THERMOPLASTIC ELASTOMERS FROM ISOTACTIC POLYPROPYLENE/NITRILE RUBBER BLENDS: EFFECT OF COMPATIBILISATION AND DYNAMIC VULCANISATION

THESIS SUBMITTED TO
THE MAHATMA GANDHI UNIVERSITY
IN PARTIAL FULFILMENT OF THE REQUIREMENTS FOR
THE AWARD OF THE DEGREE OF

DOCTOR OF PHILOSOPHY

IN CHEMISTRY
UNDER THE FACULTY OF SCIENCE

BY

SNOOPPY GEORGE

SCHOOL OF CHEMICAL SCIENCES
MAHATMA GANDHI UNIVERSITY
KOTTAYAM, KERALA, INDIA

JUNE, 1998

Dr. SABU THOMAS B. Tech., Ph.D.
READER IN POLYMER SCIENCE & TECHNOLOGY
SCHOOL OF CHEMICAL SCIENCES
MAHATMA GANDHI UNIVERSITY
PRIYADARSHINI HILLS P.O.
KOTTAYAM 686 560
KERALA, INDIA.

PHONE: Office : (0481) 598015
Residence: (0481) 597914
(0481) 596097
Fax : 91-481-561190
: 91-481-561800
Email: mgu@md2.vsnl.net.in

Mahatma Gandhi University

Date 04.06.'98

CERTIFICATE

This is to certify that the thesis entitled **Thermoplastic Elastomers from Isotactic Polypropylene/Nitrile Rubber Blends: Effect of Compatibilisation and Dynamic Vulcanisation** is an authentic record of the research work carried out by **Ms. Snooppy George** under the joint supervision and guidance of myself and Dr. K. T. Varughese, Central Power Research Institute, Bangalore, in partial fulfilment of the requirements for the award of the degree of **Doctor of Philosophy** in Chemistry under the Faculty of Science of the Mahatma Gandhi University, Kottayam. The work presented in this thesis has not been submitted for any other degree or diploma earlier. It is also certified that Ms. Snooppy George has fulfilled the course requirements and passed the qualifying examination for the Ph.D. degree of the University.

June 1998

DR. SABU THOMAS
(Supervising Teacher)

केन्द्रीय विद्युत अनुसंधान संस्थान
[illegible]
केन्द्रीय अनुसंधान व परीक्षण प्रयोगशाला
प्रो. सर. सी.वी. रमन रोड
राजामहल विलास एक्स्टेंशन II स्टेज पी.ओ.
पी बी. सं. 9401, बेंगलूर-560 094, भारत.
CENTRAL POWER RESEARCH INSTITUTE
(A GOVERNMENT OF INDIA SOCIETY)
CENTRAL RESEARCH AND TESTING LABORATORY
PROF. SIR C. V. RAMAN ROAD
RAJAMAHAL VILAS EXTENSION, II STAGE P.O.
P.B. No. 9401, BANGALORE-560 094, INDIA.

Telegram : POWERSEARCH
Telex : 0845-2572
Telephone: Off
Fax : 91-080-2-3342 13

Dr. K. T. Varughese
Scientific Officer Grade-3

CERTIFICATE

This is to certify that the thesis entitled, **"Thermoplastic Elastomers From Isotactic Polypropylene / Nitrile Rubber Blends : Effect of Compatibilisation and Dynamic Vulacanisation"**, is an authentic record of the research work carried out by **Ms. Snooppy George** under the joint supervision and guidance of myself and Dr. Sabu Thomas, Reader, School of Chemical Sciences, Mahatma Gandhi University, in partial fulfilment of the requirements for the award of the degree of **Doctor of Philosophy in Chemistry** under the Faculty of Science of the Mahatma Gandhi University, Kottayam. The work presented in this thesis has not been submitted for any other degree or diploma earlier. It is also certified that Ms. Snooppy George has fulfilled the course requirements and passed the qualifying examination for the Ph.D. Degree of the University.

Dr. K.T. Varughese
(Supervising Teacher)

June 1, 1998

DECLARATION

I hereby declare that the thesis entitled **Thermoplastic Elastomers from Isotactic Polypropylene/Nitrile Rubber Blends: Effect of Compatibilisation and Dynamic Vulcanisation** is a record of the research work carried out by me under the joint supervision and guidance of **Dr. Sabu Thomas**, School of Chemical Sciences, Mahatma Gandhi University, Kottayam, and **Dr. K. T. Varughese**, Central Power Research Institute, Bangalore. No part of this thesis has been presented for any other degree or diploma earlier.

Kottayam
June 1998

Snooppy

SNOOPPY GEORGE

ACKNOWLEDGEMENTS

I express my deep sense of gratitude and indebtedness to my supervising teachers, Dr. Sabu Thomas, Reader, School of Chemical Sciences, Mahatma Gandhi University, Kottayam, and Dr. K. T. Varughese, Scientific Officer, Polymer Laboratory, Central Power Research Institute, Bangalore, for kindly suggesting the topic of my research work and for their valuable suggestions and encouragement throughout my research work.

I am grateful to Dr. V. N. Rajasekharan Pillai, Vice-Chancellor, Mahatma Gandhi University and former Director, School of Chemical Sciences, Mahatma Gandhi University and Dr. M. Padmanabhan, Reader-in-Charge, School of Chemical Sciences, for their continued support during the work. I would like to express my thanks to Dr. A. S. Padmanabhan, Reader, School of Chemical Sciences, for his sincere co-operation. I am grateful to the authorities of Central Power Research Institute, Bangalore, for permitting me to carry out a part of my work, in their polymer laboratory.

I express my deep sense of gratitude to Mr. S. Sridhar, Joint Director, Materials Technology Division, Central Power Research Institute, Bangalore, for his valuable suggestions during my work in CPRI. I also express my thanks to Dr. P. V. Reddy, Mr. P. Sadashivamurthy and Mr. S. Sunderrajan of Insulation Division, CPRI, for their kind co-operation. I am grateful to Prof. N. R. Neelakantan, High Polymer Division, Indian Institute of Technology, Chennai, for providing me the facilities at the centre for my work. I am grateful to Dr. R. Ramamurthy, Deputy Director and Dr. R. Janardhan, Technical Officer, Rheological Laboratory, CIPET, for permitting me to carry out the rheological work there. I remember with thanks Dr. Peter Koshy, Head, Instrumentation Division, Regional Research Laboratory, Thiruvananthapuram, for extending the SEM facilities for my work. My sincere thanks are due to Dr. N. M. Mathew, Director, Rubber Research Institute of India, Kottayam, for permitting me to carry out mechanical testings there. I would like to express my thanks for Mrs. Reethamma George, RRII, for the assistance provided to me during the mechanical property studies.

I also express my thanks to the staff, School of Chemical Sciences, for their help and co-operation throughout my Ph.D. programme.

I would like to express my deep sense of gratitude and thanks to my friends in Polymer Technology Laboratory for their help and encouragement throughout my research work. I express my special thanks to Ms. R. Asaletha, Mr. T. Johnson, Mr. George Mathew, Mr. C. Radhesh Kumar and Mr. Soney C. George, for the valuable criticisms, suggestions and help during the preparation of this manuscript.

I am thankful to University Grants Commission, New Delhi, and Council of Scientific and Industrial Research for the financial support for my research work.

I express my special thanks to the members of Copy Write, Ettumanoor, for the effort they have taken in the preparation of this manuscript.

Snooppy George

GLOSSARY OF TERMS

A	-	area
a	-	area of copolymer molecule
ABS	-	acrylonitrile butadiene styrene copolymer
a_n	-	number average diameter
A_s	-	amount of solvent absorbed
a_T	-	shift factor
BS	-	butadiene styrene rubber
C	-	capacitance
C_r	-	concentration at equilibrium
CBS	-	N-cyclohexyl benzothiazyl sulphenamide
C_{cr}	-	critical concentration of copolymer
CHMA	-	cyclohexyl methacrylate
CMC	-	critical micelle concentration
CPE	-	chlorinated polyethylene
CR	-	chloroprene rubber
CR-g-iBMA	-	chloroprene-g-isobutyl methacrylate
C_t	-	concentration at time t
D	-	diffusion coefficient
d	-	interplanar distance
DCP	-	dicumyl peroxide
DMAEMA	-	dimethyl anion ethyl methacrylate
dn	-	number of average diameter
DPH	-	9,10-dihydrophenanthrene
DSC	-	differential scanning calorimetry
$\overline{D}_n$	-	number average diameter
$\overline{D}_{vs}$	-	surface area average diameter
$\overline{D}_w$	-	weight average diameter
E	-	activation energy
E″	-	loss modulus
E′	-	storage modulus
E*	-	complex modulus of blend
E/EA/GMA	-	ethylene/ethylacrylate/glycidyl methacrylate terpolymer
E_M^*	-	complex modulus of matrix
EMA	-	ethylene methyl acrylate copolymer
E_N^*	-	complex modulus of dispersed phase
ENR	-	epoxidised natural rubber
EOR	-	ethylene olefin rubber
EPDM	-	ethylene propylene diene terpolymer
EPM	-	ethylene propylene monomer rubber
EPM-MA	-	maleic anhydride grafted-ethylene propylene rubber
EPR	-	ethylene propylene rubber
EPR-g-SA	-	succinic anhydride grafted ethylene propylene rubber
ETMQ	-	6-ethoxy-2,2,4-trimethyl-1,2-dihydroquinoline
EVA	-	poly(ethylene-co-vinyl acetate)

f	-	volume fraction of filler
f_1	-	free volume fraction of component 1
f_2	-	free volume fraction of component 2
f_m	-	frequency corresponding to maximum loss factor
FTIR	-	fourier transform infrared spectroscopy
G	-	shear modulus
G^*	-	complex shear modulus
G_i^*	-	complex shear modulus of dispersed phase
G_m^*	-	complex shear modulus of the matrix
GMA	-	glycidyl methacrylate
h	-	thickness
HAF	-	high abrasion furnace black
HCl	-	hydrogen chloride
HDPE	-	high density polyethylene
HEMA	-	2-hydroxy ethyl methacrylate
HIS	-	hydrogenated butadiene styrene rubber
HPMA	-	2-hydroxy propyl methacrylate
I_a	-	intensity due to amorphous phase
iBMA	-	isobutyl methacrylate
I_c	-	intensity due to crystalline phase
IIR	-	isobutylene isoprene rubber, butyl rubber
IPO	-	2-isopropenyl-2-oxazoline
IR	-	infrared spectroscopy
k'	-	first order rate constant
K_e	-	equilibrium sorption constant
L	-	width at half height
LCP	-	liquid crystalline polymer
LDPE	-	low density polyethylene
LLDPE	-	linear low density polyethylene
M	-	molecular weight
M_1	-	mechanical property of component 1
M_2	-	mechanical property of component 2
M_A	-	molecular weight of A block
MA-PP	-	maleic anhydride modified polypropylene
M_c	-	molar mass between crosslinks
MFI	-	melt flow index
M_L	-	lower bound series model
MMA	-	methyl methacrylate
MMA-ACN	-	methyl methacrylate acrylonitrile copolymer
MPa	-	mega pascal
M_U	-	upper bound parallel model
N	-	Avagadro's number
n	-	refractive index
n'	-	flow behaviour index
N_A	-	degree of polymerisation of copolymer segment A
$NaCl.AlCl_3$	-	sodium chloride aluminium chloride double salt
N_B	-	degree of polymerisation of copolymer segment B
NBR	-	acrylonitrile-co-butadiene rubber
NDB	-	negative deviation behaviour
NR	-	natural rubber
NR-g-PMMA	-	natural rubber-g-poly(methyl methacrylate)
NR-g-PS	-	natural rubber-g-poly(methyl methacrylate)
OPS	-	oxasotine modified polystyrene
P	-	permeation coefficient
P(S-b-MMA)	-	poly(styrene-b-methyl methacrylate)
P(S-g-EO)	-	poly(styrene-g-ethylene oxide)

P_1	-	permeation coefficient of component 1
P_2	-	permeation coefficient of component 2
P_A	-	degree of polymerisation of homopolymer A
PA	-	polyamide
PA-6-g-PP	-	polyamide-g-polypropylene
P_B	-	degree of polymerisation of homopolymer B
PB	-	polybutadiene
PBT	-	polybutylene terephthalate
PC	-	bisphenol A polycarbonate
P_c	-	permeation coefficient of blend
P_d	-	permeation coefficient of dispersed phase
PDB	-	positive deviation behaviour
PDI	-	polydispersity index
PDMS	-	polydimehtyl siloxane rubber
PE	-	polyethylene
Ph-PP	-	phenolic modified polypropylene
PHB	-	poly(D(-)3 hydroxy butyrate)
PI	-	polyisoprene
PiBMA	-	poly(isobutyl methacrylate)
PM	-	N,N'-m-phenylene-bis-maleimide
P_m	-	permeation coefficient of matrix
PMMA	-	poly(methyl methacrylate)
PMPC	-	tetramethyl polycarbonate
PNDB	-	positive negative deviation behaviour
poly(CR-co-iBMA)	-	poly(chloroprene-co-isobutyl methacrylate)
POM	-	polyoxy methylene
PP	-	polypropylene
PP-g-AA	-	acrylic acid grafted polypropylene
PP-g-MA	-	maleic anhydride grafted polypropylene
PP-g-MAH	-	maleic anhydride grafted polypropylene
PPacr	-	acrylic acid modified polypropylene
PPO	-	poly(2,6-dimethyl-p-phenylene oxide)
PS	-	polystyrene
PS-g-MA	-	maleic anhydride grafted polystyrene
PTMQ	-	poly(2,2,4-trimethyl-1,2-dihydroquinoline)
PVA	-	poly(vinyl acetate)
PVC	-	poly(vinyl chloride)
PVF_2	-	poly(vinylidene fluoride)
Q_∞	-	equilibrium mol % uptake
Q_t	-	mol % uptake at time t
R	-	volume resistivity
Rg	-	radius of gyration of A block of copolymer
R_v	-	radius of the dispersed phase
S	-	sorptivity
SAG	-	poly(styrene-co-acrylonitrile-co-glycidyl methacrylate)
SAN	-	styrene acrylonitrile copolymer
SbBgCHMA	-	poly[styrene-b-(butadiene-g-cyclohexyl methacrylate)]
SbBgMMaA	-	poly[styrene-b(butadiene-g-methyl methacrylate)]
SBS	-	styrene butadiene styrene copolymer
SBu	-	styrene butadiene copolymer
SEBA-g-MA	-	maleic anhydride grafted poly[styrene-b-(ethylene-co-butylene)-b-styrene]
SEBS	-	poly[styrene-b-(ethylene-co-butylene)-b-styrene]
SIS	-	styrene isoprene styrene copolymer
SMA	-	styrene maleic anhydride copolymer
SP-1045	-	dimethyl phenolic resin

SRF	-	semi reinforcing furnace black
T	-	temperature
t	-	time
T_0	-	initial degradation temperature
tan δ	-	dissipation factor
TBAEMA	-	t-butyl amino etnyl methacrylate
T_{degr}	-	degradation temperature
Tg	-	glass transition temperature
TGA	-	thermogravjmetric analysis
T_m	-	melting temperature
TMTD	-	tetramethyl thiuram disulphide
TPE	-	thermoplastic elastomer
Tsi	-	silane treated silica
V_1	-	volume fraction of component 1
V_2	-	volume fraction of component 2
V_{Fcr}	-	critical volume fraction of copolymer
V_H	-	volume fraction of hard phase
V_s	-	molar volume of solvent
W	-	mass of copolymer
W_e	-	Weber number
X_c	-	crystallinity
XNBR	-	carboxylated nitrile rubber
Z_c	-	degree of polymerisation of copolymer
$\dot{\gamma}$	-	shear rate
$\dot{\gamma}_w$	-	apparent shear rate
ν	-	crosslink density
ρ	-	density
χ	-	interaction parameter
Σ	-	interfacial area per copolymer joint
γ	-	interfacial tension
β	-	lattice constant
μ	-	number of effective chains
τ	-	relaxation time
η	-	viscosity
ϕ	-	volume fraction
ε'	-	dielectric constant
$\Delta\gamma$	-	interfacial tension reduction
ε''	-	loss factor
ε'_c	-	dielectric constant of blend
η_1	-	viscosity of component 1
ϕ_1	-	volume fraction of component 1
ε_1'	-	dielectric constant of component 1
τ_{12}	-	interfacial tension
η_2	-	viscosity of component 2
ϕ_2	-	volume fraction of component 2
ε_2'	-	dielectric constant of component 2
ν_{2c}	-	polymer volume fraction during crosslinking
ν_{2m}	-	polymer volume fraction at equilibrium swelling
ϕ_A	-	volume fraction of component A
ρ_{bc}	-	block copolymer density
ϕ_c	-	bulk volume fraction of copolymer
Δd	-	particle size reduction
η_d	-	viscosity of dispersed phase
ΔG_{max}	-	free energy of mixing

ΔH_{mix}	-	enthalpy of mixing
μm	-	micrometer
η_m	-	viscosity of matrix
η_{mix}	-	viscosity of blend
ϕ_p	-	bulk volume fraction of polymer
ρ_p	-	density of polymer
δ_p	-	solubility parameter of polymer
ρ_s	-	density of solvent
δ_s	-	solubility parameter of solvent
ΔS_{mix}	-	entropy of mixing
τ_T	-	shear stress at a temperature T
ρ_v	-	volume resistivity
τ_w	-	shear stress

CONTENTS

Chapter 1

Introduction

The industry's need for new polymeric materials with specific properties led to the development of various thermoplastic elastomers (TPEs). Thermoplastic elastomers possess the processability and economy of thermoplastics and the performance of rubbers.[1,2] Nowadays TPEs find applications in almost all non-tyre sectors like automotive, construction, electrical and in rubber goods and medical products. TPEs are increasingly dominating the manufacture of various components based on advanced materials. Properties of TPEs range from that of soft rubbers to hard thermoplastics, bridging the gap between plastic and rubber industries.

1.1 Advantages of TPEs

1. TPEs do not require any compounding steps which are necessary for thermoset rubbers, i.e. TPE pellets itself can be used for the fabrication of products.

2. The processing of TPE is much simpler than thermoset rubbers which require multisteps for fabrication of products. This reduces the final cost of the product.

3. TPEs can be processed using thermoplastic fabrication methods such as blow moulding, heat welding and thermoforming, but are not practical for thermoset rubbers.

4. TPEs require shorter cycle times for the fabrication of a product compared to thermoset rubbers and this increase the production rate. The lower density of TPEs compared to thermoset rubbers leads to the production of a large number of articles from a given weight. Both these factors lead to cost reduction.

5. TPE scrap can be reused with negligible loss of properties. However thermoset rubber scrap cannot be reprocessed.

6. TPEs are flexible and break at large elongation.

7. TPEs have good compression set and superior vibration damping characteristics.

8. TPEs can be reinforced with fillers such as carbon black and silica.

9. TPEs have good resistance to impact, compressive and flexural loads.

10. TPEs have high fatigue to failure resistance.

1.2 Classification of thermoplastic elastomers

1. Block copolymers
   - (a) Styrene-diene block copolymers
   - (b) Polyurethanes
   - (c) Block copolyesters
   - (d) 1,2-Polybutadiene TPEs
   - (e) Polyamide block TPEs
2. Rubber/plastic blends
3. Elastomeric alloys

Among the different types of TPEs, those obtained from rubber/plastic blends have gained lot of interest, since it is possible to achieve the desired properties at a lower cost by simple blending of polymers.[3,4] The properties of the resulting material can be varied from that of a soft rubber to a hard thermoplastic by varying the rubber/plastic ratio. Some of the properties achieved through polymer blending are improvement in processability, impact strength, solvent resistance, thermal resistance and recyclability. However, as polymer blends are physical mixtures of two or more polymers there is a problem of miscibility or compatibility between the components, as in the case of any other multicomponent systems.[5,6]

For two polymers to be miscible, the Gibb's free energy of mixing (ΔG_{mix}) must be negative as given by the thermodynamic equation, $\Delta G_{mix} = \Delta H_{mix} - T\Delta S_{mix}$, where ΔH_{mix} - change in enthalpy, ΔS_{mix} change in entropy and T - the temperature. For ΔG_{mix} to be negative, either ΔH_{mix} has a negative value or ΔS_{mix} must have a higher value. The entropy term, for mixing of high molecular weight polymers is very low, since the number of possible arrangements available to the segments of covalently linked molecules is few. Hence the thermodynamic factor contributing to the miscibility of polymers is enthalpy of mixing. For two polymers to be miscible, ΔH_{mix} has a negative value, i.e. there should be some specific interactions like dipole-dipole interactions, ion-dipole interactions, hydrogen bonding, acid-base reactions, charge transfer etc. between the polymers.

For the last few decades a large quantum of research have taken place in the area of polymer blends. These studies revealed that the properties of polymer blends depend on many factors like (1) blend ratio[7-12] (2) properties of component polymers[13, 14] (3) viscosity ratio of component polymers[15-17] (4) morphology and[18-21] (5) compatibility or miscibility between the polymers.[22,23] Generally the properties of miscible blends are an average of the properties of component polymers, while those of immiscible polymer blends are a combination of the properties of two polymers. Many of the high molecular weight polymer blends are incompatible or immiscible. Generally, the immiscible blends are preferred to miscible blends as it

is possible to tailor the properties of component polymers when they are not miscible. The immiscible blends often exhibit high interfacial tension, which leads to poor degree of dispersion of the phases and lack of phase stability, i.e., phase coarsening or stratification. Figure 1.1a shows the narrow interface between two immiscible homopolymers of infinite molecular weight.[24] The interfacial density profiles of the two homopolymers through the interphase region is shown in Figure 1.1b.

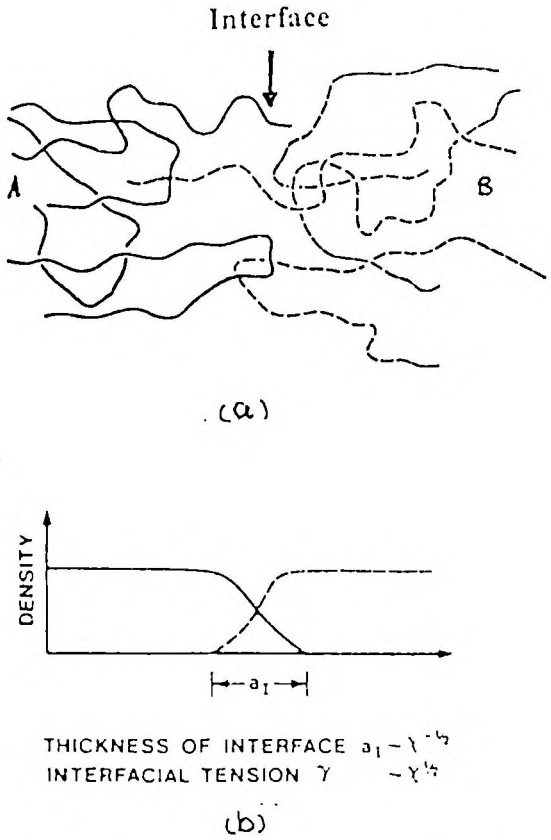

Figure 1.1. (a) Narrow interface in immiscible polymer blends and (b) interfacial density profile between immiscible polymers in a blend [Noolandi, *Polym. Eng. Sci.*, **24**, 70 (1984)].

The number of contact points between two different polymers is less in the case of sharp interfacial profile and hence the enthalpic or interaction energy contribution to the total free energy is minimised. However, the entropic contribution to the free energy arising from the turning-back entropy of the polymer

chains is also smallest for narrow interphase, leading to an increase in the total free energy. The interfacial adhesion between the phases is also low and hence immiscible blends usually give poor mechanical properties. The incompatibility or immiscibility between the polymers lead to complex rheological behaviour and anisotropy in strength of fabricated articles. The problems associated with the immiscible blends can be alleviated by different techniques like compatibilisation and dynamic vulcanisation.

1.3 Compatibilisation

The compatibilisation of immiscible polymer blends involves the improvement of properties by the addition of an interfacial agent or compatibiliser. The addition of compatibiliser to immiscible polymer blends leads to[25] (1) an increase in interfacial adhesion (2) reduction in interfacial tension (3) stability of morphology against gross phase segregation and (4) improvement in properties. Generally the materials used as compatibilisers are[26] (1) block or graft copolymers having segments identical to the components of blends and/or specific interactions with them (2) functionalised polymers which have specific reaction or interaction with the component polymers and (3) by the addition of low molecular weight materials.

1.3.1 Non-reactive compatibilisation (physical compatibilisation)

Non-reactive compatibilisation commonly known as physical compatibilisation involves the compatibilisation of immiscible blends by the addition of a third component as block and graft copolymers, which do not react with the component polymers, or homopolymers. In the compatibilisation of an immiscible blend (A/B) by a symmetric copolymer A'-B' the mechanism of the action of compatibiliser can be represented as shown in Figure 1.2.[27] If the block

A' mixes only with A and the block B' with B, the copolymer can locate at the interface as shown in the figure.

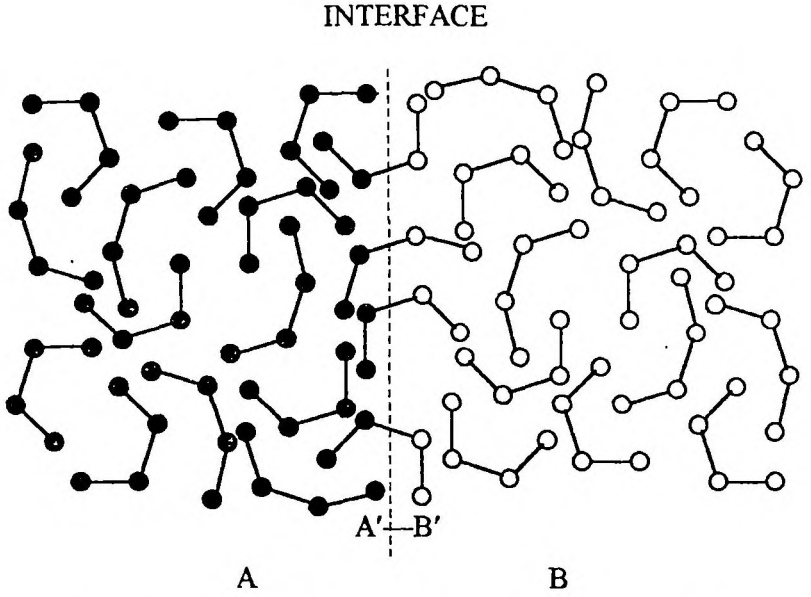

Figure 1.2. Compatibiliser effect: monolayer of a block copolymer A'-B' in the interface between the phases of two homopolymers A and B [Braun, *et al.*, *Polymer*, **37**, 3871 (1996)].

In this type of ideally compatibilised systems the interfaces are totally covered by a continuous copolymer monolayer and there are no copolymer chains outside the interfaces. In this situation, the interfacial tension is lowered drastically and the blend morphology is in equilibrium and is stable. However, though this model for compatibilisation seems very attractive there are many factors which determine the actual state of a compatibiliser in an immiscible blend. The factors affecting the efficiency of a compatibiliser are:

(i) Chemical nature of the compatibiliser

The compatibilising block or graft copolymers should have segments identical to the respective polymer phases in the blend or they have segments

miscible with one of the phases. The copolymer as a whole should not be miscible in the blend.

(ii) Copolymer chain microstructure

For a block copolymer, the compatibilising action depends on the number of blocks i.e. diblock, triblock, etc. and nature of block i.e. normal or tapered. In the case of graft copolymer, the compatibilising efficiency is also determined by the number of grafts.

(iii) Molecular weight and composition of the copolymer

The copolymer should have high molecular weight compared to homopolymers for obtaining better compatibilisation. The best compatibilising properties would be obtained only when composition is 50/50; as the copolymer needs to be located at the interface.

(iv) Concentration of the copolymer

There is an optimum concentration of copolymer, required to obtain maximum compatibilising efficiency. This optimum concentration is the amount required to saturate the interface. Above this concentration, the copolymer will form micelles in the homopolymer phases. The optimum concentration of the copolymer required for interfacial saturation depends on the conformation of the copolymer at the interface and molecular weight of the copolymer.

According to Paul the mass (W) of copolymer required to saturate the interface of an immiscible blend is given by[28]

$$W = 3\ \phi_A\ M/a\ RN \qquad (1.1)$$

where ϕ_A = volume fraction of A, M- molecular weight of the copolymer, a - area of each copolymer molecule at the interface, N-Avagadro's number and R - radius of a particle.

(v) Location of the copolymer in the blend

The copolymer should locate at the interface as a separate phase by the interpenetration of copolymer blocks into the corresponding polymer phases, rather than to disperse in the homopolymer phases.

(vi) Viscosity of the compatibiliser

The extent of dispersion of the copolymer at the interface is determined by viscosity of compatibiliser. As the viscosity of compatibiliser increases, it is more difficult to disperse the copolymer at the interphase and therefore high temperature and high shear rate are necessary for good dispersion and mixing.

(vii) Interaction parameter balance and heat of mixing

The segments of the block or graft copolymer introduced as compatibiliser into the immiscible blend should have same extent of interaction with the corresponding homopolymer phases. If the interaction of one of the segments with a homopolymer phase is more compared to that of other segments and homopolymer phase, the copolymer will get dispersed in one of the homopolymer phases; e.g., in poly(vinyl chloride)/polystyrene/poly(styrene block methyl methacrylate) [PVC/PS/P(S-b-MMA)], the major part of the copolymer is dispersed in PVC phase due to the negative heat of mixing.

(viii) Blending conditions

Method of blending, i.e., solution casting or melt blending determines the properties of compatibilised blends. In the case of melt blending, the temperature, rotor speed and time of mixing are the determining parameters. In solution casting technique, the nature of the solvent used will affect the blend properties.

(ix) Order of addition of the compatibiliser

The morphology and properties of compatibilised blends are determined by the order of addition of compatibiliser i.e. whether the compatibilised blend is prepared by one step mixing or two step mixing. In one step mixing, the

compatibiliser and homopolymers are mixed in one step, while in two step mixing the compatibiliser is added to the pre-mixed blend or by mixing with one of the homopolymers followed by blending with other polymer.

(a) *Studies related to compatibilisation by the addition of graft and block copolymers*

The compatibilisation of immiscible polymer blends using block and graft copolymers was investigated widely by various researchers. Initially researchers were interested in the use of block or graft copolymers having segments identical to the component polymers of the blend. These works include those of Molau *et al.*;[29,30] Riess *et al.*;[31,32] Gailard *et al.*;[33,34] Patterson *et al.*[35] and Paul *et al.*[36,37] for systems such as polystyrene/poly(methyl methacrylate) (PS/PMMA), polystyrene/ polyisoprene (PS/PI), polystyrene/polybutadiene (PS/PB), poly(dimethyl-siloxane)/ poly(oxymethylene-b-oxypropylene) and polyethylene/ polystyrene (PE/PS) using the corresponding block or graft copolymers. They have investigated the effects of molecular weight, structure, composition and concentration of copolymer on interfacial tension, mechanical properties and morphology of blends.

The compatibilisation of PS/PMMA blends using copolymers of styrene and methyl methacrylate was investigated by several researchers.[31-39] Riess *et al.* reported that block copolymers are more effective than graft polymers as compatibilisers in PS/PMMA system.[31,32] Their investigations also revealed that for maximum compatibilising efficiency, the composition of the block copolymer should be 50:50 and its molecular weight must be higher than that of both homopolymers. Thomas *et al.*[38] investigated the effect of molecular weight, composition, processing conditions and concentration of diblock copolymer of PS and PMMA on the morphology and miscibility of PS/PMMA blends. The authors used diblock copolymers of different molecular weights and composition. Their studies showed that the 50/50 diblock PS-PMMA copolymer with the highest molecular weight has the best compatibilising efficiency. The addition of small

amounts of copolymer (2.5%) reduced the domain size of dispersed phase sharply and above that concentration a levelling off in domain size was observed. They also reported that the size of dispersed domains depends on the solvents used for solution casting. From the amount of copolymer required to saturate the interface, the area occupied by the copolymer was calculated using the equation (1.1). By comparing this area with the area calculated from theoretical conformations of compatibiliser at the interface, the authors, have predicted a conformation for the diblock copolymer in the blend (Figure 1.3).[38]

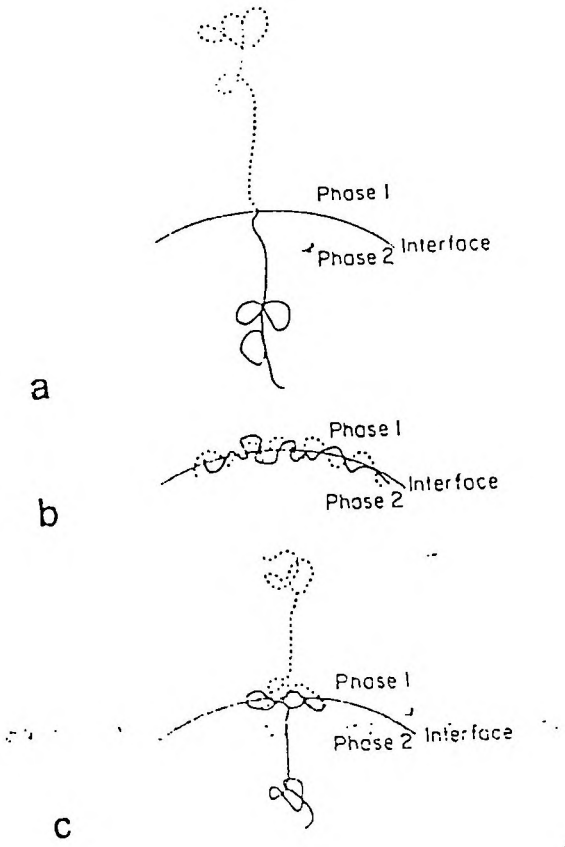

Figure 1.3. Phase models illustrating the conformation of the copolymer at the interface [Thomas and Prud'homme, *Polymer*, **33**, 4260 (1992)].

Recently Macosko *et al.*[39] have studied the influence of molecular weight of homopolymers and diblock copolymers P(S-b-MMA) on the stability of morphology during the annealing of uncompatibilised and compatibilised PS/PMMA blends. They found that even though only small amounts (1%) of copolymer was required for reduction of particle size, higher amounts were required for stable morphology during annealing. They have estimated that less than 5% of the interface is needed to be covered for preventing dynamic coalescence, i.e., for particle reduction; while 20% of the interface should be covered by the copolymer to obtain static stability.

The influence of natural rubber-graft-polymethyl methacrylate (NR-g-PMMA) copolymer as compatibiliser in PMMA/NR blends was investigated by Oommen *et al.*[40] They have studied the effect of graft copolymer concentration and molecular weight on morphology and various properties of NR/PMMA blends. Their studies showed that there is a critical concentration of compatibiliser, above which there is a levelling off in the domain size of dispersed particles and properties. The studies also revealed that the blend morphology was stabilised on compatibilisation. A graft copolymer NR-g-PS was used as a compatibiliser in NR/PS blends by Asaletha *et al.*[41] In this case also, there is a critical concentration of compatibiliser for obtaining optimum properties and stable morphology. Some of the other blends compatibilised using corresponding block copolymers investigated recently include polyester/polystyrene, polychloroprene/poly(isobutyl methacrylate), polystyrene/polyethyl acrylate, etc. The compatibilisation of poly(butylene terephthalate)/polystyrene blends using styrene-butylene terephthalate block copolymer reduced the dimensions of the dispersed phase and stabilised the morphology against annealing.[42] The tensile properties were also found to improve upon compatibilisation. Park *et al.*[43] reported that the addition of a copolymer of chloroprene and isobutyl methacrylate [poly(CR-co-iBMA)] to CR/PiBMA blends improved the miscibility of the blend

as shown by the shift in Tgs. They have also compared the compatibilising efficiency of the copolymer poly(CR-co-iBMA) with a graft copolymer of iBMA and polychloroprene (CR-g-iBMA) and found that the extent of partial miscibility becomes larger on the addition of the copolymer than the graft copolymer. The effect of number of graft per chain and graft molecular weight on the compatibilising efficiency of a graft copolymer of ethylacrylate and polystyrene in PS/polyethyl acrylate blend was investigated by Peiffer *et al.*[44] They found that the tensile strength of the blends was improved upon the addition of the graft copolymer and the tensile strength is inversely related to the graft level and directly related to the graft molecular weight. They accounted this improvement in properties to the partial phase separation of these graft copolymers in the interfacial region between the phase separated homopolymers.

Recently, researchers are interested in using block and graft copolymers chemically different but are miscible with the homopolymers i.e. in the use of A-C or C-D block copolymers in A/B blends where A and B are miscible with A and C or C and D blocks of copolymer respectively.[45-48] The compatibilisation of blend (A/B) with a block copolymer (A-B), involves a thermodynamically athermal process and in this case for better compatibilisation, the molecular weight of the copolymer segments should be higher than that the homopolymers. However, the use of a block copolymer which is miscible with the homopolymers, involves an exothermic enthalpy of mixing between miscible pairs. This is a driving force for the local miscibility in the interphase, and give compatibilising effect. Hence copolymers of low molecular weight can function as efficient compatibilisers in this case.

The use of chemically different copolymers in immiscible blends was investigated for systems such as poly(2,6-dimethyl-p-phenylene oxide)/poly(methyl methacrylate) (PPO/PMMA),[49] polypropylene/polystyrene (PP/PS),[50] polystyrene/ poly(vinyl chloride) (PS/PVC),[27] polystyrene/epoxidised natural rubber (PS/ENR),[51] polypropylene/polybutylene terephthalate (PP/PBT),[52] etc. The influence of

P(S-g-EO) copolymer on the miscibility of PPO/PMMA blends was investigated by Eklind *et al.*[49] The addition of P(S-g-EO) to the blend reduced the dimensions of the dispersed particles with increase in concentration of compatibiliser. The interfacial thickness which was not much varied with increase in concentration of P(S-g-EO) was estimated to be 47 ± 10 nm. In compatibilised blends, an additional transition was observed in between the transitions of PMMA and PPO in dynamic mechanical analysis. The authors attributed this transition to the existence of an interphase with a distinct volume fraction with its own characteristic properties. Navaratilova and Fortenly[50] investigated the effect of styrene butadiene styrene copolymer on the morphology of PP/PS blend. The size of the dispersed particles was decreased upon compatibilisation. However stability of morphology was not obtained during annealing in this case.

Recently, Braun and co-workers[27] investigated the compatibilising efficiency of a block-graft copolymer which is prepared by radical grafting on a block copolymer in immiscible PVC/PS blends. The graft copolymers used were styrene block butadiene graft cyclohexyl methacrylate (SbBgCHMA) and styrene block butadiene graft methyl methacrylate (SbBgMMA). The compatibilises were found to refine the coarse morphologies of the blend by covering the interfaces between domains of PS and PVC with monolayers. In the compatibilisers the S-block is miscible with PS phase and the grafted CHMA or MMA is miscible with the PVC phase. The central B block acts as an anchor for the graft and also helps to see the copolymer in compatibilised blends, after staining the butadiene.

The effect of molecular weight, chemical composition and architecture of the interfacial agent on the morphology of immiscible ethylene-propylene rubber/polystyrene (EPR/PS) blends was investigated by Matos *et al.*[51] The interfacial agents used were hydrogenated triblock copolymers of styrene and butadiene (SEBS) and unsaturated styrene butadiene copolymer (SBu). It was observed that the addition of 15 wt % hydrogenated triblock (SEBS) copolymer reduced the particle size by three times while for the unsaturated SBu triblock

copolymer the reduction is less than two times. The molecular weight of the triblock copolymer had little effect on the particle size of dispersed phase in this system (Figure 1.4).

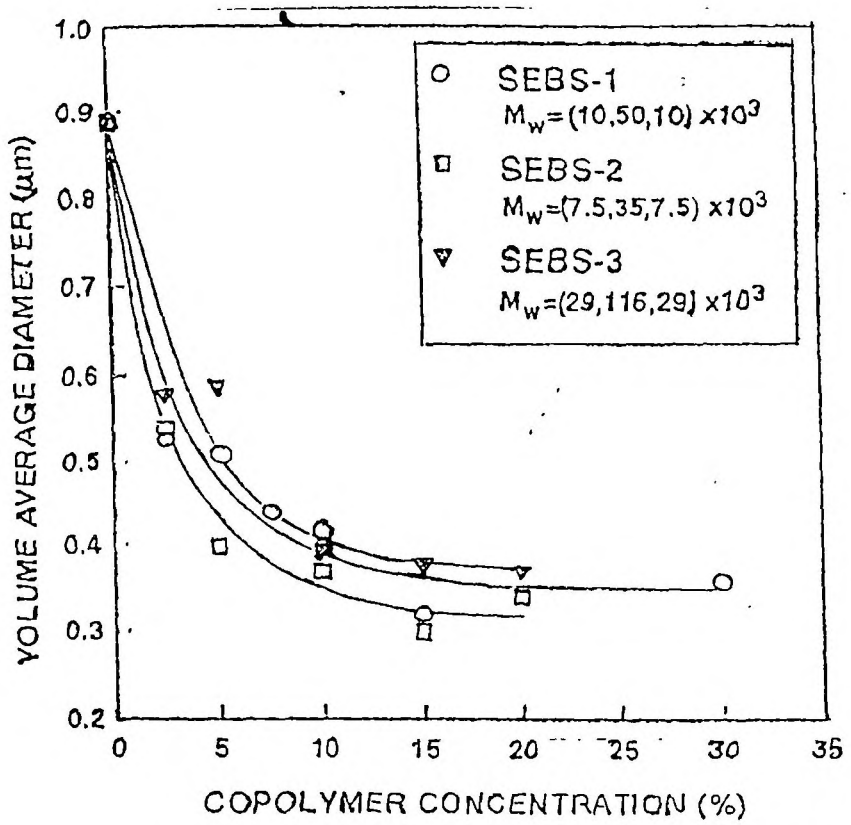

Figure 1.4. Influence of the molecular weight of the S-EB-S saturated triblock copolymer on the emulsification curve [Matos et al., *Polymer*, **36**, 3899 (1995)].

(b) Compatibilisation by the addition of third polymer

The properties of immiscible blends were also tried to improve by the addition of a third polymer which is miscible with both the components of an immiscible blend.[53,54] This third component reduces the number of unfavourable contacts between the segments of the two polymers.[55] Rio and Acosta[56] investigated the effect of poly(vinyl acetate) on the miscibility and microstructure of polystyrene/poly(vinylidene fluoride) (PS/PVF_2) blends. The addition of poly(vinyl acetate) (PVA) to the blend decreased the Tg of PVF_2 and PS as a function of PVA concentration, which indicated the compatibility. The

morphology also revealed that phase separation diminished on increasing PVA concentration. The phase behaviour and morphology of polystyrene/ polycarbonate/tetramethyl polycarbonate (PS/PC/TMPC) ternary blend was investigated by Landry *et al.*[57] The PS/PC blend is immiscible, while PS/TMPC and PC/TMPC blends are miscible. These studies indicated that the TMPC, which is miscible with the PS and PC did not solubilise the two immiscible polymers PS and PC. Single phases were observed only at very high TMPC concentrations. The effect of epoxidised natural rubber (ENR) on the miscibility and properties of chlorinated polyethylene/polyvinyl chloride (CPE/PVC) blends was investigated by Koklas *et al.*[58] The CPE/PVC blends show two transitions in dynamic mechanical analysis for both the components. As the concentration of ENR in CPE/PVC blend increases, these transitions approach each other and merge to give single transition (Figure 1.5).

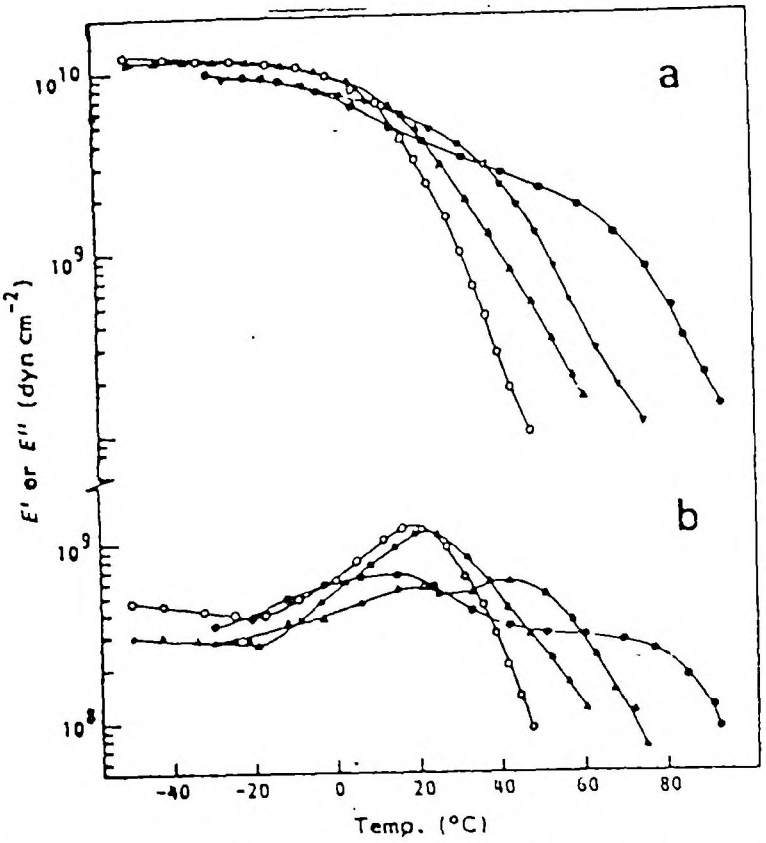

Figure 1.5. Thermomechanical spectra of PVC/ENR50/CPE48 blends: (●) 47.5/5/47.5; (△) 40/20/40; (▲) 35/30/35; (○) 30/40/30 [Koklas *et al.*, *Polymer*, **32**, 66 (1991)].

It was observed that different amounts of ENR were required to cause miscibility for different ratios of CPE/PVC blend. The mechanical properties were also improved upon the increase in concentration of ENR. Machado and Lee[59] investigated the morphology and mechanical properties of a series of immiscible blend systems styrene maleic anhydride copolymer/styrene acrylonitrile copolymer (SMA/SAN), styrene maleic anhydride copolymer/acrylonitrile butadiene styrene copolymer (SMA/ABS), PVF_2/SAN and PVF_2/ABS compatibilised by the addition of a third polymer PMMA which is miscible with each blend components. The addition of 10 wt % PMMA to these blends was found to improve the mechanical properties and reduced the size of dispersed domains. Lizymol and Thomas[60] investigated the action of PVC in styrene acrylonitrile copolymer/ethylene vinyl acetate copolymer (SAN/EVA) immiscible system and found that the addition of PVC led to a completely miscible PVC/EVA/SAN ternary system.

1.3.2 Reactive compatibilisation

Reactive compatibilisation involves the compatibilisation of immiscible polymer blends by the *in-situ* formed copolymers. Reactive compatibilisers used are grafted or ungrafted polymers and block copolymers, having reactive functional groups.[26] Such reactive groups form copolymers *in-situ* by reaction with the reactive groups in a polymer in the blend. Generally reactive compatibilisation is preferred to non-reactive compatibilisation since in non-reactive compatibilisation, the preparation of block or graft copolymers with strict molecular architecture is very difficult and costly. Some of the typical compatibilisation reactions employed in reactive compatibilisation are shown in Table 1.1.[61]

Table 1.1. Important compatibilisation reactions [Hausmann, *Proceedings of 3rd International Conference on Advances in Additives and Modifiers in Polymer and Blends*, 1994].

Carboxylic acid - amine reaction	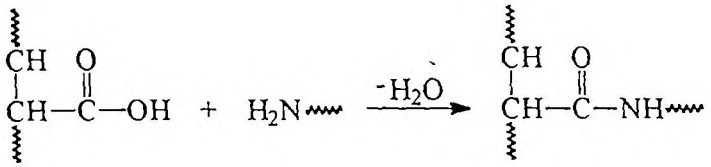
Anhydride - amine reaction	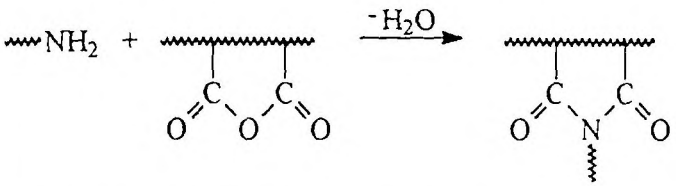
Carboxylic acid - epoxy reaction	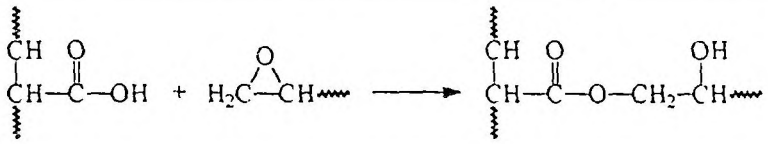
Epoxy - anhydride reaction	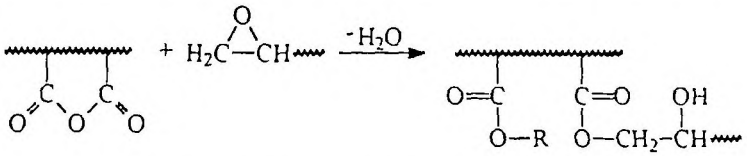
Epoxy - amine reaction	

(a) Functionalised polypropylenes

For the last few decades, the reactive compatibilisation technique has been investigated by various research groups.[62-69] Among the different types of reactive compatibilisers, modified polypropylenes were the most widely used ones. Maleic anhydride grafted polypropylene (PP-g-MAH) was used as a compatibiliser in many immiscible polymer pairs. In the compatibilisation of polypropylene/ polyamide (PP/PA) blends using PP-g-MAH, the maleic anhydride groups on

PP-g-MAH react with amino end groups of nylon to form graft copolymers, which will locate at the interface between PP and PA leading to better interfacial interactions and adhesion. Lee and Yang[70] investigated the effect of mixing procedure on the properties and morphology of PA-6/PP blends compatibilised with maleic anhydride grafted PP. The authors investigated the effect of three types of mixing procedures viz., single step mixing, two step mixing with reactive premixing and two step nonreactive blending. In two step mixing with reactive premixing, first PP-g-MAH mixed with PA-6 and then in the 2nd step with nonreactive PP and in non-reactive two step blending, first PP-g-MAH mixed with non-reactive PP and in 2nd step mixed with PA-6. The morphological investigations revealed that the size of the dispersed domains decreased upon compatibilisation and the single step mixing and two step mixing with non-reactive premixing gave fine morphology compared to two step mixing with reactive premixing. The authors attributed the coarse morphology observed in the case of two step mixing with reactive premixing to the lowered mobility and stiffness of the copolymer PA-6-g-PP formed which inhibit the copolymer to diffuse into interface. The interfacial tension in uncompatibilised and compatibilised blends was also investigated. For the calculation of interfacial tension, Oldroyds[70] model for an oscillatory shear flow was used. According to this model, the complex modulus G* can be given as

$$G^* = Gm^* \left(\frac{1 + 3\phi H}{1 - 2\phi H} \right) \tag{1.2}$$

in which

$$H = \frac{4(2G_M^* + 5G_I^*)\gamma . R_V + (G_I^* - G_M^*)(16G_M^* + 19G_I^*)}{40(G_M^* + G_I^*)\gamma . R_V (2G_I^* + 3G_M^*)(16G_M^* + 19G_I^*)} \tag{1.3}$$

where γ denotes the interfacial tension, ϕ the volume fraction and R_V the radius of the dispersed phase. The subscript M and I indicate the matrix and dispersed phase respectively. It was found that the interfacial tension decreased with increase in compatibiliser concentration up to 1.5 phr followed by a levelling off (Figure 1.6).

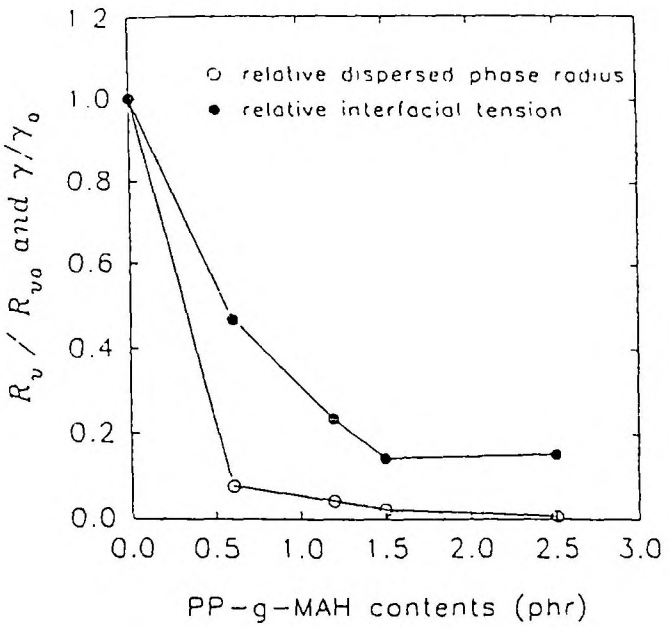

Figure 1.6. Variation of relative interfacial tension and radius of dispersed drop as a function of PP-g-MAH content in PP70/PA30 blends [Lee and Yang, *Polym. Eng. Sci.*, **35**, 1821 (1995)].

Mechanical properties were also improved upon compatibilisation. Rosch and Mulhaupt[71] recently investigated the compatibilisation of elastomer modified polypropylene/polyamide-6 blends and polypropylene/polyamide blends. The addition of PP-g-MA to PP/PA blend decreased the domain size and increased the yield stress. Haddout *et al.*[72] found that the viscosity of PP/PA blends was increased upon compatibilisation using PP-g-MA. The higher values of viscosity for compatibilised blends were correlated with the reduction in average size of the dispersed nodules and also to the better adherence between two phases in presence of a compatibiliser. The acrylic acid grafted polypropylene (PP-g-AA) was also used as compatibiliser in PP/PA blends. In this case, the compatibilisation reaction is in between the acid group of acrylic acid modified PP and amine end group of nylon-6. An increase in mixing torque upon the addition of PP-g-AA to a PP/PA blend was reported by Dagli *et al.*[73] The kinetic studies from the torque vs. time curves showed that the compatibilisation reaction follows a second order

kinetics. Valenza *et al.*[74] reported that among PP-g-MA and PP-g-AA, the PP-g-MA is more effective in compatibilising PP/PA blends due to the greater reactivity of maleic groups than acrylic groups to the amine end groups of nylon to form block copolymers. The DSC analysis of the compatibilised PP/PA blends revealed that the crystallisation peak of nylon remained unaltered while that of PP shifted toward a higher temperature in the case of PPacr and to a lower temperature in the case of PPmal. The shift in crystallisation temperature of PP to lower temperature in the case PP-g-AA compatibilisation indicated that PPacr acts as a nucleating agent. The effect of polypropylene having basic functional groups as compatibilisers in polypropylene/acrylonitrile-co-butadiene-co-acrylic acid rubber (PP/NBR) blends was investigated by Liu *et al.*[75] The basic functional groups grafted on PP are glycidyl methacrylate (GMA), 2-hydroxy ethyl methacrylate (HEMA), 2-hydroxy propyl methacrylate (HPMA), t-butyl amino ethyl methacrylate (TBAEMA), dimethyl amino ethyl methacrylate (DMAEMA) and 2-isopropenyl-2-oxazoline (IPO). Among the different functionalised polypropylenes, the GMA and IPO grafted polypropylene reduced the size of dispersed NBR particles and gave rise to a uniform distribution of particles. The other functionalised polypropylenes did not affect the blend morphology significantly. Similarly in the case of impact energy, the GMA and IPO functionalised PPs gave a nine fold improvement compared to uncompatibilised blend while the other functionalised PPs did not show much improvement. The better compatibilising efficiency of IPO and GMA grafted PP is due to the formation of copolymer by the reaction between the glycidyl or oxazoline groups in PP matrix with the carboxylic acid functionality in the NBR phase.

(b) Functionalised styrene butadiene copolymers

Maleic anhydride grafted poly[styrene-b-(ethylene-co-butylene)-b-styrene] (SEBS-g-MA) was used as compatibilisers in various immiscible blends such as PA-6/PP, PA/SEBS and PA-6/PC. Wu *et al.*[76] investigated the effect of maleic

anhydride graft ratio and concentration of SEBS-g-MA on the morphology and impact properties of PA-6/SEBS blends. The studies revealed that the addition of maleated SEBS to PA/SEBS blend improved the compatibility of the system, which is evident from the morphology and impact properties. The extent of protrusion of holes in the matrix of blends increased with increase in the concentration of maleated SEBS, which shows the better interactions in the interface. The authors also proposed a model for the interfacial action of a compatibiliser according to which the SEBS chains grafted on PA-6 interact with discrete SEBS particles through entanglements. The compatibilisation changes the crystalline structure of PA6 from γ to a mixture of γ and α forms. The impact properties also showed a tenfold improvement at 3 wt % maleated SEBS addition. The compatibilisation of PA-6/PP blends using maleic anhydride grafted SEBS was investigated by Miettinen *et al.*[77] in terms of morphology, dynamic mechanical properties and impact properties. The notched izod impact strength of the blends was increased with the addition of SEBS-g-MA. The 80/20 PA/PP with 10 wt % compatibiliser showed a much higher impact strength. The authors correlated this behaviour to the morphology. In the ternary blends, in which PA/PP ratios are 20/80, 40/60, a well dispersed phase of combined SEBS-g-MA and polyamide was present in the continuous PP matrix. At 80/20 PA/PP blend with 10 wt % SEBS-g-MA, a clear change in morphology was observed. The morphology showed a bimodal dispersion of SEBS-g-MA as the continuous phase and PA-6 as a fine dispersion of 0.04 μm with PP as a coarse dispersion of 0.4 to 1 μm. This morphology leads to exceptional impact properties. Recently Horiuchi *et al.*[78] investigated the morphology development in immiscible PA-6/PC blends containing SEBS-g-MA and PS-g-MA as one component. In the PA-6/PC blends, upon the addition of SEBS-g-MA as a third component, the morphology of the blend changes from stack formation of two dispersed phases to capsule formation of two dispersed phase by the interfacial reaction between the amino end groups of nylon and maleic anhydride groups of SEBS. According to the authors, the driving force for this

morphology development is reduction of interfacial tension by the interfacial reaction between PA-6 and SEBS-g-MA.

(c) Functionalised ethylene propylene rubbers

The functionalisation of ethylene propylene rubber using maleic anhydride grafting for the compatibilisation of ethylene propylene rubber based blends was also investigated by several researchers.[79-82] The degree of grafting of succinic anhydride on the morphology and impact properties was reported in PA-6/EPR rubber blends by Greco *et al.*[79] The compatibility and mechanical properties were improved with degree of grafting. The effect of formation of PA-6-EPM copolymer by amine-anhydride reaction in polyamide/ethylene propylene diene monomer rubber (PA-6/EPDM) blend on the morphology development during blending was investigated by Scott *et al.*[80] They reported that the major reduction in domain size occurs at shorter mixing times. In the case of reactive system, the volume average particle diameter of the dispersed phase was reduced from ~ 4 μm to 1 μm within first 90 sec of mixing. In the reactive PA/EPM/EPM-MA system, as the chemical reaction between PA and EPM-MA increased the molecular weight of the polymer, the mixing torque and temperature attained higher values than those of nonreactive systems. Kanai *et al.*[81] recently reported the impact modification of various engineering thermoplastics such as polyphenylene sulphide (PPS), polyoxymethylene (POM) and PBT. Functionalised elastomers were used as impact modifiers. They have correlated the impact strength with the particle size and interparticle distance. In the case of maleic anhydride functionalised ethylene olefin rubber (EOR) modified PBT, the impact strength did not show any significant relationship with particle size. However, the impact strength and interparticle distance gave a good correlation. The compatibility improvement of poly(D(-)3-hydroxy butyrate) (PHB)/ethylene propylene rubber blends by the use of maleic anhydride and dibutyl maleate functionalised EPR was investigated by Abbate *et al.*[82] The critical strain energy release rate and critical stress intensity

factor of these blends were improved upon the use of functionalised elastomers and among the different functionalised elastomers used, EPR-g-SA gave the highest values. This is due to the formation of a graft copolymer between PHB and EPR-g-MA as shown in Figure 1.7, which will act as an interfacial agent to improve the mode and state of dispersion of the rubbery phase, as well as its adhesion to the matrix, yielding a morphology more suitable for toughening mechanisms.

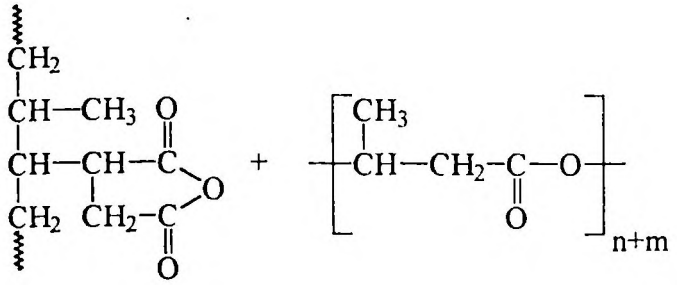

EPR-g-SA PHB

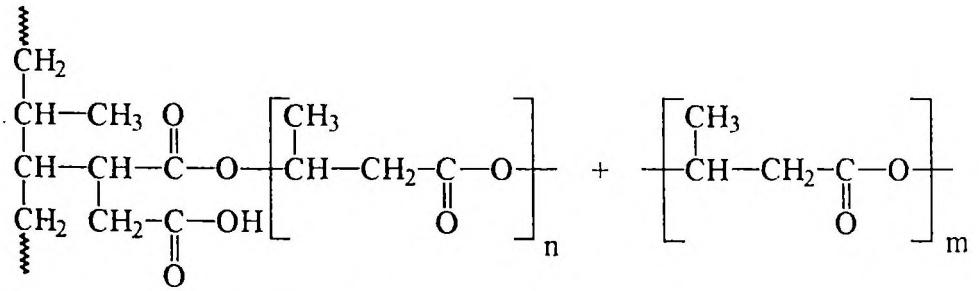

(EPR-g-SA)-g-PHB

Figure 1.7. Reaction scheme for the formation of a graft copolymer between PHB and EPR-g-MA [Abbate *et al.*, *J. Mater. Sci.*, **26**, 1119 (1991)].

(d) Modified polystyrene

The reaction between oxazoline groups on polystyrene in OPS with carboxylic groups in CPE was investigated for compatibilisation of PS/PE blends, by Baker *et al.*[63] During the reactive blending of OPS with CPE a graft copolymer is formed, which acts as an interfacial agent as shown in Figure 1.8. The authors characterised the graft copolymer formed using FTIR spectroscopy, after extracting

the copolymer with toluene. In the blending of OPS with CPE, the presence of reaction between OPS and CPE was confirmed by an increase in torque compared to non-reactive blends The morphology of reactive OPS/CPE blends showed a fine and uniform dispersion compared to non-reactive PS/PE blends. This also suggests that there is good adhesion between the two phases as a result of intermolecular reaction between the two polymers. The oxazoline modified polystyrene was also used to compatibilise PS/nylon and PS/EPM blends through the reaction between oxazoline groups in PS and amino end groups in nylon or maleic anhydride groups in EPM-g-MA.[80] The increase in mixing torque and improvement in morphology indicated that the use of oxazoline grafted PS increased the interfacial interaction in the blends.

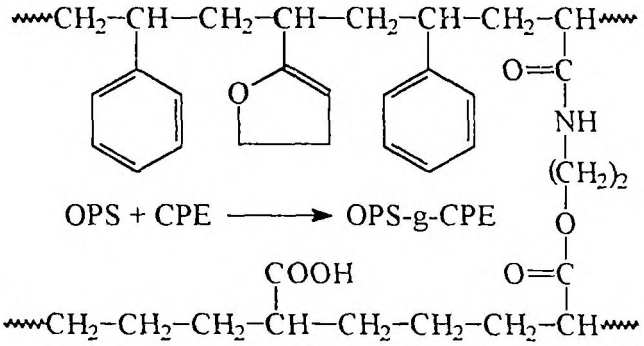

Figure 1.8. Reaction scheme for the formation of a graft copolymer between OPS and CPE [Baker and Saleem, *Polymer*, **28**, 2057 (1987)].

Reactions between carboxylic acid groups and epoxy groups have been exploited in the compatibilisation of polymer blends. Miettinen *et al.*[81] investigated the effect of epoxy functionalised polymers ethylene/ethyl acrylate/glycidyl methacrylate (E/EA/GMA) terpolymer in blends of polypropylene with polybutylene terephthalate and a liquid crystalline polyester (LCP). In the binary blends, the increased viscosity during blending, changes in crystallisation of PBT phase and the FTIR results indicated that chemical reactions occur during blending of compatibiliser with polyesters. The addition of epoxy functionalised

compatibiliser to PP/PBT and PP/LCP blends improved the impact properties of the blend. Chen *et al.*[84] reported that the *in-situ* compatibilisation of phenoxy and ABS blends using styrene-acrylonitrile-glycidyl methacrylate (SAG) reactive polymer and sodium lauryl sulphonate catalyst improved the interfacial adhesion and properties by the formation of a copolymer between SAG and phenoxy. The addition of carboxylated nitrile rubber to immiscible blends of PVC/ENR was found to make the system miscible.[85] The miscibility in this ternary system is due to the formation of a network between ENR, PVC and NBR as shown in Figure 1.9. Tg measurements indicated that the 25/75 and 50/50 PVC/ENR blends with XNBR are miscible at all compositions of XNBR, while for 75/25 PVC/ENR, 250 parts of XNBR were required to get miscibility.

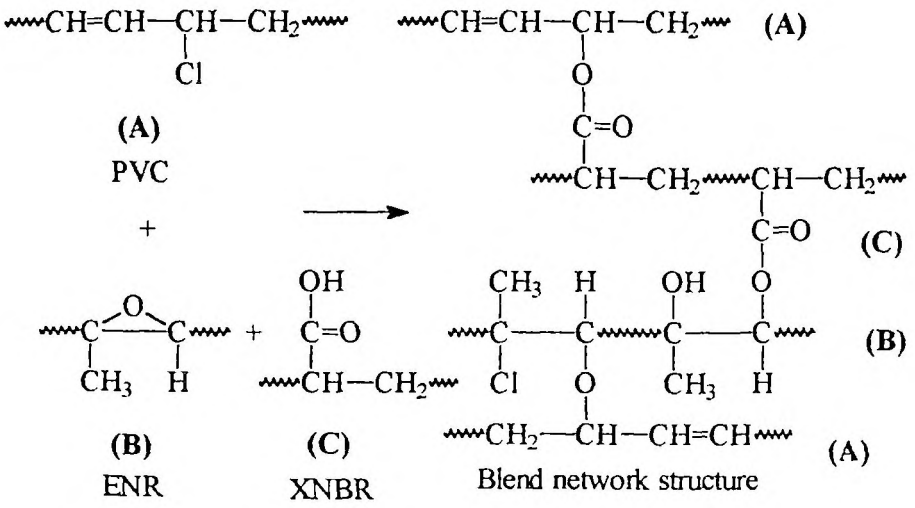

Figure 1.9. Possible mechanism of crosslinking between PVC, ENR and XNBR [Ramesh and De, *J. Appl. Polym. Sci.*, **50**, 1369 (1993)].

The reactive compatibilisation of immiscible blends such as PA/ABS,[86] LDPE/PDMS[87] and LLDPE/scrap rubber[88] using methyl methacrylate-acrylonitrile copolymer (MMA-ACN) ethylene methyl acrylate copolymer (EMA) and carboxylated polyethylene respectively was reported. Horak *et al.*[86] investigated the effect of compatibiliser preparation, mixing procedure and the type of catalyst

accelerating reaction between ester and amino groups in immiscible PA/ABS blends. Their studies revealed that a two step mixing is more effective than a single step mixing and the catalysts used for the reaction between PA and MMA-ACN accelerates the reaction. The two step blending and incorporation of catalysts reduced the crystallinity by changing the crystalline structure from α to a mixture of α and γ forms. Santra *et al.*[87] reported that EMA acts as a good compatibiliser in LDPE/PDMS blend. The IR studies of LDPE/PDMS blend with 6 wt % EMA indicated that a graft copolymer is formed between EMA and PDMS rubber. The impact strength of the blends was significantly improved upon the addition of compatibiliser (Table 1.2) and the morphology changed from a co-continuous to discrete domains in the presence of 6 wt % EMA. The crystalline structure of the blend was modified upon the addition of EMA as evidenced by the presence of new peaks. In this compatibilised system, contrary to the compatibilised PA/ABS system, the crystallinity decreased upon compatibilisation.

Table 1.2. Tensile impact strength of LDPE-PDMS rubber blends containing EMA [Santra *et al.*, *J. Appl. Polym. Sci.*, **49**, 1145 (1993)].

Sample code	Impact strength (J/m)
PES_0	765
PES_1	820
PES_2	980
PES_4	1570
PES_6	1720
PES_{10}	1730

Subscripts indicate the proportion of EMA in a 50/50 blend of polyethylene and PDMS rubber.

(e) *Reactive extrusion*

More recently, reactive extrusion, which involves the addition of low molecular weight compounds during extrusion, has been used as a compatibilisation technique in immiscible polymer blends. Usually during reactive extrusion, free radical initiators, crosslinking agents and other reactive additives are added for the chemical reaction to occur which leads to a copolymer. The effect of addition of Lewis acid $NaCl.AlCl_3$ double salt during melt mixing of PS/EPDM blends on the properties was investigated by Mori *et al.*[67] The presence of chemical reactions during mixing was evident from the increase in torque upon the addition of Lewis acid. During the reaction, the rubber was found to be more active. The rubber phase was crosslinked and or coupled with polystyrene as indicated from solvent extractions. The mechanical properties of the blend was also increased upon reactive extrusion in the presence of Lewis acid. The compatibilisation of PP/PE system by the reactive extrusion in presence of an organic peroxide 2,5-dimethyl-2,5-bis-(t-butyl-peroxy) hexyne-3 was reported by Cheung *et al.*[66] Their studies revealed that though the elongation at yield showed much improvement, other mechanical properties showed a decrease upon the addition of peroxide. The morphology studies showed that the size of the dispersed phase decreased on reactive extrusion. However, the work did not gave any evidence for the formation of a copolymer. The reactive extrusion of polypropylene/natural rubber (PP/NR) blends in the presence of a peroxide (1,3-bis(t-butyl-peroxy benzene) and a coagent trimethylol propane triacrylate was reported by Yoon *et al.*[89] The effect of peroxide and coagent content were studied in terms morphology, melt viscosity, melt flow index, thermal and mechanical properties. The melt index of the blends decreased with increase in peroxide content at a constant coagent content and shear viscosity increased with peroxide content up to 0.02 phr and decreased beyond that. The morphology studies showed that the size of dispersed rubber domains decreased at lower contents of peroxide. The reduction in domain size was attributed to the compatibilising effect of

interpolymers, which were formed *in-situ* during the melt extrusion and to the increased viscosity of PP matrix by crosslinking. The extrusion of PP and polyisoprene in the presence of maleic anhydride was reported by Els and McGill.[90] They isolated the block copolymer formed during mixing using the solvent extraction technique and characterised by means of TGA, DSC and IR spectra. The reactive extrusion of monomer, ε-caprolactone in presence of a polymer for the compatibilisation was reported by Hornsby and Tung[91] in PA-6/PP blends. In comparison to the nonreactive blend, the blend obtained by reactive extrusion, showed greater phase compatibility. The FTIR analysis of solvent extracted samples showed the formation of a graft copolymer PA-6-g-PP during reactive extrusion.

Ionomers, which contain a small number of ionic groups along with the non-ionic backbone chains have been used as compatibilisers in polymer blends.[92-95] The compatibilisation of PP/EPDM blends using Na-neutralised poly(ethylene-co-methacrylic acid) gave better results compared to the compatibilisation using Zn-neutralised EMA. Kim *et al.*[92] reported that the addition of 5 wt % ionomer to PP/EPDM blends improved the compatibility as indicated by a shift in Tgs. The melt viscosity and mechanical properties increased upon compatibilisation. The morphology became more fine upon the addition of ionomer. The compatibilising action of ionomer was attributed to the mechanical interlocking that occur among the three components due to the inherent ionic crosslinking character of Na neutralised ionomer. Poly(ethylene-co-sodium methacrylate) ionomer was found to compatibilise PBT/HDPE blend. The addition of ionomer to the blend increased the viscosity and mechanical properties. Joshi *et al.*[93] attributed the superior performance of compatibilised blends to the improved interfacial bonding in presence of ionomer. Mascia and Valenza[94] reported the use of reactive dual compatibilisers-1:1 mixtures of phenoxy and sodium ionomer of an ethylene methacrylic acid copolymer in polycarbonate/HDPE blends. During compatibilisation both components of compatibilisers formed graft polymers by reaction with PC as shown in Figure 1.10.

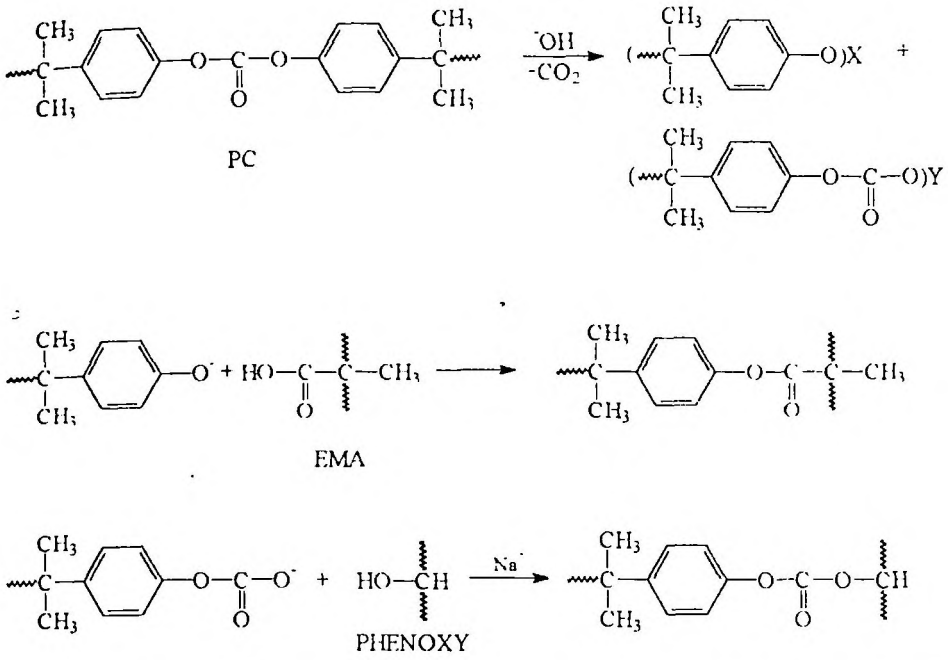

Figure 1.10. Reaction scheme for the formation of a graft copolymer between PC and ethylene-methacrylic acid, and phenoxy [Mascia and Valenza, *Adv. in Polym. Technol.*, **14**, 327 (1995)].

1.3.3 *Dynamic vulcanisation*

In recent years, crosslinking of rubber phase in thermoplastic elastomer blends during mixing has been investigated as a way to improve the properties of immiscible polymer blends. The dynamic crosslinking of TPEs generally leads to a fine and uniform distribution of rubber phase in the plastic matrix as shown in Figure 1.11.

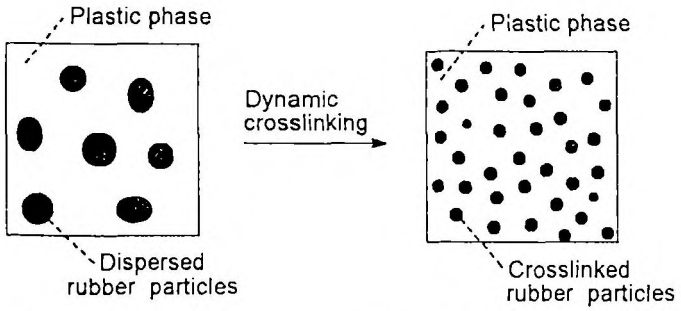

Figure 1.11. Schematic representation of the morphology of dynamic vulcanised thermoplastic elastomer.

Dynamic vulcanisation improves the mechanical properties and provides stable morphology. In dynamic vulcanised blends the size of the dispersed rubber particles depends on the extent of crosslink density and rubber concentration. The vulcanisation of rubber phase during mixing in various thermoplastic elastomers has been studied by different research groups.[96-107] One of the systems studied thoroughly among these is polypropylene/EPDM. As the dynamic vulcanised blends can be processed like thermoplastics, the researchers are interested in studying their rheological properties. Ha *et al.*[96] investigated the effect of blend ratio, curative concentration and type of dynamic vulcanisation on morphology, rheology and thermal properties of PP/EPDM blends. Two types of blending employed were (1) blend cure in which EPDM is cured in presence of PP during mixing and (2) cure-blend, here EPDM cured with dicumyl peroxide (DCP) in the absence of PP and then blended with PP. It was observed that the melt viscosity increased with DCP content for EPDM/PP-75/25 blend while in 25/75 blend it decreases in the case of blend cure. However, in the case of blend cure the melt viscosity increased at all compositions with DCP content. The decrease in viscosity in 25/75 EPDM/PP-blend cure was attributed to the degradation of PP in the presence of DCP. In 75/25 PP/EPDM blends, the crystallinity was higher than polypropylene homopolymer for both blend cure and cure blend samples. Such a crystallisation behaviour was attributed to the role of EPDM to selectively extract the defective molecules within PP crystals and also increase the mobility of neighbouring PP chains by reduction in glass transition temperature. The effect of crosslinking of PP/EPDM blends with a sulphur system with and without the compatibiliser was reported by Krulis *et al.*[100] The impact strength of PP/EPDM blends was significantly improved on dynamic vulcanisation. The extent of improvement in impact strength depends on the rate of cure (Figure 1.12).

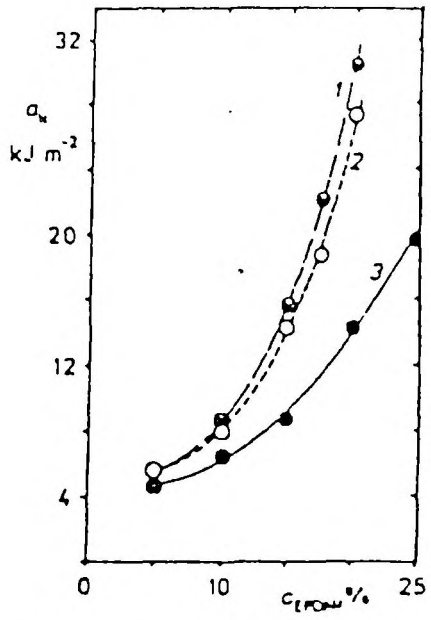

Figure 1.12. Dependence of the Charpy notched impact strength a_k at 0°C on rubber concentration c_{EPDM} for dynamically cured blends PP/EPDM-I (1) and PP/EPDM-II (2) and uncured blend PP/EPDM (3) [Krulis *et al.*, *Collect. Czech. Chem. Commun.*, **58**, 2642 (1993)].

In the curing of PP/EPDM blend with sulphur without tetramethyl thiuram disulphide (TMTD), the rate of cure is low compared to vulcanisation with TMTD formulation, and hence in the first case, long time will be obtained for the distribution of rubber particles and the coalescence of rubber phase was also blocked and led to high values of impact strength. In TMTD vulcanisation, there is a rapid start of curing reaction, and hence did not get time for fine dispersion of rubber particles which in turn reduced the impact strength.

Coran and Patel[102] investigated the properties of various dynamic vulcanised thermoplastic elastomers of NBR with polypropylene and polyamide. The curatives used were m-phenylene-bis-maleimide and dimethylol phenolic compounds as curatives. They reported that the dynamic vulcanisation of these blends improved the blend properties.

Recently Liao *et al.*[103] studied the damping behaviour of dynamically vulcanised polypropylene/butyl rubber (PP/IIR) blends and found that the damping behaviour depended on composition and curative levels. As the curative level in the blend increased the Tg corresponding to IIR shifts to high temperature region while that of PP remains constant Liao *et al.* have also analysed the applicability of PP/IIR dynamic vulcanised blends as interlayer in vibration damping laminates.[104] They reported that the incorporation of PP/IIR dynamic vulcanised blend as interlayer in laminates led to a decrease in G′ and increase in tan δ compared to maleated polypropylene based laminates.

Recently Inoue *et al.*[105,106] developed two crosslinking systems to selectively crosslink the dispersed unsaturated elastomers in saturated polyolefin matrices. One of the crosslinking systems developed comprised of N,N'-m-phenylene-bis-maleimide (PM) as the crosslinking agent and 6-ethoxy-2,2,4-trimethyl-1,2-dihydroquinoline (ETMQ) or polymerised 2,2,4-trimethyl-1,2-dihydroquinoline (PTMQ) as the activator. The PM/ETMQ and PM/PTMQ systems form charge transfer complexes to produce PM radicals and accelerates the crosslinking reaction. Another crosslinking system comprised of PM and 9,10-dihydrophenanthrene (DPH) as activator. Here the PM/DPH system acts as a hydrogen acceptor and hydrogen donor respectively and leads to the formation of PM radical by hydrogen transfer. The efficiency of these crosslinking systems was investigated for various blends such as PP/EPDM, PP/SBS, PP/SIS, PP/1,2 PB and PP/PE/EPDM. The impact strength of the blends increased upon dynamic vulcanisation. The morphology results indicated that during dynamic vulcanisation a graft copolymer between PP and elastomer is formed along with the crosslinking reaction of elastomer. This graft copolymer increased the interfacial adhesion and permits the interaction of stress concentration zones developed from the elastomer particles under deformation and promote shear yielding in PP matrix.

The development of blend morphology during *in-situ* crosslinking of dispersed phase was studied by Loor *et al.*[107] The *in-situ* crosslinking was carried out by transesterification reaction between ethylene vinyl acetate (EVA) and ethylene methyl acrylate (EMA) copolymers in presence of dibutyl tin oxide as catalyst. The matrix was polypropylene. The morphology of the resulting blend depends on the extent of reaction between EMA and EVA. The dimensions of dispersed particles are larger for the reactive (vulcanised) blends compared to nonreactive blends. As the reaction proceeds, the viscosity of dispersed phase increased due to the formation of EMA/EVA network and the break-up process was slowed down. Hence, though the coalescence of particles was modified, the particle size increased. However, the morphology of the reactive blends was stable as compared to that of nonreactive blend and showed only a small change in diameter during repeated extrusions. The investigation of the mechanical properties revealed that the impact strength and tensile strength of these blends improved upon reaction, which also indicated the formation of network in the blend.

1.4 Theories of compatibilisation

The diblock copolymers act as emulsifying agents in immiscible polymer blends like soap molecules at an oil water interface. The resulting properties of the blend depend on the ability of the copolymer to reduce the interfacial tension, which led to fine and uniform distribution of dispersed particles. Many theories have been developed in order to study the interfacial tension and particle size reduction upon the incorporation of copolymers into immiscible blends. Noolandi and Hong[24,108] have developed a theory for the interfacial tension reduction in highly incompatible polymer blends by considering the thermodynamic factors which determine the state of the block copolymers in a phase separated homopolymer system. According to them the entropy of mixing of block copolymers with the homopolymers favours a random distribution of the copolymers. Again the localisation of the block copolymers at the interphase

displaces the homopolymers away from each other and lowers the homopolymer enthalpy of mixing. The block copolymer-homopolymer enthalpy of mixing was also lowered by the preference of each block of copolymer to extend into its compatible homopolymer. The confinement of copolymer at the interface and restriction of the blocks in the respective homopolymer regions lead to a loss in entropy. Finally extension or compression of the copolymer chains as well as the effect of the excluded volume at the interphase lead to further loss of entropy. An equation for the interfacial tension of the four component system A/B/A-B/solvent was developed by Noolandi and Hong as[108]

$$\frac{\gamma}{\rho_0} = \int dx \left\{ \left(F_s'(x) - F_s(x)\right) + \frac{1}{6}\left(\chi_{AS}\sigma_{AS}^2 \frac{d\phi A}{dx}\frac{d\phi S}{dx} + \chi_{BS}\sigma_{BS}^2 \frac{d\phi B}{dx}\frac{d\phi S}{dx} + \chi_{AB}\sigma_{AB}^2 \frac{d\phi A}{dx}\frac{d\phi B}{dx} \right) \right\} \tag{1.4}$$

where $F_s'(x) = \chi_{AS}\phi_A(x) + \chi_{BS}\phi_B(x)\,\phi_S(x) + \chi_{AS}\phi_A(x)\,\phi_B(x) + \ln\phi_s(x)$

$$- [\chi_{AS}\phi_A(x)\phi_S(x) + \chi_{BS}\phi_B(x)\phi_S(x) + \chi_{AB}\phi_A(x)\phi_B(x)]$$

$$- \left[\phi_S(x) + \frac{\phi_{CA}(x)}{v_C} + \frac{\phi_{CB}(x)}{v_C} + \frac{\phi_{HA}(x)}{v_{HA}} + \frac{\phi_{HB}(x)}{v_{HB}} \right] \tag{1.5}$$

where γ - interfacial tension, ρ - density, χ - interaction parameter, ϕ - volume fraction, A and B stand for homopolymers, C for the copolymer and S for solvent.

The interfacial tension in PS/PBD/copolymer/styrene system was calculated using the above equation in order to study the effect of molecular weight and copolymer concentration by Noolandi and Hong. Figure 1.13 shows the variation of interfacial tension with increasing weight fraction of the block copolymer for various values of copolymer molecular weight. Increasing the molecular weight and copolymer concentration lead to a decrease in interfacial tension. The comparison of the interfacial density profiles for different points in the calculated curves shows that at higher molecular weights of copolymer blocks, the copolymer occupy most of the interphase region and the homopolymer have been displaced away from the interphase (Figure 1.14).

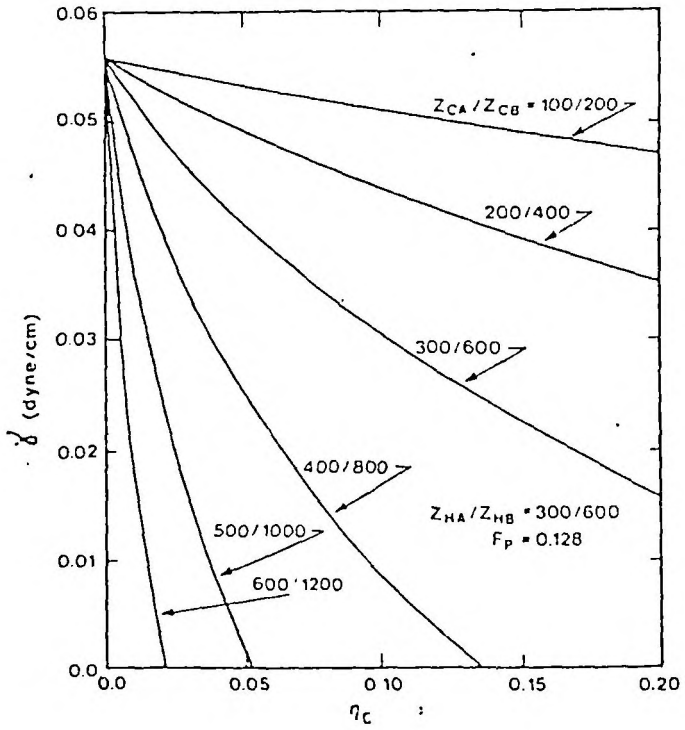

Figure 1.13. Calculations of interfacial tension for the PS-PBD-CopSBD-S system under the same conditions for the finite degrees of polymerisation of the polystyrene (HA) and polybutadiene (HB) homopolymers [Noolandi and Hong, *Macromolecules*, **15**, 482 (1982)].

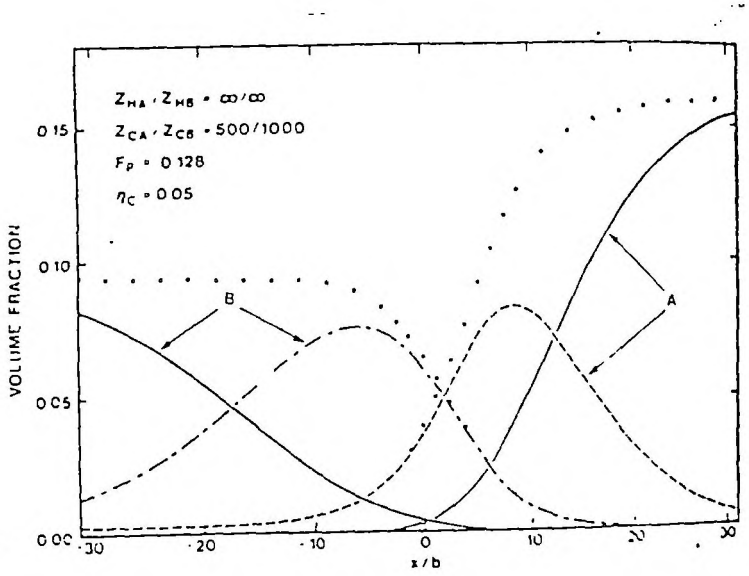

Figure 1.14. Interfacial density profiles with increased degrees of polymerisation of the polystyrene (CA) and polybutadiene (CB) blocks of the copolymer [Noolandi and Hong, *Macromolecules*, **15**, 482 (1982)].

Noolandi and Hong[24,109] derived an equation for the interfacial tension reduction in immiscible polymer blends (A/B) compatibilised with a block copolymer A-B. For a symmetric diblock copolymer, homopolymers of infinite molecular weight and a symmetric solvent the interfacial tension reduction $\Delta\gamma$, with increasing copolymer molecular weight and concentration arose mainly from the energetically preferred orientation of the blocks at the interphase so as to extend into their respective compatible homopolymers. According to Noolandi and Hong, the interfacial tension reduction in the presence of a solvent is given by

$$\Delta\gamma = d\phi_c \, 1/2 \, \chi \, \phi_p + 1/Z_c - 1/Z_c \exp\left(Z_c \chi \phi_p / 2\right) \qquad (1.6)$$

where d is the width at half height of the copolymer profile given by Kuhn statistical segment length, ϕ_c is the bulk volume fraction of the copolymer in the system; ϕ_p is the bulk volume fraction of polymer; χ is the Flory-Huggins interaction parameter between A and B segments of the copolymer and Z_c is the degree of polymerisation of the copolymer. According to this equation, the $\Delta\gamma$ depends on both molecular weight and concentration of copolymer In the absence of a solvent the total polymer volume fraction ϕ_p goes to 1 and the equation for $\Delta\gamma$ reduces to

$$\Delta\gamma = d\phi_c \, 1/2 \, \chi + 1/Z_c - 1/Z_c \exp\left(Z_c \chi / 2\right) \qquad (1.7)$$

As the derivation of equation arises from the assumption of preferential location of the copolymer at the interphase, at higher concentrations of copolymer, i.e., above critical micelle concentration (CMC) where the copolymer forms micelles in the bulk phase, rather than located at the interphase, the above equation is not valid.

Anastasiadis *et al.*[110] testified the thermodynamic theories of Noolandi and Hong for PS/1,2-polybutadiene/poly(styrene-block-1,2-butadiene) system. The authors investigated the reduction in interfacial tension between PS and PB by varying the concentration of copolymer. The results showed that the interfacial

tension decreased sharply with copolymer at lower loadings and at higher loading a levelling off was observed due to interfacial saturation. The comparison of the data with Noolandi's theory indicates that the interfacial tension reduction ($\Delta\gamma$) varies linearly with copolymer concentration below CMC as predicted by Noolandi and Hong (Figure 1.15).

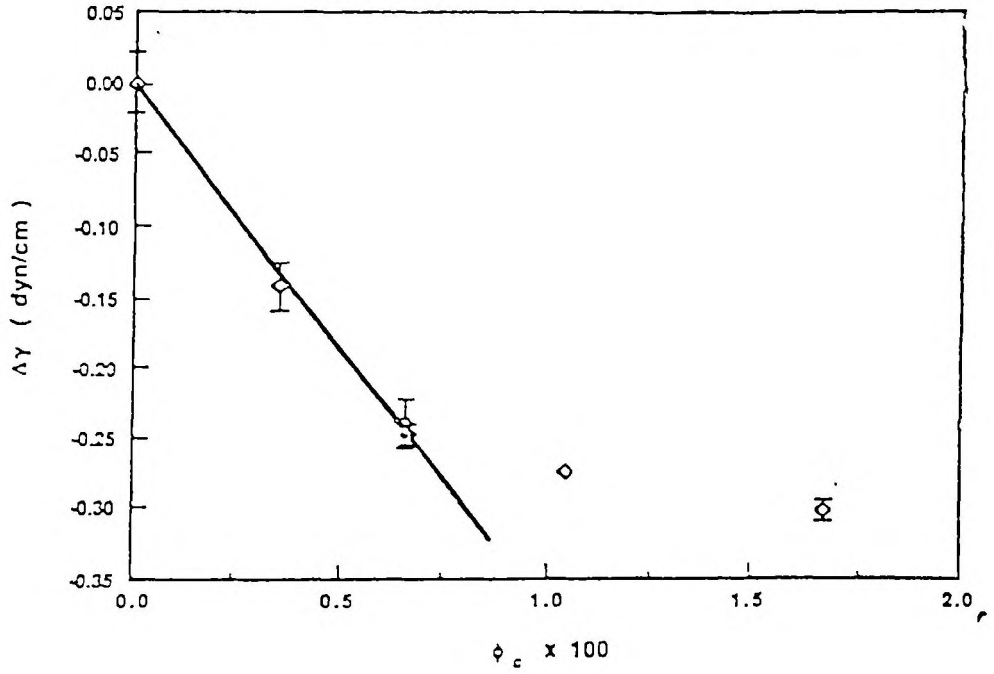

Figure 1.15. Interfacial tension reduction vs. copolymer volume fraction for the system PS/PB/P(S-b-B) at 145°C [Anastasiadis *et al.*, *Macromolecules*, **22**, 1449 (1989)].

Leibler[111] developed a simple mean field formalism for the interfacial properties of nearly compatible blend A/B compatibilised with A-B block copolymer. In nearly miscible blends, the copolymer plays an important emulsifying role. The addition of copolymers first displaces the critical point of demixing and may even cause a two phase blend to become one phase. Second the copolymer chains are present in both phases of the blend and favour a closer mixing of the chemical species A and B. Leibler calculated the interfacial

concentration profile and interfacial tension in these systems. According to Leibler, for nearly compatible species [$2 < \chi N < 4\ (2)^{1/2}$] two mechanisms of interfacial activity of copolymer chains are to be distinguished, i.e., (i) the species A and B are closely mixed as copolymer chains are present in both phases and (ii) copolymers have a certain tendency to locate at the interface. The interfacial tension γ may be expressed as

$$\gamma = \gamma_0 - \gamma_i \quad . \tag{1.8}$$

Here γ_0 represents the interfacial energy arises due to the first mechanism and γ_I represents the decrease in interfacial tension arises due to second mechanism.

Later Leibler[112] developed a theory for the reduction in interfacial tension in terms of molecular parameters of homopolymers and copolymers (molecular weight, copolymer composition, incompatibility degree) and of the concentration of copolymer molecules accumulated at the interface for the incompatible blends. Leibler calculated the interfacial tension reduction induced by the adsorption of the copolymers and is given as

$$\frac{a^2\Delta\gamma}{KT} = \left(\frac{3}{4}\right)^{1/3} (\Sigma/a^2)^{-5/3} (N_A P_A^{-2/3} + N_B P_B^{-2/3}) \tag{1.9}$$

for long copolymers and

$$\frac{a^2\Delta\gamma}{KT} = 3\ (\Sigma/a^2)^{-3} N \tag{1.10}$$

for short copolymer molecules ($N_I < P_I^{2/3}$) and $\Sigma < N^{1/2}$ where $\Delta\gamma$ is the interfacial tension reduction; Σ, the interfacial area per copolymer joint; P_A and P_B, the degree of polymerisation of homopolymers A and B respectively; a, the monomer length; N_A and N_B, the degree of polymerisation of copolymer segments A and B, respectively.

The longer copolymers are found to be more effective than shorter ones for the same surface area perchain. At equilibrium, the number of adsorbed

copolymers is determined by a competition between enthalpic effects which tend to reduce the overall number of A-B contacts in the system and the loss of entropy associated with an accumulation of chains at the interface.

Lomellini *et al.*[113] have developed an equation for the calculation of minimum amount of block copolymer needed to saturate the interface in the melt mixing of immiscible polymer blends. The saturation point is considered as the point where the dispersed phase size is no longer significantly dependent on the amount of interfacial agent. For the calculation of saturation concentration, the authors assume the geometrical model of one phase (phase B) dispersed in the continuous matrix of phase A in the form of particles with radius R and an A-B block copolymer where A and B denotes chemical identity or chemical affinity for the two phases and assume a geometrically sharp interface (Figure 1.16).

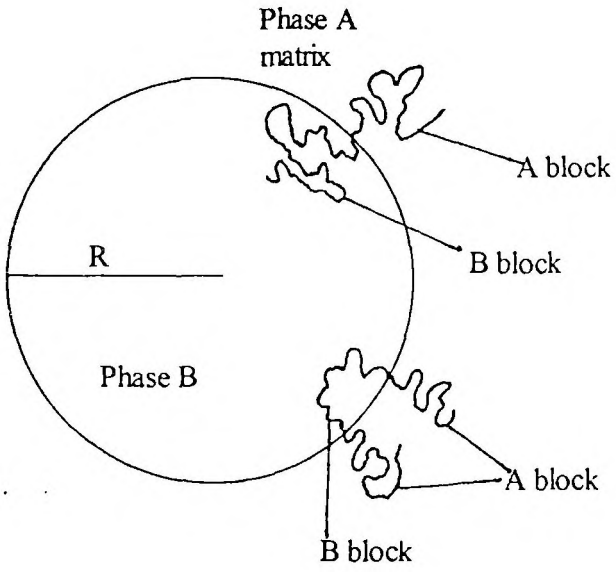

Figure 1.16. Block copolymer in an immiscible blends with spherical domains the case of an A-B diblock and A-B-A triblock copolymer at the interfacial region [Lomellini *et al.*, *Polymer*, **37**, 5689 (1996)].

At interfacial saturation it is assumed that the particle surface being homogeneously covered with a given level of A blocks to make a stable colloidal dispersion of B particles in the A matrix. It is also assumed that there is no adsorption of A blocks into the dispersed particle surface. The authors estimated the critical concentration of block copolymers required to saturate the interface per unit volume (C_{cr}) of dispersed phase as

$$C_{cr} = k \frac{\pi R^2}{Rg^2} \frac{M_A}{N_{AVO}} \frac{1}{\frac{4}{3}\pi R^3} \frac{1}{\rho_{bc} WA} = \frac{3kM_A}{4R_g^2, RN_{AVO}} \frac{1}{\rho_{bc} W_A} \qquad (1.11)$$

where R_g is the radius of gyration of A block; M_A, the molecular weight of the A block; and ρ_{bc}, the block copolymer density.

The critical volume fraction (V_{Fcr}) of block copolymer normalised unit volume of the blend is given by

$$V_{Fcr} = \frac{1}{\rho_{bc} W_A} \frac{3kM_A}{4R_g^2 N_{AVO}} \frac{\phi}{R} \qquad (1.12)$$

where ϕ is the volume fraction of dispersed phase.

According to this model, the critical amount of copolymer required to saturate the interface depends on the interfacial area and composition of copolymer and not on molecular weight.

1.5 Scope and objectives of the work

Thermoplastic elastomers from blends of isotactic polypropylene (iPP)/acrylonitrile-co-butadiene rubber (NBR) combine the oil resistant properties of nitrile rubber and the excellent processability characteristics and mechanical properties of polypropylene. These can be successfully used for high temperature oil resistant applications. However these blends are found to be incompatible and immiscible. They are characterised by a sharp interface, coarse morphology and

poor physical and chemical interactions across the phase boundaries. Hence it is necessary to improve the compatibility of these blends in order to use them for practical applications. It has been found that the compatibilisation and dynamic vulcanisation of immiscible blends lead to better compatibility and properties. However, till date no systematic studies have been made on the compatibilisation and dynamic vulcanisation of PP/NBR blends. Although some studies have been reported on the thermodynamics, structural properties and compatibilisation of NBR/PP blends, detailed investigation relating morphology to the properties and compatibilising efficiency to the nature and concentration of the copolymer are lacking.[114,115] In this thesis an attempt has been made to investigate systematically, the effect of compatibilisation and dynamic vulcanisation on the morphology and properties of PP/NBR blends. The important objectives of the work are given below.

1.5.1 Morphology and mechanical properties

The investigation of mechanical properties of raw materials is important in order to design products for various application since these materials usually undergo various types of deformation during service. It was found that the properties of polymer blends are strongly depended on the blend morphology. Hence the morphology and mechanical properties like tensile strength, modulus, tear strength , tensile impact strength, etc. of PP/NBR blends have been studied. The analysis of morphology and mechanical properties indicated that the PP/NBR blends are immiscible. Hence the properties of these blends have been improved by compatibilisation and dynamic vulcanisation. The effect of compatibiliser concentrations on the morphology and properties was investigated. Two types of compatibilisers, i.e., maleic anhydride modified polypropylene and dimethylol phenolic modified polypropylene have been used for the studies. The experimental results have been compared with theoretical predictions. The variation in morphology and mechanical properties upon dynamic vulcanisation was also investigated. The vulcanising systems used were sulphur, peroxide and a mixed

system comprised of sulphur and peroxide. Finally, the effect of addition of fillers such as carbon black, cork, silica and treated silica on the mechanical properties was studied.

1.5.2 *Dynamic mechanical properties*

As the polymeric materials usually undergo cyclic stressing during various applications, the investigation of dynamic mechanical properties is important. Dynamic mechanical investigations can be used to predict the miscibility of the blends. The viscoelastic properties like storage modulus, loss modulus and tan δ of PP/NBR blends were investigated with special reference to the effect of blend ratio, compatibiliser loading and dynamic vulcanisation. The properties were correlated with blend morphology. The experimental storage modulus was compared with various theoretical predictions.

1.5.3 *Rheological properties*

The investigation of the rheological properties over a wide range of shear rate and temperature is important in order to optimise the processing conditions like temperature, shear rate, time of flow, etc. required for each blend. Hence the melt rheology of PP/NBR blends was investigated for the uncompatibilised, compatibilised and dynamically vulcanised blends. The compatibiliser concentration was varied in these studies. The effect of shear rate and temperature on the melt viscosity was studied, and time-temperature superposition master curves have been constructed. The melt viscosity values were correlated with melt flow index values. The extrudate morphology of these blends was also investigated. Finally, the effect of annealing on the morphology of uncompatibilised and compatibilised blends was studied.

1.5.4 Thermal properties and crystallisation behaviour

For the development of durable industrial products it is necessary to study the thermal stability of polymeric materials. Hence the thermal stability of PP/NBR blends was investigated with special reference to the effect of blend ratio, compatibilisation and dynamic vulcanisation using thermogravimetric analysis. In polymer blends with a crystallisable component, the final properties strongly depend on the crystalline structure and crystallinity of the blends. The crystallisation behaviour of PP/NBR blends was investigated using differential scanning calorimetry and wide angle X-ray scattering technique.

1.5.5 Electrical properties

Polypropylene possess excellent insulating properties. Hence it is important to study the electrical properties of PP/NBR blends in order to explore the possibility of using these materials in insulating applications. The dielectric properties like volume resistivity, dielectric constant, loss factor and dissipation factor of PP/NBR blends were investigated for the uncompatibilised and dynamic vulcanised blends. The effect of fillers on the dielectric behaviour was also studied. The experimental dielectric constant values were compared with various theoretical predictions.

1.5.6 Transport properties

The investigation of the transport properties of PP/NBR blends is important, since it is possible to use these materials in various barrier applications due to their solvent resistant properties. The sorption and diffusion of various aromatic solvents through PP/NBR blends were investigated. The effects of blend ratio, type of crosslinking system, i.e., sulphur, peroxide or mixed system and fillers on transport were studied. The activation energy and thermodynamic parameters for diffusion has been calculated. Finally the experimental results were compared with theoretical predictions.

1.6 References

1. B M Walker (Ed.), *Hand Book of Thermoplastic Elastomers*, Van Nostrand Reinhold, New York, 1979.
2. N R. Legge, G. Holden and H. E. Schoeder (Eds.), *Thermoplastic Elastomers--A Comprehensive Review*, Hanser Publishers, Munich, 1987.
3. S. K. De and A. K. Bhowmick (Eds.), *Thermoplastic Elastomers from Rubber-Plastic Blends*, Ellis Horwood, New York, 1990.
4. A. K. Bhowmick and H. L. Stephen (Eds.), *Hand Book of Elastomers- New Development and Technology*, Marcel Dekker, New York, 1988.
5. D. R. Paul and S. Newman (Eds.), *Polymer Blends*, Academic Press, New York, 1978.
6. O. Olabisi, L. M. Robeson and M. T. Shaw, *Polymer-Polymer Miscibility*, Academic Press, New York, 1978.
7. A. Y. Coran, *Hand Book of Elastomers—New Developments and Technology* (Eds., A. K. Bhowmick and H. L. Stephen), Marcel Dekker, New York, 1988, p. 249.
8. B. Pukanszky and F. H. J. Maurer, *Polymer*, **36**, 1617 (1995).
9. C. Qin, J. Yin and B. Huang, *Rubber Chem. Technol.*, **63**, 77 (1989).
10. A. L. Nazareth da Silva and F. M. B. Coutinho, *Polymer Testing*, **15**, 45 (1996).
11. B. Kuriakose and S. K. De, *Polym. Eng. Sci.*, **25**, 630 (1985).
12. S. Thomas, *Mater. Lett.*, **5**, 360 (1987).
13. D. IL. Kang, C. S. Ha and W. J. Cho, *Eur. Polym. J.*, **28**, 565 (1992).
14. K. T. Varughese, *J. Appl. Polym. Sci.*, **39**, 205 (1990).
15. P. Potschke, K. Wallheinke, H. Fritsche and H. Stutz, *J. Appl. Polym. Sci.*, **64**, 749 (1997).
16. G. D. Choi, W. H. Jo and H. G. Kim, *J. Appl. Polym. Sci.*, **59**, 443 (1996).
17. B. D. Favis and J. M. Willis, *J. Polym. Sci. B. Polym. Phys.*, **28**, 2259 (1990).
18. B. D. Favis, *J. Appl. Polym. Sci.*, **39**, 285 (1990).
19. S. Danesi and R. S. Porter, *Polymer*, **19**, 448 (1978).
20. K. T. Varughese, G. B. Nando, P. P. De and S. K. De, *J. Mater. Sci.*, **23**, 3894 (1988).
21. B. Ohlsson, H. Hassander and B. Tornell, *Polym. Eng. Sci.*, **36**, 501 (1996).
22. B. K. Kim, G. S. Shin, Y. T. Kim and T. S. Park, *J. Appl. Polym. Sci.*, **47**, 1581 (1993).

23. T Nomura, T. Nishio, T. Fujii, J Sakai, M. Yamamoto, A. Uemura and M. Kakugo, *Polym. Eng. Sci.*, **35**, 1261 (1995).

24. J. Noolandi, *Polym. Eng. Sci.*, **24**, 70 (1984).

25. D. R. Paul and G. W. Barlow, *ACS Adv. Chem. Ser.*, **176**, 315 (1979).

26. M. Xanthos, *Polym. Eng. Sci.*, **28**, 1392 (1988).

27. D. Braun, M. Fischer and G. P. Hellman, *Polymer*, **37**, 3871 (1996).

28. D. R. Paul, in *Polymer Blends* (Eds., D. R. Paul and S. Newman), Academic Press, New York, 1978, Ch. 12.

29. G. E. Molau, *J. Polym. Sci.*, **A3**, 1267 (1965).

30. G. E. Molau and W M Wittbrodt, *Macromoleules*, **1**, 260 (1968).

31. G. Riess, J. Kohler, C. Tournut and A. Banderet, *Makromol. Chem.*, **101**, 58 (1967).

32. G. Riess, J. Kohler, C. Tournut and A. Banderet, *Eur. Polym. J.*, **4**, 187 (1968).

33. P. Gailard, M. Ossenbach-Sauter and G. Riess, *Makromol. Chem. Rapid Commun.*, **1**, 771 (1980).

34. P. Gailard, M. Ossenbach-Sauter and G. Riess, in *Polymer Compatibility and Incompatibility: Principles and Practice* (Ed., K. Sole), MMI Symposium Series2, Harwood, New York, 1982.

35. H. T. Patterson, K. H. Hu and T. H. Grindstaff, *J. Polym. Sci. C*, **34**, 31 (1971).

36. C. R. Lindsey, D. R. Paul and J. W. Barlow, *J. Appl. Polym. Sci.*, **26**, 1 (1981).

37. M. C. Schwarz, J. W. Barlow and D. R. Paul, *J. Appl. Polym. Sci.*, **37**, 403 (1989).

38. S. Thomas and R. E. Prud'homme, *Polymer*, **33**, 4260 (1992).

39. C. W. Macosko, P. Guegan, A. K. Khandpur, A. Nakayama, P. Marechal and T. Inoue, *Macromoleules*, **29**, 5590 (1996).

40. Z. Oommen, M. R. Gopinathan Nair and S. Thomas, *Polym. Eng. Sci.*, **36**, 1 (1996).

41. R. Asaletha, M. G. Kumaran and S. Thomas, *Rubber Chem. Technol.*, **68**, 671 (1995).

42. M. Yoshida, J. J. Ma, K. Min, J. L. White and R. P. Quirk, *Polym. Eng. Sci.*, **30**, 30 (1990).

43. C. K. Park, C. S. Ha, J. K. Lee and W. J. Cho, *J. Appl. Polym. Sci.*, **50**, 1239 (1993).

44. D. G. Peiffer and M. Rabeony, *J. Appl. Polym. Sci.*, **51**, 1283 (1994).

45. J. Heuschen, J. M. Vion, R. Jerome, Ph. Teyssie, *Polymer*, **31**, 1473 (1990).

46. C. Creton, H. R. Brown and V. R. Deline, *Macromolecules*, **27**, 1774 (1994).

47. C Auschra, R. Stadler, *Macromolecules*, **26**, 6364 (1993).

48. H. C. Kim, K. H. Nam and W. H. Jo, *Polymer*, **34**, 4043 (1993).

49. H. Eklind, S. Schantz, F. H. J. Maurer, P. Jannasch and B. Wesslen, *Macromolecules*, **29**, 984 (1996).

50. E. Navaratilova and I. Fortenly, *Polym. Networks Blends*, **6**, 127 (1996).

51. M. Matos, B. D. Favis and P. Lomellini, *Polymer*, **36**, 3899 (1995).

52. B. Boutevin, M. Khamlichi, Y. Pietrasanta and J. J. Robin, *Polym. Bullet.*, **34**, 117 (1995).

53. T. K. Kwei, H. C. Frisch, W. Radigan and S. Vogel, *Macromolecules*, **10**, 157 (1977).

54. S. Klotz and H. J. Cantow, *Polymer*, **31**, 315 (1990).

55. D. Rigby, J. L. Lin and R. J. Roe, *Macromolecules*, **18**, 2269 (1985).

56. C. del Rio and J. L. Acosta, *Polym. International*, **30**, 47 (1993).

57. C. J. T. Landry, H. Yang and J. S. Machell, *Polymer*, **32**, 44 (1991).

58. S. N. Koklas, D. D. Sotiropoulou, J. K. Kallitsis and N. K., Kalfoglou, *Polymer*, **32**, 66 (1991).

59. J. M. Machado and C. S. Lee, *Polym. Eng. Sci.*, **34**, 59 (1994).

60. P. P. Lizymol and S. Thomas, *Thermochemica Acta*, **233**, 283 (1994).

61. K. Hausmann, *Proceedings of 3rd International Conference on Advances in Additives and Modifiers in Polymer and Blends*, F1, 1994.

62. J. P. Sang, K. K. Byung and M. J. Han, *Eur. Polym. J.*, **26**, 131 (1990).

63. W. E. Baker and M. Saleem, *Polymer*, **28**, 2057 (1987).

64. F. Ide and A. J. Hasegawa, *J. Appl. Polym. Sci.*, **18**, 963 (1974).

65. N. R. Choudhury and A. K. Bhowmick, J. Appl. Polym. Sci., **38**, 1091 (1989).

66. P. Cheung, D. Suwanda and S. T. Balke, *Polym. Eng. Sci.*, **30**, 1063 (1990).

67. E. Mori, B. Pukanszky, T. Kelen and F. Tudos, *Polym. Bullet.*, **12**, 157 (1984).

68. V. P. Ballegooie and A. Rudin, *Polym. Eng. Sci.*, **28**, 21 (1988).

69. J. M. Willis and B. D. Favis, *Polym. Eng. Sci.*, **30**, 1073 (1990).

70. J. D. Lee and S. M. Yang, *Polym. Eng. Sci.*, **35**, 1821 (1995).

71. J. Rosch and R. Mulhaupt, *J. Appl. Polym. Sci.*, **56,** 1599 (1995).

72. A. Haddout, J. Villoutreix and G. Villoutreix, *International Polym. Process.*, **10**, 1 (1995).

73. S. S. Dagli, M. Xanthos and J. A. Beissenberger, *Polym. Eng. Sci.*, **34**, 1720 (1994).

74. A. Valenza and D. Acierno, *Eur. Polym. J.*, **30**, 1121 (1994).

75. N. C. Liu, H. Q. Xie and W. E. Baker, Polymer, **34**, 4680 (1993).

76. C J. Wu, J. F. Kuo and C. Y. Chen, *Polym. Eng. Sci.*, **33**, 1329 (1993).

77. R. M. H. Miettinen, J. V. Seppala, O. T. Ikkala and I. T. Riema, *Polym. Eng. Sci.*, **34**, 395 (1994).

78 S Horiuchi, N. Matchariyakul, K. Yase and T. Kitano, *Macromoleucles*, **30**, 3664 (1997).

79. R Greco, M. Maliconico, E. Martuscelli, G. Ragosta and G. Scarinzi, *Polymer*, **28**, 1185 (1987).

80. C. E. Scott and C. W. Macosko, *Polymer*, **36**, 461 (1995)

81. H. Kanai, V. Sullivan and A. Auerbach, *J. Appl. Polym. Sci.*, **53**, 527 (1994).

82. M. Abbate, E. Martuscelli, G. Ragosta and G. Scarinzi, *J. Mater. Sci.*, **26**, 1119 (1991).

83. R. M. H. Miettinen, M. T. Heino and J. V. Seppala, *J. Appl. Polym. Sci.*, **57**, 573 (1995).

84. S. H. Chen and F. C. Chang, *J. Appl. Polym. Sci.*, **51**, 955 (1994).

85. P. Ramesh and S. K. De, *J. Appl. Polym. Sci.*, **50**, 1369 (1993).

86. Z. Horak, Z. Kulis, J. Baldrian, I. Fortenly and D. Konecny, *Polym. Networks Blends*, **7**, 43 (1997).

87. R. N. Santra, B. K. Samantaray, A. K. Bhowmick and G. B. Nando, *J. Appl. Polym. Sci.*, **49**, 1145 (1993).

88. J. R. M. Duhaime and W. E. Baker, *Plast. Rubber Comp. Proc. Appl.*, **15**, 87 (1991).

89. L. K. Yoon, L. H. Choi and B. K. Kim, *J. Appl. Polym. Sci.*, **56**, 239 (1995)

90. C. Els and W. J. McGill, *Plast. Rubber Comp. Proc. Appl.*, **21**, 115 (1994).

91. P. R. Hornsby and J. F. Tung, *Plast. Rubber Comp. Proc. Appl.*, **24**, 69 (1995).

92. Y. Kim, C. S. Ha, T. K. Kang, Y. Kim and W. J. Cho, *J. Appl. Polym. Sci.*, **51**, 1453 (1994).

93. M. Joshi, S. N. Maiti and A. Misra, *J. Appl. Polym. Sci.*, **45**, 1837 (1992).

94. L. Mascia and A. Valenza, *Adv. in Polym. Technol.*, **14**, 327 (1995).

95. S. Fellahi, B. Fisa and B. D. Favis, *J. Appl. Polym. Sci.*, **57**, 1319 (1995).

96. C. S. Ha and S. C. Kim, *J. Appl. Polym. Sci.*, **35**, 2211 (1988).

97. C. S. Ha and S. C. Kim, *J. Appl. Polym. Sci.*, **37**, 317 (1989).

98. C. S. Ha, D. J. Ihm and S. C. Kim, *J. Appl. Polym. Sci.*, **32**, 6281 (1986).

99 D J. Ihm, C S Ha and S. C. Kim, *Polymer (Korea)*, **12**, 249 (1988).

100 Z Krulis, I. Fortelny and J. Kovar, *Collect. Czech. Chem. Commun.*, **58**, 2642 (1993)

101 P. K Han and J. L. White, *Rubber Chem. Technol.*, **68**, 728 (1995).

102. A. Y. Coran and R. Patel, *Rubber Chem. Technol.*, **54**, 892 (1981b).

103. F. S. Liao, A. C. Su and T. C. J. Hsu, *Polymer*, **35**, 2579 (1994).

104. F. S. Liao, T. C. J. Hsu and A. C. Su, *J. Appl. Polym. Sci.*, **48**, 1801 (1993).

105. T. Inoue, *J. Appl. Polym. Sci.*, **54**, 709 (1994).

106. T. Inoue, *J. Appl. Polym. Sci.*, **54**, 723 (1994).

107. A. De Loor, P. Cassagnau, A. Michel and B. Vergnes, *J. Appl. Polym. Sci.*, **63**, 1385 (1997).

108. J. Noolandi and K. M. Hong, *Macromolecules*, **15**, 482 (1982).

109. J. Noolandi and K. M. Hong, *Macromolecules*, **17**, 1531 (1984).

110. S. H. Anastasiadis, I. Gancarz and J. T. Koberstein, *Macromolecules*, **22**, 1449 (1989).

111. L. Leibler, *Macromolecules*, **15**, 1283 (1982).

112. L. Leibler, *Makromol. Chem. Macromol. Symp.*, **16**, 1 (1988).

113. P. Lomellini, M. Matos and B. D. Favis, *Polymer*, **37**, 5689 (1996).

114. A. Y. Coran and R. Patel, *Rubber Chem. Technol.*, **56**, 1045 (1983).

115. R. Frenkel, V. Duchacek, T. Kirillove, and E. Kuzmin, *J. Appl. Polym. Sci.*, **34**, 1301 (1987).

Chapter 2

Experimental

2.1 Materials used

Isotactic polypropylene (PP) (Koylene M3060) having MFI of 3 g/10 min was supplied by IPCL, Vadodara, India. Nitrile rubber (NBR) having 32% acrylonitrile content was supplied by Synthetics and Chemicals, Bareli, U.P., India.

Maleic modified polypropylene (MA-PP) was prepared by melt mixing polypropylene with maleic anhydride (5 parts), benzoquinone (0.75 parts) and dicumyl peroxide (3 parts) in a Brabender Plasticorder at 180°C.[1] Phenolic modified polypropylene (Ph-PP) was prepared by melt mixing polypropylene with dimethylol phenolic resin [SP-1045 (4 parts)], and stannous chloride (0.8 parts) at 180°C.[1]

The fillers used were HAF (N 330), silane, treated silica and cork powder. The treated silica was prepared by the treatment of silica (100 g) with Union Carbide A174 silane coupling agent (5 g).

2.2 Blend preparation

The blends of isotactic polypropylene with nitrile rubber were prepared by melt mixing PP with NBR in a Brabender Plasticorder (model PLE-330) at a temperature of 180°C. The rotor speed was 60 rev.min^{-1} and the blending was carried out for 6 min. In the case of binary blends, PP was first melted for 2 min in the chamber and then NBR was added and mixing continued for another 6 min. In the case of compatibilised blends, the compatibilisers were added prior to the

addition of NBR. The compatibiliser concentrations were varied from 1 to 15 wt %. The binary blends are designated as P_{100}, P_{70}, P_{50}, P_{30} and P_0, where the subscripts denote the weight percentage of PP in the blend. The Ph-PP and MA-PP compatibilised PP/NBR blends are designated as PP_{70x} and PM_{70x}, respectively where x denotes the weight percentage of compatibiliser in the blend. The dynamic vulcanisation of the blends was done by using three crosslinking systems, viz., sulphur, peroxide and a mixed system consisting of sulphur and peroxide. The formulation of the dynamic vulcanised blends is shown in Table 2.1. The PP/NBR blends vulcanised with sulphur, peroxide and mixed system are designated as PS_x, PC_x and PM_x, respectively where x denotes the weight percentage of PP in the blends. The filled PP/NBR blends were prepared using different fillers, viz., carbon black, cork, silica and silane treated silica. The filler loading was varied between 10 to 30 phr. The filled blends are designated as P_xC_y, P_xK_y, P_xS_{iy} and P_xTs_{iy} for carbon black, cork, silica and silane treated silica filled blends respectively. In this x denotes the weight percentage of PP and y denotes that of filler in the blend. In the case of dynamic vulcanised and filled blends, the amount of vulcanising agents and filler were taken with reference to the rubber phase, i.e., NBR only.

Table 2.1. Formulation of dynamic vulcanised blends.

Sample	PS_{70}	PC_{70}	PM_{70}	PS_{50}	PC_{50}	PM_{50}	PS_{30}	PC_{30}	PM_{30}
PP	70	70	70	50	50	50	30	30	30
NBR	30	30	30	50	50	50	70	70	70
Sulphur	0.2	-	0.1	0.2	-	0.1	0.2	-	0.1
DCP*	-	2	1	-	2	1	-	2	1
TMTD**	2.5	-	2.5	2.5	-	2.5	2.5	-	2.5
CBS***	2	-	2	2	-	2	2	-	2
Zinc oxide	5	-	5	5	-	5	5	-	5
Stearic acid	2	-	2	2	-	2	2	-	2

**Dicumyl peroxide, **Tetramethyl thiuram disulphide, ***N-cyclohexyl benzothiazyl sulphenamide.*

2.3 Physical testing of the samples

The samples for physical property measurements were prepared by compression moulding the mixes at 180°C in a hydraulic press in to 15 x 15 x 0.15 cm size sheets. The tensile property measurements were done on a Zwick Universal Testing machine (Model 1474) using dumb-bell shaped specimens at a crosshead speed of 500 mm/min. in accordance with ASTM D412-81. The tear strength of the samples was determined using unnicked 90° angle test pieces at a cross head speed of 500 mm/min in a Zwick Universal Testing machine in accordance with ASTM D624-81. Tensile impact strength of the samples was measured on a Ceast Impact Tester (Model 6545/000) using dumb-bell shaped specimen. Hardness values of the samples were measured using shore A and shore D Hardness Durometer.

2.4 Morphology studies

The samples for morphology studies were prepared by cryogenic fracturing of the samples in liquid nitrogen. The fractured end of the samples were kept immersed in chloroform for two weeks. The samples were then dried in an oven. For morphology studies, samples (NBR phase was preferentially extracted) were sputter coated with gold and the photographs were taken in a JEOL scanning electron microscope. The domain size was measured from the SEM photomicrographs. Several micrographs were taken for each blend and about 300 domains were taken for number average domain diameter measurements. The apparent number, weight and surface area average domain diameter was obtained from the measurements of hole diameter obtained as a result of the extraction of the rubber phase.

2.5 Dynamic mechanical testing

Dynamic mechanical properties of the blends were measured using a Rheovibron DDV-II at a frequency of 35 Hz. Compression moulded samples of dimensions 5 x 0.5 x 0.05 cm were used for testing. The temperature range used was -50 to +150°C.

2.6 Rheological measurements

Rheological measurements were done in an Instron capillary rheometer (Model 3211) at different plunger speeds. The plunger speed was varied from 0.06 to 20 cm/min. The melt was extruded through the capillary at predetermined plunger speeds after a warm up period of 5 min. The measurements were done at a temperature of 200°C. For studying the effect of temperature, the samples P_{100}, P_{70}, PP_{7010} and P_0 were analysed at 190, 200 and 210°C.

The true shear rate $\dot{\gamma}$ was calculated from the apparent shear rate ($\dot{\gamma}_{wa}$) from the following equation

$$\dot{\gamma} = \left(\frac{3n'+1}{4n'}\right)\dot{\gamma}_{wa} \tag{2.1}$$

n' - the flow behaviour index is defined as

$$n' = \frac{d(\log \tau_w)}{d(\log \dot{\gamma}_{wa})} \tag{2.2}$$

and was determined by regression analysis.

The shear viscosity, η, was calculated using the equation

$$\eta = \frac{\tau_w}{\dot{\gamma}_w} \tag{2.3}$$

2.7 Determination of MFI

Melt flow index (MFI) was determined using melt flow indexer, Tinius Olsen, USA (Model), MP993, with 3.26 kg load. The measurements were made at a temperature of 200°C.

2.8 Extrudate swell

The extrudates were carefully collected as these emerged out from the capillary die, taking care to avoid any deformation. The diameter of the extrudate was measured after 24 h. The die swell was calculated using the equation d_e/d_c where d_e is the diameter of the extrudate and d_c is the diameter of the capillary.

2.9 Extrudate morphology

The morphology of the extrudates was analysed using scanning electron microscope. The samples for morphology measurement were prepared by cryogenically fracturing the samples in liquid nitrogen. The NBR phase was preferentially extracted using chloroform.

2.10 Determination of crosslink density

The molar mass between crosslinks (M_c) crosslinks of dynamic vulcanised samples was measured by equilibrium swelling method using the equation[2]

$$M_c = \frac{-\rho_p V_s \phi^{1/3}}{[\ln(1-\phi)+\phi+\chi\phi^2]} \qquad (2.4)$$

where ρ_p is the density of polymer; V_s, the molar volume of solvent; and ϕ, the volume fraction of swollen rubber which is given by

$$\phi = \frac{(d-fw)\rho_p^{-1}}{(d-fw)\rho_p^{-1} + A_s\rho_s^{-1}} \qquad (2.5)$$

where d is the deswollen weight of the sample; f, the volume fraction of filler; w, the initial weight of the sample, ρ_s, the density of solvent, and A_s, the amount of solvent absorbed. The interaction parameter χ is given by

$$\chi = \beta + (V_s/RT)(\delta_s - \delta_p)^2 \quad (2.6)$$

where β is the lattice constant (0.34); V_s, the molar volume of solvent; R, the gas constant; and T, the temperature in °K and δ_s and δ_p the solubility parameters of solvent and polymer respectively. The crosslink density (ν) was measured from M_c as

$$\nu = 1/2M_c \quad (2.7)$$

2.11 Thermogravimetric analysis

The thermogravimetry (TGA) and derivative thermogravimetry (DTG) were carried out in a Delta Series TGA7. The samples were scanned from 30 to 600°C at a heating rate of 10°C/min in nitrogen atmosphere.

2.12 Differential scanning calorimetry

The melting behaviour and crystallinity of PP/NBR blends were studied using a Perkin Elmer DSC thermal analyser. The samples were scanned at a heating rate of 10°C/min in nitrogen atmosphere. The weight percentage crystallinity of PP and blends was determined using DSC from the ratio of the heat of fusion of the blend to that of 100% crystalline PP (ΔH_{pp} = 138 Jg^{-1}).[3]

2.13 Wide angle X-ray scattering

The crystallisation behaviour of PP/NBR blends was analysed on a wide angle X-ray diffractometer using copper k_α radiation in the 2θ range from 5 to 30°.

2.14 Electrical property measurements

The samples for electrical property measurements were prepared by compression moulding the samples into 2 mm thick sheets in a hydraulic press at a temperature of 200°C. The samples for volume resistivity measurements were prepared by compression moulding the samples into 0.3 mm thick films.

Volume resistance of the samples were measured at a Twenty Million Meghommeter Model 29A at room temperature. The volume resistivity (ρ_v) was calculated using the following equation.

$$\rho_v = R \cdot A/t \ \Omega \text{ cm} \qquad (2.8)$$

where, R is the volume resistance; A, the area; and t, the thickness of the sample.

The capacitance and tan δ of the blends were measured at frequencies ranging from 31.6 Hz - 10 MHz at room temperature using a 4192 Impedance Analyser. The dielectric constant was measured from capacitance using the equation

$$\varepsilon' = C \cdot t/\varepsilon_0 \cdot A \qquad (2.9)$$

where c is the capacitance; t, the thickness; A, the area and ε_0, is 8.85×10^{-12} F/m and

$$\text{Loss factor, } \varepsilon'' = \varepsilon' \cdot \tan \delta \qquad (2.10)$$

2.15 Sorption experiments

Circular shaped samples of diameter 20 mm was punched out from 2 mm thick sheets for diffusion studies. The samples were soaked in 20 ml solvent in diffusion bottles and kept at constant temperature by keeping them in a thermostatically controlled heating oven. The weight of the swollen samples was measured at frequent intervals until equilibrium swelling is reached. The experiments were conducted at 30, 40, 50 and 65°C. A possible source of error in

this measurements is that arises during weighing since the sample has to be taken out from the solvent for weighing. However, since the weighing is completed within 20-30 sec; the error can be neglected.[4] The results of diffusion experiments were expressed as moles of solvent uptake by 100 g of polymer sample, Q_t mol%.

$$Q_t \text{ mol\%} = \frac{\left(\frac{\text{Mass of solvent sorbed}}{\text{Molar mass of solvent}}\right)}{\text{Mass of polymer}} \times 100 \qquad (2.11)$$

2.16 References

1. A. Y. Coran and R. Patel, *Rubber Chem. Technol.*, **56**, 1045 (1983).
2. G. Boder, *Structural Investigations of Polymers*, Ellis Horwood, New York, 1991.
3. P. J. Flory and J. Rehner, *J. Chem. Phys.*, **1**, 25 (1943).
4. G. Unnikrishnan, S. Thomas and S. Varghese, *Polymer*, **37**, 2687 (1996).

Chapter 3

Morphology and Mechanical Properties: Effect of Blend Ratio, Compatibilisation and Dynamic Vulcanisation

---

The results of this chapter have been published in
(i) *Polymer*, **36**, 4405 (1995),
(ii) *Materials Letters*, **26**, 51 (1996)

3.1 Introduction

The properties of rubber-plastic blends are determined by (1) material properties of rubber and plastic phases (2) rubber/plastic proportions (3) phase morphology and (4) interaction at the interface.[1-3] A thorough understanding of the blend morphology is important since the properties of polymer blends are strongly dependant on the blend morphology.[4-8] The morphology of heterogeneous polymer blends depends on blend composition, viscosity of individual components and processing history. Danesi and Porter[5] reported that for blends with same processing history, the morphology is determined by melt viscosity ratio and composition. Generally, the least viscous component was observed to form the continuous phase over a larger composition range.[3] During the last few years a large number of studies on the morphology and properties of thermoplastic elastomers from rubber/plastic blends have been reported.[9-13]

Thermoplastic elastomers from blends of polypropylene (PP) and nitrile rubber (NBR) find applications in cables, oil seals, hoses and other moulded articles by virtue of their easy processability, low density, excellent oil resistance and good mechanical properties. Hence, it is important to study the mechanical properties of these materials in order to understand the final properties of the material.

Several studies have been reported on the rubber modification of polypropylene. The morphology and mechanical properties of PP/EVA blends have been studied by Thomas and co-workers.[14,15] Kuriakose *et al.* reported on the NR modification of PP.[16] Blends of polypropylene with ethylene-propylene

rubbers have been studied by different research groups.[17,18] The mechanical and thermal properties of PP/polybutadiene blends have been reported by Gupta and Ratnam[19]. Coran and Patel[20] reported the technological compatibilisation of PP/NBR and PE/NBR blends. They have studied the effect of addition of graft copolymer and dynamic vulcanisation on the mechanical properties of these blends. Recently, Baker and co-workers[21] studied the effectiveness of various basic functional groups in polypropylene as compatibilisers in a PP/NBR system using morphological and impact property measurements.

In this chapter, the influence of blend ratio on the morphology and mechanical properties of PP/NBR blends has been presented. The effects of concentration of two compatibilisers, maleic modified polypropylene and phenolic modified polypropylene on the morphology and mechanical properties of the blend are quantitatively investigated. The experimental results have been applied to testify the current compatibilisation theories of Noolandi and Hong. The effects of dynamic vulcanisation and filler addition on the mechanical properties are also investigated.

3.2 Results and discussion

3.2.1 Binary blends

(a) Processing characteristics

The processing characteristics of the blends have been studied from the Brabender Plastographs. The torque-time and torque-temperature relationships obtained from Brabender Plastographs are shown in Figure 3.1. In all the cases, the mixing torque falls rapidly within 3 min of mixing time and then levels off to give uniform values at the end of the mixing cycle indicating good degree of mixing. Favis[8] has reported that the final morphology of the blend is strongly influenced by the time of mixing. All the blends show higher mixing torque than PP, and the torque is found to increase with increase in NBR content. This

is due to the higher melt viscosity of NBR as compared to PP. These results clearly indicate that all the blends have higher melt viscosity than polypropylene. It is also seen from the figure that the mixing temperature of the blends increases with increase in NBR content. This is due to the fact that high shear forces are involved as NBR content increases owing to its higher viscosity compared to PP.

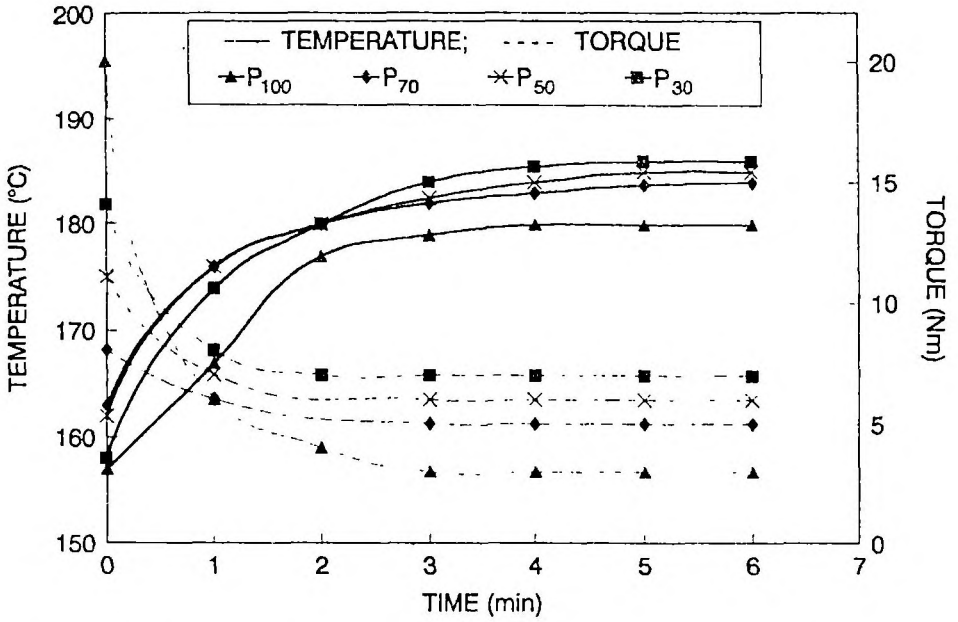

Figure 3.1. Brabender plastographs showing the variation of mixing torque and temperature with time of mixing.

(b) Morphology of the binary blends

The scanning electron micrographs of P_{70}, P_{50} and P_{30} from which the NBR phase has been extracted are shown in Figures 3.2a–3.2c. In the P_{70} NBR is found to be dispersed as domains in the continuous PP matrix. This is due to the higher melt viscosity and lower NBR content compared to PP in the blend. As the rubber in the blend increases from 30 to 50 wt % the average size of the dispersed NBR phase increases from 5.87 to 17.90 μm The bigger particle size of the rubber

phase with increase in rubber content is attributed to the reagglomeration or coalescence of the dispersed rubber particles. Occurrence of coalescence at higher concentrations of one of the components has been reported by many authors.[22-24] In P_{30}, both NBR and PP phases exist as co-continuous phases. This is associated with the higher proportions of NBR and low viscosity of the PP phase.

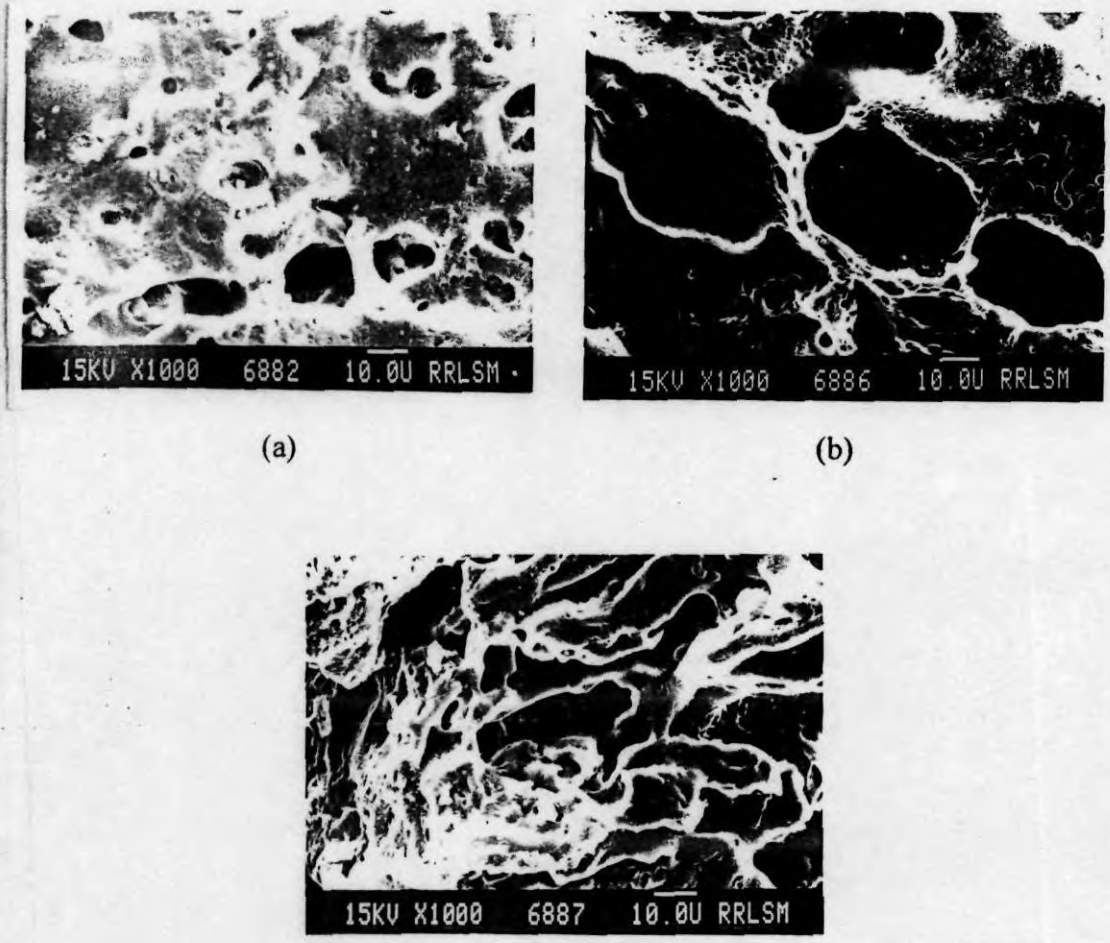

Figure 3.2. Scanning electron photomicrographs of NBR/PP blends from which NBR was extracted using chloroform: (a) 30/70 NBR/PP blend. NBR is dispersed as domains in the continuous PP matrix; (b) 50/50 NBR/PP blend: NBR is dispersed as domains in the continuous PP matrix; and (c) 70/30 NBR/PP blend with co-continuous morphology.

(c) *Mechanical properties*

The stress-strain curves of the P_{100}, P_{70}, P_{50}, P_{30} and P_0 are shown in Figure 3.3. From the stress-strain curves it is possible to determine the differences in the deformation characteristics of the blends under an applied load. The stress-strain curve of PP is similar to that of a brittle material. It shows very high initial modulus with a definite yield point. The addition of NBR changes the nature of stress- strain curves considerably. The stress-strain curves of PP and blends containing higher proportion of PP have distinct elastic and inelastic regions. In the inelastic region they undergo yielding. The elastic moduli of the blends are found to be reduced considerably with the increase in rubber concentration. The improved rubbery behaviour of P_{30} compared to P_{70} and P_{50} can be explained in terms of the phase inversion of NBR from dispersed to continuous phase on passing from P_{50} to P_{30}. The stress-strain behaviour of NBR is typical of uncrosslinked soft elastomer.

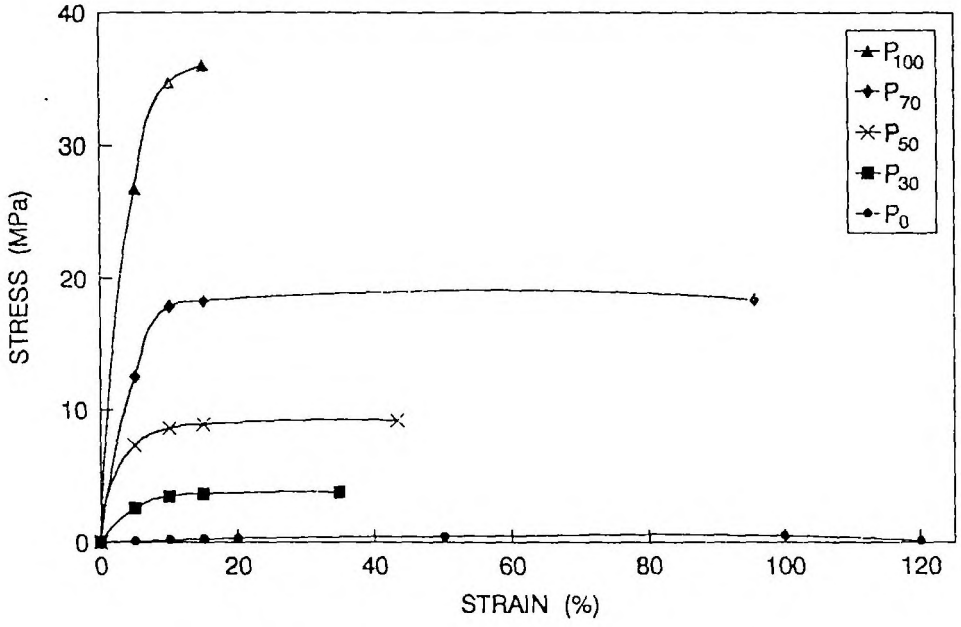

Figure 3.3. Stress strain curves of the samples.

Figure 3.4 shows the load displacement curves of PP/NBR blends during tearing. Polypropylene tears at a higher load and at a small displacement. NBR undergoes the largest displacement with the minimum tearing force. The tearing behaviour of NBR/PP blends are intermediate between those of PP and NBR. As the NBR content in the blend increases the load required to tear the samples decreases and the displacement increases. This increase in displacement with rubber content may be due to the increased stretching of rubber particles which can bridge the matrix cracks. From the figure it is also seen that the modulus of the blends decreases with increase in rubber content and this reduction is more pronounced in the case of P_{30}. In PP/EVA blends similar behaviour has been reported by Thomas *et al.*[4] They correlated this behaviour with the morphology of the blends.

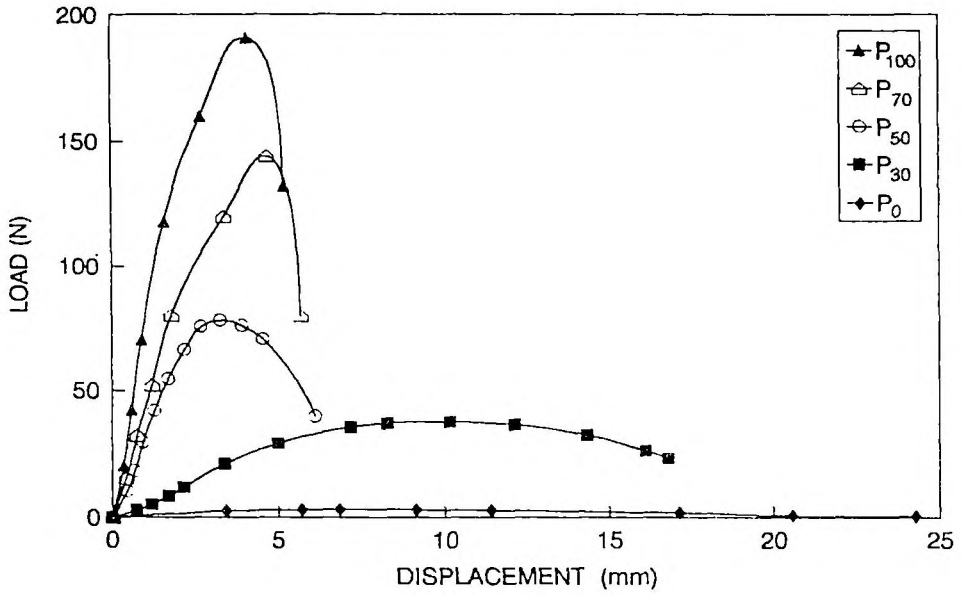

Figure 3.4. Tear load-displacement curves of NBR/PP blends.

Table 3.1 and Figure 3.5 show the variation of mechanical properties as a function of wt % of NBR. Pure iPP has the maximum tensile strength, tear strength and Young's modulus. From the table it is seen that with the increase in

NBR content, the tensile strength, tear strength and Young's modulus decrease. The strength of NBR/PP blends depends on the strength of PP phase, which in turn depends on the extent of crystallinity. It has been observed that the crystallinity of the blend was decreased by the incorporation of NBR (Table 3.2). Martuscelli *et al.*[25] have stated that the spherulite growth of iPP in blends with rubber is hindered by the presence of the rubber phase. Hence the observed decrease in tensile strength, tear strength and Young's modulus with increase in NBR content is due to the presence of the soft rubber phase and drop in crystallinity of PP phase. It can be noticed from Figure 3.5 that the tensile strength-composition curve shows a negative deviation i.e., blend properties lie below the additivity line. The observed negative deviation is due to the poor interfacial adhesion between the non-polar PP and polar NBR phases, which causes poor stress transfer between the matrix and the dispersed phase. A clear change in the slope of this tensile strength-composition curve is seen between the composition range 50/50 PP/NBR to 30/70 PP/NBR. This is attributed to phase inversion of NBR from dispersed to continuous phase. Such deviation in the slope of mechanical property-composition curves had been reported by Danesi and Porter for PP/EPDM system.[5]

Table 3.1. Mechanical properties of binary PP/NBR blends.

Property	P_{100}	P_{70}	P_{50}	P_{30}	P_0
Tensile strength (MPa)	35	18.30	9.20	3.50	0.475
Young's modulus (MPa)	500	250	135	47	1.5
Elongation at break (%)	15.6	95.58	43.45	38.64	1267
Tear strength (N/m)	117.90	85.40	50	21.10	5.36
Tensile impact strength (J/m^2)	1110	1008	320	1448	-
Hardness shore A	95	95	93	83	28

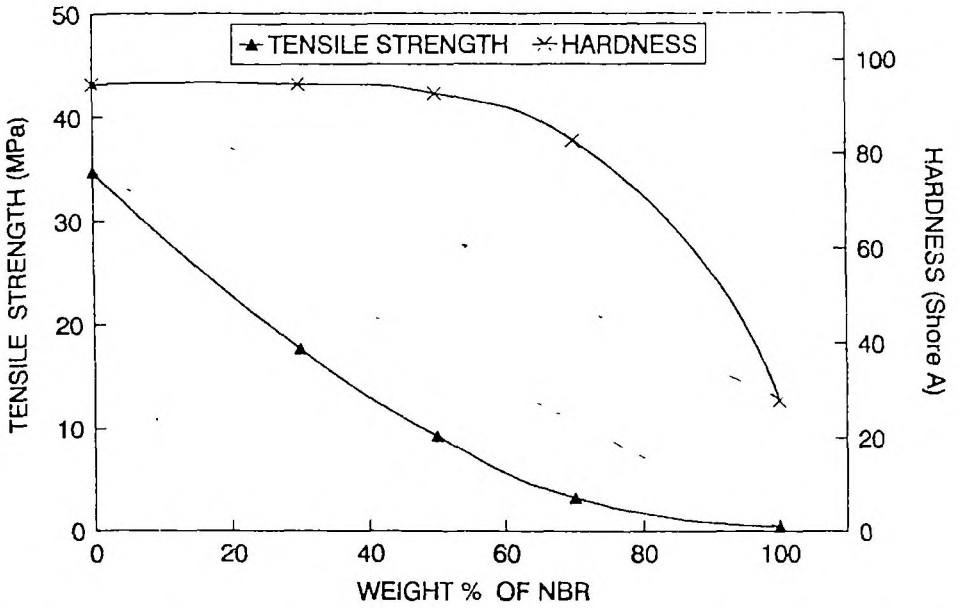

Figure 3.5. Effect of weight percent of NBR on tensile strength and shore A hardness of NBR/PP blends.

Table 3.2. Crystallinity of PP/NBR blends (from DSC data).

Composition	Crystallinity (%)
P_{100}	55.3
P_{70}	33.9
P_{50}	20.9
P_{30}	13.7

The elongation at break of PP/NBR blend is found to increase with the addition of 30 wt % NBR and after that it decreases with increase in rubber content (Table 3.1). The elongation at break also shows negative deviation. This decrease in elongation at break at higher rubber content is due to the poor interfacial adhesion between the homopolymers.

From the table, it is also seen that the tensile impact strength decreases with the addition of NBR up to 50 wt %. In immiscible blends, the tensile impact strength usually depends on the particle size of the dispersed phase. Smaller and uniformly distributed particles are more effective to initiate crazes and to terminate them before they develop into catastrophic sizes. The decrease in tensile impact strength in PP/NBR blends up to 50 wt % of NBR is due to the poor interfacial adhesion and higher particle size of the dispersed NBR phase as seen in the SEM photographs of P_{70} and P_{50} (Figure 3.2). The poor interfacial adhesion causes premature failure as a result of the usual crack opening mechanism. Karger-Kocsis *et al.*[26] have shown that with the increase in the particle size of the dispersed rubber phase, the tensile impact strength of PP/EPDM blend decreases. After 50 wt % of NBR, the tensile impact strength is found to increase sharply. This sharp increase in impact strength may be due to the continuous nature of the NBR phase, which forms a co-continuous structure with the plastic phase (Figure 3.2). Similar results were reported in the case of PP-EVA system.[27]

From Table 3.1 it is seen that the addition of 30 wt % of NBR does not change the hardness However, further addition of NBR decreases the hardness. The hardness- composition curve shows a slope change beyond 50 wt % of NBR (Figure 3.5). The reduction in hardness and the slope change in the curve at higher proportion of NBR (>50%) can be explained by the phase inversion of NBR from dispersed to continuous phase on passing from 50/50 PP/NBR to 30/70 PP/NBR blend. It is interesting to see that the hardness values show a positive deviation.

Applicability of various composite models such as parallel, series, Halpin-Tsai and Coran's models has been used to predict the mechanical properties of these blends. The highest upper bound parallel model is given by the rule of mixtures

$$M = M_1\phi_1 + M_2\phi_2 \qquad (3.1)$$

where M is any mechanical property of the composite, M_1 and M_2 are the mechanical properties of component 1 and 2 respectively and ϕ_1 and ϕ_2 are the volume fractions of components 1 and 2 respectively. This equation holds for models in which the components are arranged parallel to one another so that an applied stress elongates each component by the same amount. The lowest lower bound series model is found in models in which the components are arranged in series with the applied stress. The equation for this case is

$$1/M = \phi_1/M_1 + \phi_2/M_2 \tag{3.2}$$

According to Halpin-Tsai equation[28,29]

$$M_1/M = (1+AiBi\phi_2)/(1-Bi\phi_2) \tag{3.3}$$

$$Bi = (M_1/M_2 - 1)/(M_1/M_2 + Ai) \tag{3.4}$$

In the Halpin-Tsai equation, subscripts 1 and 2 refer to the continuous phase and dispersed phase respectively. The constant Ai is defined by the morphology of the system. For elastomer domains dispersed in a continuous hard matrix, Ai = 0.66.

For an incompatible blend, values of mechanical properties are expected to be in between upper bound parallel model (M_U) and lower bound series model (M_L). According to Coran's equation,[3]

$$M = f(M_U - M_L) + M_1 \tag{3.5}$$

where f can vary between zero and unity. The value of f is a function of phase morphology. The value of f is given by

$$f = V_H^n (nV_S + 1) \tag{3.6}$$

where n - contains the aspects of phase morphology, V_H and V_S are the volume fractions of hard phase and soft phase respectively. The change in f with respect to V_H is greatest when $V_H = (n-1)/n$. Thus the value of (n-1)/n could be considered as the volume fraction of hard phase material that corresponds to a phase inversion.

Figure 3.6 shows the experimental and theoretical curves of Young's modulus as a function of soft phase volume fraction. It can be seen from the figure that experimental data are very close to the Coran's model, in which the value of n = 2.2. The value of n = 2.2, corresponds to $V_H = 0.545$ as the hard phase volume fraction that corresponds to a phase inversion of NBR from dispersed to continuous phase. This result is consistent with the experimental results from morphology and mechanical property studies.

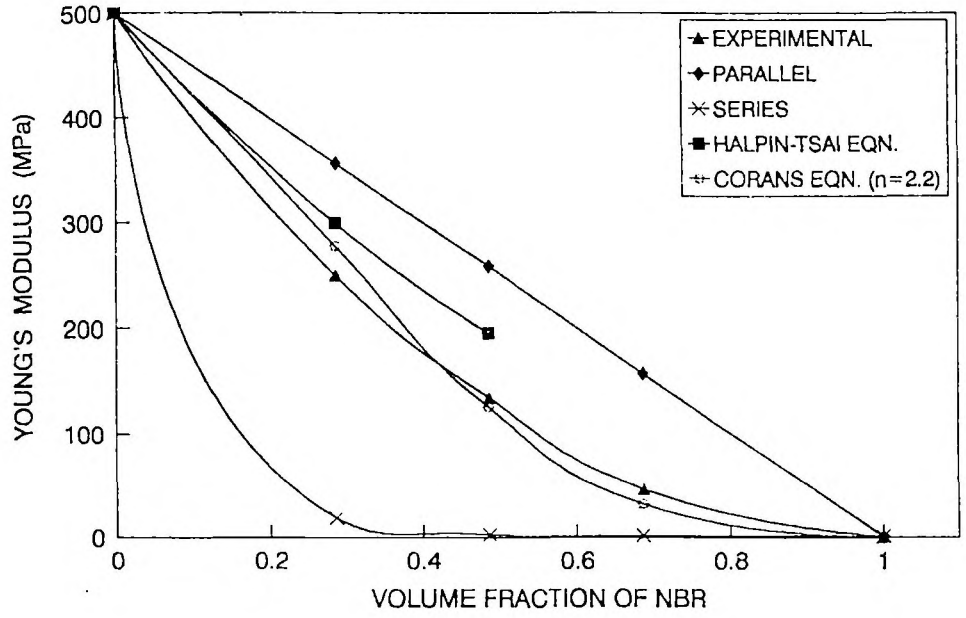

Figure 3.6. Experimental and theoretical values of Young's modulus as a function of volume fraction of NBR phase.

3.2.2 Compatibilisation

(a) *Morphology of compatibilised blends*

The effect of maleic anhydride modified polypropylene and phenolic modified polypropylene as compatibilisers on the morphology of the 70/30 PP/NBR blend is shown by the SEM micrographs of Figures 3.7 and 3.8, respectively. The micrographs 3.7a–3.7d indicate blends containing 1, 5, 10 and 15% MA-PP respectively and micrographs 3.8a–d indicate blends containing

3, 7.5, 10 and 15% Ph-PP, respectively. The morphology of uncompatibilised blend was already given in Figure 3.2a. From the SEM micrographs, it is seen that the size of the dispersed NBR phase decreases with the addition of modified polymers. This reduction in particle size with the addition of modified polymers is due to the reduction in interfacial tension between the dispersed NBR phase and polypropylene matrix.

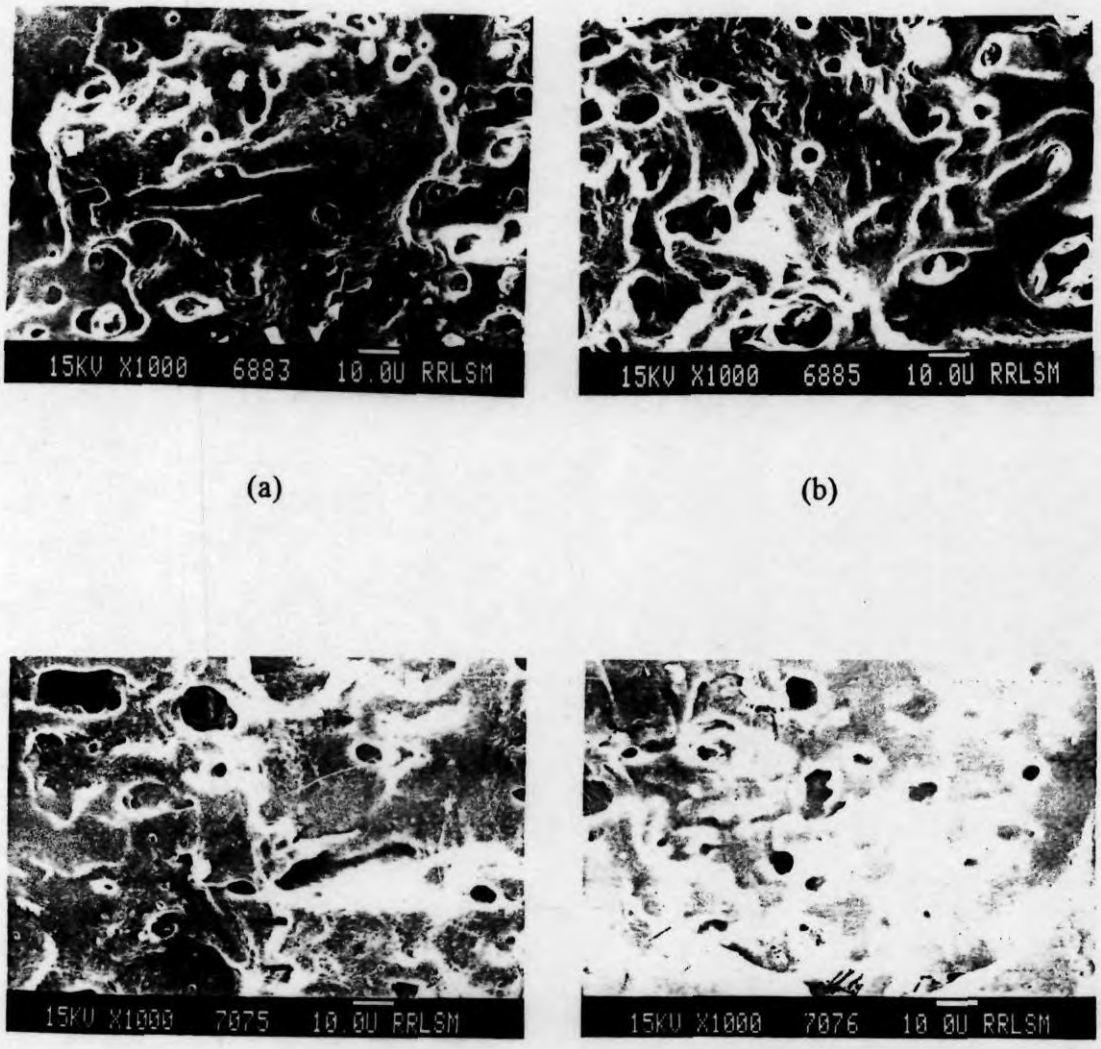

(a) (b)

(c) (d)

Figure 3.7. Scanning electron micrographs of P_{70} blends compatibilised with MA-PP: (a) 1% Ma-PP, (b) 5% MA-PP, (c) 10% MA-PP and (d) 15% MA-PP.

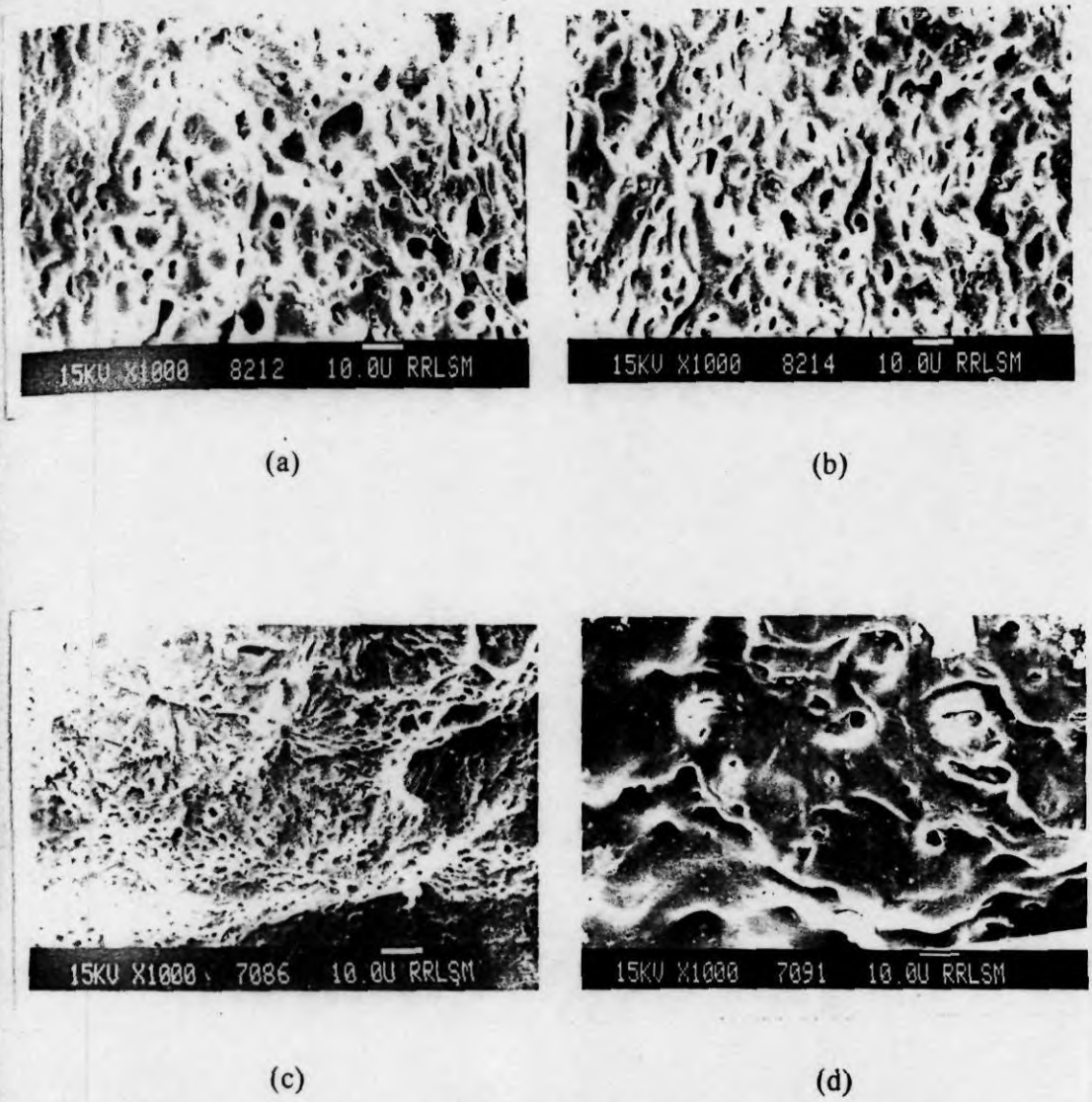

Figure 3.8. Scanning electron micrographs of P_{70} blends compatibilised with Ph-PP: (a) 3% Ph-PP, (b) 7.5% Ph-PP, (c) 10% Ph-PP and (d) 15% Ph-PP.

The average domain size of the compatibilised blends were analysed as a function of compatibiliser concentration (Figure 3.9). The number average domain size of the unmodified blend is 5.87 μm. From the Figure, it is seen that in the case of MA-PP compatibilised blends, addition of 1% MA-PP causes a domain size reduction of 35%. Further addition of MA-PP does not change the domain

size considerably, but a levelling off is observed. In the case of Ph-PP compatibilised blends, the average diameter of the dispersed NBR phase decreases up to the addition of 10 wt % Ph-PP. By the addition of 10 wt % Ph-PP, the domain size is reduced by 77% of the domain size of the unmodified blend. However, further addition of compatibiliser increases the domain size. The equilibrium concentration at which the domain size levelled off can be considered as the so-called critical micelle concentration (CMC), i.e., the concentration at which micelles are formed. Generally, CMC is estimated from the plot of interfacial tension versus copolymer concentration. Since the interfacial tension is directly proportional to the domain size, the estimation of CMC from the plot of domain size versus concentration is warranted.[30] The CMC values indicate the critical amount of compatibiliser required to saturate unit volume of interface. The increase in domain size above CMC may be due to the formation of micelles of compatibiliser at the continuous polypropylene phase. This is schematically represented in Figure 3.10. Several authors have reported the interfacial saturation of binary polymer blends by the addition of compatibilisers.[31-34] Thomas and Prud'homme[31] reported that in PS/PMMA blends at lower concentrations of copolymer, the dispersed phase size decreases linearly with increasing copolymer concentration, whereas at higher concentration, it levelled off. Noolandi and Hong[35,36] also suggested that there is a critical concentration of block copolymer at which micelles are formed in the homopolymer phases. All the above experimental observations including the present study and theoretical predictions of Noolandi and Hong suggest that there is a critical concentration of compatibiliser required to saturate the interface of a binary blend. The compatibiliser concentration above this critical concentration, may not modify the interface any more, but forms compatibiliser micelles at the bulk phase.

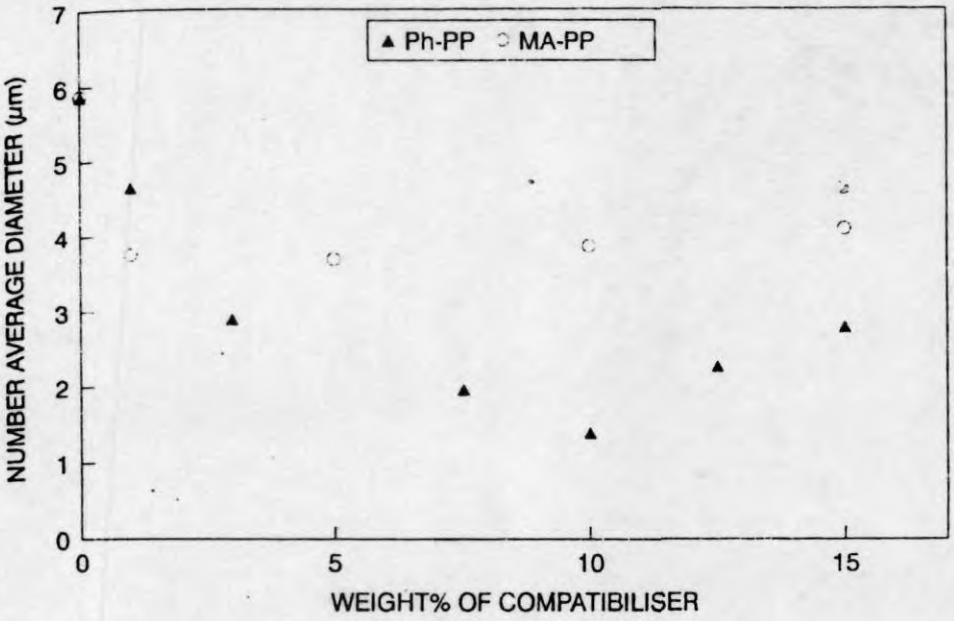

Figure 3.9. Effect of compatibiliser concentration on the domain size of the dispersed phase of P_{70}.

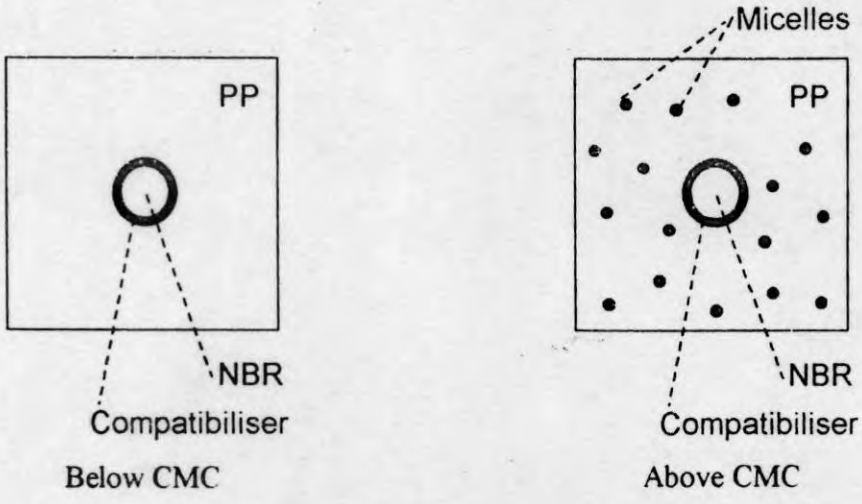

Figure 3.10. Schematic representation of the formation of micelle above critical micelle concentration.

The interfacial saturation point can be further explained by Taylors theory. In Taylors theory[37] of particle deformation the critical Weber number, We, is given by the equation

$$W_e = \frac{\eta_m dn\dot{\gamma}}{2\tau_{12}} \qquad (3.7)$$

where η_m is the viscosity of the matrix, dn the number average diameter of the dispersed phase, $\dot{\gamma}$ is the shear rate and τ_{12} is the interfacial tension. From the equation, it is clear that there is a critical value of We below which there is no particle deformation and as a result there is a point of critical particle size. At this point the compatibiliser attains maximum interfacial area and therefore there must be a maximum quantity of compatibiliser required to saturate the interface.

The theories of Noolandi and Hong can be applied to these highly incompatible PP/NBR blends for concentrations less than CMC. According to them the interfacial tension is expected to decrease linearly with the addition of compatibiliser below CMC, and above the CMC a levelling off is expected. The expression for interfacial tension reduction ($\Delta\gamma$) in a binary blend A/B upon the addition of a divalent copolymer A-b-B is given by equation (1.1).[35,36]

According to this equation, the plot of interfacial tension reduction versus ϕ_c should yield a straight line. Although this, theory was developed for the action of symmetrical diblock copolymer A-b-B in incompatible binary system (A/B), this theory can be successfully applied to other systems, in which the compatibilising action is not strictly by the addition of symmetrical block copolymers.[38] Since interfacial tension reduction is directly proportional to the particle size reduction as suggested by Wu,[30] we can replace the interfacial tension reduction term by the particle size reduction (Δd) term in Noolandi and Hong's equation. Therefore:

$$\Delta d = Kd\phi_c[(1/2\chi + 1/Z_c) - 1/Z_c\exp(Z_c\chi/2)] \qquad (3.8)$$

where K is a proportionality constant.

The plot of particle size reduction as a function of the volume percent of the compatibiliser is shown in Figure 3.11. It can be seen that at low copolymer concentrations (below the CMC), Δd decreases linearly with increasing copolymer volume fraction, whereas at higher concentrations (above the CMC), it levels off, and this is in agreement with the theories of Noolandi and Hong.

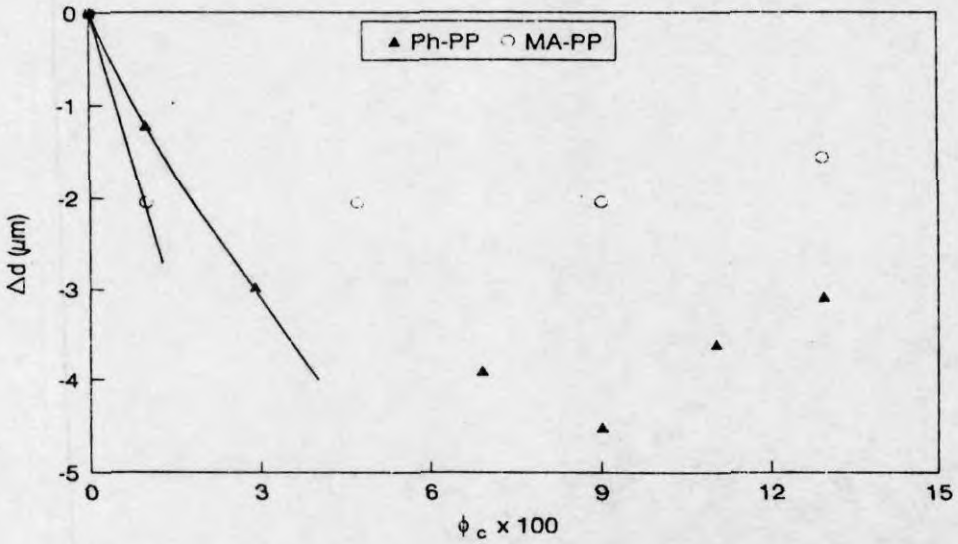

Figure 3.11. Effect of volume fraction of compatibiliser on the particle size reduction of P_{70}.

The domain size distribution curves for the MA-PP and Ph-PP compatibilised blends are shown in Figures 3.12 and 3.13 respectively. In the case of unmodified blend, a high degree of polydispersity is evident by the large width of the distribution curve. With the increasing concentration of the compatibiliser (Ph-PP and MA-PP) the polydispersity decreases as evidenced by the decrease in the width of the distribution curve. In the case of Ph-PP compatibilised blend, a sharp distribution is obtained with the addition of 10% Ph-PP. Willis and Favis[32] have also shown that the addition of compatibiliser to polyolefin/polyamide system not only reduces the dimensions of the minor phase, but also results in uniform distribution of minor phase.

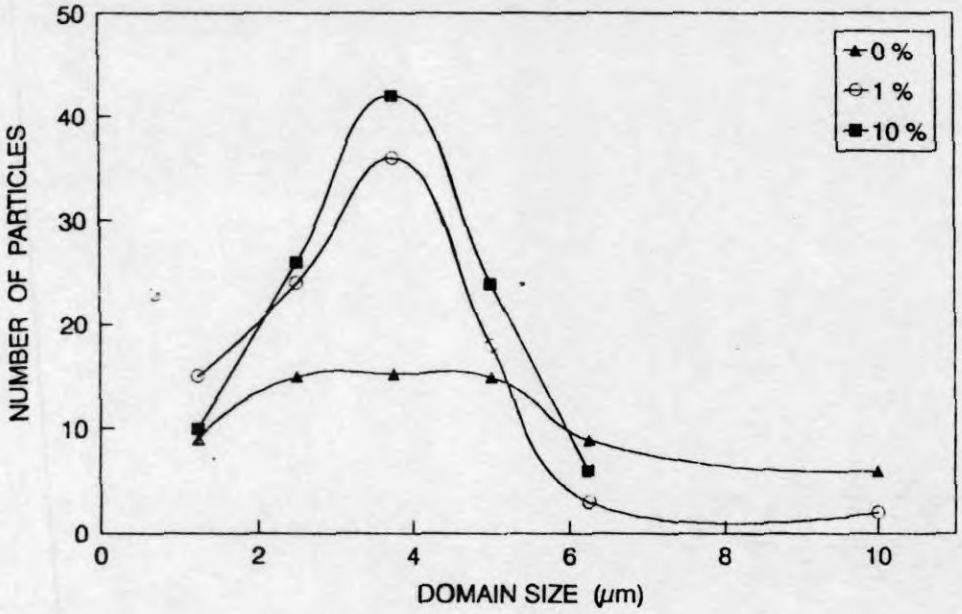

Figure 3.12. Effect of MA-PP concentration on domain size distribution of P_{70}.

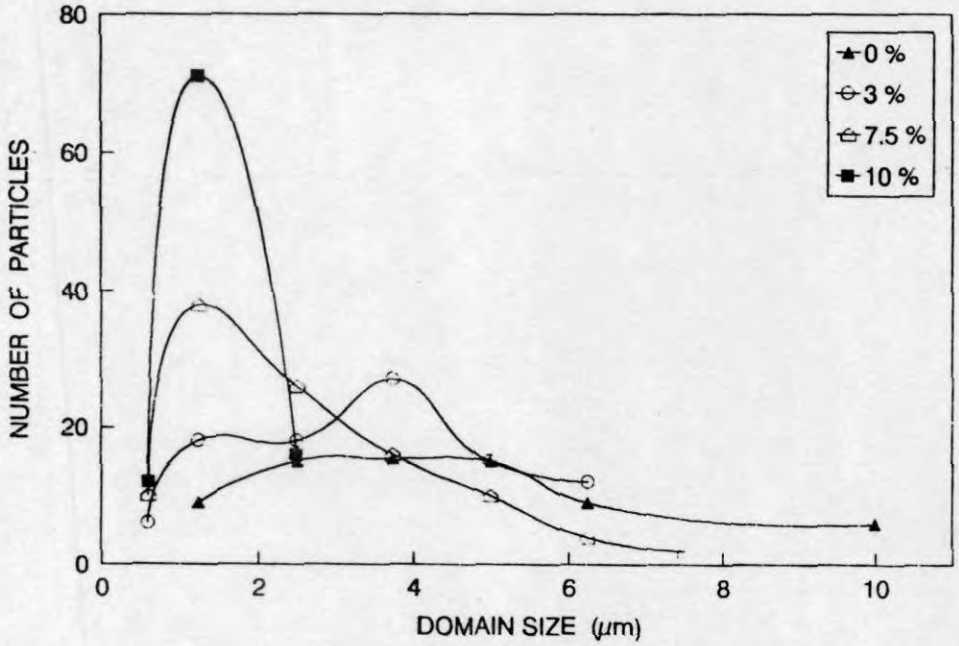

Figure 3.13. Effect of Ph-PP concentration on domain size distribution of P_{70}.

The mechanism of compatibilising action and the difference in the behaviour of MA-PP and Ph-PP as compatibilisers in NBR/PP can be explained as follows. In the maleic anhydride modified polypropylene, maleic anhydride groups are grafted on to PP chain back bone as shown in Figure 3.14.

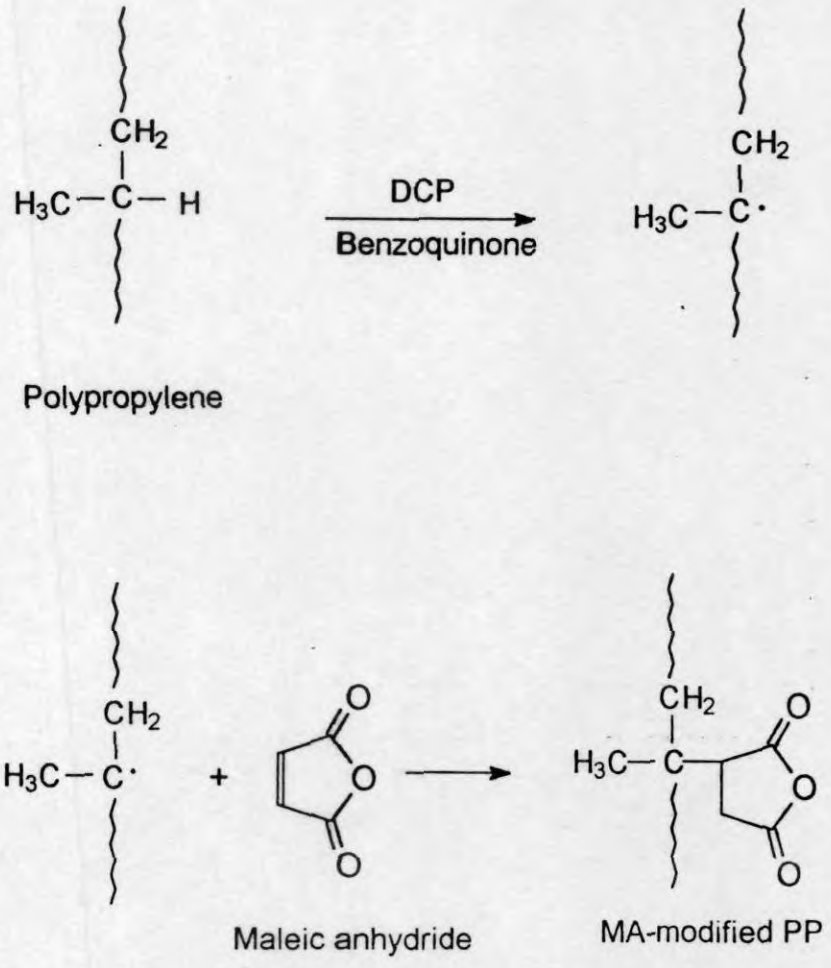

Figure 3.14. Reaction scheme for the maleic anhydride modification of polypropylene.

The FTIR spectrum of maleic anhydride grafted PP is shown in Figure 3.15. The peak present at 1710 cm^{-1} indicate the presence of carboxyl groups, originating from maleic anhydride grafted on PP chains. The compatibilising action of this

MA-PP is due to the dipolar interaction between the maleic anhydride groups of MA-PP and NBR.

When PP is melt mixed with dimethylol phenolic resin and $SnCl_2$, dimethylol groups are grafted on to PP backbone chain as shown in Figure 3.16. When the Ph-PP was added to PP/NBR blend, there is a possibility for the formation of graft copolymer between PP and NBR as shown in Figure 3.16.[20] This graft copolymer acts as an emulsifier at the interface and thus reduces interfacial tension leading to small and uniform distribution of NBR phase as seen in the SEM micrographs (Figure 3.8). It is also important to mention that the Ph-PP can also act as compatibiliser due to the dipolar interaction between the dimethylol groups of Ph-PP and polar NBR phase.

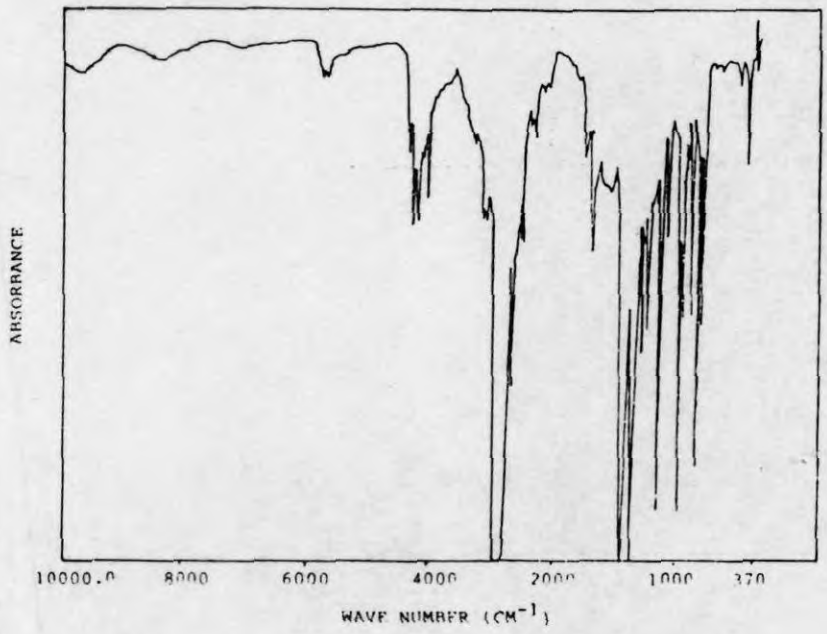

Figure 3.15. FTIR spectrum of the maleic anhydride modified polypropylene.

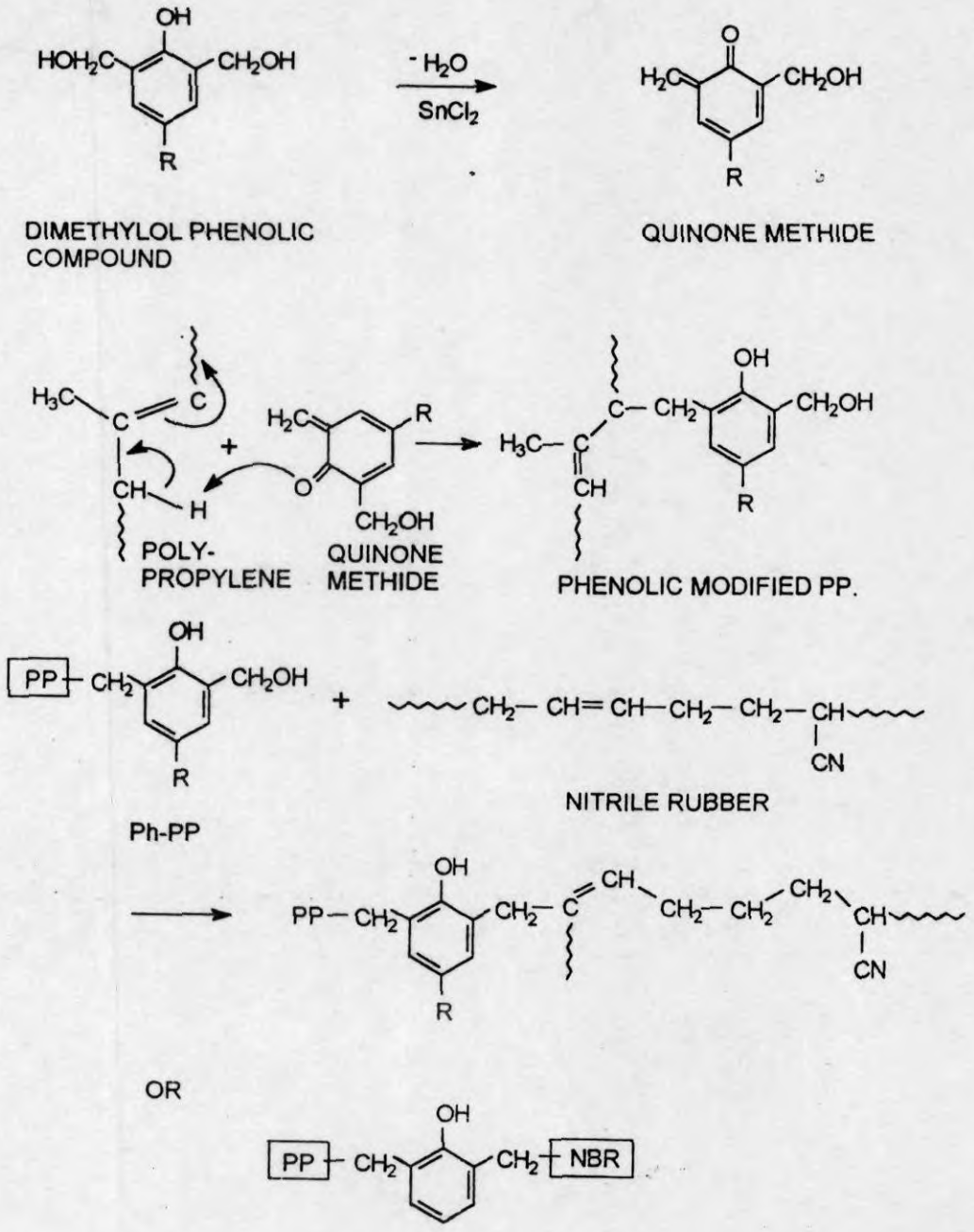

Figure 3.16. Reaction scheme for the dimethylol phenolic modification of polypropylene.

(b) Mechanical properties of compatibilised blends

The mechanical properties of immiscible polymer blends are affected by the addition of compatibilisers. Figure 3.17 shows the variation of tensile strength of 70/30 PP/NBR blend with weight percent of two compatibilisers Ph-PP and MA-PP. With the increase in compatibiliser concentration, the tensile strength is found to increase up to 10 weight percent of compatibiliser and then levels off for both the compatibilisers. This increase in tensile strength is due to the increase in interfacial adhesion between PP and NBR phases which is evident from the SEM micrographs (Figures 3.7 and 3.8). The highest tensile strength of 10% Ph-PP compatibilised blend is due to the lowest particle size of NBR domains in this system. In the case of MA-PP compatibilised blends, the increase in tensile strength is due to the increased dipolar interaction between the MA-PP and NBR phase which causes an increase in interfacial adhesion between PP and NBR phases, although there is no reduction in particle size with the increase in MA-PP concentration beyond 1%. Similar results have been reported for Nylon/PP system.[39]

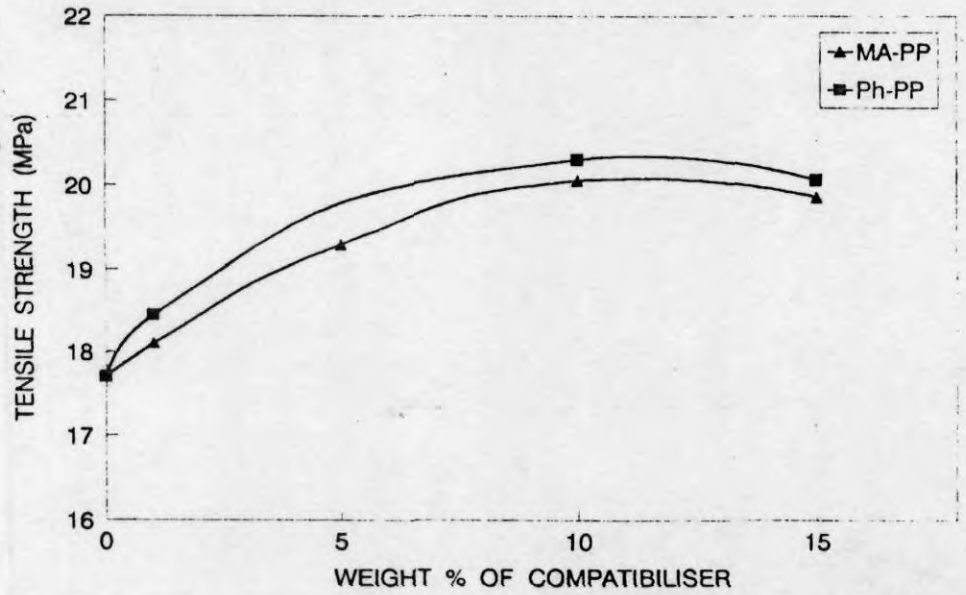

Figure 3.17. Effect of compatibiliser concentration on the tensile strength of P_{70}.

The variation of tensile modulus at 5 and 10% elongation and tensile impact strength with the Ph-PP concentration is shown in Figure 3.18. The tensile modulus is found to increase with increase in concentration of Ph-PP up to 10% and after that it levels off. From the figure it is seen that the tensile impact strength of the blend increases significantly with the addition of Ph-PP up to 10% and after that it decreases drastically. This result is consistent with the literature reports on the increase of the tensile impact strength with reduction in particle size of dispersed phase. The reduction in tensile impact strength for the blend containing 15 wt % Ph-PP is due to the formation of compatibiliser micelles in the homopolymer phases. Similar results have been reported for LDPE/PDMS system by Santra *et al.*[40]

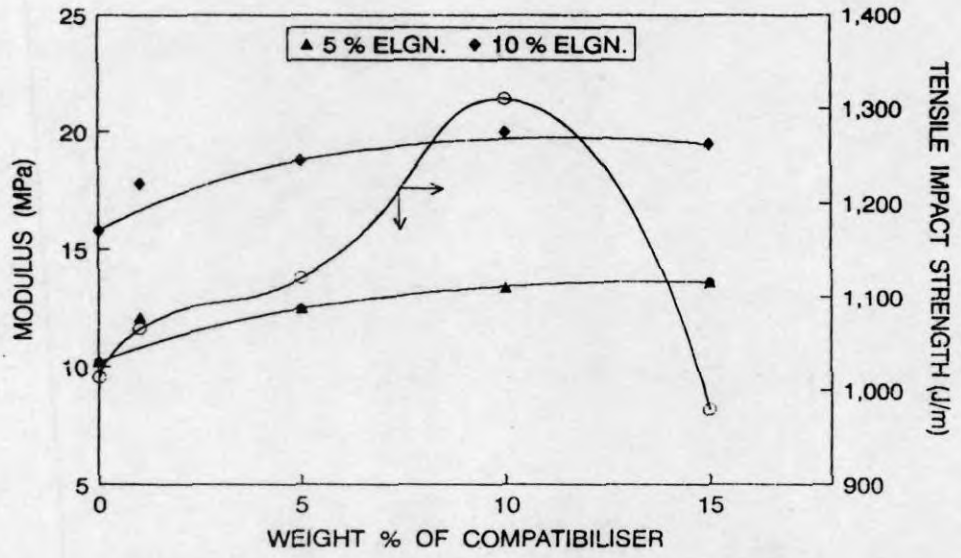

Figure 3.18. Effect of Ph-PP concentration on the modulus at 5% and 10% elongation and tensile impact strength of P_{70}.

The effect of phenolic modified polypropylene on the tear strength of 70/30 PP/NBR blend is shown in Figure 3.19. It is observed that the tear strength of the blend increases with increase in Ph-PP concentration up to 10 wt % and after that it levels off. It can be noticed that the tear strength of the blend is increased by 50%

upon the addition of 10% compatibiliser. The increase in tear strength with Ph-PP concentration is due to the increased interfacial adhesion between the PP and NBR phases and also due to the reduction in particle size of the dispersed NBR phase. During tearing, usually the rubber particles which bridge the growing crack stretch to large extent before failing.[41-42] The tearing strain of the rubber particles increases with the reduction in particle size. It has been reported that the stretched rubber particles span the crack during crack propagation by acting like little springs between its faces.[41] Thus in PP/NBR blend, the addition of Ph- PP decreases the size of NBR domains which bridge the growing crack and this reduction in domain size leads to increased stretching of NBR particles during tearing. Again the increased interfacial adhesion between PP and NBR phase helps to inhibit the propagation of growing crack during tearing. This will obviously increase the tear strength of PP/NBR blends with the addition of Ph-PP. The levelling off observed in the tear strength after 10 wt % of Ph-PP is due to the interfacial saturation.

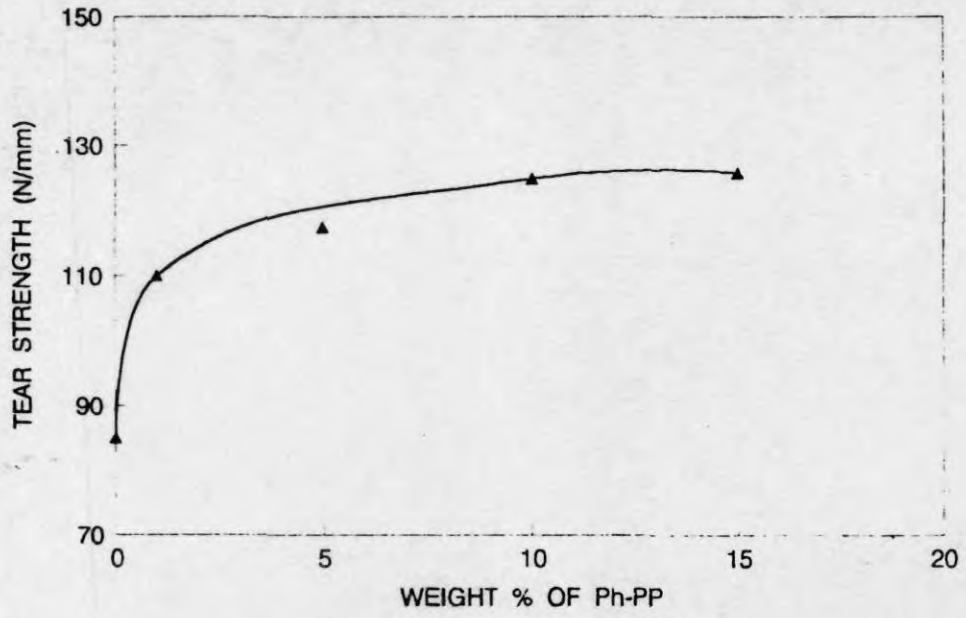

Figure 3.19. Effect of Ph-PP concentration on the tear strength of P_{70}.

3.2.3 *Dynamic vulcanisation*

The vulcanisation of rubber phase during mixing has been investigated as a way to improve the physical properties of several thermoplastic elastomers based on rubber/plastic blends.[43] In the present study, three types of crosslinking systems have been used. These include accelerated sulphur vulcanisation which produces predominantly S-S linkages, peroxide system which give rise to only C-C linkages and mixed system which produces both sulphide linkages and C-C linkages. The schematic representation of the network structure in the three cases are shown in Figure 3.20.

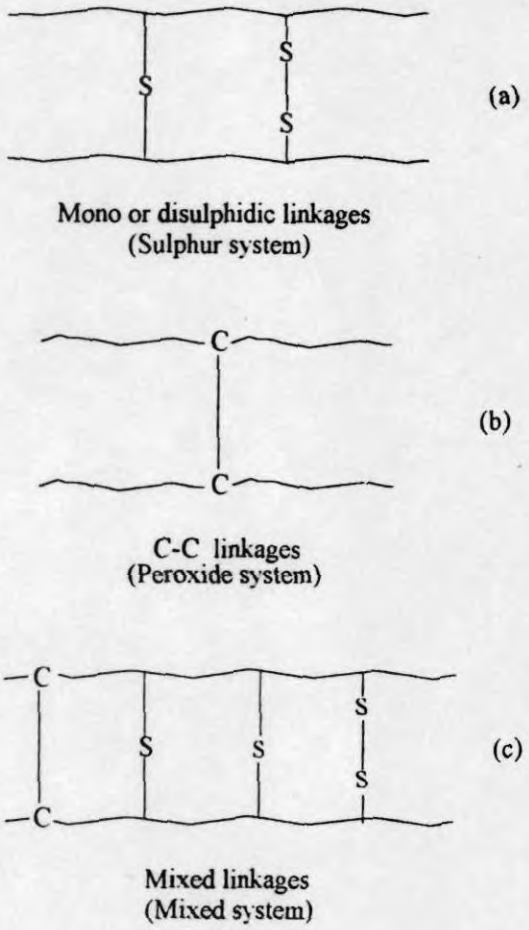

Figure 3.20. Schematic representation of the network formed during dynamic vulcanisation using (a) sulphur, (b) peroxide and (c) mixed systems.

The morphology of 70/30 PP/NBR blends vulcanised with sulphur, DCP and mixed systems is shown in Figure 3.21. From the figures it is seen that in sulphur cured system, the size of the dispersed NBR domains is larger than those of peroxide and mixed systems. In peroxide cured system, the distribution is more fine and uniform and hence the crosslinking is more effective in DCP system. However this effect of crosslinking is not so predominant on the properties of the peroxide vulcanised system due to the degradation of PP phase in presence of DCP.[43]

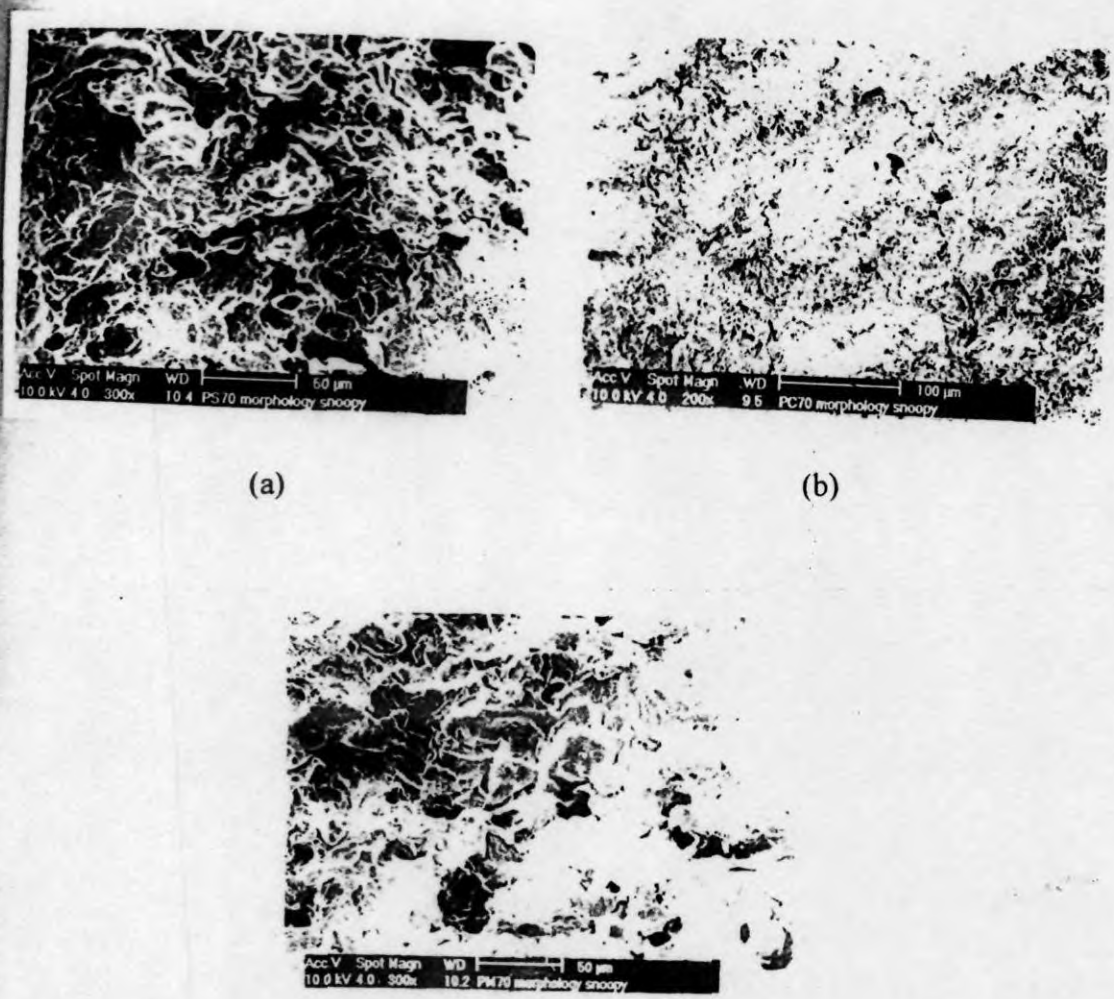

(a) (b)

(c)

Figure 3.21. Morphology of dynamically vulcanised P_{70} blends: (a) PS_{70}, (b) PC_{70} and (c) PM_{70}.

The stress-strain curves of dynamic vulcanised PP/NBR blends are shown in Figure 3.22. The effect of vulcanising systems on deformation behaviour can be obtained from the stress-strain curves. The modulus of the blends were lowered by dynamic vulcanisation. It can also be seen from the figure that the elongation at break decreased upon dynamic vulcanisation for blends with higher loadings of PP. The blends with higher concentrations of PP showed distinct elastic and inelastic regions and in the inelastic region the systems undergo necking/yielding.

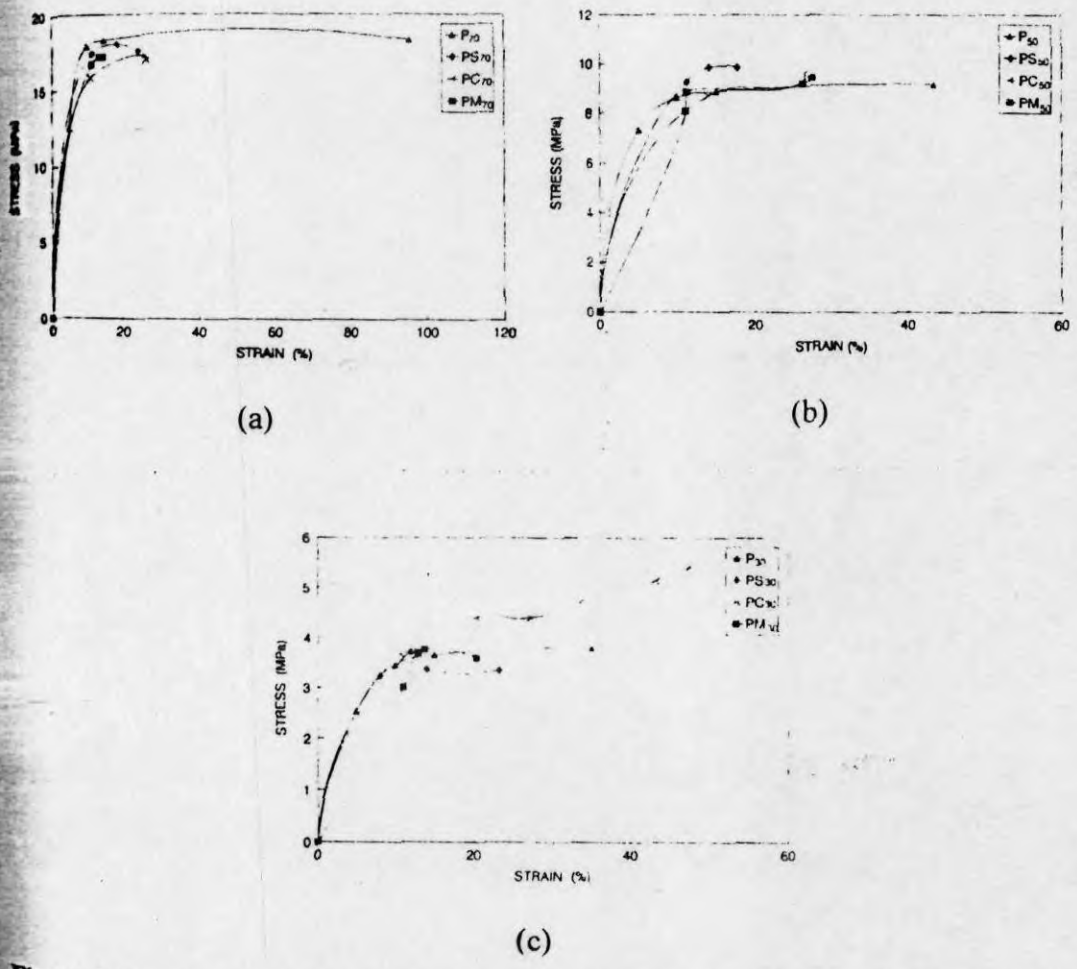

Figure 3.22. Stress-strain curves of unvulcanised and dynamically vulcanised: (a) P_{70}, (b) P_{50} and (c) P_{30} blends.

The tensile strength and tear strength of dynamic vulcanised blends are shown in Table 3.3. The mechanical properties of the blends with 70 wt % of PP decreased upon dynamic vulcanisation and that with 50 and 30 wt % of PP show an increase for tensile strength values. When considering the various vulcanised systems, it can be seen that for blends with higher loadings of PP, the sulphur vulcanisation gave comparatively better effect. As the concentration of rubber increases, the trend gets reversed, and DCP vulcanisation leads to better properties. The mixed vulcanised system takes an intermediate position. In the case of thermoplastic elastomers the strength depends mainly on the strength of hard phase matrix. We have seen that in P_{70} and P_{50}, NBR is the dispersed phase and PP the matrix. Therefore, the blends the strength depends mainly on the strength of PP phase. The vulcanisation of PP based blends using DCP leads to the degradation of PP phase. Hence for blends with higher loadings of PP, showed lower properties on dynamic vulcanisation using DCP though the crosslinking is more effective by DCP. However at higher loadings of rubber, the DCP crosslink the rubber phase preferentially than degrading PP and hence leads to better properties.

Table 3.3. Mechanical properties of dynamic vulcanised PP/NBR blends.

Sample	Tensile strength (MPa)	Tear strength (N/m)
PS_{70}	18.364	79.77
PC_{70}	17.23	63.01
PM_{70}	17.17	81.28
PS_{50}	9.88	47.64
PC_{50}	9.94	53.4
PM_{50}	9.47	49.45
PS_{30}	3.71	18.24
PC_{30}	5.43	21.38
PM_{30}	3.78	18.26

3.2.4 *Filled PP/NBR blends*

The mechanical properties of filled PP/NBR blends were studied for various fillers such as carbon black, cork, silica and silane treated silica. The stress-strain curves of unvulcanised P_{70} and P_{30} blends with 30 phr filler loadings are given in Figures 3.23a and 3.23b, respectively. The stress-strain curves indicate that the modulus of the blends decreased upon the incorporation of fillers. The deformation behaviour of the blends are not much varied on the filler addition. The blend with 70 wt % of PP shows higher initial modulus, and yielding. The P_{30} blends showed lower initial modulus. The stress-strain curves of both the blends show distinct elastic and inelastic regions.

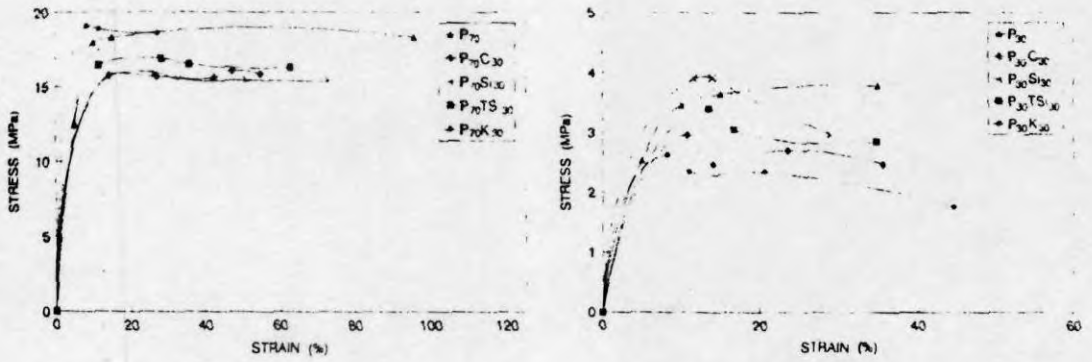

(a) (b)

Figure 3.23. Stress-strain curves of (a) P_{70} and (b) P_{30} blends with 30 phr filler loading.

The tensile and tear properties of unvulcanised PP/NBR blends with 30 phr filler loading is given in Table 3.4. From the table it is seen that the properties of blend with various fillers vary with concentration of rubber phase. At 30 wt % NBR, among the different fillers, cork showed highest improvement in tensile and tear strength values while silica showed the lowest value. At 50 wt % NBR also, cork filler showed oetter properties. However, as the NBR content increased to 70 wt % the trend is reversed, cork filled system showed the lowest tensile and tear strength and silica filled system showed the highest values. It can also be seen

from the table that the addition of carbon black adversely affects the properties in all cases. The treatment of silica with silane coupling agent improved the properties only in the case of 70 wt % of PP and in other two blend compositions the properties decrease.

Table 3.4. Mechanical properties of filled PP/NBR blends with 30 phr filler loading.

Sample	Tensile strength (MPa)	Tear strength (N/m)	Elongation at break (%)
P_{70}	18.30	89.00	95.68
$P_{70}C_{30}$	16.76	82.82	22.97
$P_{70}K_{30}$	19.02	95.54	8.38
$P_{70}Si_{30}$	15.95	86.44	26.44
$P_{70}TSi_{30}$	16.89	91.89	28.35
P_{50}	9.20	50.00	43.45
$P_{50}C_{30}$	8.05	39.77	44.70
$P_{50}K_{30}$	9.73	45.05	18.47
$P_{50}Si_{30}$	8.05	39.60	44.23
$P_{50}TSi_{30}$	7.59	34.81	34.38
P_{30}	3.50	21.00	38.64
$P_{30}C_{30}$	2.97	18.16	11.64
$P_{30}K_{30}$	2.64	16.88	8.23
$P_{30}Si_{30}$	4.06	28.60	21.29
$P_{30}TSi_{30}$	3.41	19.10	13.52

The effect of filler loading on mechanical properties was also studied. The stress-strain curves of unvulcanised P_{50} blends with 10, 20 and 30 phr loading of carbon black and silica are shown in Figures 3.24a and 3.24b respectively. From

Table 3.5. Mechanical properties of filled P_{50} blends.

Sample	Tensile strength (MPa)		Tear strength (N/m)		Elongation at break (%)	
	Unvulca-nised	Vulca-nised	Unvulca-nised	Vulca-nised	Unvulca-nised	Vulca-nised
P_{50}	9.20	9.88	50.00	47.64	43.14	17.76
$P_{50}Si_{10}$	10.28	8.67	53.13	45.10	39.60	37.35
$P_{50}Si_{20}$	9.21	8.03	42.31	44.76	58.47	24.52
$P_{50}Si_{30}$	8.05	8.34	39.60	49.38	39.30	55.94
$P_{50}TSi_{10}$	9.94	9.06	46.40	54.00	55.47	12.14
$P_{50}TSi_{20}$	8.43	10.37	42.00	51.14	44.67	41.97
$P_{50}TSi_{30}$	7.59	8.45	34.81	49.60	34.38	32.26
$P_{50}K_{10}$	9.55	10.53	48.54	46.18	32.26	14.76
$P_{50}K_{20}$	8.81	10.35	49.24	45.05	38.35	26.21
$P_{50}K_{30}$	9.73	9.00	45.05	37.94	18.47	18.44
$P_{50}C_{10}$	10.05	9.22	49.66	45.68	47.70	28.97
$P_{50}C_{20}$	7.97	9.08	41.24	40.20	35.26	41.80
$P_{50}C_{30}$	8.05	8.31	39.77	35.12	44.70	31.58

3.3 References

1. B. M. Walker (Ed.), *Handbook of Thermoplastic Elastomers*, Van Nonstrand Reinhold, New York, 1979.
2. S. K. De and A. K. Bhowmick (Eds.), *Thermoplastic Elastomers from Rubber-Plastic Blends*, Ellis Horwood, New York, 1990.
3. A. Y. Coran, *Handbook of Elastomers—New Development and Technology* (Eds., A. K. Bhowmick and H. L. Stephens), Marcel Dekker, New York, 1988, p. 249.
4. S. Thomas, S. K. De and B. R. Gupta, *Kauts. Gummi Kunst.*, **40**, 7, 665 (1987).
5. S. Danesi and R. S. Porter, *Polymer*, **19**, 448 (1978).

the curves it is seen that the incorporation of fillers did not improve the modulus, for all loadings. However, the nature of stress-strain curves are not changed with filler addition, i.e., filled samples also show elastic and inelastic sections, with yielding in the inelastic section. The tensile strength, tear strength and elongation at break values of the blends are given in Table 3.5 for both unvulcanised and vulcanised blends. The addition of 10 phr silica, T-silica, cork and carbon black increased the tensile strength values, however further addition reduces the values; for both crosslinked and uncrosslinked blends. It is also seen from the table that in the case of crosslinked filled blends, the treatment of silica with silane coupling agent improved the tensile and tear properties.

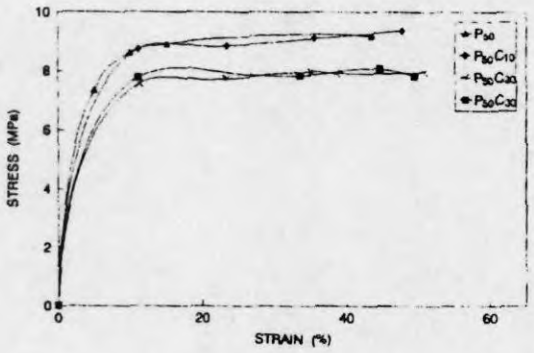

(a)

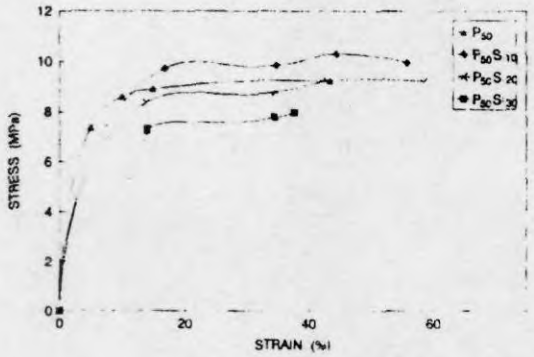

(b)

Figure 3.24. Stress-strain curves of P_{50} blends with (a) carbon black and (b) silica.

6. F. C. Stehling, T. Huff, C. S. Speed and G. Wissler, *J. Appl. Polym. Sci.*, **26**, 2693 (1981).

7. J. Jancar, A. Di Anselmo, A. T. Di Benedetto and J. Kucera, *Polymer*, **34**, 8, 1684 (1993).

8. B. D. Favis, *J. Appl. Polym. Sci.*, **39**, 285 (1990).

9. E. N. Kresge, *J. Appl. Polym. Sci. Appl. Polym. Symp.*, **39**, 37 (1984).

10. D. S. Campbell, D. J. Elliot and M. A. Wheelans, *NR Technol.*, **9**, 21 (1978)

11. B. Kuriakose and S. K. De, *Polym. Eng. Sci.*, **25**, 630 (1985).

12. S. Akhtar, P. P. De and S. K. De, *Mater. Chem. Phys.*, **12**, 235 (1985).

13. A. Y. Coran, R. Patel and D. Williams, *Rubb. Chem. Technol.*, **55**, 116 (1982a).

14. S. Thomas, S. K. De and B. R. Gupta, *Kauts. Gummi Kunst.*, **40**, 665 (1987).

15. S. Thomas, B. R. Gupta and S. K. De, *J. Mater. Sci.*, **22**, 3209 (1987).

16. B. Kuriakose and S. K. De, *Int. J. Polym. Mater.*, **11**, 101 (1986).

17. E. N. Kresge, *J. Appl. Polym. Sci. Polym. Symp.*, **39**, 37 (1984).

18. R. Greco, C. Mancarella, E. Martuscelli, G. Ragosta and J. Jinghua, *Polymer*, **28**, 1929 (1987).

19. A. K. Gupta and B. K. Ratnam, *J. Appl. Polym. Sci.*, **42**, 297 (1991).

20. A. Y. Coran and R. Patel, *Rubber Chem. Technol.*, **56**, 1045 (1983b).

21. N. C. Liu, H. Q. Xie and W. E. Baker, *Polymer*, **34**, 4680 (1993).

22. K. C. Dao, *Polymer*, **25**, 1527 (1984).

23. D. Heikens and Barentsen, *Polymer*, **18**, 69 (1977).

24. Z. K. Walczak, *J. Appl. Polym. Sci.*, **17**,169 (1973).

25. E. Martuscelli, C. Silvestre and G. Abate, *Polymer*, **23**, 229 (1982).

26. J. Karger-Kocsis, L. Kiss and Kuleznev, *Int. Polym. Sci. Technol.*, **8**, T/21 (1981).

27. S. Thomas, *Mater. Lett.*, **5**, 9, 360 (1987).

28. N. E. Nielsen, *Rheol. Acta*, **13**, 86 (1974).

29. J. C. Halpin, *J. Compos. Mater.*, **3**, 732 (1970).

30. S. Wu, *Polym. Eng. Sci.*, **27**, 335 (1987).

31. S. Thomas and R. E. Prud'homme, *Polymer*, **33**, 4260 (1992).

32. J. M. Willis, B. D. Favis, *Polym. Eng. Sci.*, **30**, 1073 (1990).

33. H. A. Spiros, I. Gancarz and J. T. Koberstein, *Macromolecules*, **22**, 1449 (1989).

34. R. Fayt, R. Jerome and Ph. Teyssie, *Makromol. Chem.*, **187**, 837 (1986).

35. J. Noolandi, *Polym. Eng. Sci.*, **24**, 70 (1984).

36. J. Noolandi and K. M. Hong, *Macromolecules*, **15**, 482 (1982).

37. J. M. Willis and B. D. Favis, *Polym. Eng. Sci.*, **28**, 1416 (1988).

38. Z Oommen, S. Thomas and M. R. G. Nair, *Polym. Eng. Sci.*, **36**, 1 (1996).

39. F. Ide and A. Hasegawa, *J. Appl. Polym. Sci.*, **18**, 963 (1974).

40. R. N. Santra, B. K. Samantaray, A. K. Bhowmick and G. B. Nando, *J. Appl. Polym. Sci.*, **49**, 1145 (1993).

41. G. B. Bucknall and R. R. Smith, *Polymer*, **6**, 437 (1965).

42. J. A. Schmitt and H. Keskkula, *J. Appl. Polym. Sci.*, **3**, 132 (1960).

43. B. Kuriakose, S. K. De, S. S. Bhagawan, R. Sivaramakrishnan and S. K. Athithan, *J. Appl. Polym. Sci.*, **32**, 5509 (1986).

Chapter 4

Dynamic Mechanical Properties: Effects of Blend Ratio, Reactive Compatibilisation and Dynamic Vulcanisation

---

The results of this chapter have been published in
Journal of Polymer Science Part B Polymer Physics,
35, 2309 (1997)

4.1 Introduction

Miscibility between two polymers is usually characterised by dynamic mechanical analysis or viscoelastic data. The viscoelastic properties like storage modulus, loss modulus and loss tangent of polymer depend on structure, crystallinity, extent of crosslinking, etc.[1] Karger-Kocsis and Kiss[2] have investigated the effect of morphology on the dynamic mechanical properties of PP/EPDM blends. The presence of two phase morphology and two separate damping peaks for blend components remaining at their original positions in the dynamic mechanical spectrum indicated the incompatibility of the system. Influence of microstructure on the viscoelastic behaviour of polycarbonate/styrene acrylonitrile copolymer (PC/SAN) blend has been studied by McLaughlin[3] and Guest and Daly.[4] The compatibility of polycarbonate with polystyrene and polyester was investigated by Li *et al.*[5] using dynamic mechanical and DSC measurements. Their investigations indicated that the PS/PC system is partially miscible since the Tg values corresponding to PC and PS are composition dependent. Wippler[6] reported on the dynamic mechanical properties of PC/PE blends. They have used Takayanagi model to predict the behaviour of experimental storage modulus.

The effect of polychloroprene (CR) content on the storage moduli of ABS was reported by Kang *et al.*[7] They found that the storage moduli of the blends increase with increase in CR content. Recently, the influence of blend composition on the viscoelastic properties of NR-EVA and NBR-EVA blends has been investigated.[8,9] The damping factors of these blends are found to increase with increase in rubber content, and this behaviour has been correlated with the phase morphology of the system.

The miscibility of poly(vinyl chloride) (PVC) with 50% epoxidised natural rubber (ENR) was investigated by Varughese *et al.*[10] using dynamic mechanical and DSC measurements. These blends showed a single Tg lying between the Tg's of pure components, which indicated the miscibility of the system. They also found that a moderate level of broadening of glass transition temperature region occurs with increasing PVC concentration.

The effect of compatibilisation on the dynamic mechanical properties of various polymer blends has been reported.[11-15] The investigations of Brahimi *et al.*[11] indicated that the addition of pure and tapered diblock copolymers into PE/PS blends enhances the phase dispersion and interphase interactions of these blends and that the addition of excess copolymer create micelles. Ramesh and De[12] investigated the effect of carboxylated nitrile rubber as a reactive compatibiliser in PVC/ENR blends in terms of dynamic mechanical data. The DMA results indicated that an immiscible composition of PVC/ENR blends becomes progressively miscible by the addition of XNBR. The addition of ethylene-methyl acrylate copolymer as a compatibiliser in LDPE/PDMS blends was found to shift the Tg values corresponding to the homopolymers.[13] Cohen and Ramos[15] have used the mechanical model of Takayanagi to describe the viscoelastic behaviour of binary

and ternary blends of cis-1,4-polyisoprene, 1,4-polybutadiene and the polyisoprene-polybutadiene block copolymer.

The effect of static and dynamic vulcanisation on the dynamic mechanical properties of polymer blends has been reported.[8,16-18] Kuriakose *et al.*[16] investigated the effect of dynamic vulcanisation of PP/NR blends on the viscoelastic properties. They found that the increase in storage modulus and decrease in loss modulus becomes more remarkable as extent of crosslinking increases. Thomas *et al.*[8] investigated the effect of dynamic vulcanisation on the dynamic mechanical properties of NR/EVA blends. Liao *et al.*[17] reported that the damping characteristics of the dynamically cured IIR/PP blend depend on blend composition and the curative level. PVC/ENR blends upon dimaleimide vulcanisation showed a lowering in storage and loss moduli in the glassy zone. The damping peak became narrow upon dynamic vulcanisation.[18]

In many practical applications, since the materials usually undergo cyclic stressing, the study of viscoelastic properties are very important. In this chapter the effect of blend composition and morphology on dynamic mechanical properties of PP/NBR blends have been investigated. The effect of compatibiliser concentration and dynamic vulcanisation was also investigated. The dynamic mechanical properties have been correlated with the morphology of the blend. Attempts have also been made to predict the experimental dynamic mechanical properties using existing theoretical models.

4.2 Results and discussion

4.2.1 *Binary blends*

The dynamic mechanical properties such as storage modulus (E′), loss modulus (E″) and damping (tan δ) of the pure components and the blends were

evaluated from -50 to 150°C. Figures 4.1–4.3 show the variation of tan δ, E″ and E′ Vs temperature for the homopolymers. The tan δ curve of nitrile rubber shows a peak at -16°C due to the α-transition arising from the segmental motion. This corresponds to the glass transition temperature (Tg) of nitrile rubber. Polypropylene shows glass transition temperature at 25°C, as shown by a tan δ peak at 25°C in the tan δ Vs temperature curve. Nitrile rubber has higher damping than polypropylene because of its rubbery nature. The loss modulus (E″) curve also shows the presence of loss maxima for NBR and PP at -20 and 25°C, respectively (Figure 4.2).

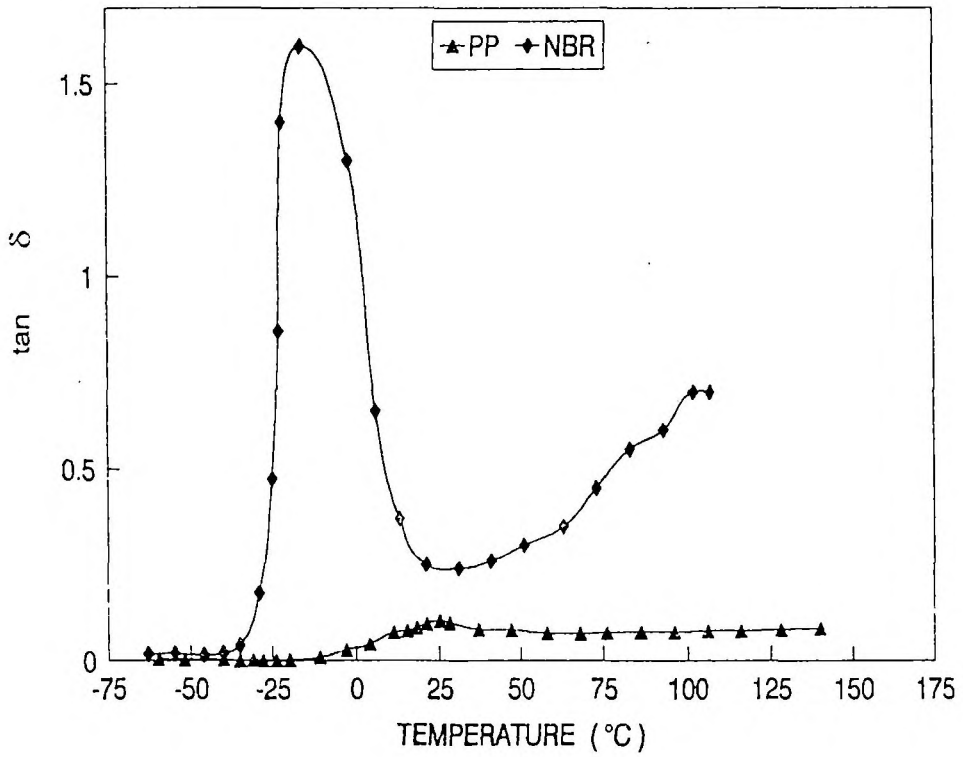

Figure 4.1. Variation of tan δ of PP and NBR with temperature.

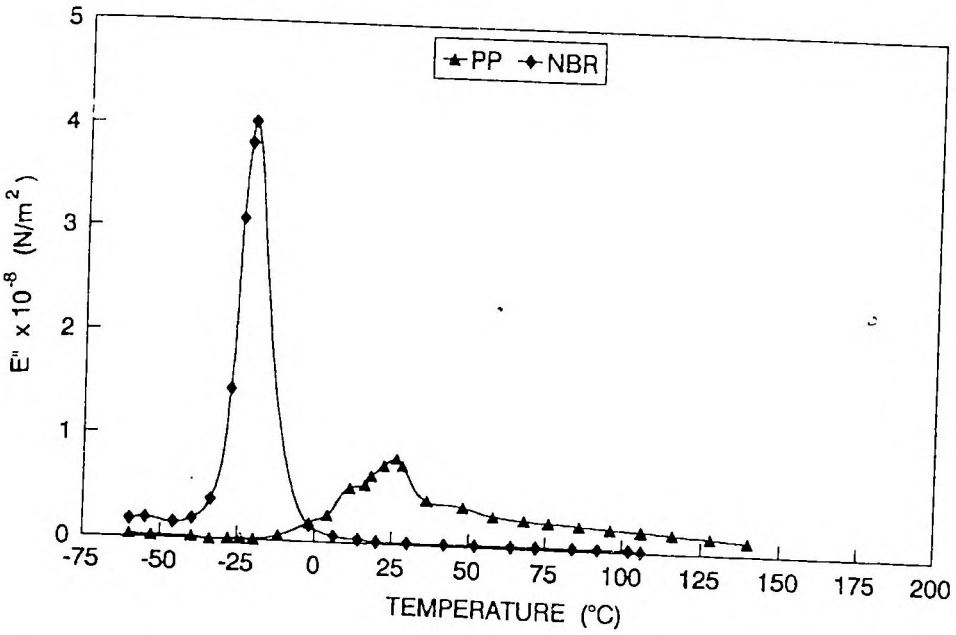

Figure 4.2. Variation of loss modulus (E″) of PP and NBR with temperature.

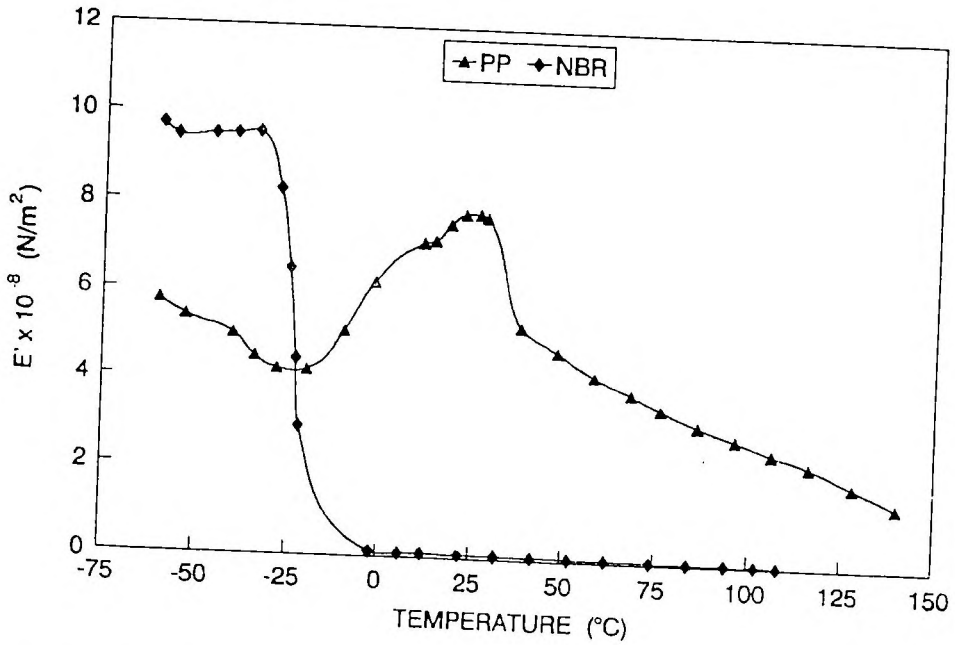

Figure 4.3. Variation of storage modulus (E′) of PP and NBR with temperature.

Nitrile rubber has higher storage modulus than polypropylene below the Tg region and the trend is reversed beyond the relaxation stage. In the case of nitrile rubber, the storage modulus shows a drastic fall around Tg while for polypropylene, because of its crystalline nature, the modulus drop is at a slower rate. The higher modulus of NBR compared to PP below the transition region is due to the fact that at this stage the entire molecular chains of amorphous NBR is frozen to form a fully glassy state. As NBR undergoes transition from the fully formed glassy state to the rubbery state, the storage modulus decreases considerably. In crystalline materials, during transition, only the amorphous part undergoes segmental motion, while the crystalline region remains as solid until its temperature of melting (Tm). Hence in the case of polypropylene, due to its crystalline nature, the storage modulus drops only at a lesser extent than that in NBR during the relaxation process.

Dynamic mechanical data was used to predict the miscibility of the system by various researchers.[10,19-21] If two polymers are not compatible, the tan δ vs. temperature curve shows the presence of two separate damping peaks corresponding to the glass transition temperatures of individual polymers.[19] For a highly compatible blend the curve will show only a single peak[10] lying between the Tgs of the component polymers, whereas in partially compatible system a broadening of Tg is noticed.[21] In the case of compatible and partially compatible blends the Tgs are shifted to higher or lower temperatures as a function of composition. The variation of tan δ with temperature of PP/NBR blends is shown in Figure 4.4. The blends show two tan δ peaks around -20°C and +20°C, which correspond to the Tgs of nitrile rubber and polypropylene, respectively. Two separate peaks corresponding to the Tgs of PP and NBR indicate that the blends are not compatible. The Tg corresponding to PP component is shifted to lower

temperature on the addition of NBR. This may be due to the plasticizing effect of NBR, by which the chain mobility of PP is increased. The damping of the blends increases with increase in concentration of nitrile rubber The variation of tan δ_{max} of the blends as a function of NBR content is shown in Figure 4.5. The increase in the damping and tan δ_{max} with increase in NBR content is due to the reduction in the crystalline volume of the system on increasing the concentration of NBR whose damping is always higher than PP. The variation of tan δ_{max} is more pronounced above 50 wt % of NBR. This behaviour can be explained in terms of the morphology of the blends. In P_{70} and P_{50}, the NBR phase is dispersed as domains in the continuous PP matrix. In P_{30}, the NBR phase also forms a continuous phase resulting in a co-continuous morphology (Figure 3.2). Since above 50 wt % of NBR, it forms continuous phase, the tan δ_{max} shows a pronounced variation due to the higher contribution of tan δ_{max} from NBR phase.

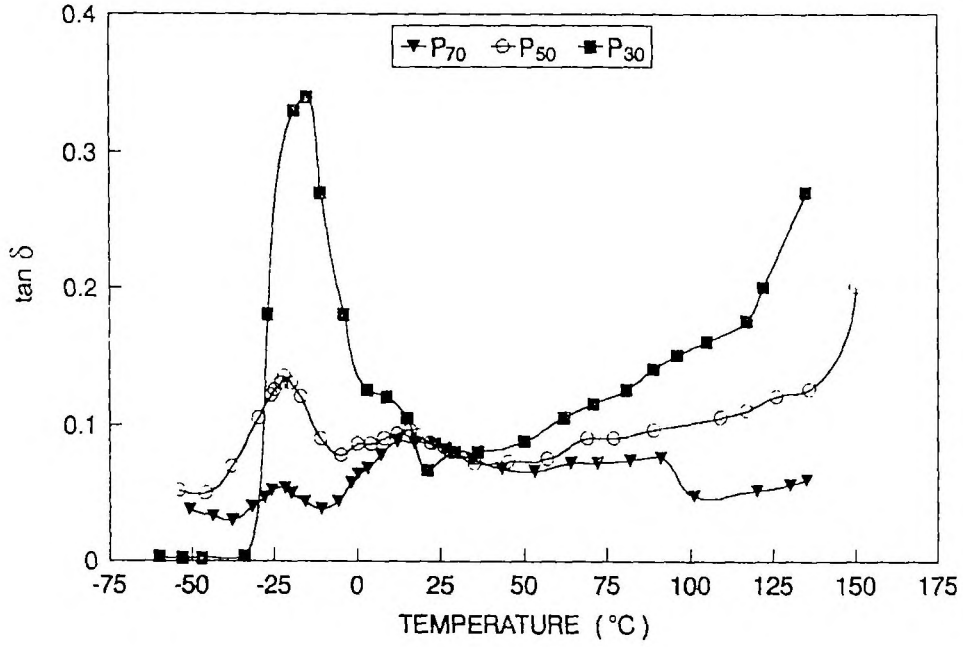

Figure 4.4. Variation of tan δ of PP/NBR binary blends with temperature.

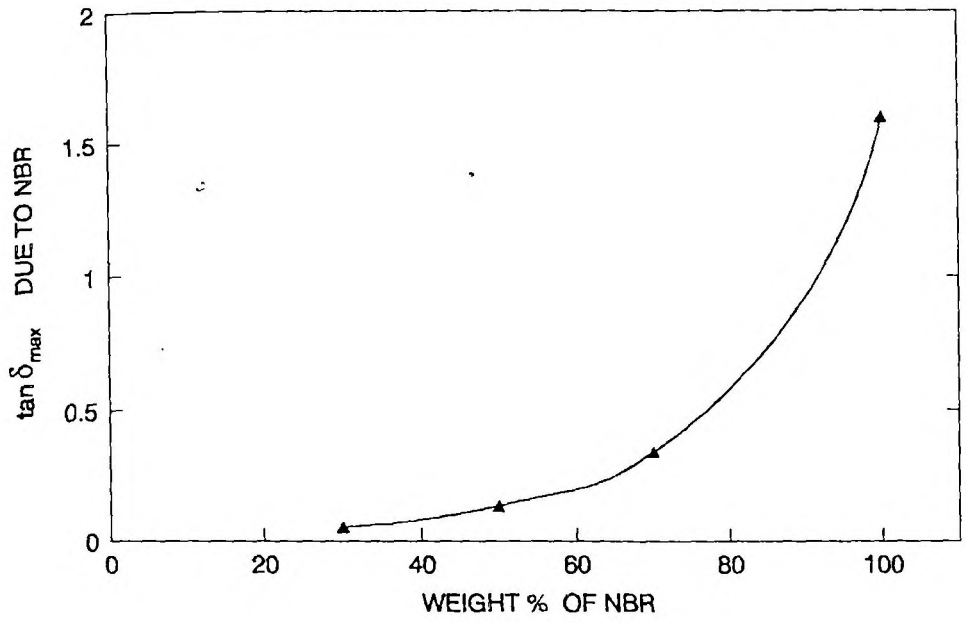

Figure 4.5. Variation of tan δ_{max} due to NBR of PP/NBR binary blends with wt % of NBR.

The variation of storage modulus E′ of various blends as a function of temperature is shown in Figure 4.6. As in the case of blend components the modulus of the blends decreases with increase in temperature. It is seen from this figure that the modulus of the blends decreases with increase in NBR content. At the glassy region, E′ becomes higher for high NBR blends and its value drops down several decades faster above Tg. This behaviour can be attributed to the better glass forming characteristics of NBR with a higher degree of modulus value. Thus, P_{30} in which NBR is also distributed as continuous phase, has the higher storage modulus below the transition region than the other ones in which NBR is in the form of dispersed phase only. Above the transition region, E′ is higher for low NBR blends due to the influence of crystalline PP.

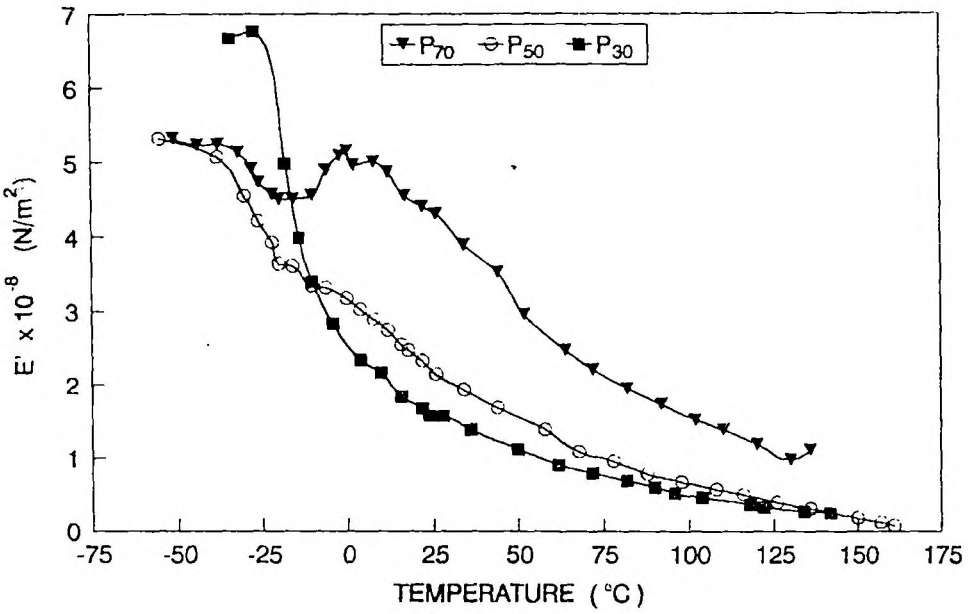

Figure 4.6. Variation of storage modulus (E′) of binary PP/NBR blends with temperature.

Figure 4.7 shows the variation of storage modulus at 30°C as a function of NBR content. As we have already discussed the modulus decreases with increase in rubber concentration and the curve shows a negative deviation from the additivity line. This negative deviation is due to the lack of interfacial interaction and adhesion between the non-polar crystalline PP and polar nitrile rubber phases. The curve shows a slope change from P_{50} to P_{30} due to the phase inversion of NBR from dispersed to continuous phase.

The variation of loss modulus with temperature (Figure 4.8) also shows the same trend as that of tan δ, i.e., the curves show two maxima corresponding to the glass transition temperatures of polypropylene and nitrile rubber. The loss modulus also increases with increase in NBR content.

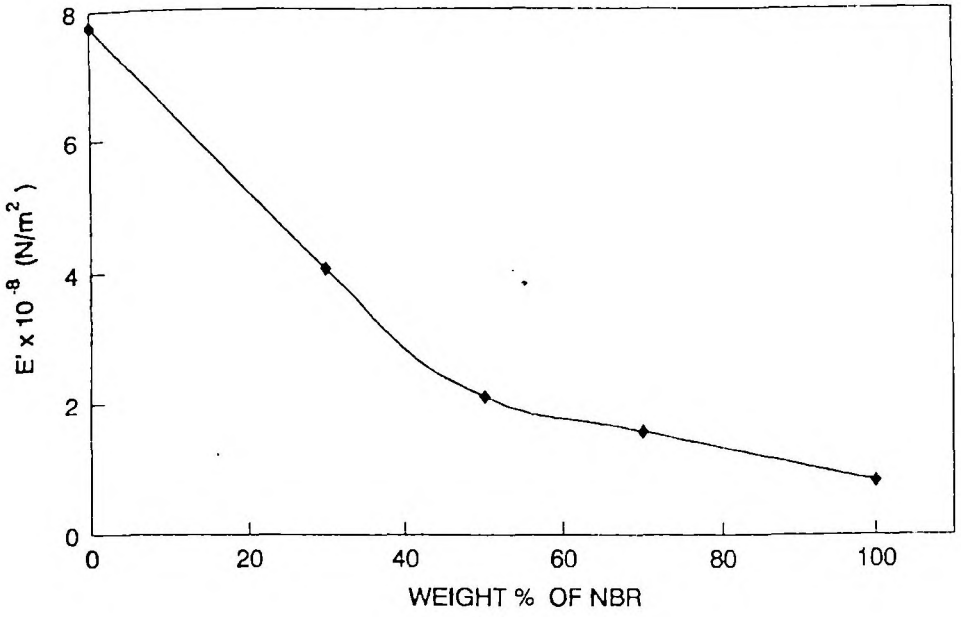

Figure 4.7. Variation of storage modulus (E') of binary PP/NBR blends with wt % of NBR at 30°C.

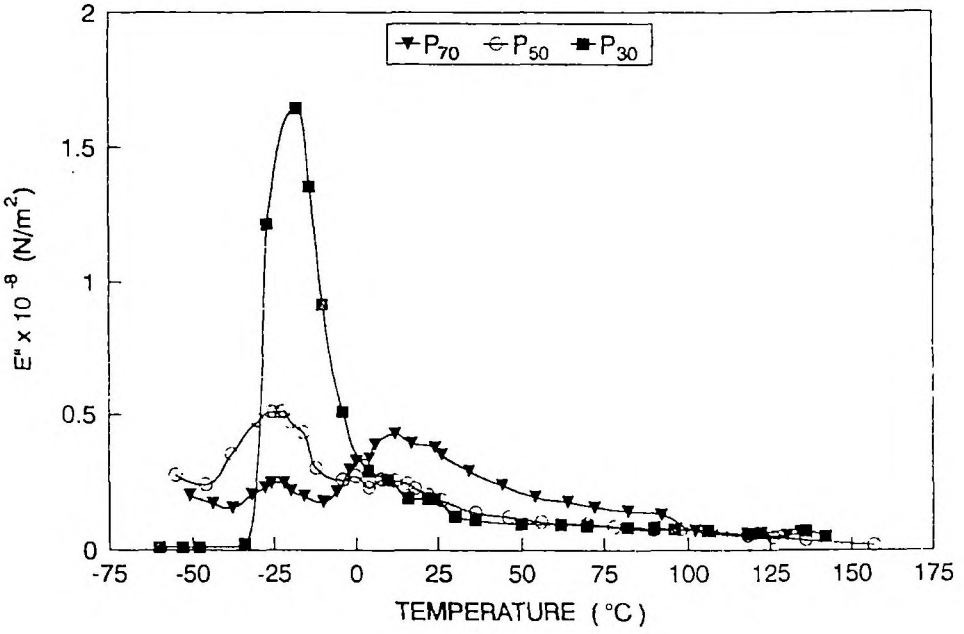

Figure 4.8. Variation of loss modulus (E") of binary PP/NBR blends with temperature.

4.2.2 *Modelling of viscoelastic properties*

Various composite models such as parallel, series, Halpin-Tsai, Coran's and Takayanagi's models have been applied to predict the viscoelastic behaviour of the binary blends. The storage modulus of PP/NBR blends was calculated for parallel, series, Halpin-Tsai and Coran's model using equations (3.2-3.6).

The viscoelastic behaviour of heterogeneous polymer blends can be predicted using Takayanagi's model. The Takayanagi model is given by[15]

$$E^* = (1-\lambda)E_M^* + \left[\left\{(1-\phi)/E_M^*\right\} + \left(\phi/E_N^*\right)\right]^{-1} \qquad (4.1)$$

where E^* is the complex modulus of blend; E_M^*, the complex modulus of matrix phase; E_N^*, the complex modulus of the dispersed phase; and $\lambda\phi$, the volume fraction of the dispersed phase and the values of λ and ϕ related to the degree of series-parallel coupling.

As suggested by Cohen and Ramos, degree of parallel coupling of the model can be expressed by

$$\% \text{ parallel} = [\phi(1-\lambda)/(1-\phi\lambda)] \times 100 \qquad (4.2)$$

Figure 4.9 shows the experimental and theoretical curves of storage modulus of PP/NBR blends as a function of NBR volume fraction. As expected the storage modulus values of these blends lie in between those of parallel and series models. The experimental values are close to Halpin-Tsai and Coran model ($n = 2.2$) up to 50 wt % NBR. In the case of Takayanagi model, which is widely used for the prediction of viscoelastic data, the experimental values can be described with 20% parallel coupling. However for the P_{30} blend the experimental values are higher than those obtained from any other theoretical models. This may be due to the fact that all theoretical values are calculated, based on the assumption that NBR phase is dispersed in the continuous PP matrix. But in the case of P_{30},

the NBR also forms a continuous phase leading to a co-continuous morphology of the blend (Figure 3.2c).

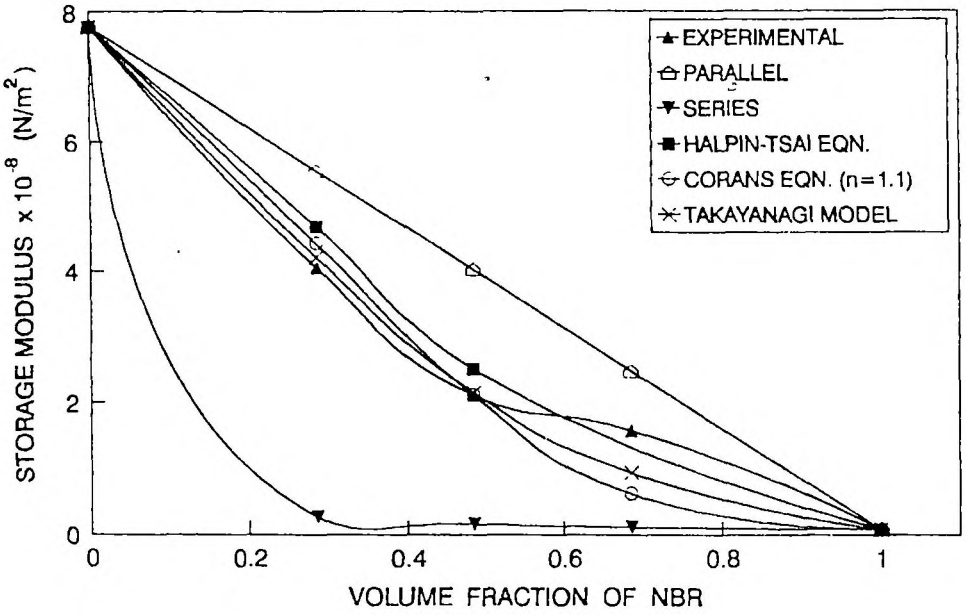

Figure 4.9. Experimental and theoretical curves of storage modulus of binary PP/NBR blends as a function of wt % of NBR at 30°C.

4.2.3 Effect of compatibilisation

The variation of storage modulus as a function of temperature of 70/30 PP/NBR blends compatibilised with different concentrations of phenolic modified polypropylene is shown in Figure 4.10. With the addition of 3% Ph-PP the modulus of the unmodified blend is increased at lower temperatures i.e., below glass transition temperature. However with further addition of compatibiliser (7.5 and 10 wt % Ph-PP) the storage modulus is decreased from the levels of P_{70} containing 3% Ph-PP. The increase in the modulus with the addition of 3% Ph-PP is due to the increase in the interfacial adhesion caused by the emulsifying effect of the block copolymer formed by the interaction between the phenolic modified

polypropylene and nitrile rubber (Figure 3.16). The better interaction between PP and NBR in presence of Ph-PP is evident from the morphology observed in SEM micrographs (Figure 3.8) At lower concentration of compatibiliser, the average domain size of NBR particles decreased due to interfacial tension reduction and high interfacial interaction. The decrease in modulus at higher concentration of the copolymer is due to the formation of micelles of the compatibiliser in the polypropylene matrix. As the micelle formation starts some of the copolymer already at the interface leaves the interface. This increases the domain size. Similar behaviour has been reported in the compatibilisation of PS/PE blends by PS-b-PE copolymers [11] Brahimi *et al.*[11] reported that the modulus of PE/PS blend increased by compatibilisation using PS-PE block copolymers up to interface saturation concentration and after that the modulus decreased. At higher temperatures all the blends of PP/NBR showed approximately the same modulus.

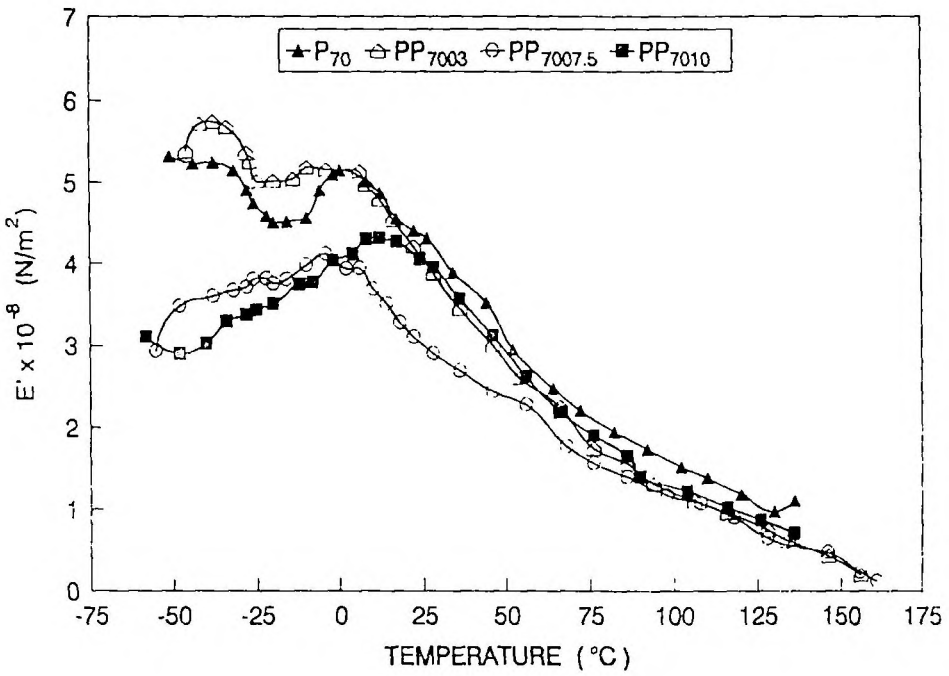

Figure 4.10. Variation of storage modulus (E') of Ph-PP compatibilised PP/NBR blends with temperature.

Figure 4.11 depicts the variation of storage modulus E′ of 70/30 PP/NBR blend compatibilised with maleic anhydride modified polypropylene. In this case also the addition of 1% maleic anhydride modified polypropylene increases the modulus of the blend as compared to the unmodified one at lower temperatures i.e., below grass transition temperature of PP. At high temperatures the values are lower than the P_{70} blend. When the concentration of MA-PP is increased to 10% the modulus shows lower values than that of P_{70} At higher temperatures it shows values higher than that of the blend modified with 1% MA-PP. At temperatures above 50°C all the blends show nearly the same values of E′. In the modification of PP/NBR with maleic anhydride modified polypropylene (MA-PP), the MA-PP increases the interfacial interaction between PP and NBR by the dipolar interaction between polar maleic anhydride groups of MA-PP and polar NBR. The increased interaction at the interface may be the reason for the increase in the modulus upon the addition of 1% MA-PP. The further decrease in E′ by the addition of 10% MA-PP indicates the formation of micelles in the PP matrix. Here also, the increased interfacial interaction is evident from the small and uniform dispersion of NBR particles upon the addition of MA- PP. Above 1% MA-PP the domain size levelled off due to interfacial saturation (Figure 3.9).

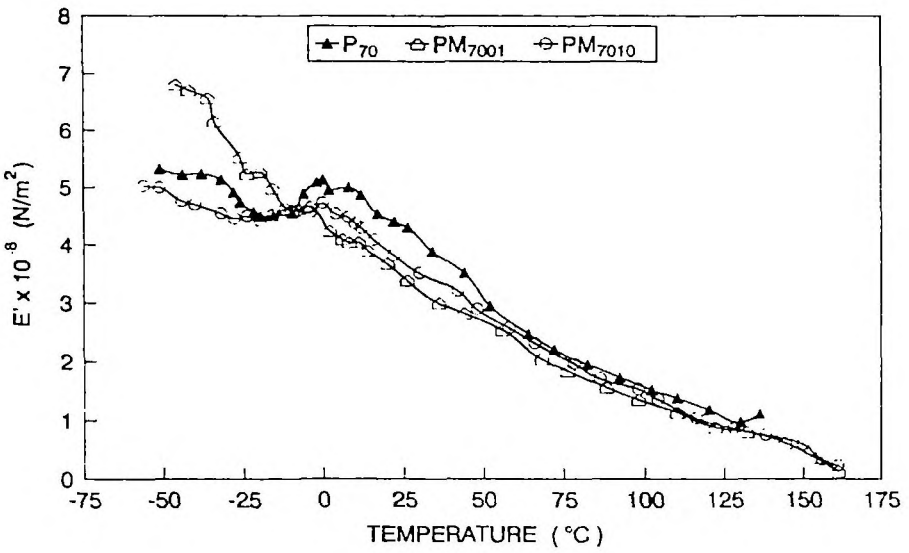

Figure 4.11. Variation of modulus (E′) of MA-PP compatibilised PP/NBR blends.

The variation of tan δ as a function of temperature of Ph-PP compatibilised blends is shown in Figure 4.12. The compatibilised blends also show the same behaviour for the tan δ curve as that of unmodified blend, i.e., the compatibilised blends show the presence of two maximas corresponding to the glass transition temperature of polypropylene and nitrile rubber. This indicates that the compatibilisation does not alter the level of miscibility. In other words, presence of a compatibiliser does not promote molecular level miscibility. This is in agreement with the conclusions made by Paul[22] who suggested that if two polymers are far from being miscible, then no copolymer is likely to make one phase system. In a completely immiscible system, the main role of the compatibiliser is to act as an interfacial agent. At lower temperatures the tan δ values show an increase for 3 and 7.5% of Ph-PP. However, at intermediate temperatures the tan δ values of these blends are lower than that of unmodified blend. When the concentration of Ph-PP is increased to 10% the tan δ values decrease and the values are lower than those of P_{70}. All the compatibilised systems show higher values of tan δ than unmodified blend at higher temperatures. This increase in tan δ indicates that the interfacial interaction caused by the presence of Ph-PP in PP/NBR blend may be weakened at higher temperatures. The decrease in interfacial interaction at higher temperature will decrease the interfacial adhesion and hence leads to increased segmental motion. The glass transition temperature corresponding to NBR remains unaltered by the incorporation of Ph-PP. However, Tg values corresponding to PP changes slightly with the incorporation of Ph-PP. On the addition of 3% Ph-PP, the Tg value remains the same as that of P_{70}. However, in the case of 7.5 and 10% Ph-PP incorporation, the Tg values shift to a slightly higher temperatures.

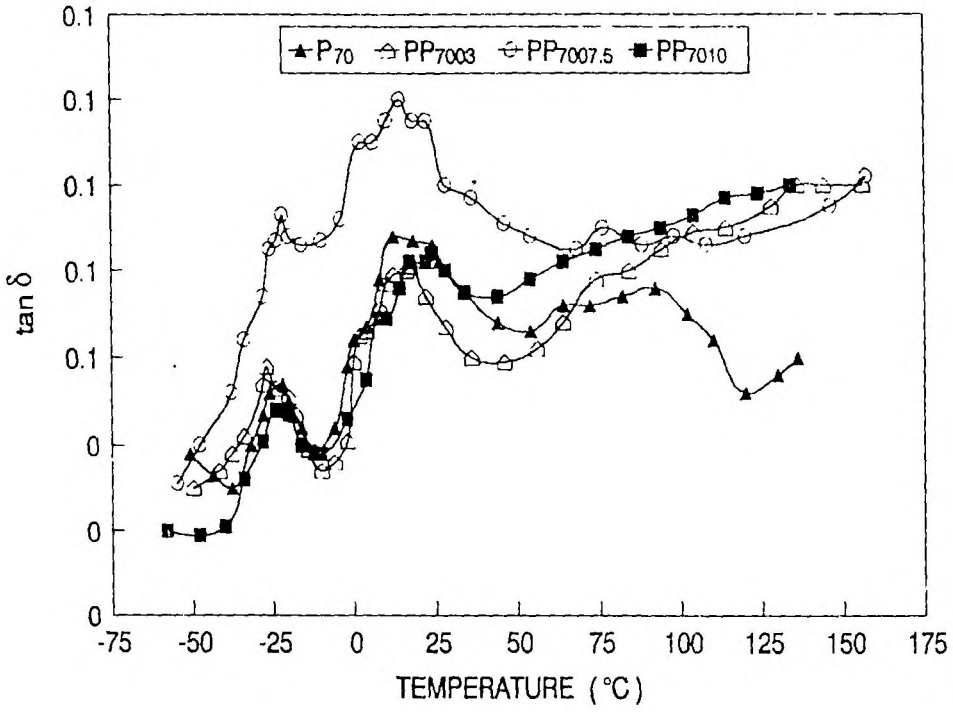

Figure 4.12. Variation of tan δ of Ph-PP compatibilised PP/NBR blends as a function of temperature.

The variation of tan δ of MA-PP compatibilised PP/NBR blends is shown in Figure 4.13 By the incorporation of 1% MA-PP, the tan δ values increase for the whole temperature range. When the concentration of MA-PP is increased to 10 wt % the tan δ shows an increase at lower temperature and at intermediate temperature it decreases. In this case also, the decrease in tan δ is due to the increase in interfacial interaction caused by the presence of MA-PP. The compatibilised blends have higher tan δ than the uncompatibilised system at higher temperatures

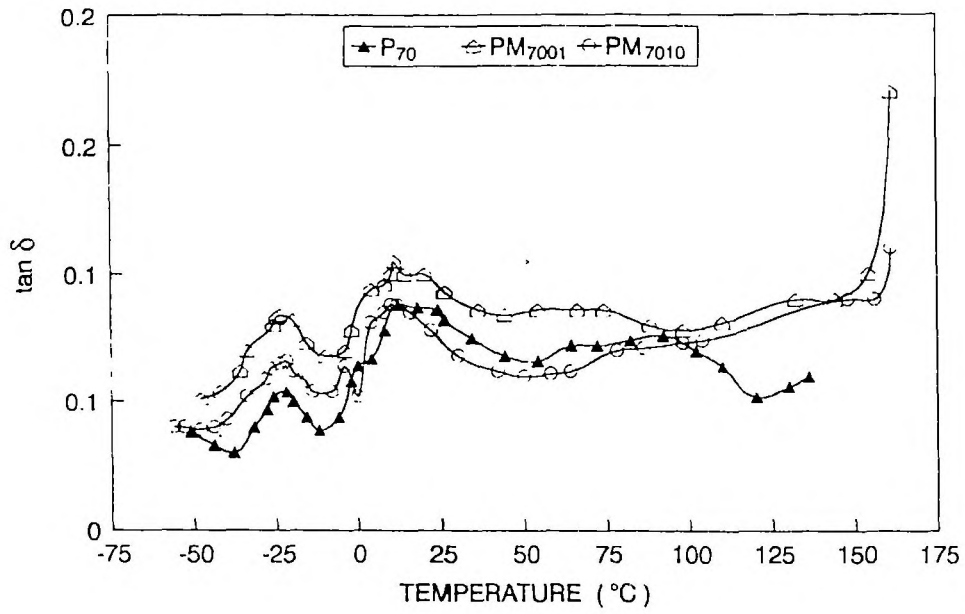

Figure 4.13. Variation of tan δ of MA-PP compatibilised PP/NBR blends as a function of temperature.

Figure 4.14 depicts the variation of loss modulus (E″) as a function of temperature of Ph-PP compatibilised blends The loss modulus shows a similar trend as that of tan δ curves. The E″ curves show the presence of two peaks corresponding to the glass transition temperature of PP and NBR. Similar to tan δ curves, here also the addition of 3 and 7.5% Ph-PP increases the E″. The values are lower than those of P_{70} at lower temperatures. At intermediate temperatures all the compatibilised blends show slightly lower E″ values than P_{70}.

In MA-PP compatibilised blends, the variation of loss modulus is shown in Figure 4.15. The behaviour is similar to tan δ curves. It shows the presence of two peaks corresponding to NBR and PP. At lower temperatures, 1 and 10% MA-PP modified blends show higher values of E″ than those of the unmodified blend. At intermediate temperature the values of E″ lie below that of unmodified blend. Here also at higher temperatures the compatibilised blends show higher values of E″.

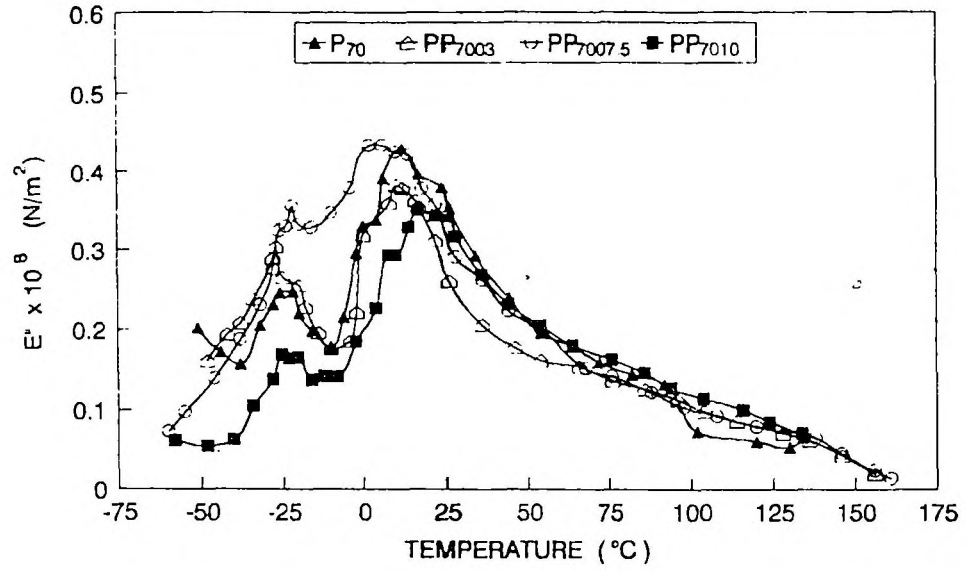

Figure 4.14. Variation of loss modulus (E″) of Ph-PP compatibilised PP/NBR blends as a function of temperature.

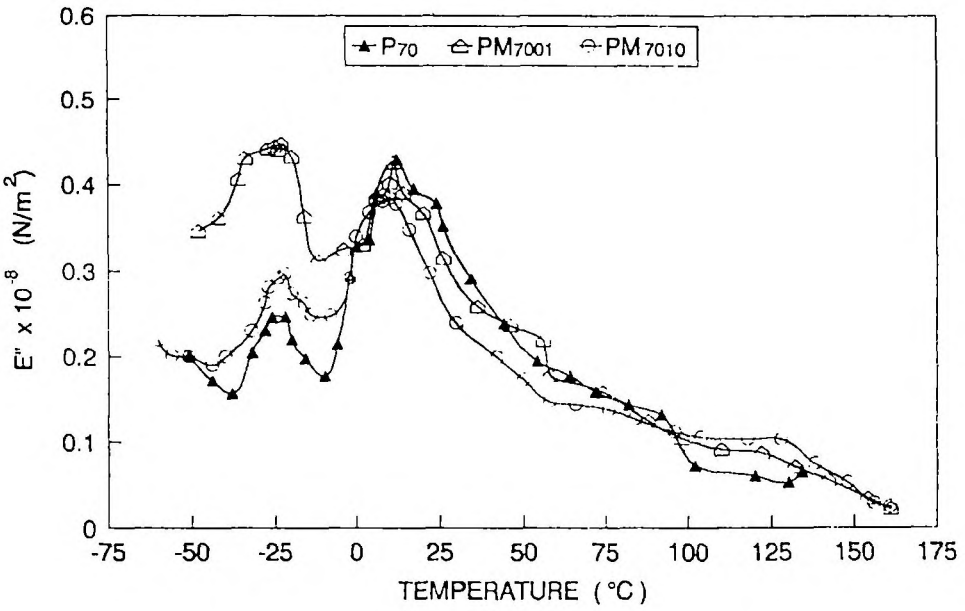

Figure 4.15. Variation of loss modulus (E″) of MA-PP compatibilised blends as a function of temperature.

4.2.4 *Effect of dynamic vulcanisation*

The variation of E′, E″ and tan δ of P_{70} blend crosslinked with sulphur, dicumyl peroxide and mixed systems are shown in Figures 4.16–4.18. The modulus of the blends vulcanised with DCP and mixed systems shows higher values than the uncrosslinked system, while the sulphur crosslinked system shows the lowest value In PP/NBR blends, on peroxide vulcanisation, there is a possibility of degradation of PP phase in the presence of DCP. However, the results from the figure indicates that the crosslinking reaction predominates over degradation reactions in the case of DCP vulcanisation. The increase in modulus for DCP system is also due to the crosslinking of NBR phase. In the case of sulphur system, sulphur crosslinks only the NBR phase and so shows the lowest modulus value. As expected the mixed system shows an intermediate behaviour.

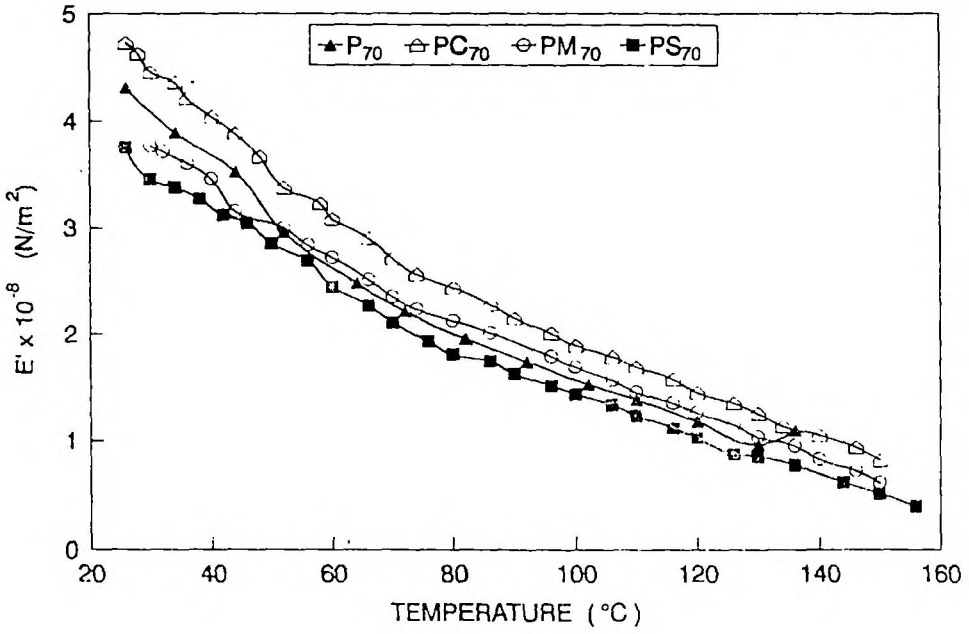

Figure 4.16. Variation of storage modulus (E′) of sulphur, DCP and mixed (DCP + sulphur) vulcanised 70/30 PP/NBR blends with temperature.

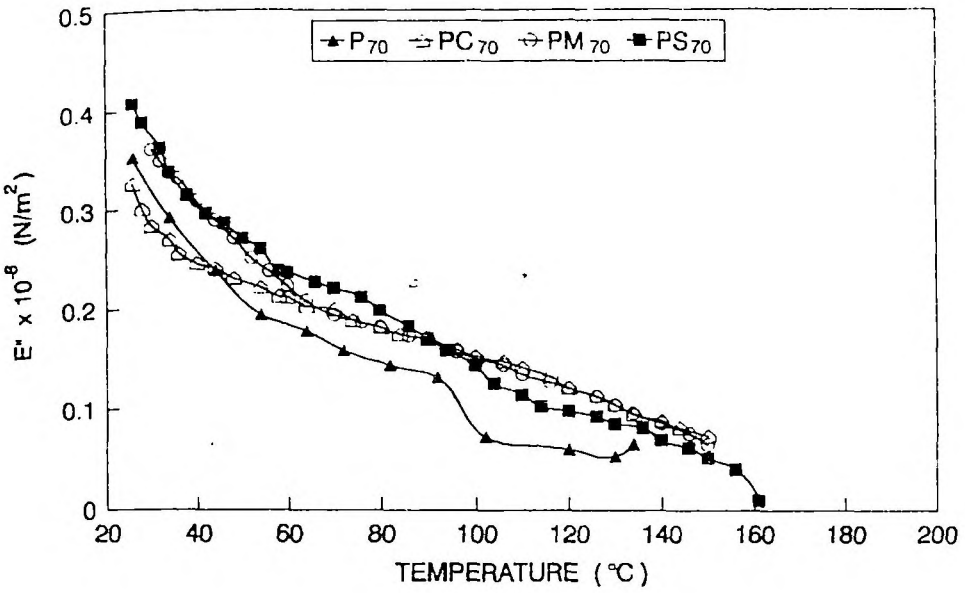

Figure 4.17. Variation of loss modulus (E″) of sulphur, DCP and mixed (DCP + sulphur) vulcanised PP/NBR blends with temperature.

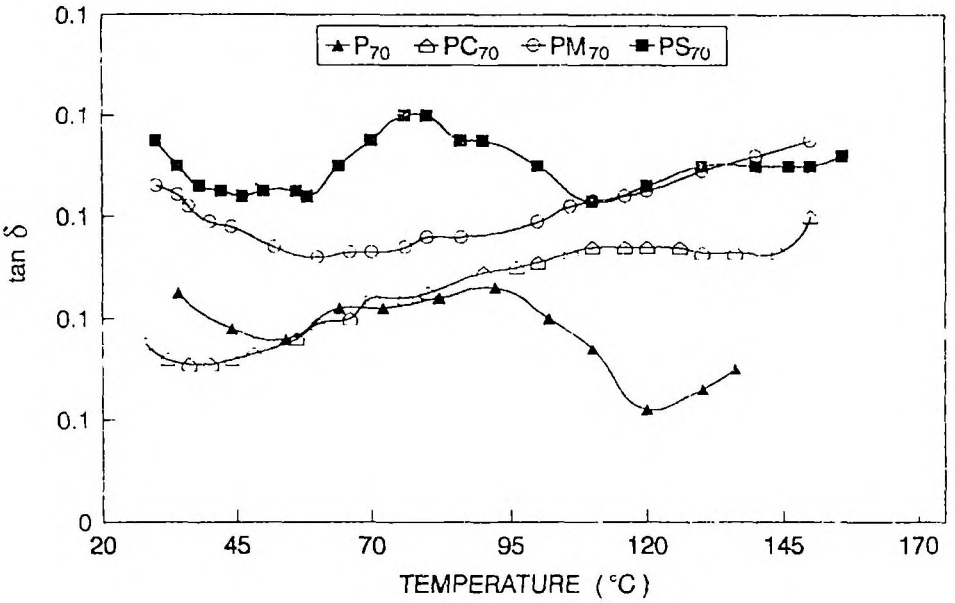

Figure 4.18. Variation of tan δ of sulphur, DCP and mixed (DCP + sulphur) vulcanised PP/NBR blends with temperature.

The loss modulus values of the vulcanised systems shown in Figure 4.17 indicate that the loss modulus increases upon vulcanisation. Here also DCP system shows the lowest E″ and sulphur system shows the highest E″ values. The mixed system shows intermediate behaviour.

The variation of tan δ with temperature (Figure 4.18) also shows the same trend as that of loss modulus i.e., among the crosslinked samples, the DCP crosslinked system shows the lowest tan δ values and sulphur system the highest value. The mixed system shows intermediate values. In all cases the introduction of crosslinks increases the tan δ values.

The morphology obtained from scanning electron micrographs (Figure 3.21) indicates that the crosslinking is more effective in DCP vulcanised system as proved by the presence of fine and uniform distribution of rubber particles in this case. However, this effect of crosslinking is not so predominant on the properties of the peroxide vulcanised system due to the degradation of PP phase in presence of DCP.

4.3 References

1. T. M. Murayama (Ed.), *Dynamic Mechanical Analysis of Polymeric Materials*, Elsevier, New York, 1978.
2. J. Karger-Kocsis and L. Kiss, *Polym. Eng. Sci.*, **27**, 4, 254 (1987).
3. K. W. McLaughlin, *Polym. Eng. Sci.*, **29**, 22, 1560 (1989).
4. M. J. Guest and J. H. Daly, *Eur. Polym. J.*, **26**, 6, 603 (1990)
5. Y. Li and H. L. Williams, *J. Appl. Polym. Sci.*, **40**, 1891 (1990).
6. C. Wippler, *Polym. Eng. Sci.*, **30**, 17 (1990).
7. D. IL, Kang, C. S. Ha and W. J. Cho, *Eur. Polym. J.*, **28**, 6, 565 (1992).
8. A. T. Koshy, B. Kuriakose, S. Varghese and S. Thomas, *Polymer*, **34**, 3428 (1993).
9. H. Varghese, S. S. Bhagawan and S. Thomas, *Eur. Polym. J.*, **31**, 957 (1995).
10. K. T. Varughese, G. B. Nando, P. P. De and S. K. De, *J. Mater. Sci.*, **23**, 3894 (1988).

11. B. Brahimi, A. Ait-Kadi, A. Ajji and R. Fayt, *J. Polym. Sci. Part B. Polym. Phys.*, **29**, 946 (1991).

12. P. Ramesh and S. K. De, *J. Appl. Polym. Sci.*, **50**, 1369 (1993).

13. R N Santra, B. K. Samantaray, A. K Bhowmick and G. B. Nando, *J. Appl. Polym. Sci.*, **49**, 1145 (1993).

14. R M. Holsti-Miettinen, J. V. Seppala, O. T. Ikkala and I. T. Reima, *Polym. Eng. Sci.*, **34**, 5, 395 (1994).

15. R. E. Cohen and A. R. Ramos, *J. Macromol. Sci. Phys.*, **B17(4)**, 625 (1980)

16. B. Kuriakose, S. K. De, S. S. Bhagawan, R. Sivaramakrishnan and S. K. Athithan, *J. Appl. Polym. Sci.*, **32**, 5509 (1986).

17. F. S. Liao, A. C. Su and Tzu-Chien J Hsu, *Polymer*, **35**, 2579 (1994).

18. K. T. Varughese, P. P. De and S. K. Sanyal, *Die Angewandte Makromolekulare Chemie*, **182**, 73 (1990).

19. S. Thomas and A. George, *Eur. Polym. J.*, **28**, 145 (1992).

20. D. J. Walsh and J. S. Higgins, *Polymer*, **23**, 336 (1982).

21. S. Thomas, B. R. Gupta and S. K. De, *J. Vinyl Technol.*, **9**, 71 (1987).

22. D. R. Paul, S. Newman, Eds., *Polymer Blends*, Academic Press, New York, 1978.

Chapter 5

Rheological Properties: Effect of Blend Ratio, Reactive Compatibilisation and Dynamic Vulcanisation

---

The results of this chapter have been accepted for publication in *Polymer*

5.1 Introduction

For the last few decades, as the commercial importance of polymer blends are increasing, it is necessary to optimise the processing conditions required for each blend. Generally for homopolymers, the flow behaviour depends on the flow geometry and processing conditions like temperature, shear rate, time of flow etc. In the case of polymer blends, the flow behaviour becomes more complex and is influenced by additional factors like the miscibility of the system, morphology, interfacial adhesion and interfacial thickness. The complex rheological behaviour of polymer blends has been investigated by several researchers.[1-10] Utracki and Kamal[1] have reviewed the rheological behaviour of various polymer blends. Normally the melt viscosity of polymer blends shows three types of behaviour: (1) positive deviation behaviour (PDB) where the blend viscosities show a synergistic behaviour, i.e., blend viscosity is higher than the log additivity value; (2) negative deviation behaviour (NDB) where the blend viscosity shows a negative deviation from log additivity values; and (3) a positive-negative deviation behaviour (PNDB). In this case the same blend exhibits both positive and negative deviation behaviour depending on the composition, morphology and processing conditions.

The miscibility of polymer components has a significant effect on the flow behaviour of polymer blends. Kim and co-workers[2] investigated the effect of

miscibility on the rheological behaviour by studying the poly(methyl methacrylate) (PMMA)/acrylonitrile butadiene styrene copolymer (ABS) blends with ABS having different acrylonitrile content. Their studies showed that blends containing ABS with 24 and 27 wt % acrylonitrile content are miscible with PMMA, while ABS with 35 wt % acrylonitrile content is immiscible with PMMA. The rheological study of these blends indicated that the miscible blends showed viscosities lower than the additive values due to the dilution effect while immiscible blends with ABS rich phase showed positive deviation. Recently, in this laboratory the flow behaviours of various thermoplastic elastomer blends have been investigated by Thomas *et al.*[3,4] They found that in natural rubber (NR)/ poly(ethylene-co-vinyl acetate) (EVA) blends, at low concentration of EVA, the system showed positive deviation. This behaviour has been explained to be due to the strong interactions among EVA domains. At higher concentration of EVA a negative deviation was observed. The viscosity of the blend was found to increase with NR concentration. Such an increase in viscosity upon the incorporation of rubber in plastic phase has been reported in systems such as plasticised polyvinyl chloride (PVC)/epoxidised natural rubber (ENR), polypropylene (PP)/NR, high density polyethylene (HDPE)/NR and PP/ethylene propylene diene rubber (EPDM).[5-10] In PVC/ENR miscible blends, the observed negative deviation is attributed to the composition dependent plasticising effect of ENR.[5,6] Another important class of polymer blends whose rheological behaviour studied widely are those with liquid crystalline polymers and thermoplastics. In these types of blends, the melt viscosity decreases with the addition of liquid crystalline polymers.[11,12]

The addition of compatibilisers to polymer blends extensively affects their flow behaviour.[13-17] Chemical reactions occurring between the components of the blend upon compatibilisation generally increases the viscosity of the system. The viscosity of PP/polyamide (PA) blend was found to increase upon compatibilisation using maleic anhydride grafted styrene-ethylene-co-butylene-styrene copolymer (SEBS-g-MA), due to the chemical reactions taking place between amine and anhydride groups.[13] Germain *et al.*[14] reported the effect of a block copolymer on the

rheological behaviour of PP/PA blends. A dual flow behaviour was observed in these blends, i.e. at low shear rates the blend viscosity is higher than the matrix and at high shear rates, the viscosity is lower than matrix. They have correlated this behaviour with the morphology of the system and have used emulsion model to predict the behaviour at low shear rate region. The flow behaviour of PMMA/NR blends compatibilised with poly(methyl methacrylate) grafted natural rubber (PMMA-g-NR) copolymer was investigated in this lab by Thomas *et al.*.[17] The binary blends show positive deviation at low shear rates. On compatibilisation the viscosity of these blends was found to be increasing due to the high interfacial interaction.

Recently Okoroafor *et al.*[18] have analysed the viscosity of immiscible polymer blends using different rheological models of flow behaviour. In these models, the viscosity of polymer blend has contributions from both the viscosities of pure components and also from the viscosity of interphase. According to the authors, in mechanically mixed polymer blends in which the components have neither a strong interphase nor chemical interactions, the positive and negative deviation behaviours (PDB and NDB) entirely depend on the viscosity ratio, η_d/η_m. In the case of blends with an interphase, the synergism is related to both the viscoelastic properties of the interphase and its volume fraction (ϕ_i) in the blend.

The effects of dynamic vulcanisation on the rheological behaviour of various rubber-plastic blends have been investigated by several researchers.[19-22] It has been reported that the viscosity of the blends increased with increase in the curative concentration.[19] De *et al.*[7,20] investigated the effect of various vulcanising agents on the rheological behaviour of PP/NR and HDPE/NR blends.

In this chapter, the rheological properties of PP/NBR blends have been investigated. The dependence of blend ratio, compatibiliser concentration and dynamic vulcanisation on the flow characteristics have been studied. The morphology of the extrudates was also examined and correlated with the flow properties.

5.2 Results and discussion

5.2.1 *Effects of blend ratio and shear stress on viscosity*

The effect of shear stress on the viscosity of polypropylene, nitrile rubber and their binary blends at different shear rates are shown in Figure 5.1. The viscosities of pure components and their blends decrease with increase in shear stress indicating pseudoplastic flow behaviour. The pseudoplastic nature of polymers arises from the randomly oriented and entangled nature of polymer chains, which on application of high shear rates gets oriented and disentangled and results in reduction in viscosity. The nitrile rubber shows the highest viscosity and polypropylene the lowest. The viscosity of the NBR decreases at a lower rate than polypropylene and blends. At low shear rates PP shows higher viscosity than P_{70} and P_{50} and at high shear rates, the viscosity of blends lies in between that of the homopolymers.

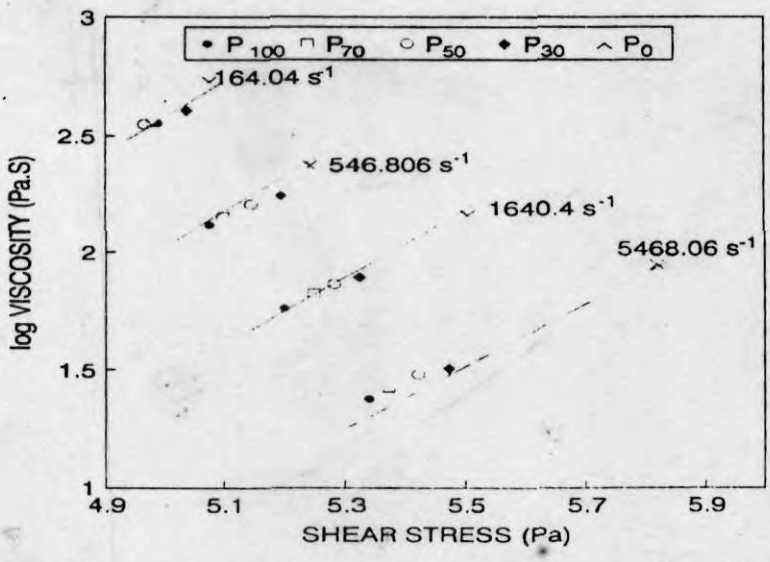

Figure 5.1. Effect of shear stress on melt viscosity of PP/NBR blends at different shear rates.

Figure 5.2 shows the variation of viscosity with blend composition at different shear rates. As the rubber content in the blend increases the blend viscosity is increased. Such an increase in viscosity on incorporation of rubber phase was already reported for several systems.[5-9] In polymer blends, since there is

interlayer slip along with orientation and disentanglement of chains on application of shear stress the viscosity depends on the interfacial thickness and adhesion in addition to the characteristics of component polymers. From Figure 5.2 it is seen that the PP/NBR blend viscosity shows negative deviation and indicates the incompatibility of the system. When a shear stress is applied to a blend it undergoes an elongational flow. If the interface is strong, deformation of the dispersed phase will be effectively transferred to the continuous phase. However, in the case of weak interphases the interlayer slip occurs and therefore the viscosity of the system decreases. The extent of negative deviation is more prominent at high shear rate region than at low shear rate region. It can be seen that viscosity increases marginally up to 50% NBR content, followed by a sharp increase at higher NBR content. This behaviour can be explained in terms of the morphology of the system. The SEM micrographs of cross-section of the extrudates of PP/NBR blends are shown in Figure 5.3. In P_{70} and P_{50}, NBR is dispersed as spherical domains with number average diameter 8.16 and 11.59 μm respectively in the continuous PP matrix, while in P_{30}, NBR also forms continuous phase resulting in a co-continuous morphology. The co-continuous nature of PP and NBR in P_{30} is responsible for the sharp increase in viscosity in this blend.

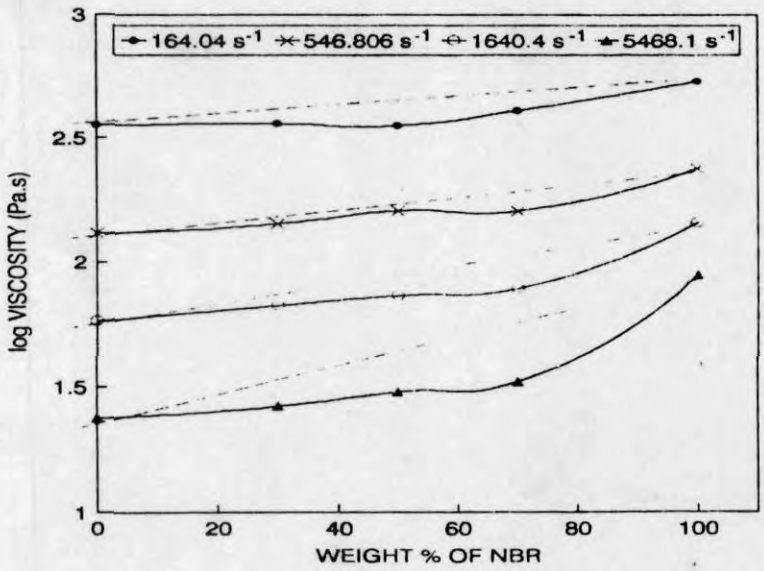

Figure 5.2. Variation of melt viscosity of PP/NBR blend with NBR concentration at different shear rates.

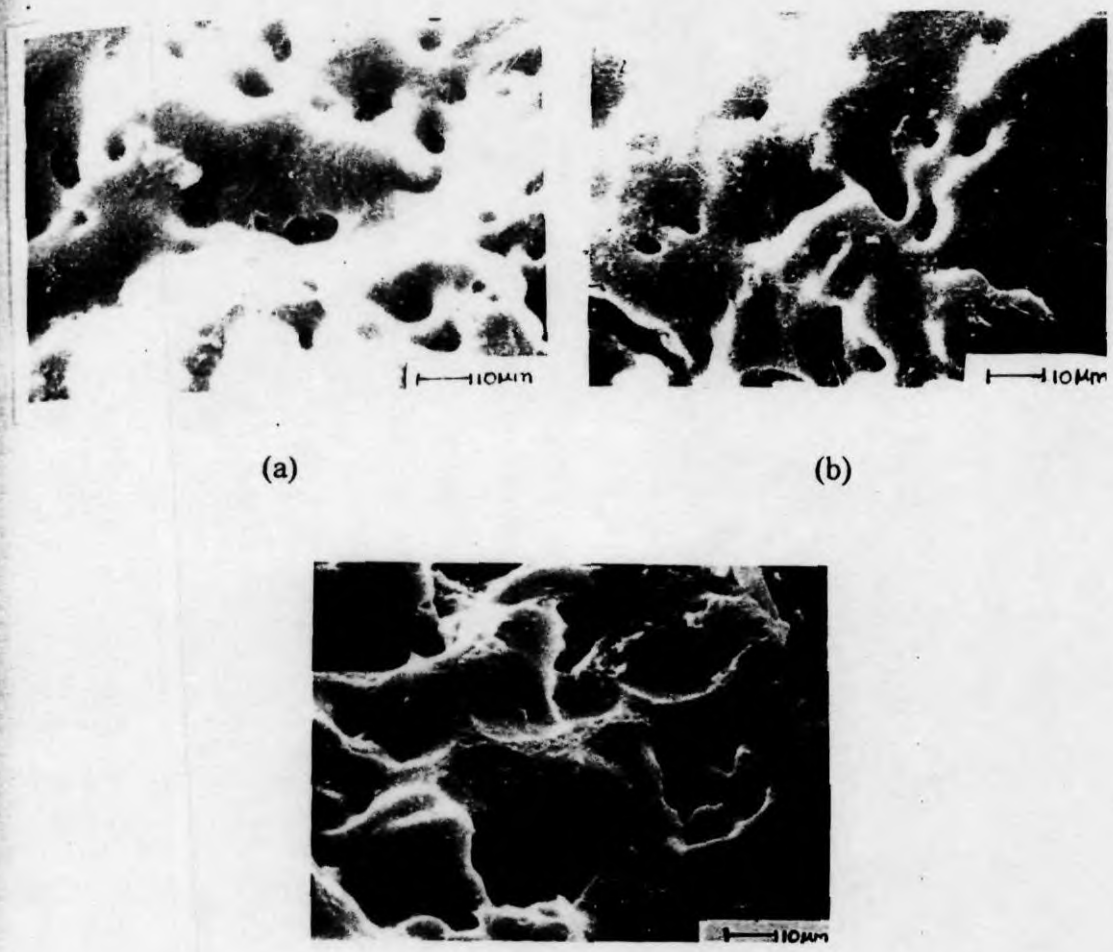

(a) (b)

(c)

Figure 5.3. The extrudate morphology of (a) P_{70}, (b) P_{50} and (c) P_{30} blends.

5.2.2 *Comparison with theoretical predictions*

The viscosities of these blends have been correlated with various theoretical models. The following models have been used to calculate the viscosity.

$$\eta = \eta_1\phi_1 + \eta_2\phi_2 \qquad \text{(Model 1)} \qquad (5.1)$$

where η_1 and η_2 are the viscosities of the components and ϕ_1 and ϕ_2 their volume fractions.

According to Hashin's upper and lower limit models.[23]

$$\eta_{mix} = \eta_2 + \frac{\phi_1}{1/(\eta_1 - \eta_2) + \phi_2 / 2\eta_2} \qquad \text{(Model 2)} \qquad (5.2)$$

$$\eta_{mix} = \eta_1 + \frac{\phi_2}{1/(\eta_2 - \eta_1) + \phi_1 / 2\eta_1} \qquad \text{(Model 3)} \qquad (5.3)$$

where η_1, η_2, ϕ_1 and ϕ_2 have the same significance as explained before.

An altered free volume model developed by Mashelkar and co-workers[24] was also used to calculate the viscosity. According to this equation.

$$\ln \eta_{mix} = \frac{\phi_1(\alpha - 1 - \gamma\phi_2)\ln \eta_1 + \alpha\phi_2(\alpha - 1 + \gamma\phi_1)\ln \eta_2}{\phi_1(\alpha - 1 - \gamma\phi_2) + \alpha\phi_2(\alpha - 1 + \gamma\phi_1)} \qquad \text{(Model 4)} \qquad (5.4)$$

where $$\alpha = \frac{f_2}{f_1} \qquad (5.5)$$

and $$\gamma = \frac{\beta}{f_1} \qquad (5.6)$$

where f_1 and f_2 are free volume fractions of components I and II respectively and β is the interaction parameter.

$$f = f_g + \alpha(T - T_g) \qquad (5.7)$$

where $f_g = 0.025$

$$\alpha_f = \frac{B}{2.303 C_1 C_2} \qquad (5.8)$$

where $B = 0.9 \pm 0.3 \approx 1$, $C_1 = 17.44$, and $C_2 = 51.6$ K.

For the calculations, the value of γ was varied to obtain best fit values with experimental results. Figure 5.4 presents viscosity values from theoretical models and also from the experiments. It is seen from the figure that the viscosity of the blend shows negative deviation and the experimental curve lies in between those of Hashin's upper and lower limit models. The viscosity values can be better explained using Mashelkar Model with $\gamma = -0.04$. This value of γ corresponds to an interaction parameter of $\beta = -4.376 \times 10^{-3}$ according to equation (5.6).

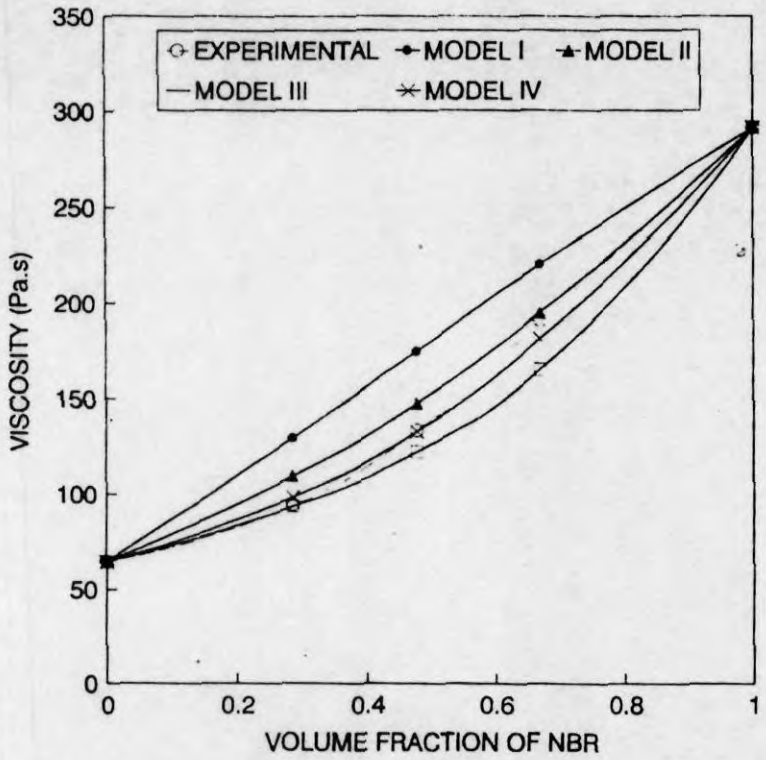

Figure 5.4. Theoretical and experimental viscosity values of PP/NBR blends.

5.2.3 Effect of compatibilisation

The effect of shear stress on the viscosity of 70/30 PP/NBR blend containing phenolic modified polypropylene is shown in Figure 5.5. It is seen from the figure that at lower shear rates, the viscosity of the compatibilised system is higher compared to the uncompatibilised system. At high shear rates the viscosity seems to be unaffected by compatibilisation. Figure 5.6 depicts the variation of viscosity as a function of compatibiliser concentration. With the increase in compatibiliser loading the viscosity initially increases which then levels off at higher loading. The variation in viscosity is more pronounced at low shear rates. Such an increase in viscosity on compatibilisation of immiscible polymer blends has been already reported by several researchers.[13-17] In the introductory part we

have already discussed that the viscosity of a polymer blend has a contribution from the interphase. Upon compatibilisation of an immiscible blend, the compatibiliser will preferentially locate at the interface between the dispersed phase and matrix. This will lead to an increase in interfacial thickness. According to Okoroafor *et al.*[18] the viscosity of the compatibilised blend is given by

$$\frac{1}{\eta_{blend}} = \frac{\phi_m}{\eta_m} + \frac{\phi_i}{\eta_d} + \frac{\phi_i}{\eta_i} - \left(\frac{1}{\eta_m} - \frac{1}{\eta_d}\right)\phi_m\phi_d + \left(\frac{\phi_m}{\eta_m} - \frac{\phi_d}{\eta_d}\right)\phi_i + \frac{\phi_i}{\eta_m}(\phi_d - \phi_m) \quad (5.9)$$

where ϕ is the volume fraction; η, the viscosity; and the subscripts m, d and i denote matrix, dispersed phase and interphase, respectively.

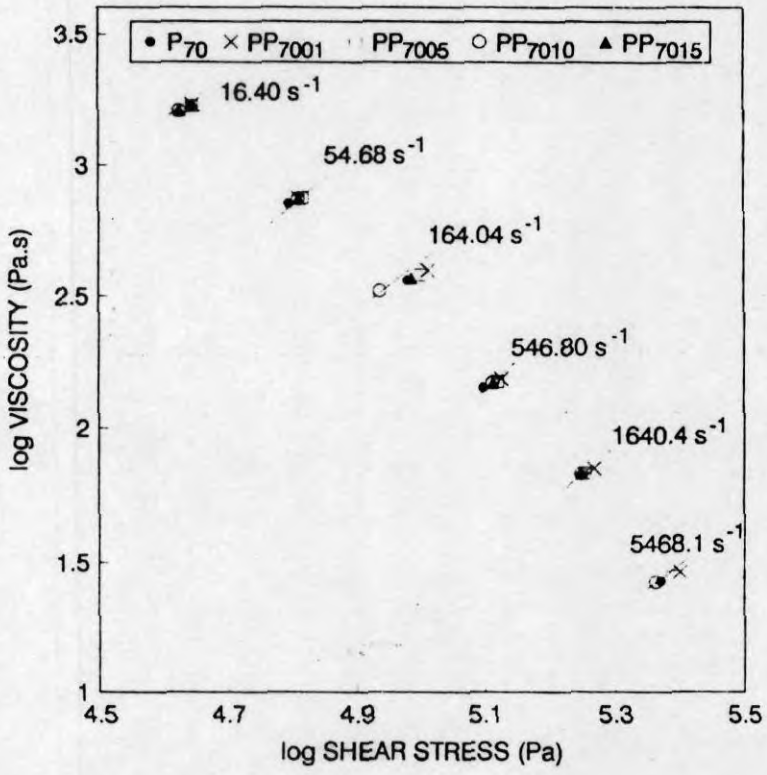

Figure 5.5. The effect of shear stress on the melt viscosity of Ph-PP compatibilised 70/30 PP/NBR blends at different shear rates.

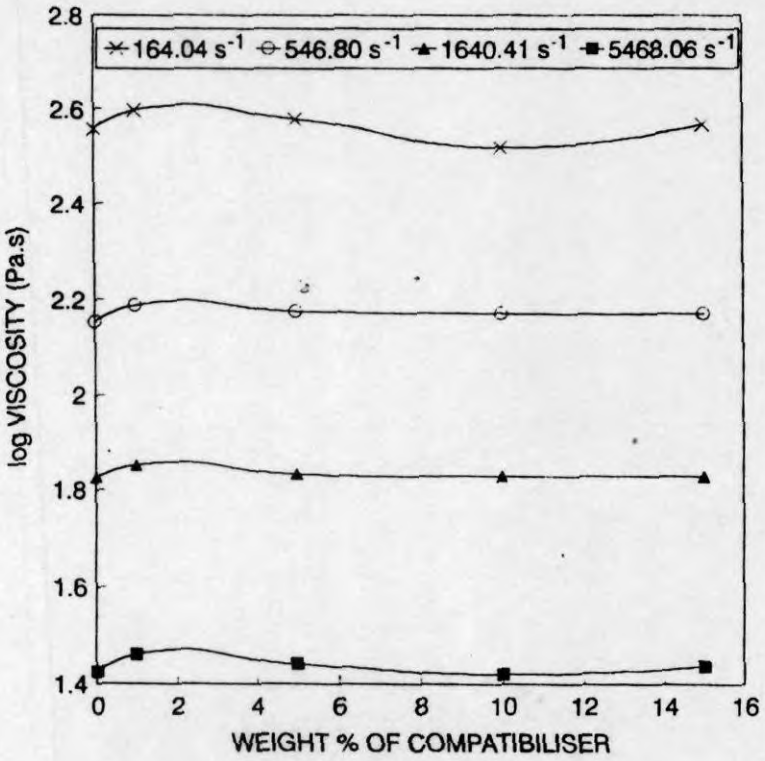

Figure 5.6. Variation of viscosity with compatibiliser concentration.

Hence the viscosities of these blends depend on the interphase volume fraction and also on the viscosity of the interface. In the case of PP/NBR blends compatibilised with Ph-PP, Ph-PP reacts with NBR to form a copolymer as shown in Figure 3.16. As a result of the addition of Ph-PP the thickness of the interphase increases and this leads to an effective stress transfer between the dispersed phase and the continuous phase and an increase in interfacial adhesion. This contributes to the reduction in interlayer slip and therefore an increase in viscosity. The levelling off in the viscosity vs. compatibiliser loading curve at higher concentrations of Ph-PP can be understood from the morphology of the system. The SEM micrographs of the extrudates of 70/30 blend compatibilised with Ph-PP is shown in Figure 5.7. As the concentration of Ph-PP increases the size of the dispersed NBR phase decreases.

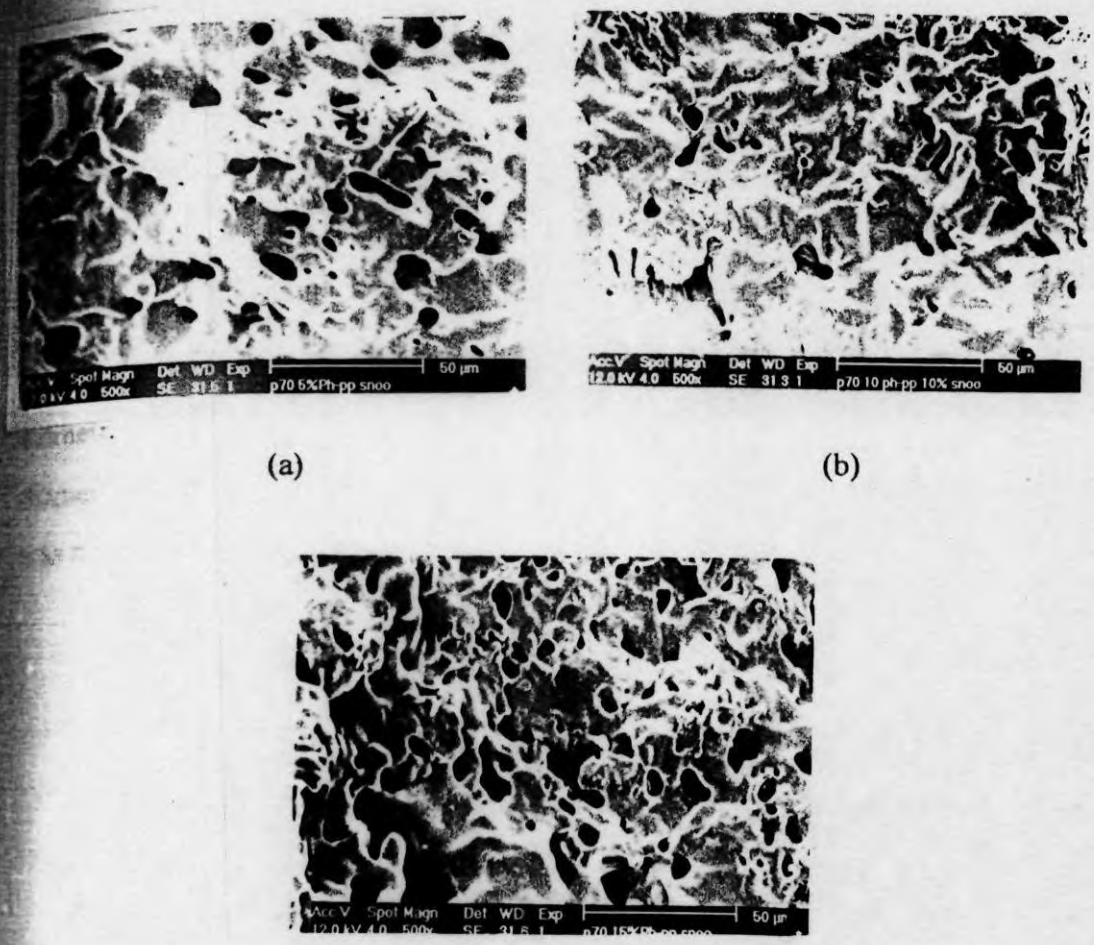

(a) (b)

(c)

Figure 5.7. Effect of addition of Ph-PP on the morphology of 70/30 PP/NBR blend: (a) 5 wt %, (b) 10 wt % and (c) 15 wt %/Ph-PP.

The domain size distribution curves of P_{70} blend compatibilised with different Ph-PP loadings is shown in Figure 5.8. Large number of domains (>300) from different micrographs were considered for the determination of domain diameter. The uncompatibilised blend shows a broader distribution curve, showing the non-uniform distribution of NBR domains. As the compatibiliser loading increases the distribution curve becomes narrow and the size of the NBR domains also decreases. The size of the NBR domains measured from the SEM micrographs is expressed in different ways as given by the equations,

$$\overline{D}_n = \frac{\Sigma NiDi}{\Sigma Ni} \quad (5.10)$$

$$\overline{D}_w = \frac{\Sigma NiDi^2}{\Sigma NiDi} \quad (5.11)$$

and $$\overline{D}_{vs} = \frac{\Sigma Di^3}{\Sigma Di^2} \quad (5.12)$$

where, Ni is the number of domains having diameter Di; $\overline{D}_n$, the number average diameter; $\overline{D}_w$, the weight average diameter; and $\overline{D}_{vs}$, the surface area average diameter. The polydispersity index which is a measure of domain size distribution was also calculated using the equation.

$$PDI = \frac{\overline{D}_w}{\overline{D}_n} \quad (5.13)$$

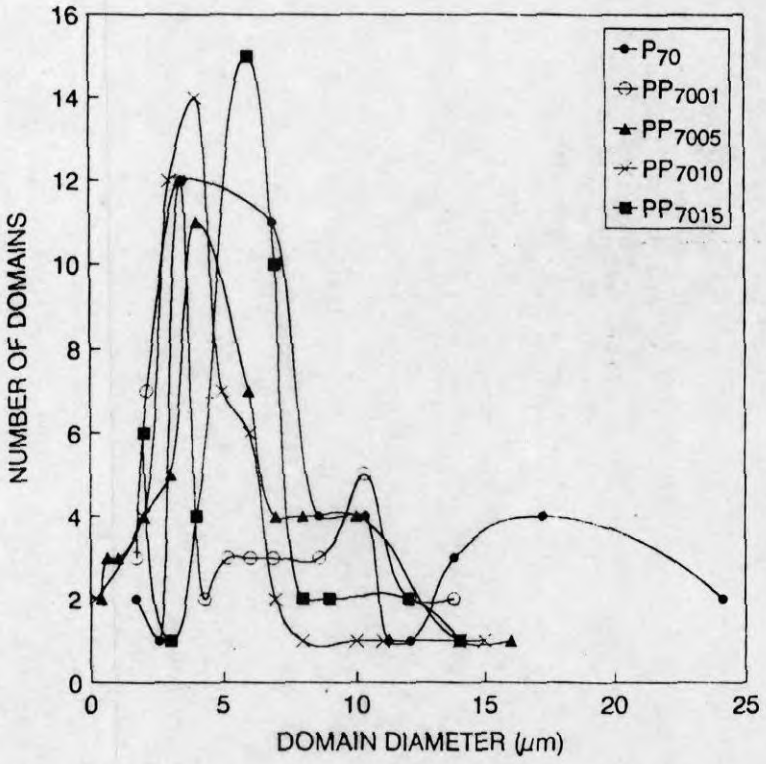

Figure 5.8. Domain size distribution curves of Ph-PP compatibilised P_{70} blends.

Table 5.1 shows the results of these measurements. It is seen from the table that the domain diameter decreases with increase in compatibiliser loading up to 5% and after that it shows a slight increase. The increase in domain size at high concentrations is due to the formation of micelles in the continuous polypropylene matrix. The polydispersity index values decrease with increase in compatibiliser loading which confirms the fact that loading of compatibiliser increases the uniformity of domain size.

Table 5.1. Average diameter of NBR domains in Ph-PP compatibilised P_{70} blends.

Sample	$\overline{D}_n$ (μm)	$\overline{D}_w$ (μm)	$\overline{D}_{vs}$ (μm)	PDI ($\overline{D}_w/\overline{D}_n$)
P_{70}	8.168	11.59	15.001	1.418
P_{7001}	5.322	7.516	9.3073	1.412
P_{7005}	4.9918	7.34	9.264	1.472
P_{7010}	5.06	6.17	10.219	1.219
P_{7015}	6.19	7.72	9.028	1.24

Figure 5.9 depicts the variation of domain size of NBR phase and viscosity of 70/30 PP/NBR blend as a function of compatibiliser concentration. As the Ph-PP concentration increases the size of the NBR domains decreases followed by a levelling off at higher concentrations. The decrease in domain size upon the addition of Ph-PP in PP/NBR blends indicates that the interfacial interaction between PP and NBR phases increases and interfacial tension decreases with Ph-PP loading. The levelling off at higher concentration is due to the interfacial saturation above which the compatibiliser form micelles in the continuous PP phase. The variation of viscosity with compatibiliser concentration indicates that the viscosity increases with Ph-PP loading up to the interfacial saturation point. Above the interfacial saturation point the viscosity gets levelled off.

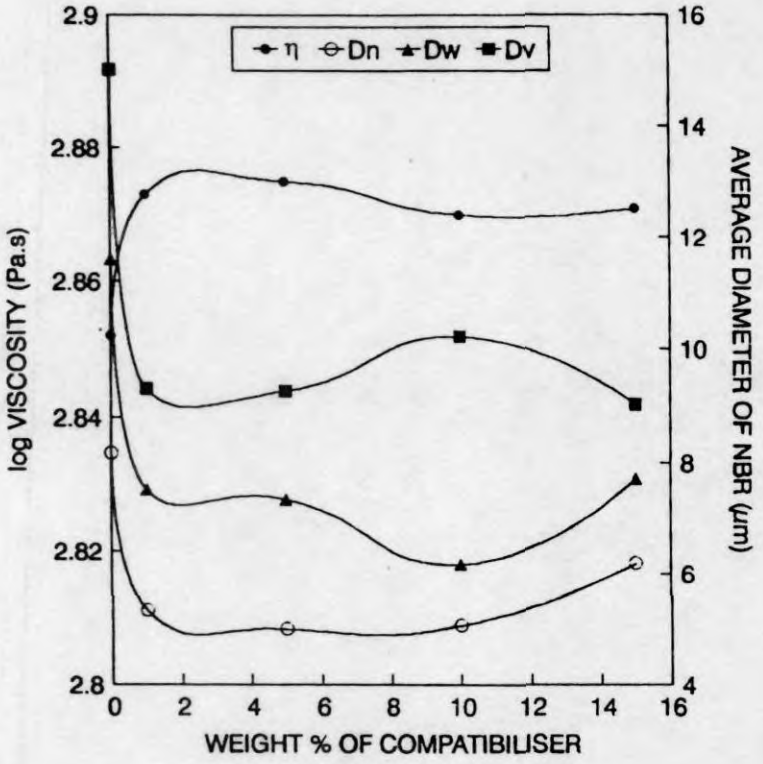

Figure 5.9. Variation of domain size of NBR and viscosity with compatibiliser concentration.

The influence of interfacial energy and viscosity ratio on the particle size of the dispersed phase is given by the relationship proposed by Wu.[25]

$$G\,\eta_m a_n/\gamma = 4(\eta_d/\eta_m)^{0.84} \text{ for } p>1 \qquad (5.14)$$

where p is η_d/η_m; G, the shear rate; a_n, the number average diameter of the domains; γ, the interfacial tension; and η_d and η_m, the viscosities of dispersed phase and matrix, respectively.

It is seen from this equation that at constant shear rate and viscosity ratio, the reduction in particle size is due to the reduction in interfacial tension. In PP/NBR blends the size of the dispersed NBR phase decreases by the increasing

concentration of Ph-PP as compatibiliser (Figure 5.7). Hence these results indicate that upon the incorporation of Ph-PP in PP/NBR blends the interfacial tension decreases. The interfacial tension of uncompatibilised and compatibilised blends were calculated using the equation (5.14). The calculation of interfacial tension using equation (5.14) gives higher values compared to literature values. However, we are interested in the trend in the variation of interfacial tension with compatibiliser concentration and the results show that the interfacial tension decreases with the incorporation of Ph-PP as compatibiliser (Figure 5.10).

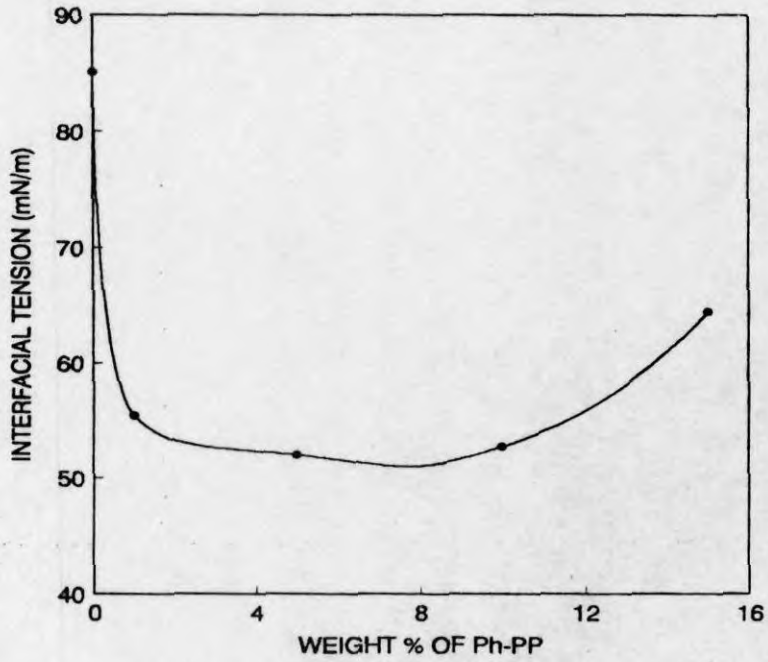

Figure 5.10. Variation of interfacial tension of 70/30 PP/NBR blends with compatibiliser concentration.

5.2.4 *Effect of dynamic vulcanisation*

The effect of dynamic vulcanisation of 70/30 PP/NBR blend using sulphur, peroxide and mixed system on the viscosity as a function of shear stress at different shear rates is shown in Figure 5.11. Here also the viscosity decreases with

increasing shear stress which indicates pseudoplastic behaviour. Among the three vulcanising systems studied the sulphur cured system shows the highest viscosity compared to other systems. At low shear rates the peroxide cured system shows slightly higher viscosity than mixed system and at high shear rates the trend is reversed. In mixed and peroxide cured systems, during shearing at high temperature the peroxide degrades the polypropylene phase and as a result the viscosity decreases. In these systems (peroxide and mixed systems) the degradation of PP overshadows the effect of crosslinking of NBR phase. But in the case of sulphur cured system the NBR phase is crosslinked and no degradation of PP takes place.

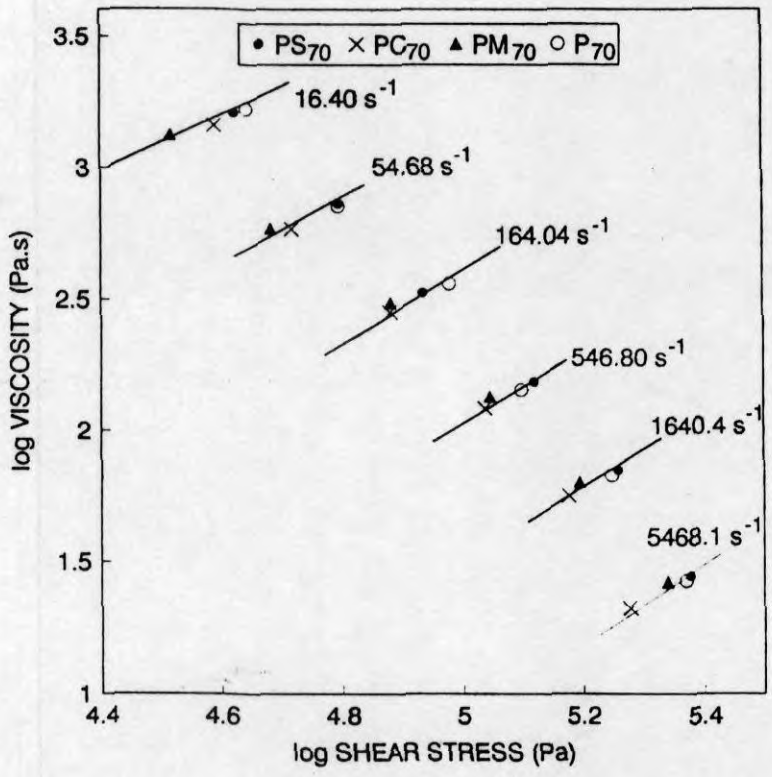

Figure 5.11. Effect of shear stress on melt viscosity of dynamically vulcanised PP/NBR blends.

The morphology of the extrudates of PP/NBR blends vulcanised with sulphur, DCP and mixed system is shown in Figure 5.12. From the figures it can be seen that in sulphur cured system, the size of the dispersed NBR domains is larger than those of peroxide and mixed cured systems. In peroxide cured system, the distribution of NBR domains is fine and uniform and the crosslinking is more effective (Table 5.2). However this effect of crosslinking is not so predominant on the properties of the peroxide vulcanised system due to the degradation of PP phase in presence of DCP.

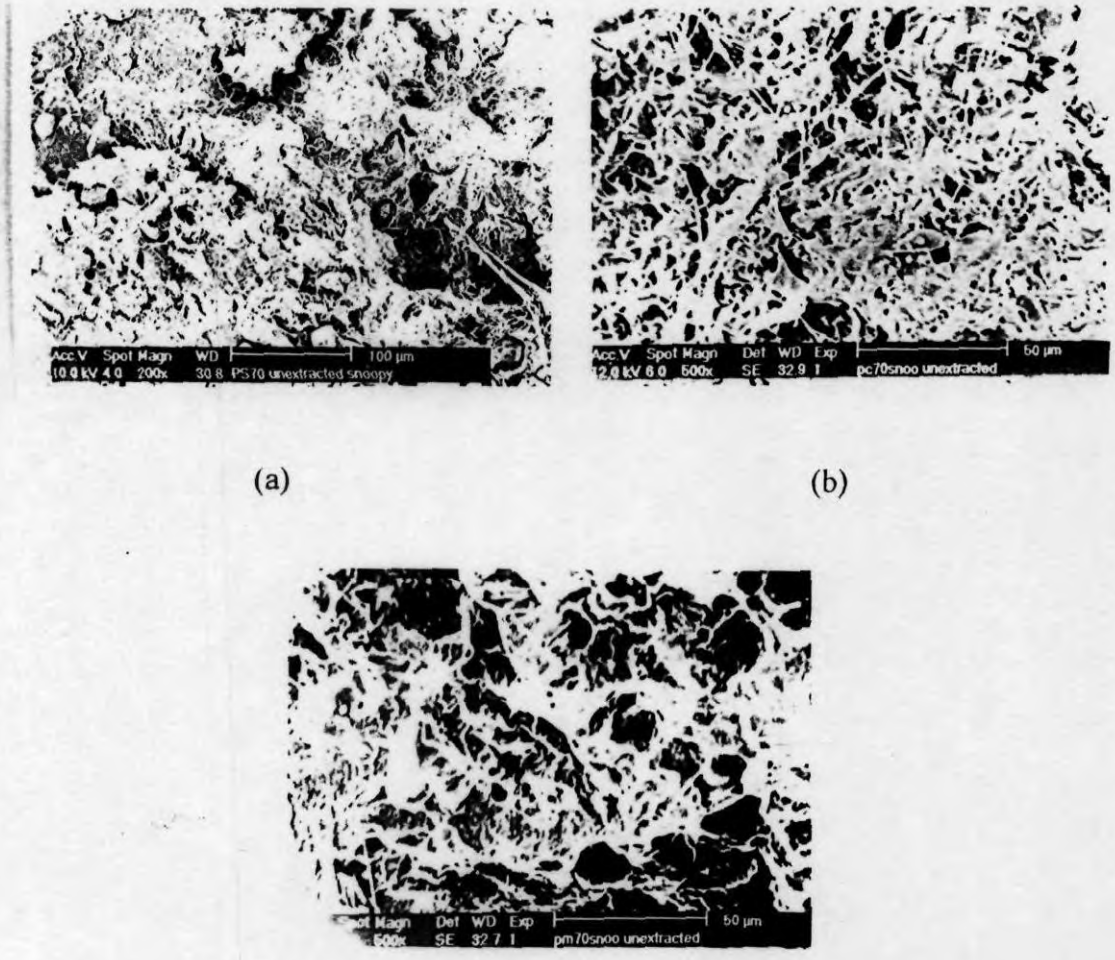

(a) (b)

(c)

Figure 5.12. Morphology of dynamically vulcanised 70/30 PP/NBR blends: (a) PS_{70}, (b) PC_{70}, and (c) PM_{70}.

Table 5.2. Crosslink density values of dynamically vulcanised P_{70} blends.

Sample	Crosslink density x 10^5 mol/cm^3
PS_{70}	2.06
PC_{70}	2.33
PM_{70}	2.04

5.2.5 *Effect of temperature*

The effect of temperature on the melt viscosity of PP, NBR and 70/30 PP/NBR blend is shown in Figure 5.13. In the case of polypropylene, the viscosity decreases with increase in temperature, while for nitrile rubber, it initially decreases, followed by an increase at high temperature. This increase in viscosity of NBR at high temperatures is due to the crosslinking of NBR phase. In the case of 70/30 PP/NBR blend, the viscosity reduction upon increase in temperature from 200 to 210°C is lower compared to neat polypropylene. This may be due to the crosslinking of the NBR phase in the blend. In fact, two reactions take place in the blend at high temperature: Crosslinking of NBR phase and degradation of PP phase. The activation energy was calculated from the plot of log η vs. 1/T curve for polypropylene, 70/30 PP/NBR blend and the compatibilised blend. The plots are shown in Figure 5 14 and the activation energies are given in Table 5.3. It can be seen from the table that on blending PP with NBR, the activation energy decreases while compatibilisation increases the activation energy. Generally higher the activation energy the more temperature sensitive the material will be. Hence upon compatibilisation the temperature sensitivity of the material increases. This type of increase in activation energy on compatibilisation was reported earlier.[17] It is important to add that the activation energy values are useful in choosing the temperature to be used during various processing methods like injection moulding, calendering and extrusions.

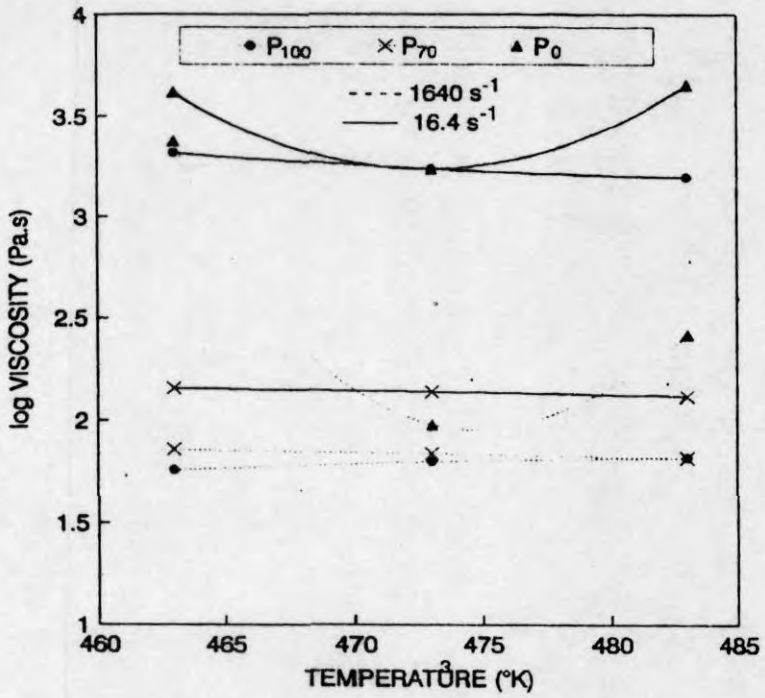

Figure 5.13. Effect of temperature on the melt viscosity of polypropylene, nitrile rubber and 70/30 PP/NBR blend.

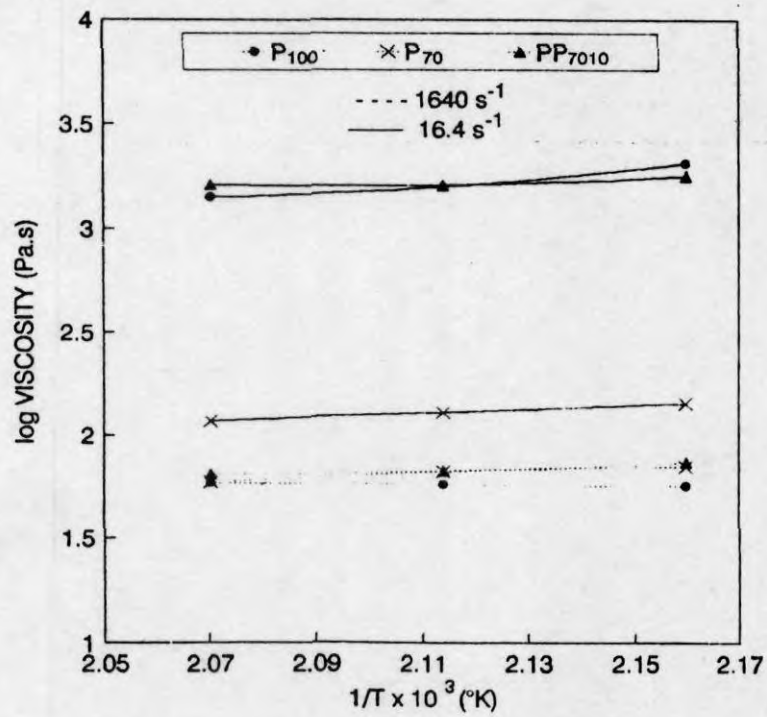

Figure 5.14. Arrhenius plots of P_{100}, P_{70} and PP_{7010} blends.

Table 5.3. Activation energies of PP/NBR blends.

Sample	E (kJ/mol)
P_{100}	46.62
P_{70}	18.39
PP_{7010}	44.35

The shear rate temperature superposition analysis has been used to predict the melt viscosity of polymers.[26] The super position shift factors were obtained using the following equation,

$$a_T = \frac{\tau_{ref}}{\tau_{(T)constant\,\dot{\gamma}}} \qquad (5.15)$$

The shear rate-temperature superposition master curves of PP/NBR 70/30 blend and P_{100} have been constructed by plotting modified shear stress ($\tau \times a_T$) vs. $\dot{\gamma}$ at a reference temperature of 200°C. In the case of polypropylene and P_{70} blend, the super position of the data was obtained in the temperature range and shear rate studied (Figure 5.15 and 5.16).

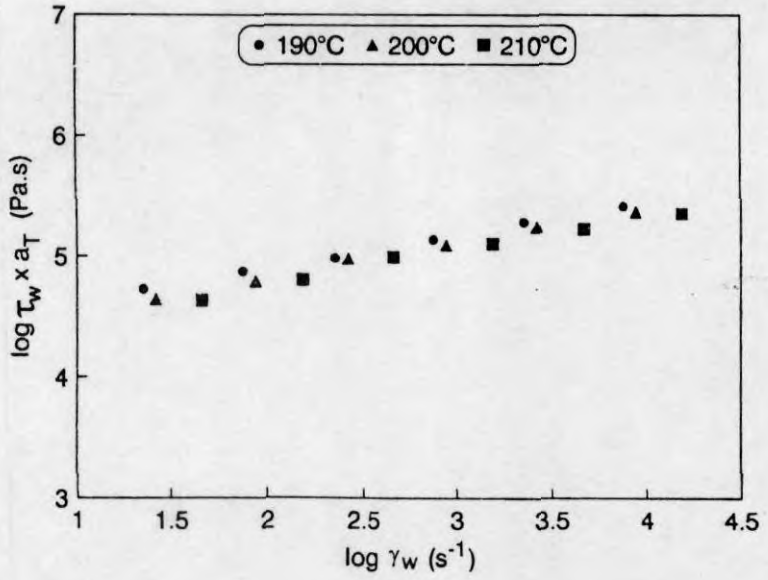

Figure 5.15. Shear rate-temperature super position master curve of P_{100}.

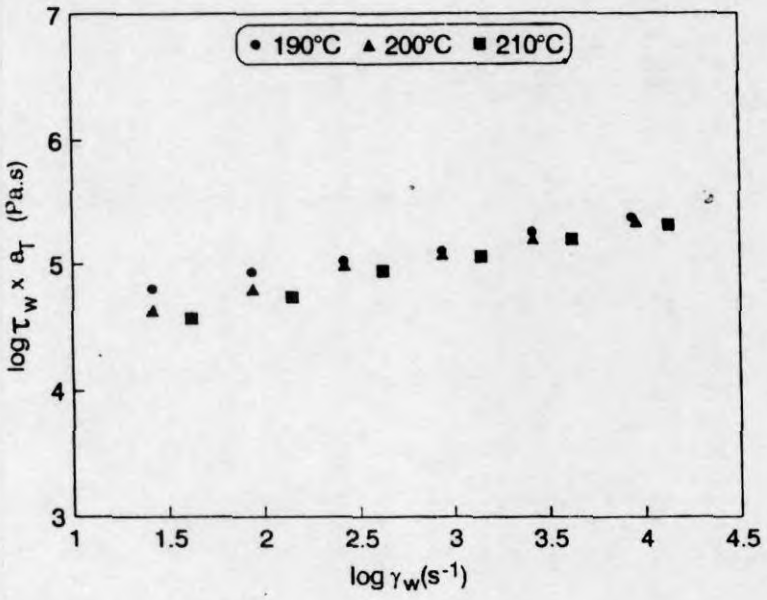

Figure 5.16. Shear rate-temperature super position master curve of P_{70}.

The values of a_T for different temperatures of P_{100} and P_{70} are shown in Table 5.4. Hence it is possible to develop the rheograms at different temperatures from the rheogram at any temperature by knowing the shift factor (a_T) values.

Table 5.4. Shift factor (a_T) values of P_{100} and P_{70}

Temperature (°C)	P_{100}	P_{70}
190	0.842	0.834
200	1	1
210	1.535	1.629

5.2.6 *Flow behaviour index (n')*

The flow behaviour index (n') gives an idea about the nature of flow whether it is Newtonian or non-Newtonian. Most polymers show pseudoplastic behaviour with flow behaviour index n' less than 1. For Newtonian liquids n' value is 1. The effect of blend ratio on the flow behaviour index is shown in Figure 5.17. The low values of n' for PP, NBR and blends indicate their pseudoplastic behaviour. The incorporation of NBR slightly increases the flow behaviour index, i.e., the incorporation of NBR does not change the flow behaviour of polypropylene considerably. The effect of compatibilisation and dynamic vulcanisation on the flow behaviour index is given in Table 5.5. It is clear from the table that, the compatibilisation and dynamic vulcanisation using sulphur and mixed systems increase the n' values showing an increased Newtonian behaviour. However, the DCP vulcanised system shows a lower n' value.

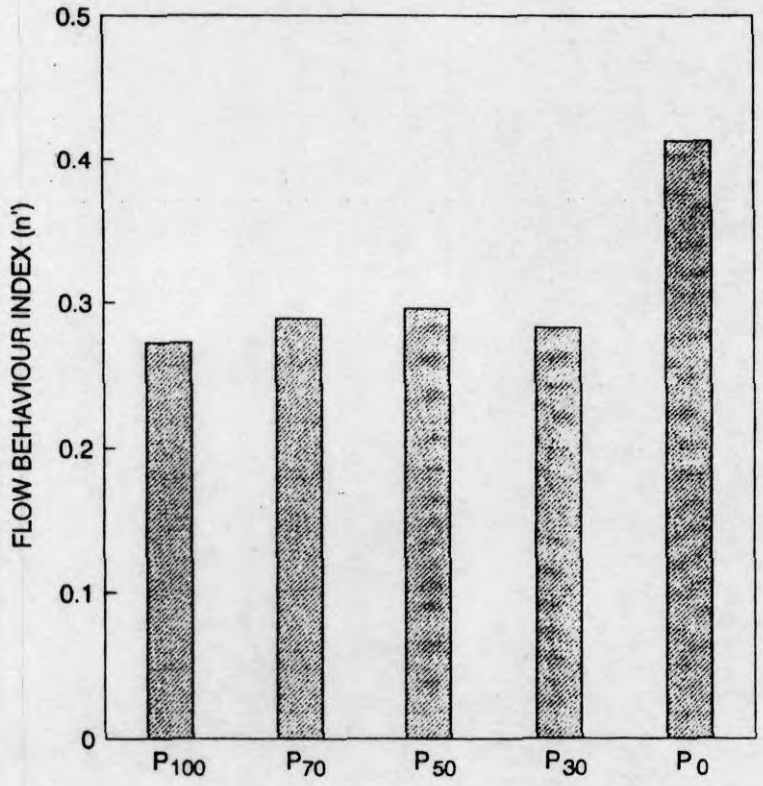

Figure 5.17. Effect of blend ratio on flow behaviour index n'.

Table 5.5. Flow behaviour index and die swell value d_e/d_c of compatibilised and dynamic vulcanised samples.

Sample	n′	d_e/d_c
P_{70}	0.289	1.44
PP_{7001}	0.298	1.43
PP_{7010}	0.294	1.42
PS_{70}	0.303	1.286
PC_{70}	0.281	1.162
PM_{70}	0.329	1.136

5.2.7 *Extrudate morphology*

The extrudate morphology of the blends depends on many factors such as the viscosity of individual components, composition, interfacial tension and shear rate. According to Danesi and Porter[27] when the polymers have similar melt viscosities, the minor component will be finely and uniformly distributed in the major component. When the two polymers have different melt viscosities, the morphology of the blend depends on whether the minor component has lower or higher melt viscosity than the major one. Generally, the least viscous component forms the continuous phase irrespective of the composition.[28] In PP/NBR blends, we have already seen that polypropylene has lower viscosity than nitrile rubber. Thus in P_{70} in which NBR is the minor phase, the NBR forms dispersed phase, i.e., NBR is dispersed as spherical domains in the continuous PP matrix as expected. In P_{50}, the intermediate composition also NBR forms dispersed phase and in this case the size of the dispersed NBR domains increases due to coalescence of the rubber domains during shearing. The domain size of P_{70} and P_{50} blends is shown in Table 5.6. In P_{30}, where the minor component PP has a lower viscosity, both NBR and

PP form continuous phase resulting in a co-continuous morphology. This is due to the fact that low viscosity phase has a tendency to form continuous phase irrespective of the composition. The effect of shear rate on the extrudate morphology is shown in Figure 5.18. As the shear rate increases the size of the dispersed domains decreases and becomes more uniform. The domain size distribution curves of 70/30 PP/NBR blends extruded at different shear rates are shown in Figure 5.19. As the shear rate increases from 16.4 to 1640 s^{-1}, the distribution curve becomes narrow indicating more uniform distribution at high shear rates. The number and weight average diameter of NBR domains and the polydispersity index values are given in Table 5.7. As the shear rate increases the average diameter of NBR domains decreases and the distribution of NBR domains becomes more uniform as shown by the low values of polydispersity index. Under the action of shear, the dispersed phase undergoes elongational deformation and finally the droplet will break up as shown schematically in Figure 5.20. The droplet break up depends on the viscosity ratio (η_d/η_m). The break up is easier when the viscosity ratio η_d/η_m is close to unity. Taylor's equation has been developed for the deformation of a Newtonian drop suspended in Newtonian matrix.[29] The equation gives the deformation of droplet in terms of critical Weber number. According to Taylor's equation

$$W_e = \dot{\gamma}\, \eta_m d_n/\tau_{12} \qquad (5.16)$$

where $\dot{\gamma}$ is the shear rate; η_m, the viscosity of matrix phase; d_n, the average diameter of the dispersed rubber particle; and τ_{12}, the interfacial tension.

Table 5.6. Average diameter of NBR domains in PP/NBR blends.

Sample	$\overline{D}_n$ (μm)	$\overline{D}_w$ (μm)	PDI ($\overline{D}_w/\overline{D}_n$)	$\overline{D}_{vs}$ (μm)
P_{70}	8.168	11.59	1.418	15.00
P_{50}	11.89	15.68	1.318	18.65

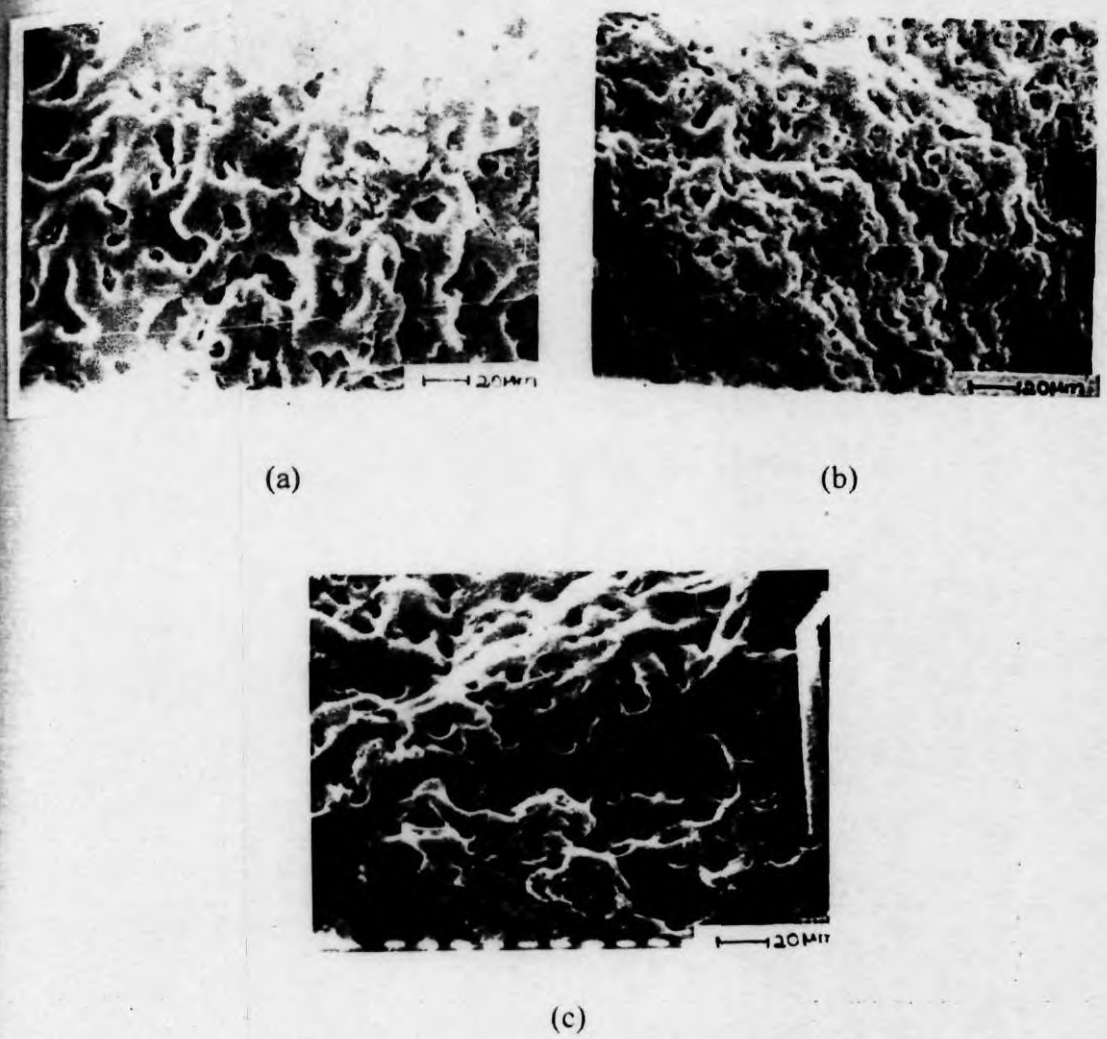

Figure 5.18. The effect of shear rate on the extrudate morphology of 70/30 PP/NBR blends: (a) 16.46 s^{-1}, (b) 164.04 s^{-1} and (c) 1640.4 s^{-1}.

Table 5.7. Average domain diameter of NBR in P_{70} extruded at different shear rates.

Shear rate (s^{-1})	$\overline{D}_n$ (μm)	$\overline{D}_w$ (μm)	PDI
16.4	9.57	13.962	1.459
164.04	8.168	11.59	1.418
1640.4	4.398	5.915	1.345

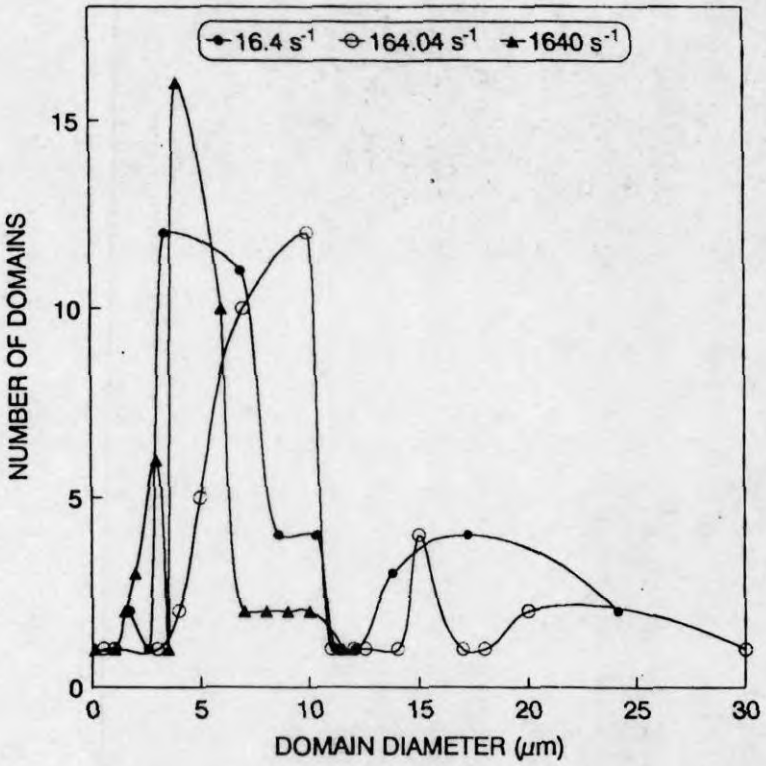

Figure 5.19. Domain size distribution curves of P_{70} extruded at different shear rates.

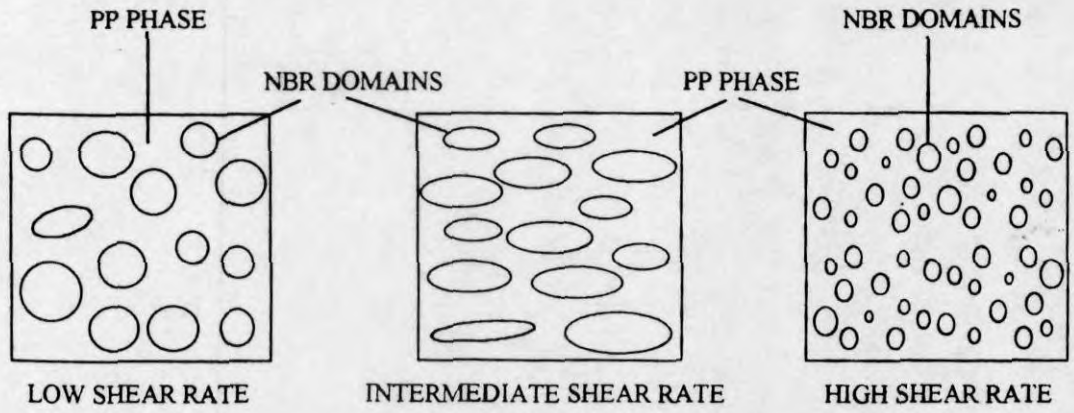

Figure 5.20. Schematic representation of the droplet break-up during shearing.

According to Wu's equation (5.14) it is clear that the average size of the particles is small, when the shear rate is high, interfacial tension is low and when η_d/η_m ratio is less. Thus, as the shear rate increased, in PP/NBR blends, the dispersed NBR domains are elongated in the direction of flow and at higher shear rates the elongated NBR phase is broken down into small particles.

5.2.8 *Extrudate swell*

The melt elasticity of polymers leads to different phenomena like extrudate swell, melt fracture, shark skin etc. during flow through a capillary.[6] In the capillary the polymer molecules undergo orientation under the action of shear. On emerging out from the die, the oriented molecules has a tendency to recoil, as a result, lateral expansion takes place which leads to extrudate swell. The extrudate deformation characteristics of these blends are shown in Figures 5.21a and 5.21b. At low shear rate, the deformation of the extrudates is less and at high shear rate, the deformation is very prominent. This is associated with the melt fracture which occurs at high shear forces, where the shear stress exceeds the strength of the melt. As the concentration of rubber increases the surface of the blend exhibits more roughness and the extrudates have non-uniform diameter since the elastic response increases with increase in the concentration of the rubber phase. It is clear from the figure that compatibilisation and dynamic vulcanisation reduce the extrudate deformation. In unvulcanised blends during extrusion, the rubber particles undergo large extent of deformation in the die or broken down into small particles at high shear rates and after extrusion, they show a deformed morphology. However in dynamic vulcanised blends, the rubber particles undergo less deformation during extrusion through the die, and therefore they retain their morphology after extrusion. The change in morphology of dynamic vulcanised blend during extrusion process is shown schematically in Figure 5.22.

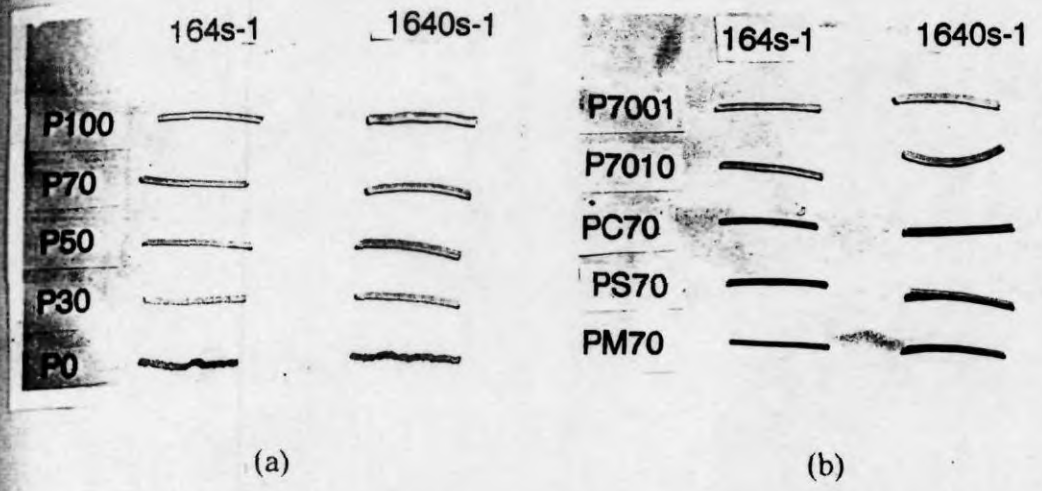

Figure 5.21. Photographs of the extrudates of (a) PP/NBR binary blends, and (b) dynamic vulcanised and compatibilised blends at shear rates 164 and 1640 s^{-1}.

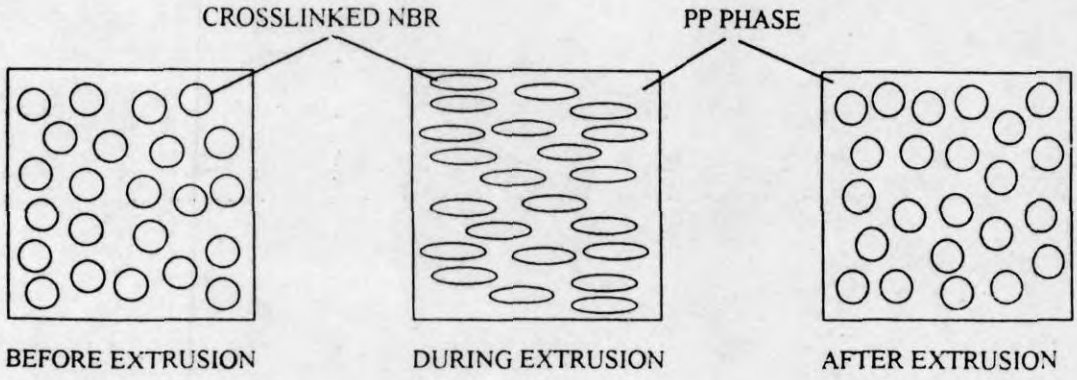

Figure 5.22. Schematic representation of morphology changes during extrusion of dynamic vulcanised blends.

Kuriakose *et al.*[20] have reported that on dynamic vulcanisation of PP/NR blends, the extrudate distortion decreases due to the less deformation and quick recovery of the crosslinked rubber particles in these blends. The effect of addition of NBR on the extrudate swell (d_e/d_c) of PP/NBR blend is shown in Table 5.8. As

the rubber content in the blend increases the extrudate swell decreases. This is due to the elasticity of the rubber phase. The effect of shear rate and temperature on the die swell value of 70/30 PP/NBR blend is shown in Table 5.9. As expected the increase in shear rate increases the die swell values, while increase in temperature decreases the values. Compatibilisation of the blend marginally decreases the die swell. The dynamic vulcanisation has a significant effect on die swell values (Table 5.5) due to the elasticity of the network resulting from dynamic vulcanisation. On dynamic vulcanisation of PP/NBR blend using sulphur, peroxide and mixed system the die swell values decrease and the effect is more pronounced in the case of mixed cured system. Coran[28] reported that in the case of dynamically vulcanised thermoplastic elastomers, the die swell values are negligibly small or even absent, since viscosity can approach infinity at zero shear rate in these types of thermoplastic vulcanisates upon emerging from the die.

Table 5.8. Die swell ratio of PP/NBR blends.

Sample	d_e/d_c
P_{100}	1.48
P_{70}	1.44
P_{50}	1.43

Table 5.9. Die swell ratio of 70/30 PP/NBR blends.

Shear rate (s^{-1})	Temperature (°C)		
	190°C	200°C	210°C
16.4	1.33	1.34	1.34
164.04	1.49	1.44	1.38
1640.4	2.07	1.88	1.71

5.2.9 *Melt flow index*

The MFI values of PP/NBR blends are given in Table 5.10. The melt flow index of the blends decreases with increase in the concentration of nitrile rubber, which is in good agreement with the viscosity data obtained from capillary measurements. The MFI values, give an idea about the processing behaviour of polymers. However, the actual processing conditions like temperature and shear rate employed in the product development differ from that of the conditions used in MFI tests. Several authors have made attempt to correlate the MFI values with rheograms and to develop master curves.[30,31] Recently, in this laboratory Oommen *et al.*,[17] George *et al.*[32] and Asaletha *et al.*[33] combined the MFI data and capillary rheometer data to provide master curves.

Table 5.10. MFI values of PP/NBR blends.

Sample	MFI (g/10 min)	Viscosity (Pa.s)
P_{100}	2.014	4169.1
P_{70}	0.68	11282.1
P_{50}	0.487	19194.2
P_{30}	0.239	47675.8

In PP/NBR blends, a master curve is obtained by combining the MFI values and capillary rheometer data as shown in Figure 5.23. For different blend compositions the plots of $\dot{\gamma} \times \rho / MFI$ vs. $\eta \times MFI/\rho$ (where ρ is density for various PP/NBR blends) unified into a single curve. Thus, it is possible to generate, the viscosity versus shear rate curves from the mastercurve by simply knowing the MFI values without the use of sophisticated rheological instruments.

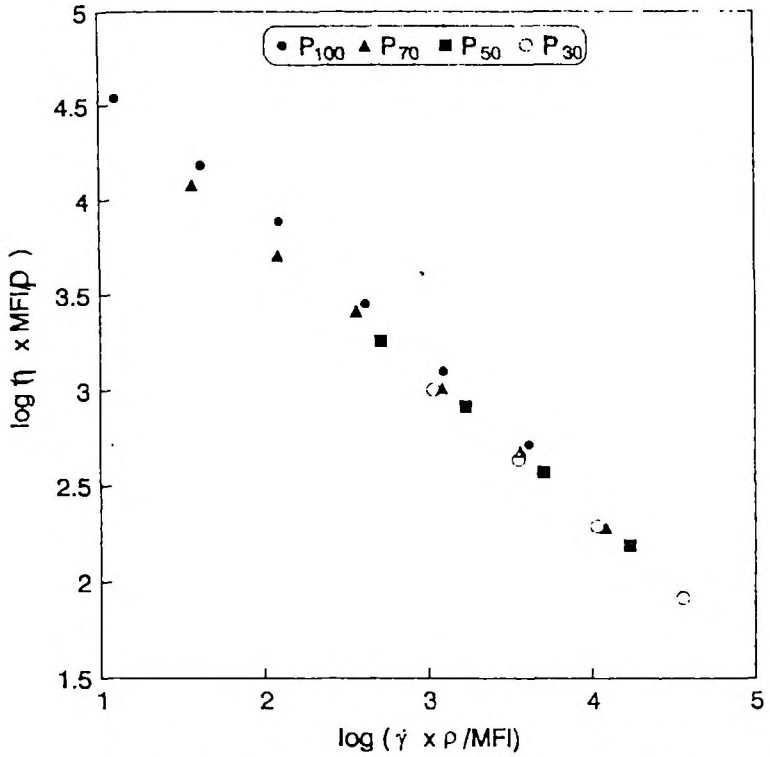

Figure 5.23. Master curve of modified shear viscosity vs. modified shear rates as a function of blend ratio at 200°C.

5.2.10 Effect of annealing

The influence of phase coarsening and coalescence that occurs during annealing on the morphology of polymer blends is important since these materials often undergo annealing during processing and fabrication steps. The phase coarsening and coalescence phenomena in polymer blends have been reported by various researchers.[17,34-36] The coalescence of dispersed particles leads to unstable morphology and poor mechanical properties. A schematic model illustrates the coalescence phenomena in the blends is shown in Figure 5.24. It has been reported that coalescence in immiscible blends can be prevented by compatibilisation. In the case of compatibilised blends, the compatibiliser forms a shell around the dispersed phase, therefore the coalescence is suppressed.[37] The SEM micrographs of the annealed P_{70} and P_{7010} blends are shown in Figure 5.25. The samples were annealed by keeping the samples in barrel for one hour before extrusion at 200°C.

It is seen from the figure that during annealing, the size of the dispersed NBR particles increases in P_{70}. However in the presence of compatibiliser, the domain size is unaffected upon annealing. The increase in domain size during annealing is due to the coalescence of dispersed NBR particles. On compatibilisation using Ph-PP, it forms a shell around NBR particles, which prevents the rubber particles from coalescence and this leads to a stable morphology. Hence in compatibilised blends, the size of the dispersed phase is unaffected on annealing. The dispersed phase size of P_{70} and P_{7010} blend before and after extrusion is shown in Table 5.11.

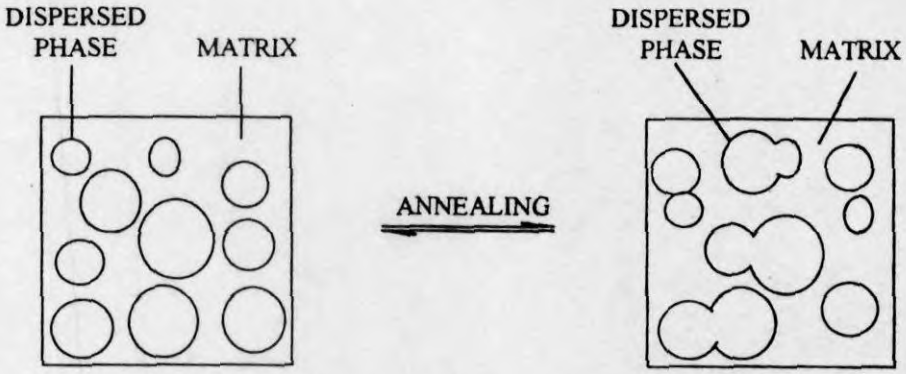

Figure 5.24. Schematic representation of coalescence phenomena in PP/NBR blends.

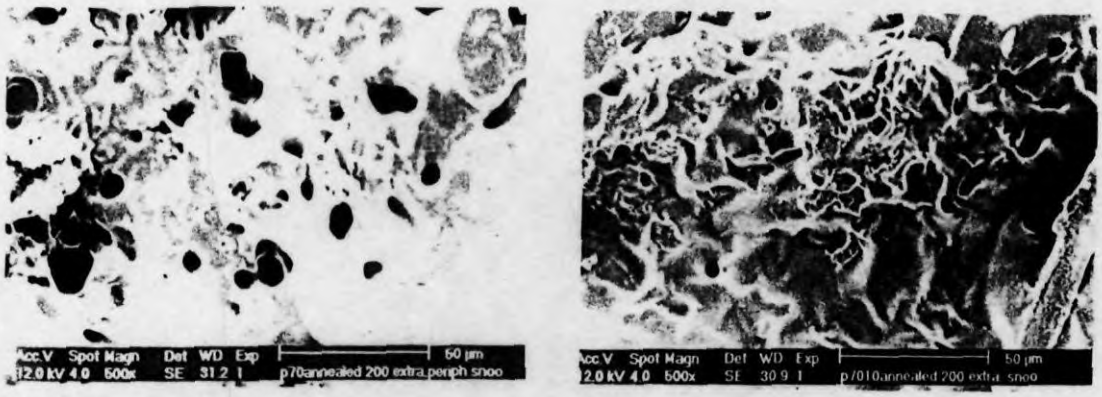

(a) (b)

Figure 5.25. SEM micrographs of (a) P_{70} and (b) PP_{7010} annealed for one hour at 200°C.

Table 5.11. Average diameter of NBR domains in annealed samples.

Sample	$\bar{D}_n$ (μm)	$\bar{D}_w$ (μm)	PDI
P_{70}	8.168	11.59	1.418
P_{70} annealed	9.711	13.438	1.283
PP_{7010}	5.06	6.17	1.219
P_{7010} annealed	5 0	6.673	1.37

Oommen *et al.*[17] reported that the compatibilisation of PMMA/NR blend using PMMA-g-NR prevents coalescence of dispersed domains. Danesi and Porter reported that in PP/EP blend, the PP particles coalesce into larger domains during annealing and have indicated the high instability of the morphological species with annealing above the melting point of polypropylene [27]

5.3 References

1 L. A. Utracki and M. R. Kamal, *Polym. Eng. Sci.*, **26**, 96 (1982).

2. Y. J. Kim, G. S. Shin, I. T. Lee and B. K. Kim, *J. Appl. Polym. Sci.*, **47**, 295 (1993).

3. A. T. Koshy, B. Kuriakose, C. K. Premalatha and S. Thomas, *J. Appl. Polym. Sci.*, **49**, 901 (1993).

4. H. Varghese, K. Ramamurthy, R. Janardhan, S. S. Bhagawan and S. Thomas, *Polym. Plast. Technol. Eng.* (In Press).

5 K. T. Varughese, P. P. De, G. B. Nando and S K De, *J. Vinyl Technol.*, **9**, 161 (1987).

6 K. T. Varughese, *J. Appl. Polym. Sci.*, **39**, 205 (1990).

7. S. Akhtar, B. Kuriakose, P. P. De and S. K De, *Plast. Rubber Process. Appl.* 7, 11 (1987).

8. B. Kuriakose, *Kaust. Gummi Kunst.*, **37**, 1044 (1984).

9. I. Duvdevani, P. K. Agarwal and R D. Lundberg, *Polym. Eng. Sci.*, **22**, 8, 499 (1982).

10. B. K. Kim, H. M. Jeong and Y. H Lee, *J. Appl. Polym. Sci.*, **40**, 1805 (1990).

11. W. Brostow, T. Sterzynski and S. Triouleyre, *Polymer*, **37**, 9, 1561 (1996).

12. P. Zhuang, T. Kyu and J. L. White, *Polym. Eng. Sci.*, **28**, 1095 (1988).

13. R. M. H. Miettinen, J. V. Seppala, O. T. Ikkala and I. T. Reima, *Polym. Eng. Sci.*, **34**, 5, 395 (1994).

14. Y. Germain, B. Ernst, O. Genelot and L. Dhamini, *J. Rheol.*, **38**, 3, 681 (1994).

15. A. Valenza and D. Acierno, *Eur. Polym. J.*, **30**, 10, 1121 (1994).

16. M. Joshi, S. N. Maiti and A. Misra, *J. Appl. Polym. Sci.*, **15**, 1837 (1992).

17. Z. Oommen, C. K. Premalatha, B. Kuriakose and S. Thomas, *Polymer*, **38**, 5611 (1997).

18. E. U. Okoroafor, J. P. Villemuire and J. F. Agassant, *Polymer*, **33**, 24, 5264 (1992).

19. C. S. Ha and S. C. Kim, *J. Appl. Polym. Sci.*, **35**, 2211 (1988).

20. B. Kuriakose and S. K. De, *Polym. Eng. Sci.*, **25**, 10, 630 (1985).

21. S. Thomas, B. Kuriakose, B. R. Gupta and S. K. De, *Plast. Rubber Process. Appl.*, **6**, 1, 85 (1986).

22. P. K. Han and J. L. White, *Rubber Chem. Technol.*, **68**, 728 (1995).

23. Z. Hashin, in *Second Order Effects in Elasticity, Plasticity and Fluid Dynamics* (Eds., M. Reiner and S. Abir) MacMillan, New York, 1964.

24. R. Sood, M. G. Kulkarni, A. Dutta and R. A. Mashelkar, *Polym. Eng. Sci.*, **28**, 1, 20 (1988).

25. S. Wu, *Polym. Eng. Sci.*, **27**, 5, 335 (1987).

26. J. S. Anand, *Int. Plast. Eng. Technol.*, **1**, 25 (1994).

27. S. Danesi and R. S. Porter, *Polymer*, **19**, 448 (1978).

28. A. Y. Coran, *Handbook of Elastomers—Development and Technology* (Eds., A. K. Bhowmick and H. L. Stephens), Marcel Dekker, New York, 1988.

29. G. I. Taylor, *Proc. R. Soc.*, London, **226A**, 34 (1954).

30 A. V. Shenoy, D. R. Saini and V. M. Nadkarni, *Polymer*, **24**, 722 (1983).

31. S. S. Bhagawan, D. K. Tripathy and S. K. De, *Polym. Eng. Sci.*, **28**, 648 (1988).

32. J. George, R. Janardhan, J. S. Anand, S. S. Bhagawan and S. Thomas, *Polymer*, **37**, 5421 (1996).

33. R. Asaletha, M. G. Kumaran and S. Thomas, *J. Appl. Polym. Sci.* (Communicated).

34. J. D. Lee and S. M. Yang, *Polym. Eng. Sci.*, **35**, 1821 (1995).

35. C C. Chen, E. Fontan, K. Min and J. L. White, *Polym. Eng. Sci.*, **28**, 69 (1988).

36. B. D. Favis, *J. Appl. Polym. Sci.*, **39**, 285 (1990).

37. U. Sundararaj and C. W. Macosko, *Macromolecules*, **28**, 2647 (1995).

Chapter 6

Thermal and Crystallisation Behaviour

The results of this chapter have been submitted for publication in *Journal of Thermal Analysis*

6.1 Introduction

In order to develop durable industrial products it is necessary to investigate the thermal stability of these blends. Thermogravimetric analysis can be used as a technique to measure the thermal stability of polymers due to the simplicity of this weight loss method.[1,2] The thermal degradation of polymer blends was investigated by various researchers using thermogravimetric method.[3-10] The blending of a polymer with other polymers has stabilising as well as destabilising effect. Grassie *et al.*[3] reviewed these stabilising effects of blending. The complete degradation of PMMA into monomers on heating can be considerably reduced by blending with other polymers. The destabilising effect of PVC on the degradation of polymers was also investigated. Varughese *et al.*[4] reported that the blending of ENR with PVC reduced the rate of HCl elimination in the first degradation step of PVC. The thermal degradation behaviour of blends has been used to identify SBR/BR blends from SBR based compounds by Amraee *et al.*[5] from the ratio of the peak heights of DTG peaks. The effect of miscibility of polymer blends on thermal degradation behaviour was investigated by Lizymol *et al.*[6] Among the different blends studied (PVC/EVA, EVA/SAN and PVC/SAN), the thermal stability was improved in the case of miscible PVC/EVA system. In immiscible EVA/SAN and PVC/SAN blends, there was not much improvement in thermal stability. Subhra *et al.*[7] reported that blends of ENR with poly(ethylene-co-acrylic acid) showed the

existence of a single phase at low concentrations of ENR i.e at 10, 20 and 30 wt %, as shown by the two step degradation exist in these blends.

In polymer blends with a crystallisable component, the final properties are determined by (1) mode and state of dispersion of rubbery domains in the crystalline matrix (2) the texture, dimensions and size distribution of spherulites of the matrix (3) the inner structure of spherulites i.e. lamellar and inter lamellar thickness (4) physical structure of inter spherulitic boundary regions and amorphous inter lamellar regions and (5) the adhesion between the rubbery domains and the crystalline matrix.[11] The effects of the nature of crystalline structure and the extent of crystallinity on the properties of various polymer blends were investigated.[18-28] Martuscelli *et al.*[12,13] investigated the nucleation and growth of spherulites in various rubber/plastic blends. Hlavata *et al.*[14] investigated the change in crystalline structure of iPP on blending with two thermoplastic elastomers, butadiene-styrene (BS) and hydrogenated butadiene styrene rubbers (HIS). The pure polypropylene and blends with BS and HIS showed the presence of a hexagonal β phase along with the α-form. The thermal and crystallisation behaviour of EVA/NR blends were investigated by Koshy and co-workers.[15] The crystallinity of the blends decreased with increase in NR content, and the interplanar distance 'd values' increased upon the addition of NR indicating the migration of NR phase into the interchain space of EVA.

The effect of compatibilisation on crystallisation behaviour was studied by Santra *et al.*[16] They reported that the crystallinity of LDPE/PDMS rubber blends increased upon compatibilisation using ethylene methyl acrylate copolymer. Wu *et al.* reported that in PA-6/SEBS blends,[17] the compatibilisation using maleated SEBS changes the α-crystalline form of PA-6 in binary blends to a mixture of α and γ-crystalline forms. The effect of dynamic vulcanisation on crystallinity and crystalline structure was reported for PP/EPDM blend.[18,19]

In this chapter, the thermal properties of binary, compatibilised and dynamically vulcanised PP/NBR blends have been presented. The crystalline structure of binary and compatibilised blends was also investigated.

6.2 Results and discussion

6.2.1 *Thermal degradation*

Thermograms and derivative thermograms of pure polypropylene, nitrile rubber and their blends are shown in Figures 6.1a–e. In the case of polypropylene, the weight loss is very low up to 250°C. Hence, the sample can be considered as stable up to this temperature in nitrogen atmosphere. The degradation of PP which starts at 250°C was completed at 385°C. The weight loss in this region (250-385°C) corresponds to the formation of volatile products which arises from the random chain scission and intermolecular transfer involving tertiary hydrogen abstractions from the polymer by the primary radical. The degradation products of PP involves monomer, 2-methyl-1-pentane, 2,4 dimethyl-1-heptane, 2-pentene and isobutene. The mechanism of degradation of PP can be represented as follows.

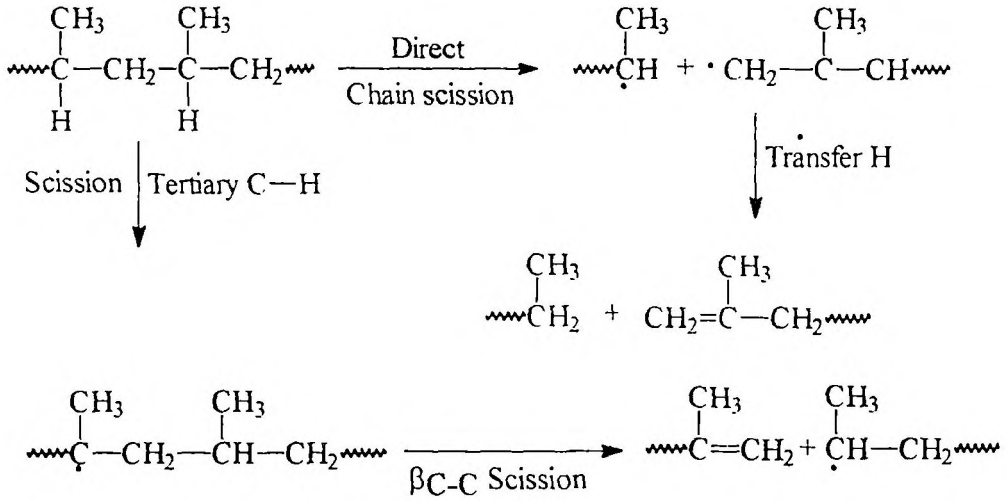

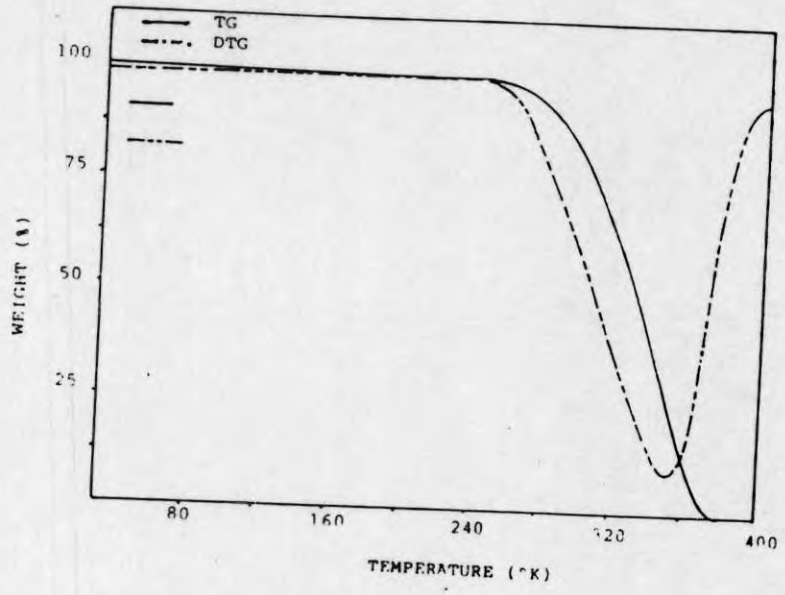
TG
DTG
100
75
50
25
WEIGHT (%)
80
160
240
320
400
TEMPERATURE (°K)

(a)

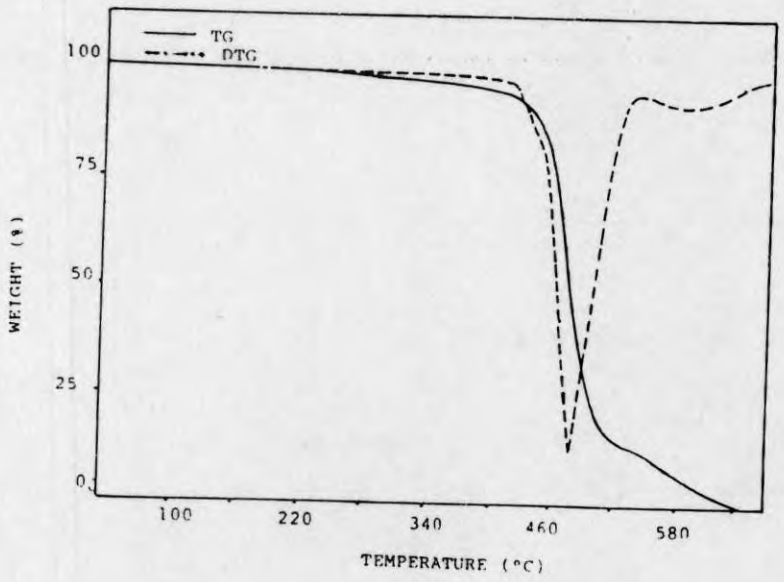
TG
DTG
100
75
50
25
0
WEIGHT (%)
100
220
340
460
580
TEMPERATURE (°C)

(b)

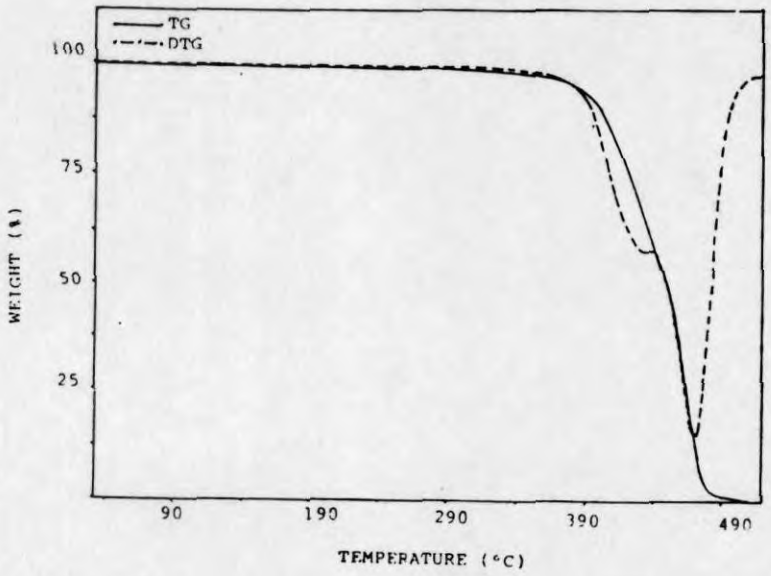
TG
DTG
100
75
50
25
WEIGHT (%)
90
190
290
390
490
TEMPERATURE (°C)

(c)

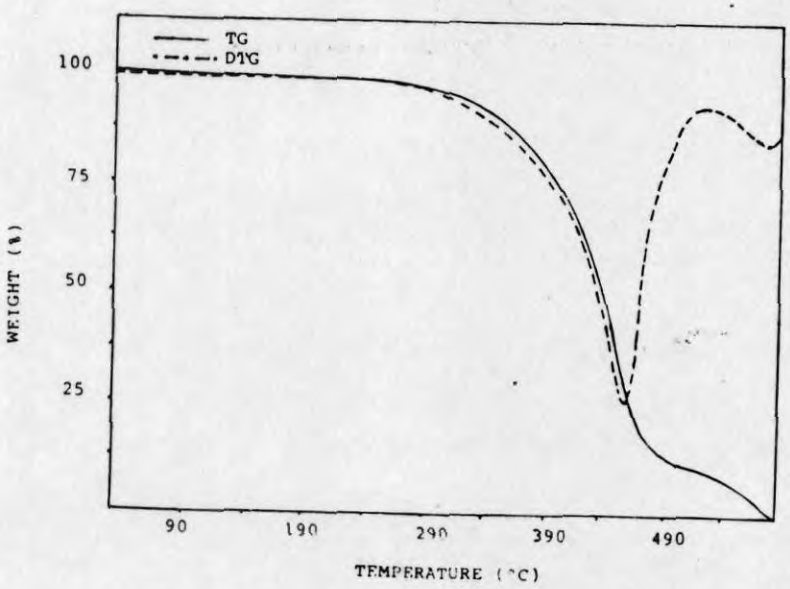
TG
DTG
100
75
50
25
WEIGHT (%)
90
190
290
390
490
TEMPERATURE (°C)

(d)

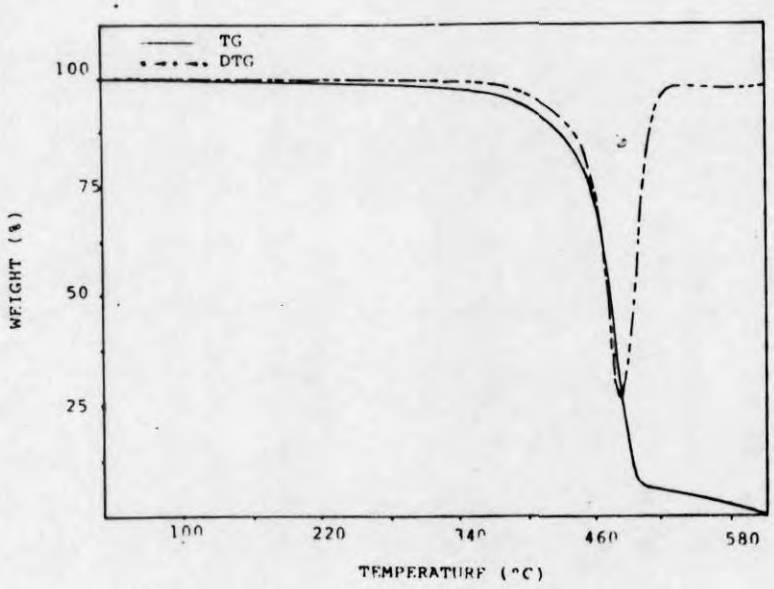

(e)

Figure 6.1. Thermograms and derivative thermograms of binary PP/NBR blends: (a) P_{100}, (b) P_{70}, (c) P_{50}, (d) P_{30} and (e) P_0.

The degradation of nitrile rubber occurs in two stages. In the first stage, which starts at 414.7°C leads to a weight loss of 80.37% and completed at 526.76°C. In the next stage, the degradation started at 543.6°C and completed at 633°C with a weight loss of 11.86%. Hence, nitrile rubber is stable up to 415°C. The two step weight loss in NBR was due to the degradation by random chain scission of butadiene part and acrylonitrile part in NBR.

In the case of blends, the incorporation of NBR into polypropylene was found to improve the thermal stability of polypropylene. The incorporation of 30 wt % NBR increases the initial degradation temperature from 250 to 380°C, while further addition of NBR i.e. at 50 wt % NBR, the initial degradation

temperature shifts to lower side i.e., 308°C. It is interesting to note that in P_{50}, the degradation occurs in two steps, while in P_{70} and P_{30} the degradation occurs in one step. This indicated the better interaction between PP and NBR in P_{70} and P_{30}. In the case of polymer blends, the thermal degradation depends on the morphology and extent of interaction between the phases. In P_{70} and P_{50} blends, NBR is dispersed as domains in the continuous PP matrix and in P_{30}, NBR also forms continuous phase along with PP phase, resulting in a co-continuous morphology (Figure 3.2). As the weight percent of NBR increased from 30 to 50 wt %, the size of NBR domains increased from 5.87 to 18.7 μm. This increase in domain size at higher loadings of NBR is due to the coalescence of NBR domains. Hence as the concentration of NBR increased from 30 to 50 wt % the interfacial area decreased and reduced the extent of interaction between the phases. The increased thermal stability of the blends compared to PP may arise from the interaction of radicals formed during the degradation of PP with nitrile rubber. Hence, the observed decrease in initial degradation temperature of P_{50} can be attributed to the decreased interaction between PP and NBR phases. At 70 wt % NBR, due to the co-continuous morphology, the possibility of interaction further increases and the initial degradation temperature (T_0) also increases.

The degradation temperature corresponding to the main weight losses, obtained from DTG curves are given in Table 6.1. The weight loss corresponding to different temperatures and the initial degradation temperature are also given in the Table 6.1. The degradation temperature of PP is 353°C and that of NBR are at 480 and 577°C. The blends show intermediate values. Among the different blends, the P_{50} blend shows the lowest degradation temperature. The total weight loss and percentage weight loss at various temperatures of PP degradation were also decreased upon the incorporation of NBR.

Table 6.1. Degradation temperature and weight loss of PP/NBR blends.

	T_0 (wt %)	T_{degr} (°C)	Total wt. loss (%)	Wt. loss at 300°C (%)	Wt. loss at 400°C (%)	Activation energy (kJ/mol)
P_{100}	250.81	353.33	97.85	16.67	100	24.82
P_{70}	380.36	472.61	93.89	1.04	89.03	42.33
P_{50}	308.29 520.51	460 575	93.84	2.08	25.69	24.8
P_{30}	382.7	480.87	89.62	1.38	6.94	66.14
P_0	415.71 543.65	480.93 577.21	92.23	1.38	3.82	58.81

6.2.2 *Effect of compatibilisation*

The thermograms and derivative thermograms of 70/30 PP/NBR blends compatibilised with phenolic modified polypropylene are given in Figure 6.2a–c.

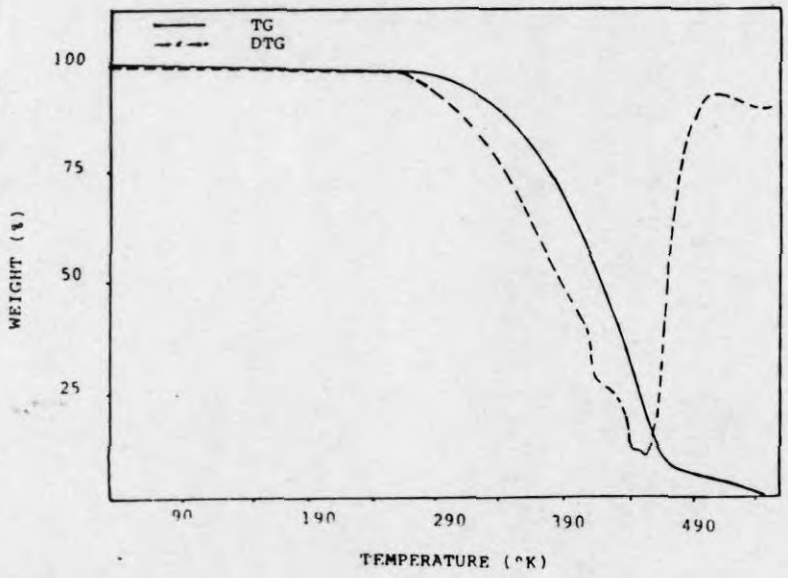

(a)

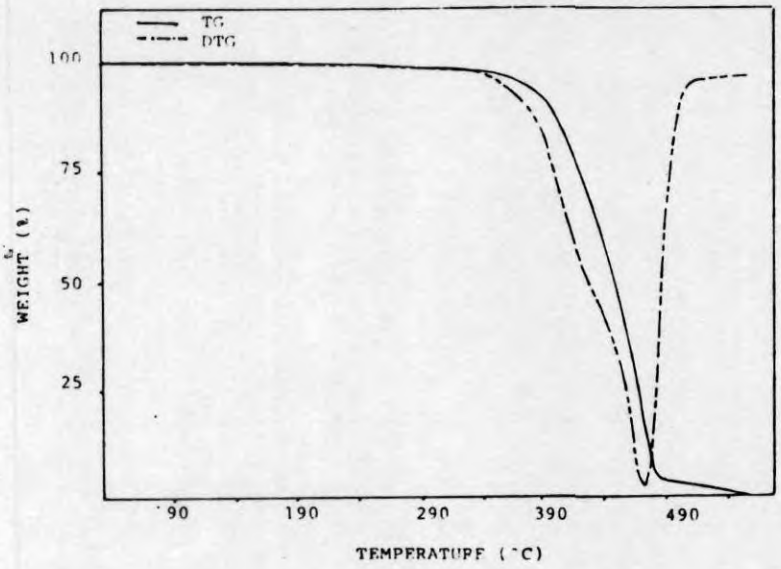

(b)

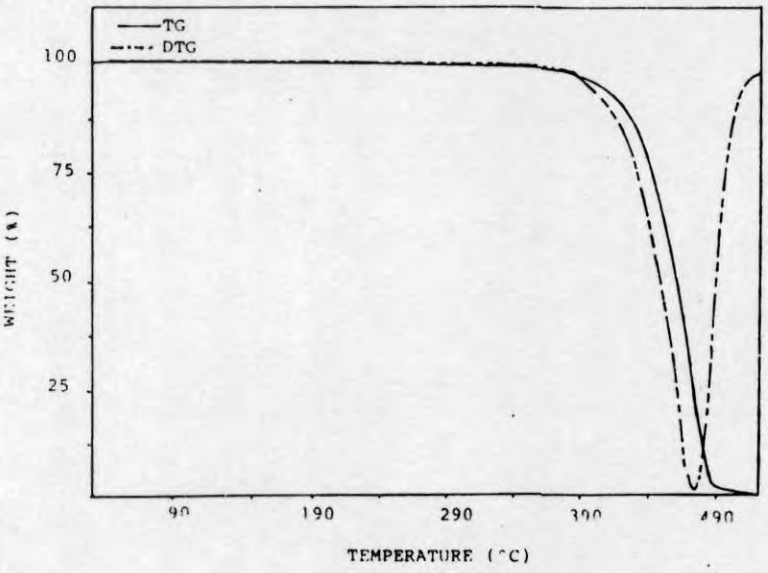

(c)

Figure 6.2. Thermograms and derivative thermograms of Ph-PP compatibilised PP/NBR blends: (a) PP_{7004}, (b) $PP_{7007.5}$ and (c) PP_{7010}.

The incorporation of 4 wt % Ph-PP in to the blend decreased the degradation temperature (Table 6.2) corresponding to the major weight loss. However at higher loadings of Ph-PP, the degradation temperature was increased. The percentage weight loss, at different temperatures increased at 4 wt % Ph-PP and decreased for further increase in Ph-PP concentration.

Table 6.2. Thermal properties of compatibilised PP/NBR blends.

	T_0 (wt %)	$T_{degr.}$ (°C)	Total wt. loss (%)	Wt. loss at 300°C (%)	Wt. loss at 400°C (%)	Activation energy (kJ/mol)
P_{70}	380.36	472.61	93.89	1.04	89.03	42.33
PP_{7004}	269.09	454.28	93.38	36.11	95.13	22.66
$PP_{707.5}$	343.85	475.71	94.98	13.88	96.52	37.09
P_{7010}	380.36	475.86	96.18	6.25	98.61	53.67
PM_{7001}	271.83	449.09	92.71	45.48	96.53	21.44
PM_{7005}	364.17	474.09	94.33	10.42	97.92	46.05
PM_{7010}	380.36	474.32	94.32	7.64	98.61	51.06

The effect of compatibilisation of 70/30 PP/NBR blend with maleic anhydride modified PP on thermal behaviour was shown in Figure 6.3a–c. As in the case of Ph-PP, at low concentration of MA-PP the degradation temperature i.e.. temperature corresponding to the major peak in DTG curves is decreased and at higher loadings it increased (Table 6.2). The improvement in degradation temperature on compatibilisation may arise from the better interactions between PP and NBR, which is evident from the micrographs (Figures 3.7 and 3.8). From the micrographs, it was observed that the size of the dispersed NBR domains decreased upon the addition of maleic anhydride modified PP (Figure 3.7). This is due to the dipolar interactions between the maleic anhydride groups of PP with polar NBR (Figure 3.14). In Ph-PP, the compatibilising action arises from the graft copolymer formed between Ph-PP and NBR, which will locate at the interface between PP

and NBR phases (Figure 3.16). This interactions will increase interfacial adhesion, which leads to better interaction of radicals formed during degradation of PP and NBR. This type of improvement in degradation temperatures upon compatibilisation of immiscible polymer blends has been reported.[7]

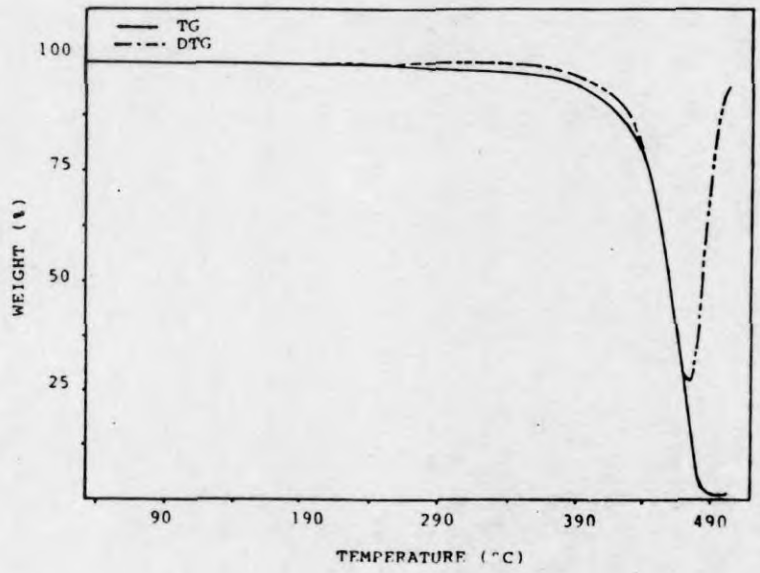

(a)

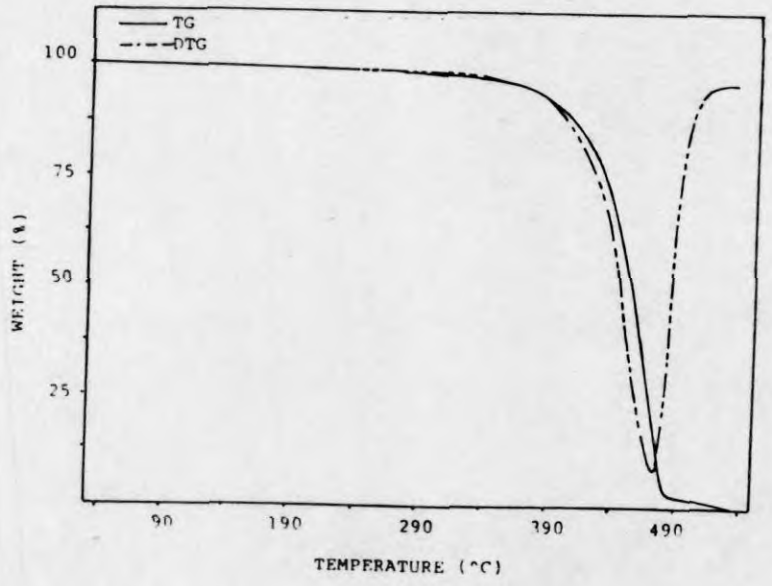

(b)

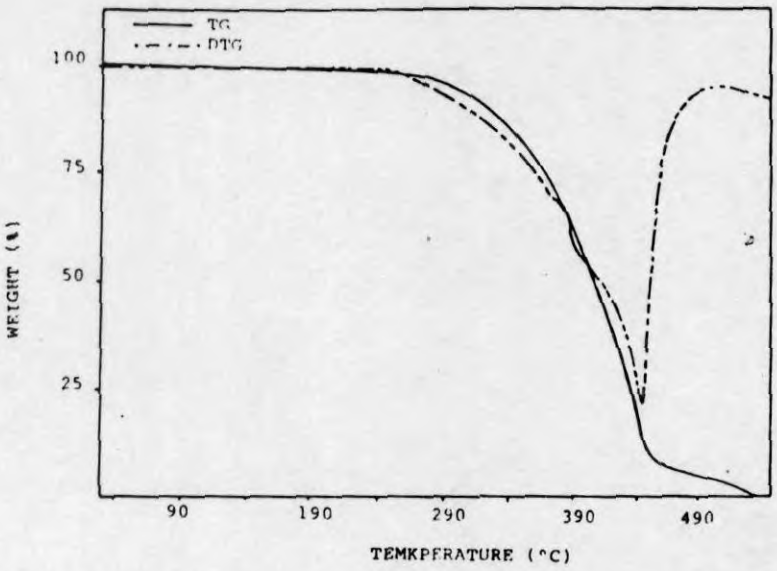

(c)

Figure 6.3. Thermograms and derivative thermograms of MA-PP compatibilised PP/NBR blends: (a) PM_{7001}, (b) PM_{7005} and (c) PM_{7010}.

6.2.3 *Effect of dynamic vulcanisation*

The vulcanisation of rubbers generally improves the degradation temperature since more energy is required to break the bonds formed during vulcanisation. Figures 6.4a–c show the thermograms and derivative thermograms of dynamic vulcanised P_{50} blends. The P_{50} blends were vulcanised using sulphur, peroxide and a mixed system composed of sulphur and peroxide. The data obtained from the thermograms and derivative thermograms are given in Table 6.3. From the table it is seen that, the initial degradation temperature (T_0) is shifted to higher temperatures on vulcanisation. The degradation temperatures corresponding to the two weight losses also show improvement upon vulcanisation. The initial degradation temperature is highest for samples cured with mixed system and lowest for sulphur system. The peroxide cured system takes an intermediate position. i.e., the degradation temperature follows the order PS<PC<PM.

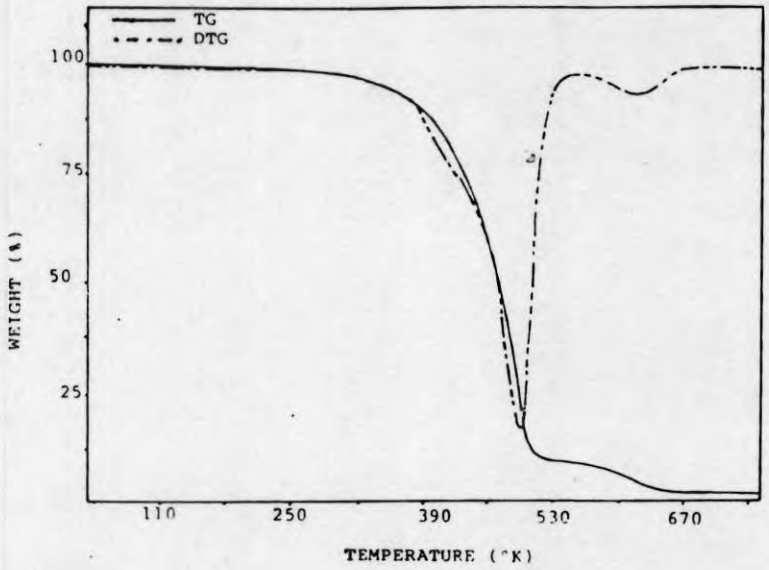
TG
DTG
100
75
50
25
WEIGHT (%)
110
250
390
530
670
TEMPERATURE (°K)

(a)

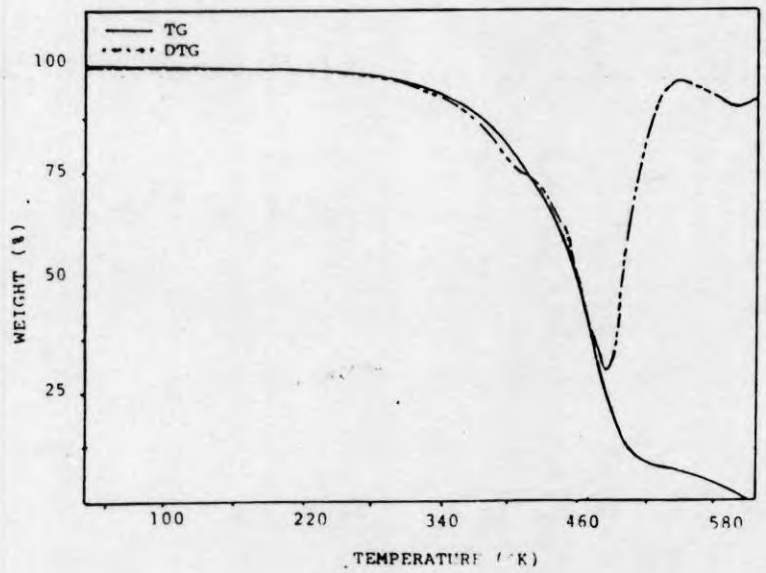
TG
DTG
100
75
50
25
WEIGHT (%)
100
220
340
460
580
TEMPERATURE (°K)

(b)

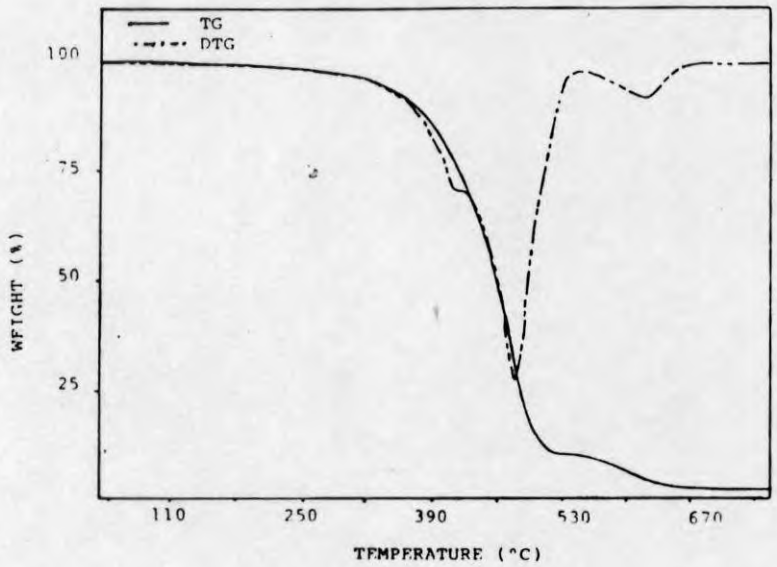

(c)

Figure 6.4. Thermograms and derivative thermograms of dynamically vulcanised PP/NBR blends: (a) PS_{50}, (b) PC_{50} and (c) PM_{50}.

Table 6.3. Thermal properties of dynamic vulcanised 50/50 PP/NBR blends.

	T_0 (wt %)	$T_{degr.}$ (°C)	Total wt. loss (%)	Wt. loss at 300°C (%)	Wt. loss at 400°C (%)	Activation energy (kJ/mol)
PS_{50}	314.56 567.12	495.00 623.86	93.90	13.89	83.33	29.08
PC_{50}	324.7 552.2	483.47 596.95	93.62	19.44	84.03	22.85
PM_{50}	340.24 564.98	482.27 615.91	90.47	14.58	83.6	28.92

This behaviour can be explained by considering the following parameters:(i) crosslink density and (ii) type of crosslinks formed. The crosslink density values of the samples obtained from swelling measurements are given in Table 6.4. Among

the different dynamically vulcanised systems, the peroxide cured system showed the highest crosslink density while sulphur system shows the lowest value. As the crosslink density increases, the number of bonds that have to be broken during degradation increases and hence the degradation temperature must increase.

Table 6.4. Crosslink density values of dynamically vulcanised 50/50 PP/NBR blends.

Sample	Crosslink density x 10^4 (gmol/cm^3)
PS_{50}	5.97
PC_{50}	7.99
PM_{50}	5.98

Another factor which is to be considered is the type of crosslinks formed. In sulphur cured system, flexible and more heat sensitive mono or disulphidic linkages are formed, while in peroxide cured system, a more stable C-C linkages are formed (Figure 3.20). In mixed cured system, both C-C and S-S linkages are formed. Among the C-C and S-S linkages, more energy is required to break C-C linkages. Hence, the initial degradation temperature (T_0) is lowest for sulphur cured system which contains S-S linkages. In peroxide and mixed cured systems, during vulcanisation in presence of peroxide the PP phase was degraded. At high temperatures, the polypropylene undergoes depolymerisation in presence of DCP as shown below.

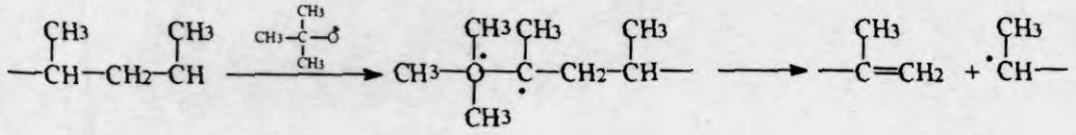

Since among PM and PC, the degradation must be more in PC system with high DCP content, which in turn reduce the initial degradation temperature of PC, though it contains more stable C-C linkages compared to PM.

The degradation temperatures corresponding to the two weight losses of PS system are higher compared to PM and PC systems. The lower degradation temperatures for PC and PM may be due to the degradation of PP, at the time of dynamic vulcanisation as explained earlier.

The activation energy for the degradation of the blends was determined using the Arrhenius equation

$$\ln W = \ln A - \frac{2.303E}{RT} \qquad (6.1)$$

where W is the weight loss at a temperature T in Kelvin, E-activation energy. Among the blend compositions, the polypropylene shows the lowest activation energy and NBR the highest (Table 6.1), i.e., polypropylene is more susceptible to degradation than NBR on increasing temperature. The P_{50} blend shows the lowest activation energy among the blends which also indicates the lowest interaction between PP and NBR in the blend. In compatibilised blends, the activation energy increases which shows the better interaction (Table 6.2). However on dynamic vulcanisation, the energy decreases for peroxide cured system. This indicates that the degradation of PP is enhanced in this system in presence of DCP (Table 6.3).

6.2.4 *Differential scanning calorimetry*

The melting behaviour of PP/NBR blends was analysed using differential scanning calorimetry. The DSC traces of the binary blends are given in Figures 6.5a–e. The results obtained from the analysis of these curves are given in Table 6.5.

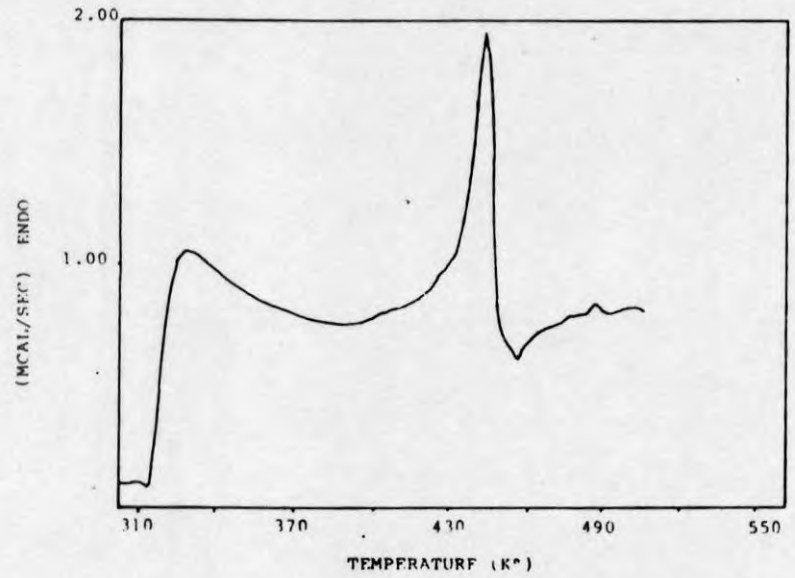
2.00
1.00
(MCAL/SEC) ENDO
310
370
430
490
550
TEMPERATURE (K°)

(a)

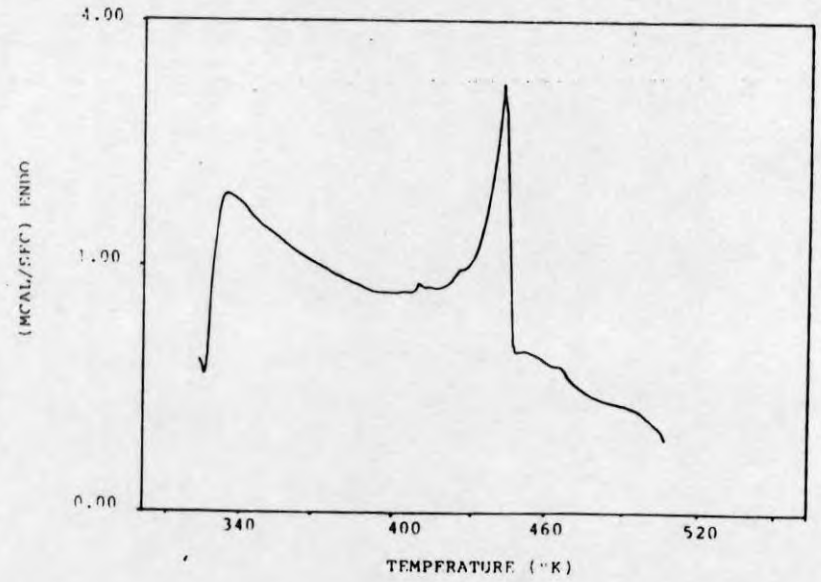
4.00
1.00
0.00
(MCAL/SEC) ENDO
340
400
460
520
TEMPERATURE (°K)

(b)

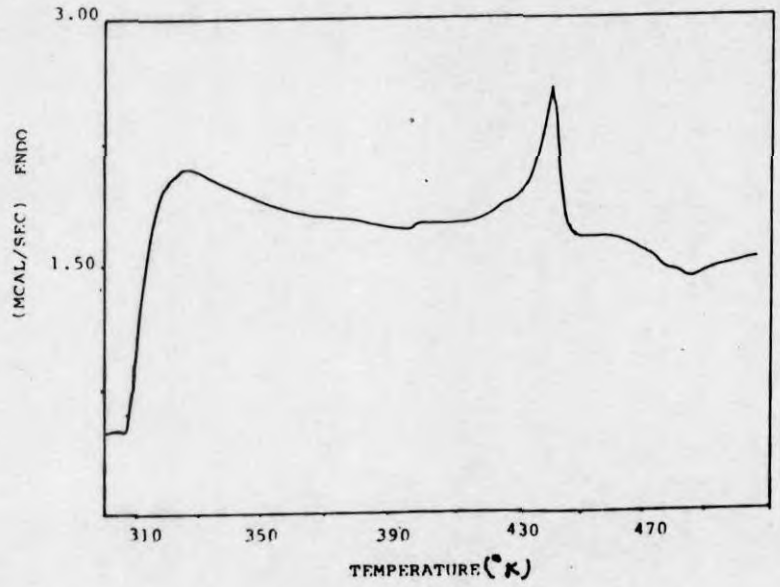
3.00
1.50
(MCAL/SEC) ENDO
310
350
390
430
470
TEMPERATURE(°K)

(c)

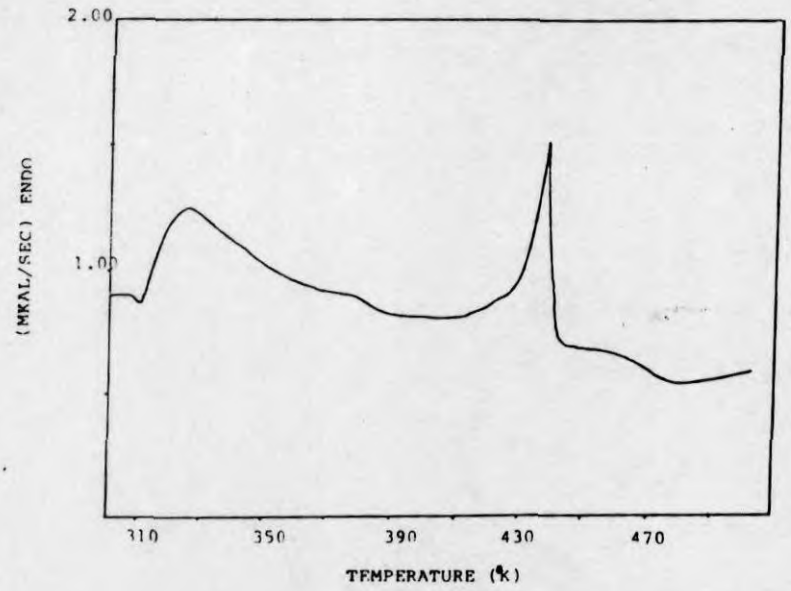
2.00
1.00
(MKAL/SEC) ENDO
310
350
390
430
470
TEMPERATURE (°K)

(d)

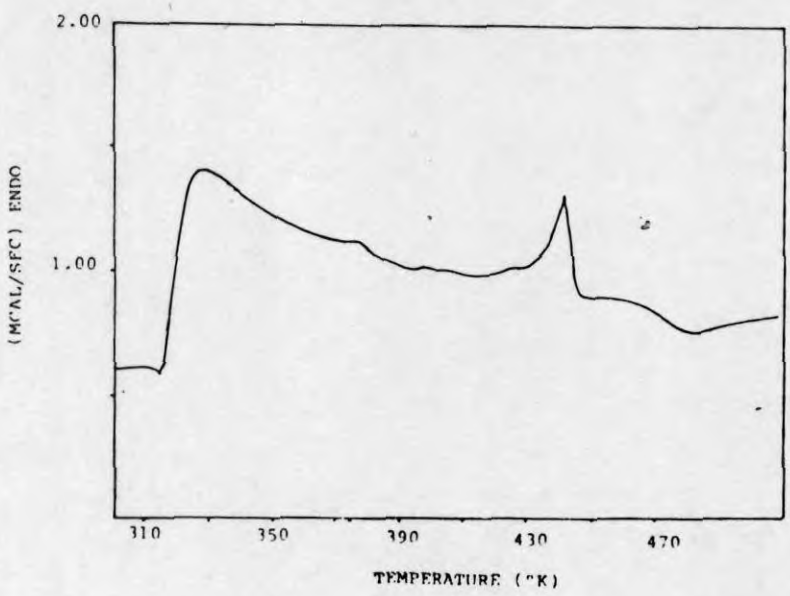

(e)

Figure 6.5. DSC curves of binary PP/NBR blends: (a) P_{100}, (b) P_{90}, (c) P_{70}, (d) P_{50} and (e) P_{30}.

Table 6.5. Melting characteristics of PP/NBR blends.

	T_{onset} (°K)	T_m (°K)	ΔH (cal/g)
P_{100}	431.81	441.5	18.45
P_{90}	432.66	441.11	12.97
P_{70}	432.3	439 93	10.88
P_{50}	430.79	437.34	8.53
P_{30}	433.84	440.08	3.7

From the table it is seen that the heat of fusion corresponding to the melting endotherm decreases upon the incorporation of NBR in to polypropylene. The heat of fusion values depend on the crystallinity of the material and hence the crystallinity of the system decreases with increase in the rubber content. This

indicates that the crystallinity of the system was affected by the presence of nitrile rubber. Martuscelli *et al.*[11,12] have made a detailed investigation on the effect of rubber phase on the crystallisation behaviour of thermoplastic elastomers and observed that, the rubber particles are present in the inter and intra spherulitic region of the crystalline phase of plastic. Hence the observed decrease in ΔH values and crystallinity (Figure 6.6) is due to the fact that the formation of crystallites in the blend was affected by the presence of nitrile rubber. Again the melting temperature corresponding to the melting endotherm also decreases upon the incorporation of rubber into polypropylene. In the case of compatible blends, the decrease in melting temperature is related to the extent of interaction between the components according to Flory-Huggins theory. However Stolp *et al.*[21] reported that in the case of incompatible blends, the melting point decreased since the noncrystallisable component retard the crystal growth which leads to imperfect crystals. Hence, the observed decrease in melting temperature on the addition of NBR is due to the impediment caused by NBR to the crystal growth of PP.

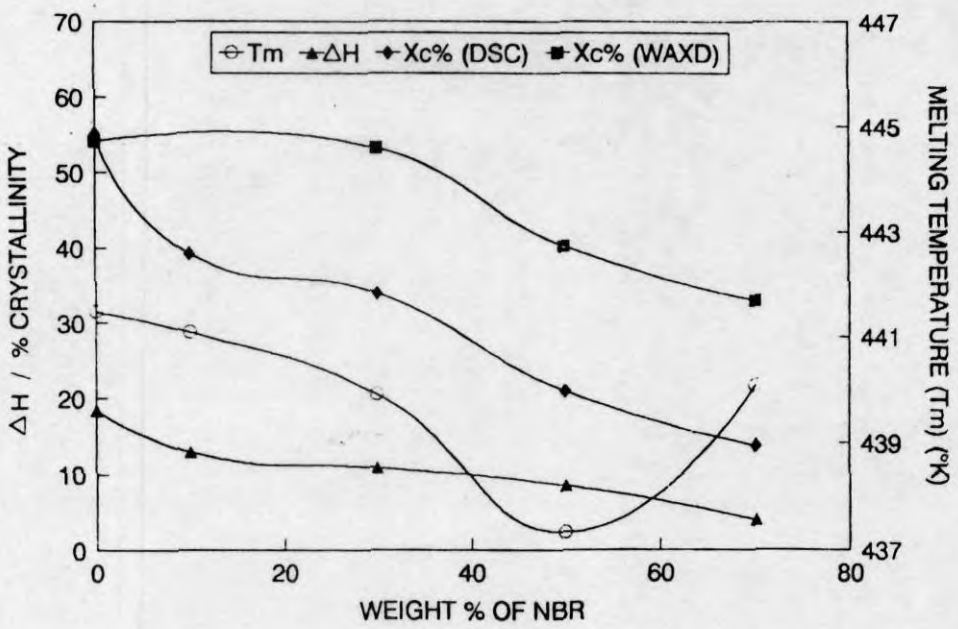

Figure 6.6. Variation of ΔH, crystallinity and melting temperature of PP/NBR blends with weight % of NBR.

6.2.5 *Wide angle X-ray scattering*

The properties of thermoplastic elastomers with a crystallisable component depends on crystalline structure and crystallinity of the blends. The wide angle X-ray scattering have been used to investigate the crystalline structure of PP/NBR blends. The X-ray diffractograms of binary PP/NBR blends are shown in Figure 6.7.

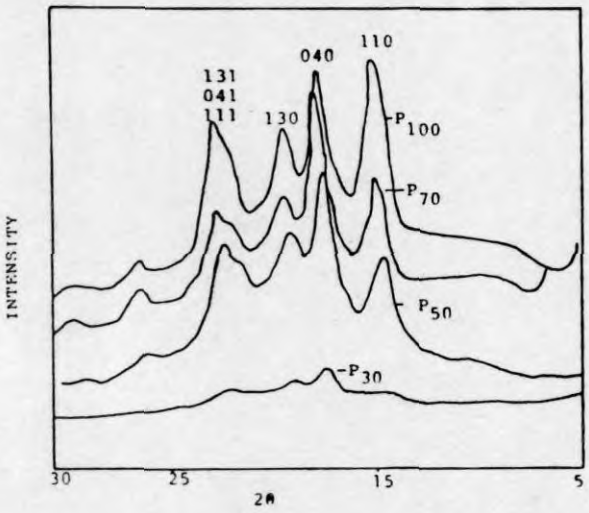

Figure 6.7. Wide angle X-ray diffractograms of binary PP/NBR blends.

The isotactic polypropylene generally has three types of crystalline structures, α, β and γ forms depending on the crystallisation conditions. The WAXD spectrum of polypropylene shows four maximas corresponding to the 110, 040, 130 and overlapping 131, 041 and 111 planes, which are characteristics of

α-monoclinic structure at 2θ of 14.1, 16.8, 18.5 and 21.2° respectively in X-ray diffractograms. The incorporation of NBR into polypropylene did not affect the crystalline structure of PP, i.e., the blends also exhibit the α-monoclinic structure. In polypropylene, the highest intense peak is at 2θ of 14.1°, however in the case of blends the highest intense peak is at 2θ of 16.8°. Table 6.6 shows the results obtained from the analysis of wide angle X-ray diffractograms of PP and the binary blends. The addition of 30 wt % of NBR into polypropylene increased the interplanar distance (d value). This indicates that rubber particles are present in the intra spherulitic structure of PP. As the concentration of NBR increased to 50 wt % and above, the d values decreased. The decrease in d values at higher concentrations of NBR may be due to the occlusion of rubber particles to inter spherulitic regions due to the large size of NBR at higher concentrations. The inter planar distance decreased in P_{30} also. This indicates the absence of rubber phase in spherulitic structure in P_{30}. This is schematically represented in Figure 6.8. The crystallinity (X_c) of the blends was also calculated using equation,

$$X_c = \frac{I_c}{I_c + I_a} \qquad (6.2)$$

where I_c and I_a represent the integrated intensity corresponding to the crystalline and amorphous phases and the results are given in Table 6.6. From the table it is seen that, the values are higher than that obtained from DSC measurements.

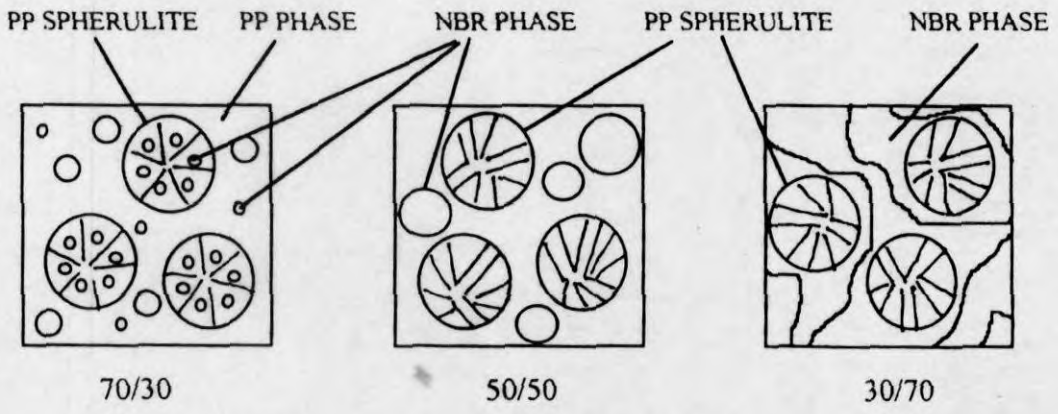

Figure 6.8. Schematic representation of the crystalline structure of PP/NBR blends.

Table 6.6. XRD datas of PP/NBR blends.

Reflection	P_{100}		P_{70}		P_{50}		P_{30}	
	2θ°	d (Å)	2θ°	d (Å)	2θ°	d (Å)	2θ°	d (Å)
110	14.05	6.30	13.99	6.33	14.04	6.31	14.08	6.29
040	16.85	5.26	16.77	5.29	16.85	5.26	17.09	5.19
130.	18.52	4.79	18.5	4.79	18.50	4.79	18.66	4.75
111	21.22	4.18	21.68	4.09	21.14	4.21	21.53	4.13
% Crystallinity	54.23		53.26		40.17		32.9	

The effect of compatibilisation of 70/30 PP/NBR blend with phenolic modified polypropylene and maleic anhydride modified polypropylene on the WAXD pattern is shown in Figures 6.9 and 6.10, respectively.

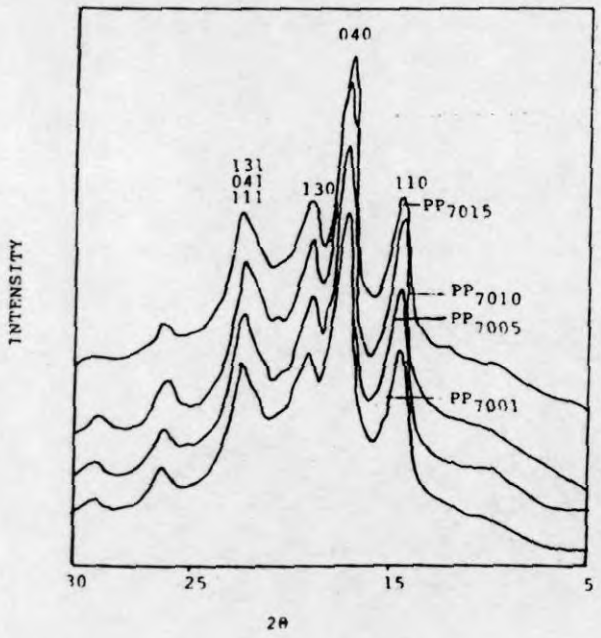

Figure 6.9. Wide angle X-ray diffractograms of Ph-PP compatibilised PP/NBR blends.

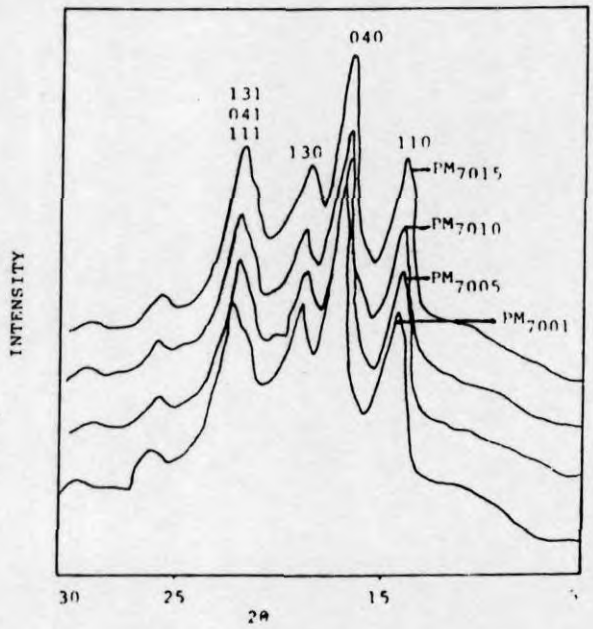

Figure 6.10. Wide angle X-ray diffractograms of MA-PP compatibilised PP/NBR blends.

The compatibilisation in PP/NBR blends did not affect the α-monoclinic structure of PP. However, in literature it has been reported that the compatibilisation of the blends leads to a change in crystalline structure.[23] The data obtained from the WAXD patterns are given in Tables 6.7 and 6.8. From the table it is seen that, the compatibilisation of the blends using phenolic modified polypropylene reduced the interplanar distance corresponding to different planes.

Table 6.7. XRD datas of Ph-PP compatibilised 70/30 PP/NBR blends.

Reflection	P_{7001}			P_{7005}			P_{7010}			P_{7015}		
	2θ°	d (Å)	L*	2θ°	d (Å)	L*	2θ°	d (A)	L*	2θ°	d (A)	L*
110	14.06	6.26	0.9	14.03	6.31	0.85	14.04	6.31	0.9	13.99	6.33	0.95
040	16.84	5.26	0.8	16.77	5.29	0.72	16.84	5.24	0.7	16.77	5.28	0.8
130	18.53	4.79	0.7	18.48	4.79	0.6	18.51	4.79	0.6	18.49	4.79	0.75
111	21.19	4.19	1.4	21.69	4.09	1.4	21.22	4.19	1.35	21.65	4.11	1.35

*The value of L was taken in arbitrary units.

Table 6.8. XRD datas of MA-PP compatibilised 70/30 PP/NBR blends.

Reflection	PM_{7001}		PM_{7005}		PM_{7010}		PM_{7015}	
	2θ°	d (Å)	2θ°	d (Å)	2θ°	d (Å)	2θ°	d (Å)
110	14.03	6.31	14.03	6.31	14.07	6.29	14.08	6.29
040	16.82	5.27	16.84	5.27	16.85	5.26	16.86	5.26
130	18.49	4.79	18.53	4.79	18.55	4.78	18.52	4.79
111	21.22	4.19	21.33	4.16	21.29	4.17	21.79	4.08

The width at half height (L) for different reflections were also calculated and it was observed that the peak width at half height which is a measure of spherulite size decreased upon compatibilisation. Hence, the size of spherulites increases upon compatibilisation since peak width at half height is inversely proportional to the size of the spherulite. These observations indicate that on compatibilisation of PP/NBR blends using Ph-PP and MA-PP lead to better crystallisation of polypropylene component.

6.3 References

1. I. C. McNeill, *Thermal Degradation in Comprehensive Polymer Science-6* (Ed., G. Allen), Pergamon Press, New York, 1989, Ch. 15.
2. W. Schnabel (Ed.), *Polymer Degradation Principles and Applications*, Hanser, New York, 1981.
3. N. Grassie (Ed.) *Developments in Polymer Degradation*, Applied Science, London Vol. 1-7.
4. K. T. Varughese, *Kaust. Gummi Kunst.*, **41**,114 (1988).
5. I. A. Amraee, A. A. Kathab and S. A. Jollah, *Rubber Chem. Technol.*, **69**, 130, 1995.
6. P. P. Lizymol and S. Thomas, *Polym. Degrad. Stab.*, **41**, 59 (1993).

7. M. Subhra, P. G. Mukunda and G. B. Nando, *Polym. Degrad. Stab.*, **50**, 21 (1995).

8. C. Chen and F. S. Lai, *Polym. Eng. Sci.*, **34**, 472 (1994).

9. L. Callandrelli, B. Immirzi, M. Malinconio, E. Martuscelli and F. Riva, *Makromol. Chem.*, **193**, 669 (1992).

10. D. IL. Kang, C. S. Ha and W. J. Cho, *Eur. Polym. J.*, **28**, 565 (1992).

11. E. Martuscelli, in *Thermoplastic Elasromers from Rubber-Plastic Blends* (Eds., S. K De and A. K. Bhowmick), Ellis Horwood, New York, 1990.

12. E. Martuscelli, C. Silvlestre and G. Abate, *Polymer*, **23**, 229 (1982).

13. Z. Bartczak, Z. A. Galeski and E. Martuscelli, *Polym. Eng. Sci.*, **24**, 1155 (1984).

14. D. Hlavata, J. Plestil, D. Zuchowska and R. Steller, *Polymer*, **32**, 3313, 1991.

15. A. T. Koshy, B. Kuriakose, S. Thomas and S. Varughese, *Polymer*, **34**, 3428 (1993).

16. R. N. Santra, B. K. Samantaray, A. K. Bhowmick and G. B. Nando, *J .Appl. Polym.. Sci.*, **49**, 1145 (1993).

17. C. J. Wu, J. F. Kuo and C. Y. Chen, *Polym. Eng. Sci.*, **33**, 1329 (1993).

18. D. J. In, C. S. Ha and S. C. Kim, *Polymer (Korea)*, **12**, 249. (1988).

19. C. S. Ha, *J. Appl. Polym. Sci.*, **35**, 2211 (1988).

20. N. R. Choudhury, T. K. Chaki, A. Dutta and A. K. Bhowmick, *Polymer*, **30**, 2047 (1989).

21. M. Stolp, R. Androsch and H. J. Radusch, *Polym. Networks Blends*, **6**, 141 (1996).

22. Z. Horak, Z. Krulis, J. Baldrian, I. Fortelny and D. Konecny, *Polym. Networks Blends*, 7, 43 (1997).

Chapter 7

Dielectric Properties: Effects of Blend Ratio, Filler Addition and Dynamic Vulcanisation

The results of this chapter have been submitted for publication in *Journal of Applied Polymer Science*

7.1 Introduction

Thermoplastic elastomers are used in various electrical applications like wire and cable as insulation and jacketing materials due to their unique combination of properties such as low temperature flexibility excellent insulating characteristics and resistance to moisture absorption.[1] By blending suitably selected plastics with elastomers, new materials with desirable final properties can be prepared. Electrical properties of various polymer blends have been investigated by different researchers.[2-8] In these reports it has been shown that the dielectric properties of polymers and blends in general depend on structure, crystallinity, morphology and presence of fillers or other additives. The dielectric constant of the blends is found to increase with increase in the effective dipole moment. In SBR/NBR blends, the permittivity ε' was found to increase with increase in concentration of C≡N dipoles.[8] The incorporation of polar components into polyethylene has increased the dielectric constant and dielectric loss of the blends.[9] The measurement of dielectric properties as a function of temperature was used as a way to study the miscibility of different polymer blend systems.[2] Dielectric monitoring of thermosets and their blends has been used for the measurement of curing.[4] In heterogeneous polymer blends, the dielectric constants of the polymers are influenced by interfacial effects i.e., due to the polarisation arising from difference in conductivities of the two phases.[9] The volume resistivity of various polymer blends upon the incorporation of fillers was also studied.[10-14]

Polypropylene has excellent electrical properties like low dielectric constant, loss factor, high volume resistivity and high surface resistivity and is used as high frequency insulators.[15,16] Nitrile rubbers have moderate insulating properties and good oil resistance. Therefore, by blending PP with NBR, materials with improved processability, good flexibility and excellent oil resistance can be achieved. In this chapter we have studied the effect of blend ratio, and dynamic vulcanisation on dielectric constant, dissipation factor, loss factor and volume resistivity of PP/NBR blends. The effect of different particulate fillers on dielectric properties is also investigated.

7.2 Results and discussion

7.2.1 *Volume resistivity*

Resistivity studies are important for insulating materials, since the most desirable characteristic of an insulator is its ability to resist the leakage of electrical current. Figure 7.1 shows the variation of volume resistivity (ρ_v) of PP/NBR blends as a function of NBR concentration. Polypropylene is a good insulator with volume resistivity in the order of 10^{16} Ω cm, while the volume resistivity of nitrile rubber is in the order of 10^{10} Ω cm. In the case of blends the ρ_v has values in between that of PP and NBR. As the concentration of NBR increases the ρ_v value decreases. This decrease in ρ_v is due to the introduction of low resistivity NBR. The curve shows a sharp change after 50 wt % NBR. This change can be correlated with the morphology of the blends. In P_{70} and P_{50}, NBR is dispersed as domains in the continuous polypropylene matrix while in P_{30}, NBR also forms a continuous phase resulting in a co-continuous morphology. (Figure 3.2) The change of NBR from dispersed phase to continuous phase should cause a sharp change in the electrical properties.

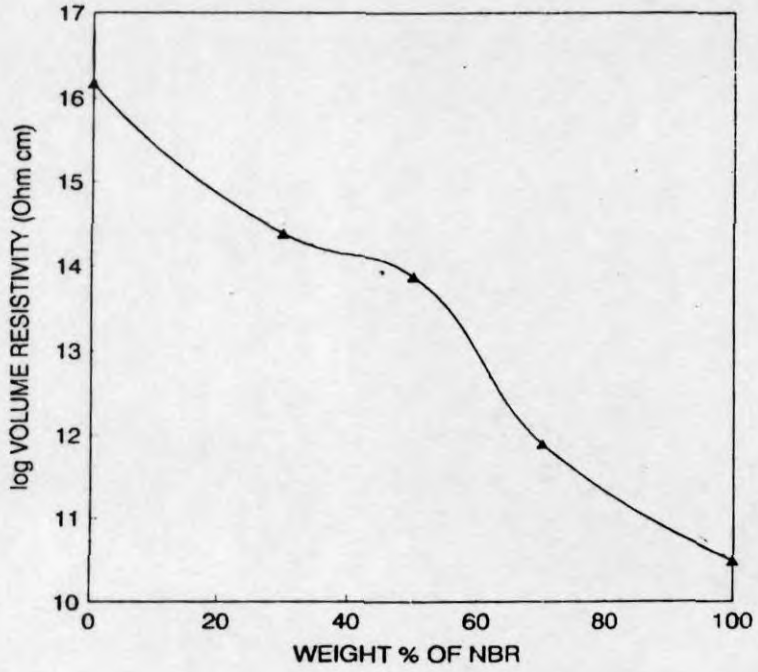

Figure 7.1. Variation of volume resistivity of PP/NBR blends with NBR content.

The effect of dynamic vulcanisation on ρ_v values of PP/NBR blends is given in Table 7.1. On dynamic vulcanisation of the blends using sulphur, the resistivity of the blends decreases for different blend compositions. Among the various vulcanised systems, the DCP system shows the highest resistivity value and sulphur the lowest. The mixed system shows an intermediate value. The difference in conductivity among the different vulcanising systems may arise because of the difference in the type of crosslinks formed during vulcanisation. In sulphur vulcanised system, S-S linkages are formed whereas in DCP crosslinked system C-C linkages are formed (Figure 3.19). In mixed vulcanised system a combination of both C-C and S-S linkages are formed. In comparison to C-C linkages, S-S linkages have ionic character, which may further increase the conductivity of the system. On vulcanisation of blends, some ionic impurities are incorporated into the blend system as vulcanising ingredients and hence the conductivity of the final system increases upon vulcanisation. In the case of

peroxide vulcanisation, there is the presence of free radicals which arise due to the degradation of PP which may also increase the conductivity.

Table 7.1. Volume resistivity values of unvulcanised and dynamically vulcanised P_{70} blends.

Sample	Volume resistivity x 10^{-12} Ω cm
P_{70}	24
PS_{70}	3.52
PC_{70}	8.65
PM_{70}	5.82

The effect of incorporation of fillers on the resistivity values is shown in Figure 7.2. It is seen from the figure that, the incorporation of 10 wt % each of carbon black, silane treated silica and cork into P_{50} blend decreases the resistivity values. In the case of carbon black and silica further increase in the loading decreases the resistivity, while in the case of cork, as the loading increases the resistivity also increases. The decrease in resistivity upon the incorporation of silica and carbon black may arise from the presence of ionic groups present in silica and carbon black which facilitate the conducting process. The non-conducting nature of the cork filler accounts for the increase in resistivity of PP/NBR blend at higher loadings of cork. By the incorporation of the conducting filler into polymers and blends, the resistivity generally decreases and there is a critical loading of filler i.e., percolation threshold at which the polymer composites change from insulating to conducting material. Abo-Hashem *et al.*[12] have reported that in SRF black loaded butyl rubber, the percolation threshold is at 30 wt % carbon black. In PP/NBR blends, the change in resistivity on increasing the loading up to 30 wt % is less and no percolation threshold is observed up to this loading.

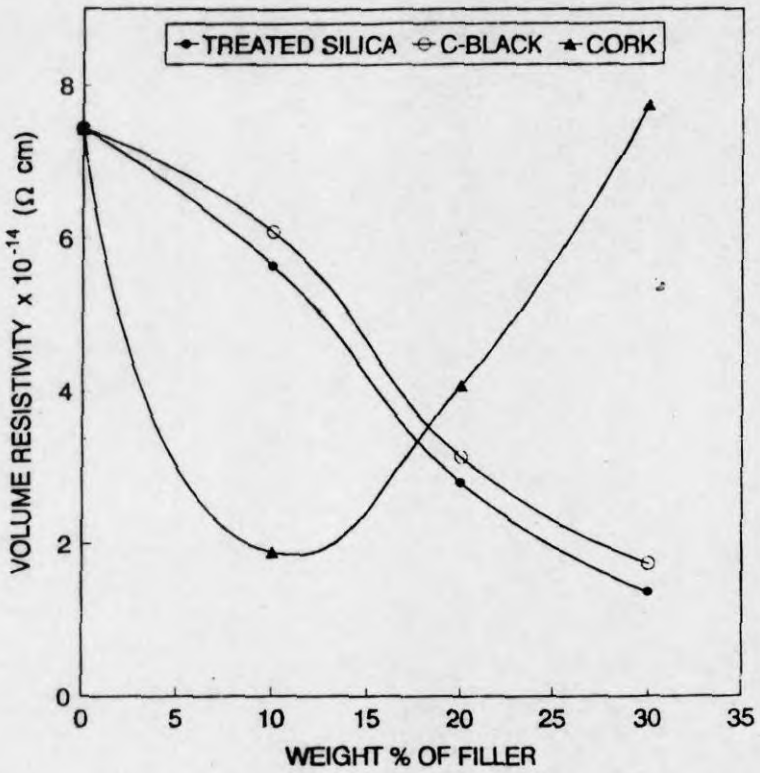

Figure 7.2. Variation of volume resistivity of 50/50 PP/NBR blends with wt % of filler for different fillers.

7.2.2 *Dielectric constant, loss factor and dissipation factor*

(a) Effect of blend ratio

The dielectric constant and loss tangent are important parameters in the selection of an insulating material. The variation of dielectric constants of pure polypropylene and the blends of PP/NBR as a function of frequency is shown in Figure 7.3. The dielectric constant values of the pure PP, NBR and their blends were decreased with increase in frequency. Generally the dielectric constant of a material arises due to the polarisation of molecules and the dielectric constant increases with increase in polarisability. The different types of polarisation possible in a material are (1) electronic polarisation (2) atomic polarisation and (3) orientation polarisation due to the orientation of dipoles parallel to the applied field.[17] In heterogeneous materials, there is the possibility for interfacial polarisation which arises due to the difference in conductivities of the two

phases.[18] The time required for each type of polarisation to reach the equilibrium level varies with the nature of polarisation.

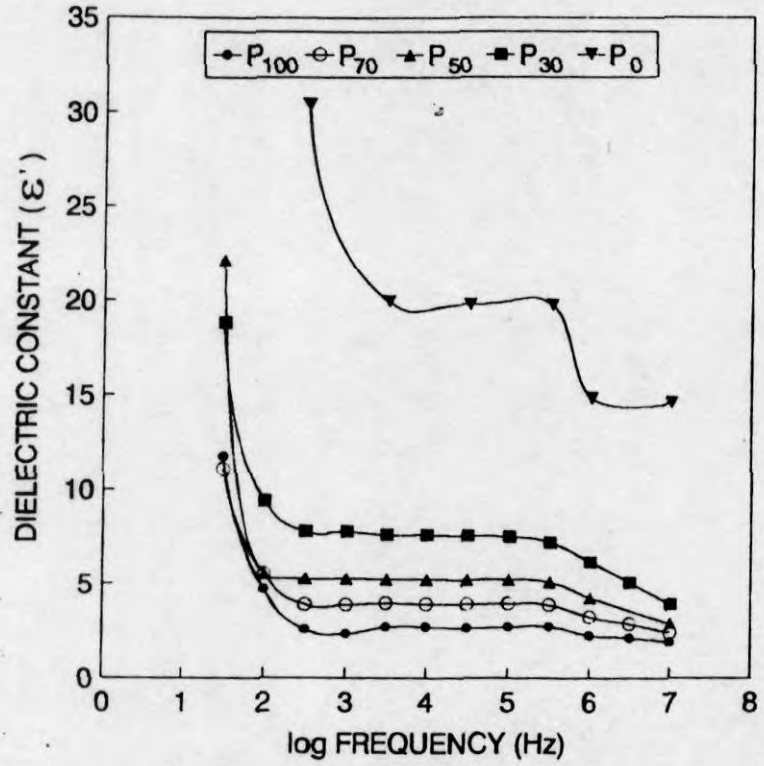

Figure 7.3. Variation of dielectric constant of PP/NBR blends with frequency.

The orientation polarisation requires more time compared to electronic and atomic polarisation to reach static field value. Therefore, at lower frequency region, the orientation polarisation decreases with increase in frequency compared to electronic and atomic polarisations. The interfacial polarisation generally occurs at much lower frequencies. In the dielectric constant vs. frequency plot of PP/NBR blends, it is seen that the reduction in ε′ is in three stages. In the first stage, high values of dielectric constant can be attributed to the interfacial polarisation effects. The high value of ε′ for polypropylene indicates the presence of impurities in polypropylene. It may also be due to the fact that the impurities in such polymers

may cause some oxidation at the site of structural defects which leading to the formation of oxidised centres which then cause interfacial polarisation.[1]

In the case of blends, due to the presence of two phases NBR and PP with different conductivities, interfacial polarisation occurs leading to an increase in dielectric constant. Since interfacial polarisation decreases with increase in frequency, as the frequency increases to 100 Hz the dielectric constant decreases considerably. In the region 3.16×10^2–10^5 Hz frequency, the dielectric constant has contribution from orientation, atomic and electronic polarisations. Here the dispersion region spreads over a wide range of frequencies. Above 3.16×10^5 Hz frequency, the ε' further reduces which may be due to the drop in orientation polarisation. At this frequency the drop in ε' increases with increase in the rubber content. It is due to the increase in dipoles in the materials at high rubber concentration, which leads to a decrease in orientation polarisation at a higher rate compared to the blends with lesser number of dipoles.

The variation of dielectric constant with weight percentage of NBR at three different frequencies is shown in Figure 7.4. Polypropylene shows the lowest ε' value, characteristic of a non-polar material and nitrile rubber shows the highest value. Generally for a non-polar material, the dielectric constant equals the square of refractive index (n^2). The refractive index of polypropylene is 1.47 and hence $\varepsilon' = 2.16$. The experimental value is 2.805. The higher values may be due to the presence of interfacial polarisation which arises due to the presence of impurities. For polar materials, the ε' values are generally greater than that of n^2 and ε' increases with increase in polarity. In the case of blends, the dielectric constant increases as the rubber content increases. This increase in ε' with the incorporation of rubber is due to increase in C≡N dipoles, which increase the orientation polarisation and also due to the presence of interfacial polarisation. Again, the orientation of dipoles depends on the crystallinity of the medium. With the incorporation of rubber, the crystallinity of the system decreases (Table 3.2). As the crystallinity of the system decreases, the dipoles can orient more easily. Such

an increase in dielectric constant upon the incorporation of polar polymers was reported.[9] The dielectric constant is related to the resistivity by the equation[19]

$$\log R_{10}(298\ K) = 23 - 2\ .\ \varepsilon'\ (298\ K) \qquad (7.1)$$

i.e., the electrical resistance of polymers decreases exponentially with increasing dielectric constant. In PP/NBR blends as the dielectric constant increases with increase in rubber content, the volume resistivity decreases (Figure 7.1). The increase in ε' is more pronounced above 50 wt % of NBR (Figure 7.4). This can be correlated with the phase inversion of NBR from dispersed to continuous phase on increasing the concentration of NBR from 50 to 70 wt % (Figure 3.2). The continuous nature of NBR phase leads to better orientation of dipoles and results in high dielectric constant.

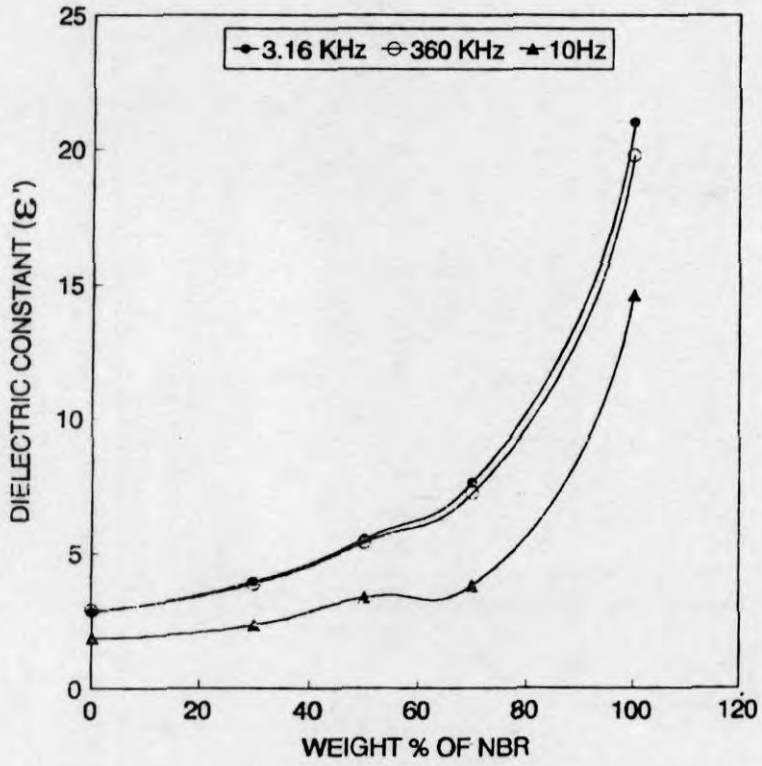

Figure 7.4. Variation of dielectric constant of PP/NBR blends with NBR content.

The experimental data can be compared with model calculations. The dielectric constant of a composite containing two components can be expressed in the general form:

$$\varepsilon'_c = V_1 \varepsilon'_1 + \varepsilon'_2 (1 - V_1) \qquad \text{(Model I)} \qquad (7.2)$$

where ε'_1, and ε'_2 are dielectric constants of components 1 and 2 and V_1 and V_2 are the volume fractions of components 1 and 2, respectively. The logarithmic variation of dielectric constant was also expressed by the equation:

$$\log \varepsilon'_c = V_1 \log \varepsilon'_1 + (1 - V_1) \log \varepsilon'_2 \qquad \text{(Model II)} \qquad (7.3)$$

The dielectric constant of two phase mixtures based on spherical particle, which consider all the possible interaction are given by Reynoulds and Hough as[20]

$$\varepsilon'_c = ¼ H + (H_2 + 8 \varepsilon'_1 \varepsilon'_2)^{1/2} \qquad \text{(Model III)} \qquad (7.4)$$

$$\text{where } H = (3V_1 - 1) \varepsilon'_1 + (2 - 3V_2) \varepsilon'_2 \qquad (7.5)$$

The Maxwell-Wagner Sillers equation was also used to predict the ε' values which is given as[21]

$$\varepsilon'_c = \varepsilon' \frac{2\varepsilon'_2 + \varepsilon'_1 + 2V_1(\varepsilon'_1 - \varepsilon'_2)}{2\varepsilon'_2 + \varepsilon'_1 + V_1(\varepsilon'_1 - \varepsilon'_2)} \qquad \text{(Model IV)} \qquad (7.6)$$

The applicability of Claussius Mossoti equation[21]

$$\varepsilon'_c = \frac{(1 - V_1) 2\varepsilon'^2_2 + 1 + (2V_1)\varepsilon'_1 \varepsilon'_2}{(1 - V_1)\varepsilon'_1 + (2 + V_1)\varepsilon'_2} \qquad \text{(Model V)} \qquad (7.7)$$

was also checked.

Figure 7.5 gives the experimental and the theoretical variation of dielectric constants with blend composition. The experimental values are lower than that of parallel model and is close to logarithmic mixing rule. The Maxwell-Wagner-Sillers equation gives better correlation of dielectric constants with experimental results.

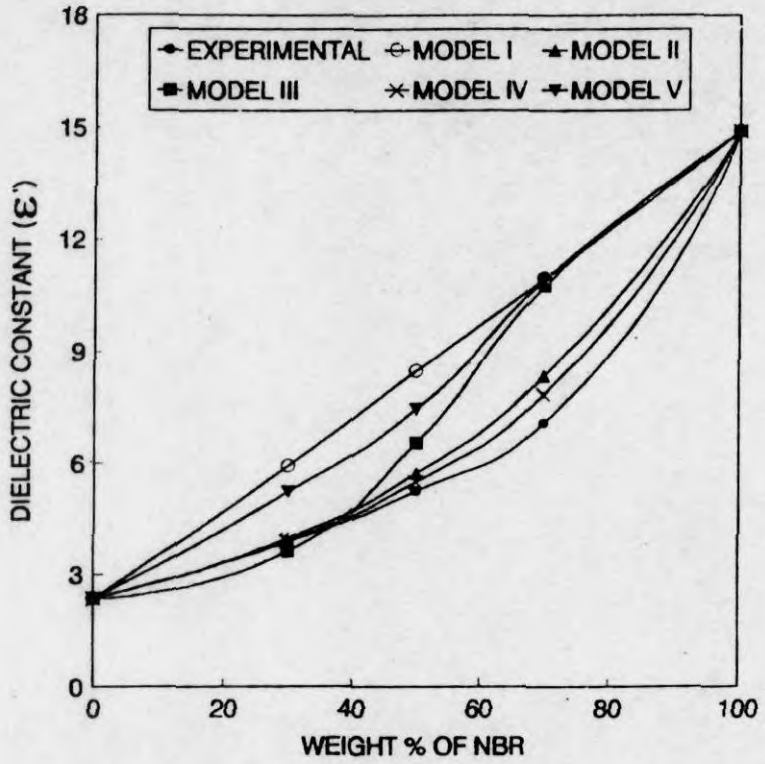

Figure 7.5. Experimental and theoretical variation of ε′ values with wt % of NBR

The measurement of dissipation factor (tan δ) and loss factor (ε″) of insulating material is important since the loss tangent is a measure of the alternating current electrical energy which is converted into heat in an insulator. This heat raises the insulator temperature and accelerates its deterioration. The variation of dissipation factor and loss factor (ε″) with frequency of PP and PP/NBR blends is shown in Figure 7.6. As the frequency increases the dissipation factor and loss factor increase for pure PP and its blends. A relaxation region is observed in the frequency range 3.16×10^5 - 3.16×10^6 Hz which may be due to a lag in dipole orientation behind the alternating electric field. Also, it is seen from the Figure 7.6 that the dissipation factor and magnitude of relaxation increase with increase in rubber content. In the case of polypropylene, the relaxation is due to the lag in electronic and atomic polarisation. But on the incorporation of nitrile rubber, dipoles are introduced into the system and this leads to lag in orientation of dipoles

on the application of electric field. Hence the dissipation factor increases with increase in rubber content. Blends of NBR with PP show the presence of a relaxation peak maximum at a frequency 10^6 Hz. As the concentration of NBR increases, the relaxation peak maximum shifts to higher frequency i.e., to 3.16 x 10^6 Hz. This suggests that the relaxation time decreases with increase in rubber content.

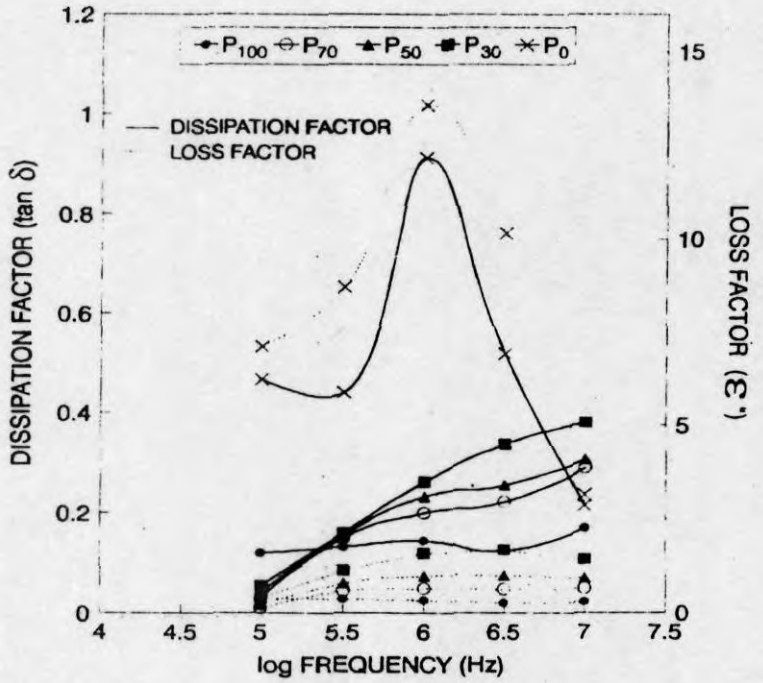

Figure 7.6. Variation of dissipation factor and loss factor of PP/NBR blends with frequency.

In polar polymers it was reported that the increase in crystallinity reduces the tan δ values and also leads to an increase in relaxation time. i.e., their peaks corresponding to the relaxation process shift to lower frequency, since relaxation time is given by

$$\tau = 1/2\pi fm \qquad (7.8)$$

where fm is the frequency corresponding to the maximum in relaxation peak. In PP/NBR blends as the concentration of NBR increases, the crystallinity of the

system decreases. Hence the observed shift in relaxation frequency or the reduction in relaxation time is due to the reduction in crystallinity. As the crystallinity of the system decreases, the rotatory motion of the dipoles becomes easy which leads to higher values of tan δ.

The sharp increase in tan δ beyond 50 wt % NBR is due to the change in morphology of the blend, i.e. the phase inversion of NBR from dispersed to continuous phase. It is seen that the incorporation of rubber into polypropylene, did not increase the value of tan δ more than 3%, which is frequently desired to avoid problems leading to failure of the insulator.

(b) Effect of fillers

Fillers are generally incorporated into TPEs to modify physical and electrical properties. The effect of addition of carbon black on ε′ values in 50/50 PP/NBR blend is shown in Figure 7.7.

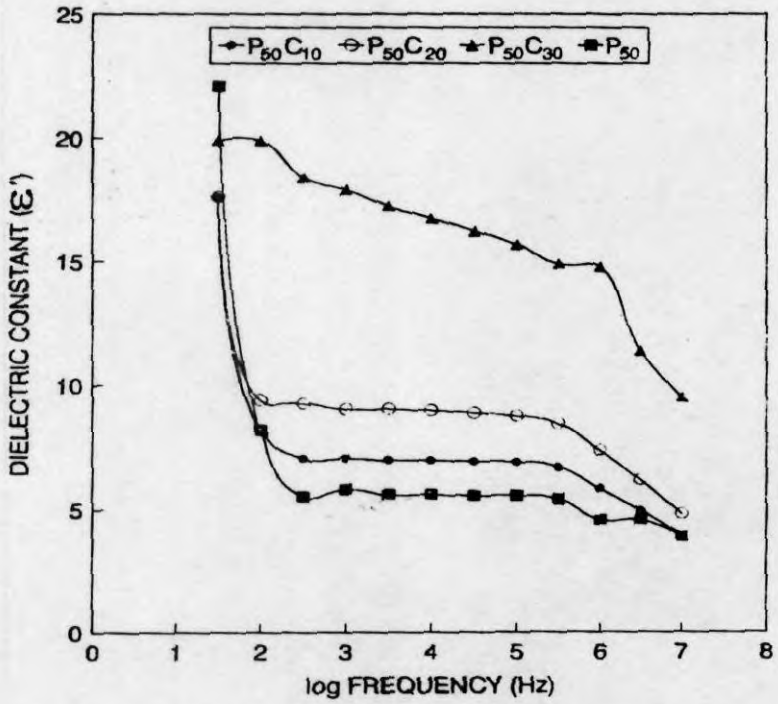

Figure 7.7. Variation of dielectric constant of carbon black loaded P_{50} blends with frequency.

The incorporation of carbon black into P_{50} blend increases the dielectric constant. The increase in ε' upon the incorporation of carbon black is due to the conducting nature of the black which is associated with conjugated bonding structure present in the crystalline regions and also due to the presence of polar groups in carbon black. It is again seen from Figure 7.7 that as the carbon black loading increases, the dielectric constant increases and this increase is more pronounced at 30% carbon black. Figure 7.8 depicts the variation of dielectric constant of PP/NBR blends at 30 wt % loading of carbon black. Upon the incorporation of carbon black the dielectric constants of all the blends are increased and this increase becomes more pronounced with increase in rubber content. It is seen from the Figure 7.8 that at 70 wt % NBR, the dielectric constant shows a sharp increase compared to P_{70} and P_{50}. This can be explained in terms of the morphology of the system.

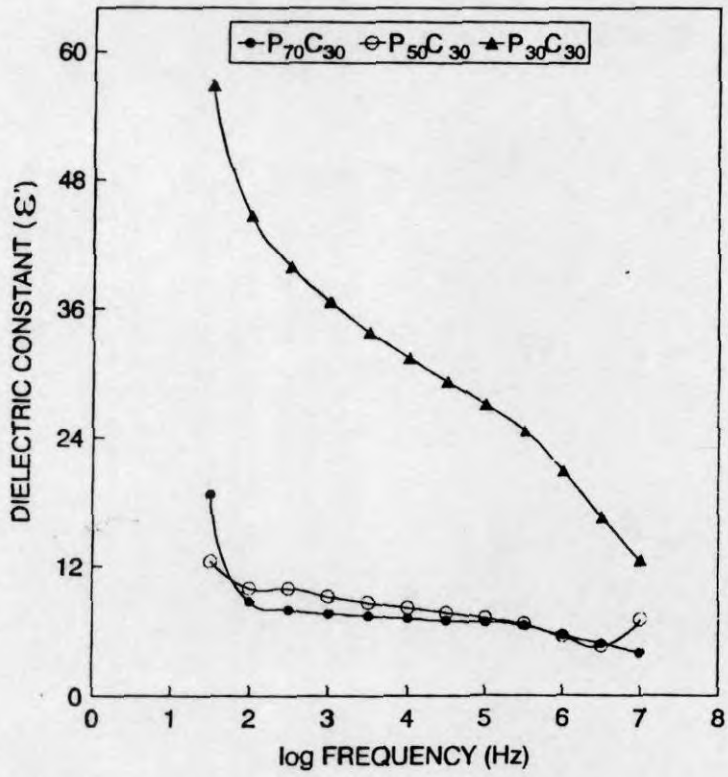

Figure 7.8. Variation of dielectric constant of 30 wt % carbon black loaded PP/NBR blends with frequency.

The morphology of filled blends can be schematically represented as shown in Figure 7.9. In P_{70} and P_{50}, NBR forms the dispersed phase in continuous PP phase while in P_{30}, NBR forms a continuous phase resulting in a co-continuous morphology. Again at this carbon black concentration (30%) the carbon black forms continuous network in the continuous nitrile rubber phase. This leads to an increase in conductivity of the system and an increase in dielectric constant. Carbon black is predominantly dispersed in the NBR phase due to its high polarity. Generally in thermoplastic elastomers the fillers locate in the rubber phase.[1]

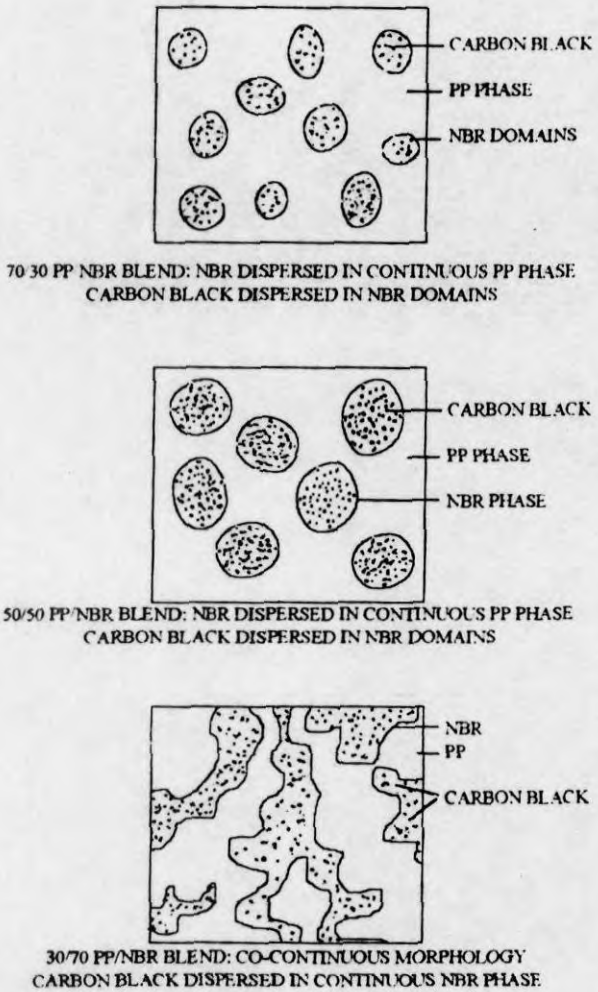

Figure 7.9. Schematic representation of the morphology of carbon black loaded PP/NBR blends.

The variation of dielectric constant with the incorporation of silane treated silica is shown in Figure 7.10. In these samples also the ε′ values decrease with frequency in three steps, due to the relaxation in interfacial and dipole polarisations. It is seen from the above figure that upon the incorporation of silica, the dielectric constant increases up to 20 wt % loading. However, at 30 wt % loading the ε′ value decreases. The increase in ε′ on the addition of silica may be due to the presence of polar groups present in the filler. As the filler loading increases, the density of the system is also increased and the extent of orientation of dipoles is retarded, and hence the ε′ shows a decrease at this concentration. Figure 7.11 shows the variation of ε′ with frequency for P_{70}, P_{50} and P_{30} blends containing 30 wt % of silane treated silica. As the concentration of rubber increases the ε′ increases and it is seen from the Figure 7.11 that the incorporation of silica into the blend increases the dielectric constant. The increase is more in the case of P_{70} blend, while in P_{50} and P_{30}, the incorporation of silica only slightly affects the ε′ values.

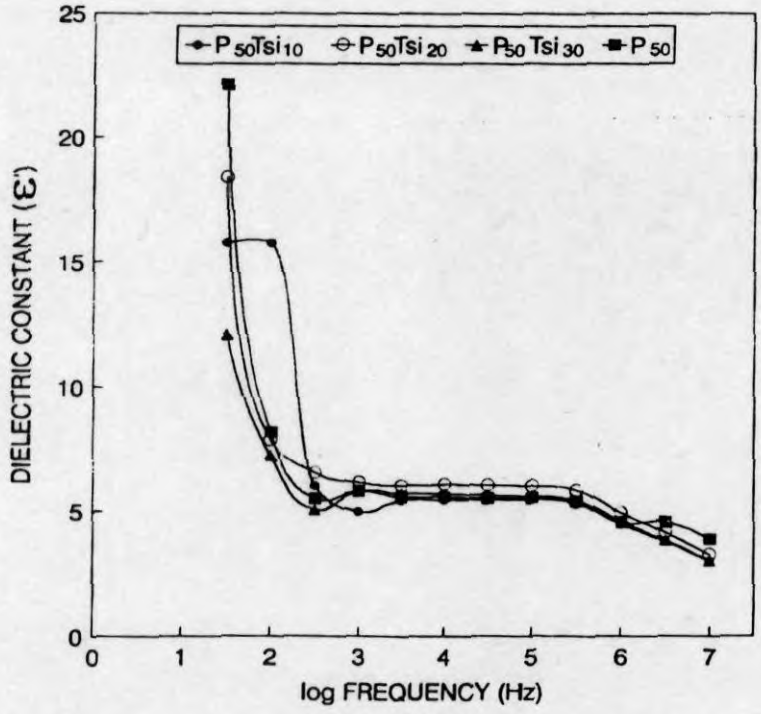

Figure 7.10. Variation of dielectric constant of silane treated silica loaded P_{50} blends with frequency.

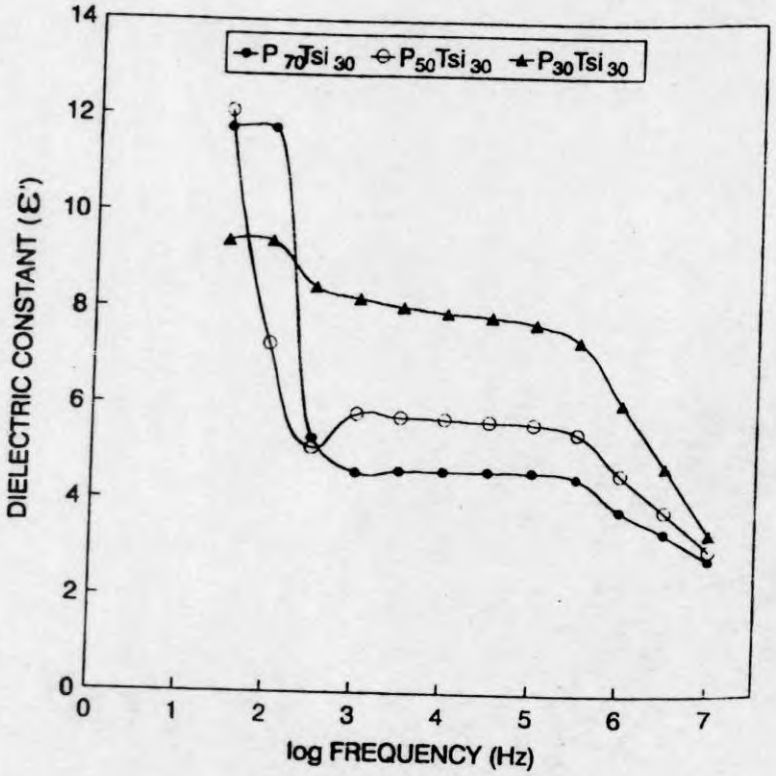

Figure 7.11. Variation of dielectric constant of 30 wt % silane treated silica loaded PP/NBR blends with frequency.

Figure 7.12 depicts the variation of ε′ with frequency for P_{50} blend containing varying concentration of cork. With the incorporation of 10 wt % cork, the ε′ increases while further increase in loading decreases the ε′ values. The increase in ε′ on the addition of cork is due to the interfacial polarisation. The variation of dielectric constant with 30 wt % of cork loaded P_{70}, P_{50} and P_{30} blends are shown in Figure 7.13. The nature of relaxation spectra is not affected by the presence of cork. Here also the dielectric constant increases with increase in rubber content, but the difference is less than those with other two fillers, which may be due to the non-conducting character of the cork compared to the other two fillers.

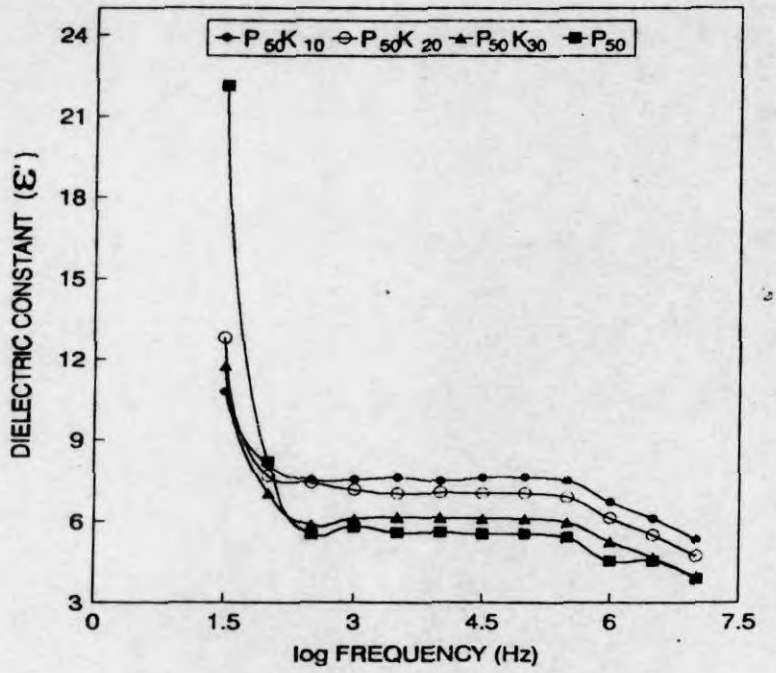

Figure 7.12. Variation of dielectric constant of cork loaded P_{50} blends with frequency.

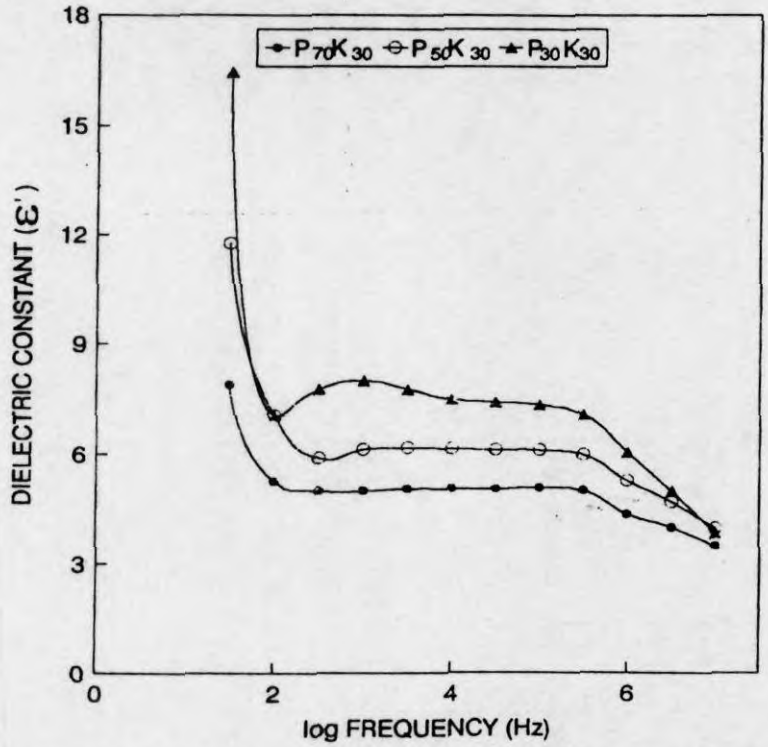

Figure 7.13. Variation of dielectric constant of 30 wt % cork loaded PP/NBR blends with frequency.

The variation of loss factor with frequency for different filler loadings of carbon black, cork and silane treated silica filled 50/50 PP/NBR blends is shown in Figures 7.14–7.16 respectively. Figure 7.14 shows the variation of loss factor, ε″, with frequency for carbon black loaded samples. The loss factor shows an increase with filler loading. The addition of carbon black did not alter the relaxation process, however the peak height corresponding to the relaxation of C≡N dipole increases. At 30 phr loading, the peak maximum shifted to a lower frequency of 10^6 Hz compared to 3.16 x 10^6 Hz for other loadings. The incorporation of filler into the blend system increases the dielectric loss and this may be due to the presence of some oxidising groups on surface of carbon black and also due to the increase in conductance loss. The shift in relaxation frequency to low values i.e., reduced relaxation time indicates that the resistance for relaxation of C≡N dipoles increases at 30 phr loading. This indicates that the filler mainly locates in rubber phase.

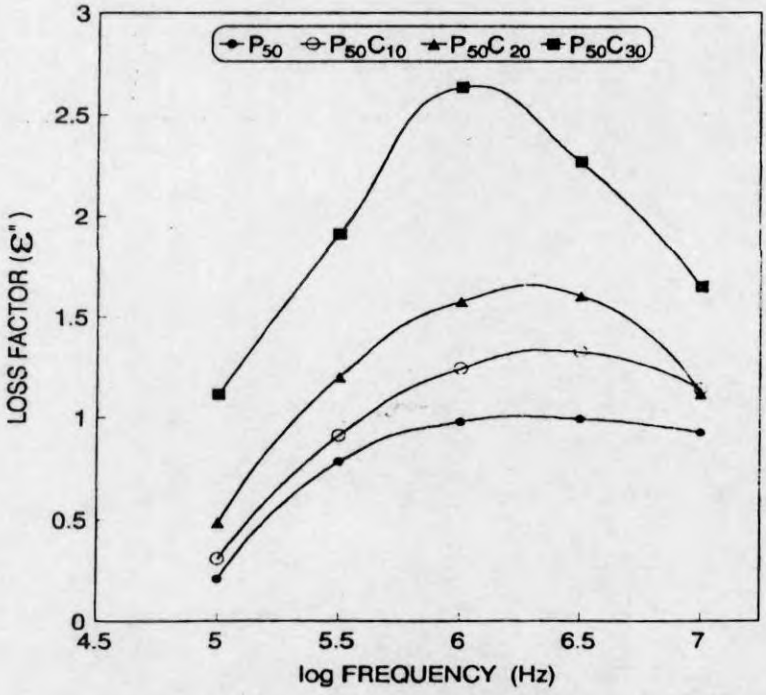

Figure 7.14. Variation of loss factor of carbon black loaded P_{50} blends with frequency.

Figure 7.15 shows the change in loss factor with frequency for different loadings of cork filler in P_{50} system. The incorporation of cork into the blend system slightly decreases the loss factor. As the loading of cork increases the loss factor also decreases. The lowest value is obtained for the blend with 30 phr filler loading. The reduction in loss factor with the incorporation of cork filler is due to the hindrance for the orientation of C≡N dipoles in presence of filler. As the loading of filler increases the orientation of dipoles is retarded by the presence of increasing amount of cork. The width of the relaxation peak also decreases with increase in filler loading.

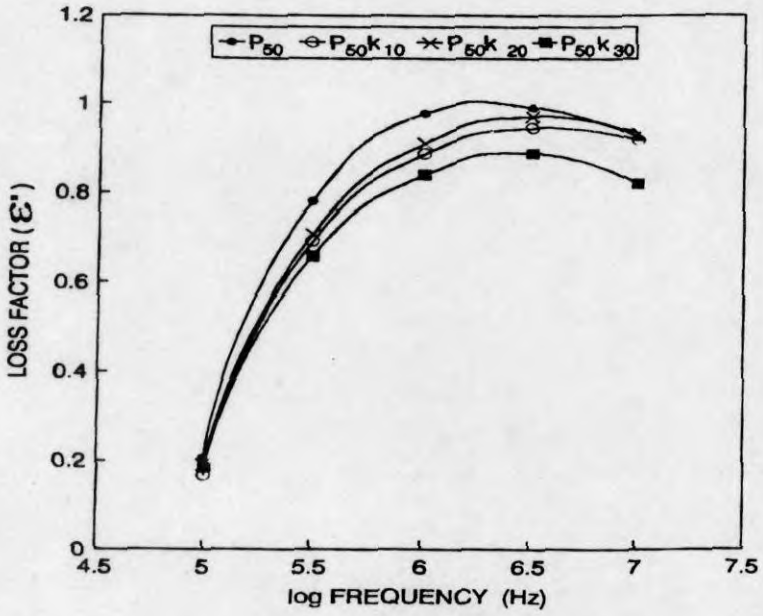

Figure 7.15. Variation of loss factor of cork loaded P_{50} blends with frequency.

In the case of silane treated silica filler, the variation of loss factor with frequency is depicted in Figure 7.16. Here the loss factor increases with the incorporation of treated silica filler up to 20 phr loading. At 30 phr loading of silica filler, the loss factor shows a decrease. The treated silica filler contains polar groups and this increases the effective dipole moment which also contributes to the loss factor. This in fact, leads to an increase of ε″ values upon the incorporation of

treated silica filler to the P_{50} blend. However for 30 phr loading, though there is an increase in the effective dipole moment, the relaxation process is retarded due to an increase in viscosity at this loading. In effect the loss factor shows a decrease at this loading.

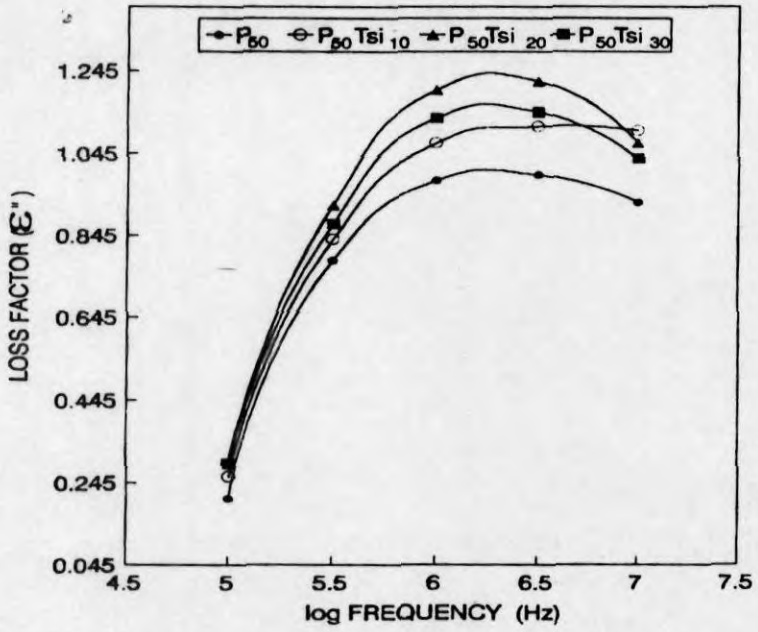

Figure 7.16. Variation of loss factor of silane treated silica loaded P_{50} blends with frequency.

Variations of loss factor with NBR content for different fillers are shown in Figures 7.17–7.19. As the rubber content in the blend increases the loss factor (ε″) increases in all cases. The increase in loss factor (ε″) with rubber content is low up to 50 wt % and after that the loss factor (ε″) increases sharply. This sharp increase in ε″ above 50 wt % NBR is due to the change in morphology i.e., phase inversion of NBR from dispersed to continuous phase above 50 wt % NBR which leads to better orientation of dipoles. Among the filled blends, for carbon black loaded samples the relaxation peak is observed at a frequency of 10^6 Hz in all composition while in silane treated silica filled samples, the peak is observed at 3.16×10^6 Hz. In cork loaded samples, the peak is at 10^6 Hz for 70/30 PP/NBR blend and at higher NBR content, the peak is shifted to higher frequency.

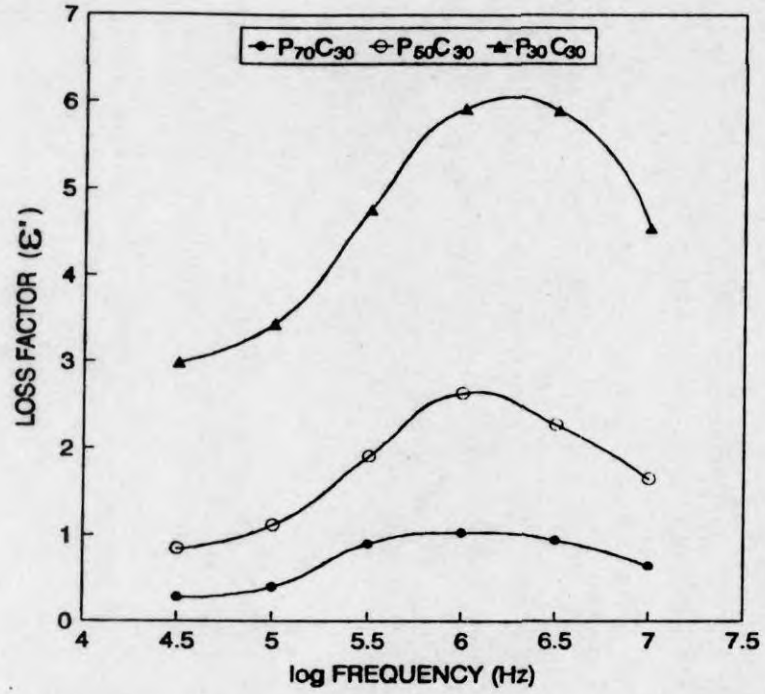

Figure 7.17 . Variation of loss factor of 30 wt % carbon black loaded PP/NBR blends with frequency.

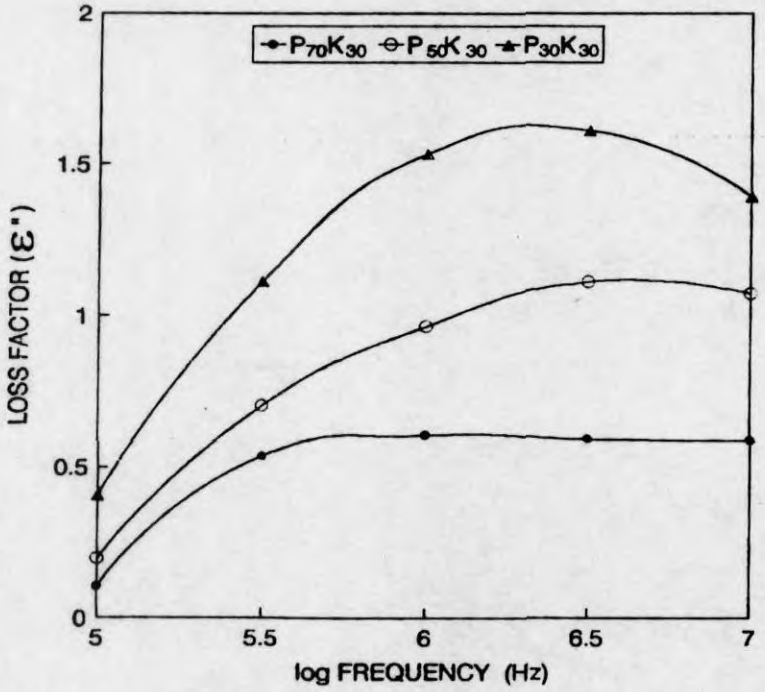

Figure 7.18. Variation of loss factor of 30 wt % cork loaded PP/NBR blends with frequency.

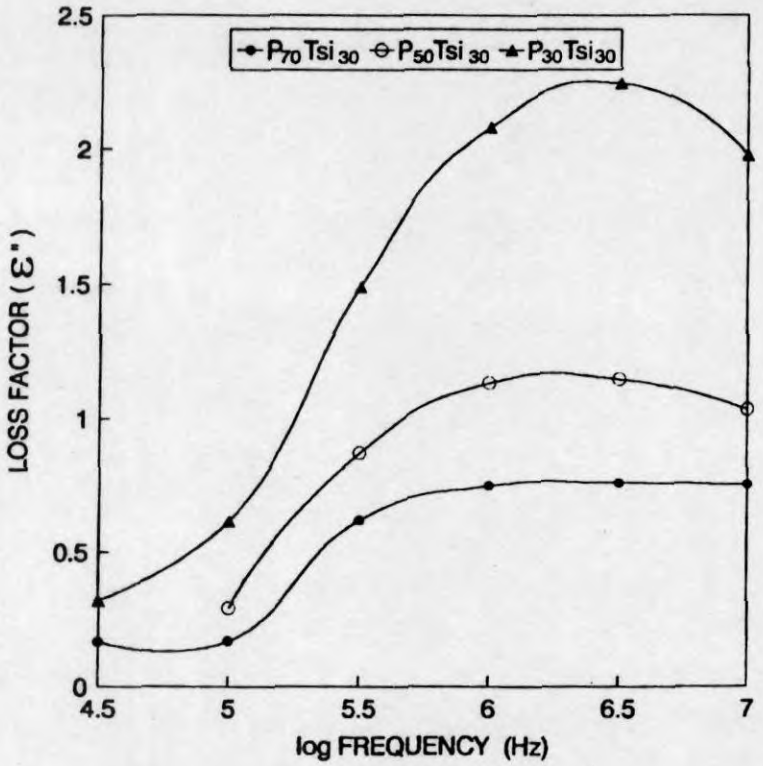

Figure 7.19. Variation of loss factor of 30 wt % silane treated silica loaded PP/NBR blends with frequency.

(c) Effect of dynamic vulcanisation

Figure 7.20 depicts the variation of dielectric constant ε′ with frequency for unvulcanised and vulcanised (sulphur, peroxide and mixed system) P_{70} blends. It is seen from the figure that the vulcanisation of rubber phase leads to an increase in dielectric constant. The variation in ε′ is marginal in the case of sulphur crosslinked system, compared to the other systems. Among the different vulcanising systems studied, the peroxide system shows the highest ε′ values while sulphur system the lowest. The mixed (S + peroxide) system shows ε′ values in between that of sulphur and peroxide systems. The higher values of peroxide and mixed systems may be due to the increased interfacial polarisation and also due to the degradation of PP phase in presence of DCP. The degradation of PP phase may decrease the crystallinity which leads to better dipole orientation. Since the

rubber particles are finely dispersed upon dynamic vulcanisation, the interfacial area increases and this leads to an increase in interfacial polarisation. Therefore the dielectric constant increases. In DCP vulcanised system, the rubber is more finely and uniformly distributed compared to mixed and sulphur vulcanised systems (Figure 3.21). The size of NBR domains increases in the order sulphur > mixed > peroxide systems. Even though DCP vulcanised system has the highest crosslink density, the effect is not observed in the properties due to the degradation of PP in presence of DCP.

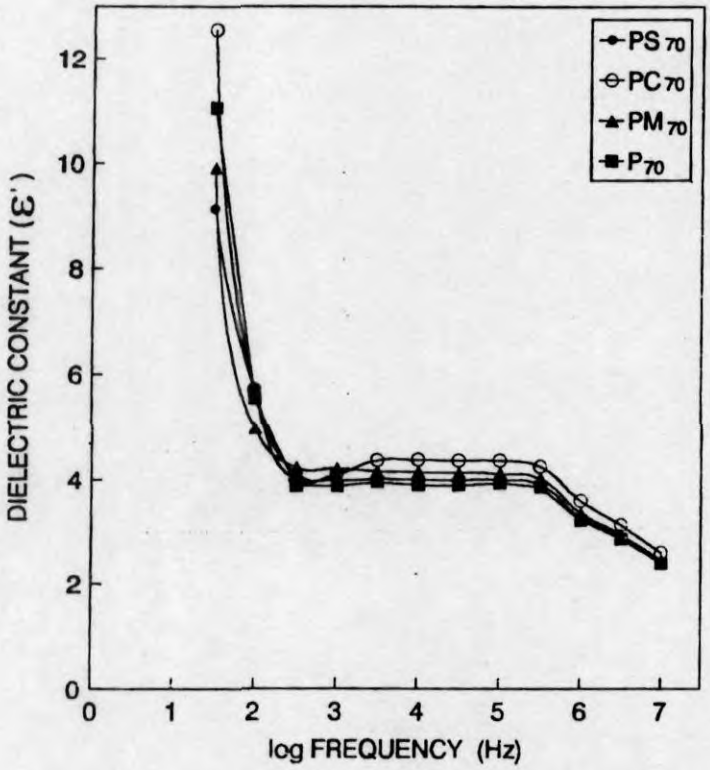

Figure 7.20. Variation of dielectric constant of unvulcanised and dynamically vulcanised 70/30 PP/NBR blends with frequency.

Figure 7.21 shows the variation of dielectric constant with frequency for P_{70}, P_{50} and P_{30} blends vulcanised with sulphur. As the concentration of rubber increases, the dielectric constant of the crosslinked blends are found to be slightly higher than that of uncrosslinked ones at low frequencies while at high

frequencies, the trend is reversed. The increase in dielectric constant for vulcanised blends at low frequencies may be due to the increase in interfacial polarisation, which reduces with increase in frequency. But at high frequencies the effect from orientation polarisation predominates. On vulcanisation of the rubber phase, the relaxation of C≡N dipoles is retarded due to the presence of crosslinks between the chains. This leads to a low value of dielectric constant which arises from orientation polarisation.

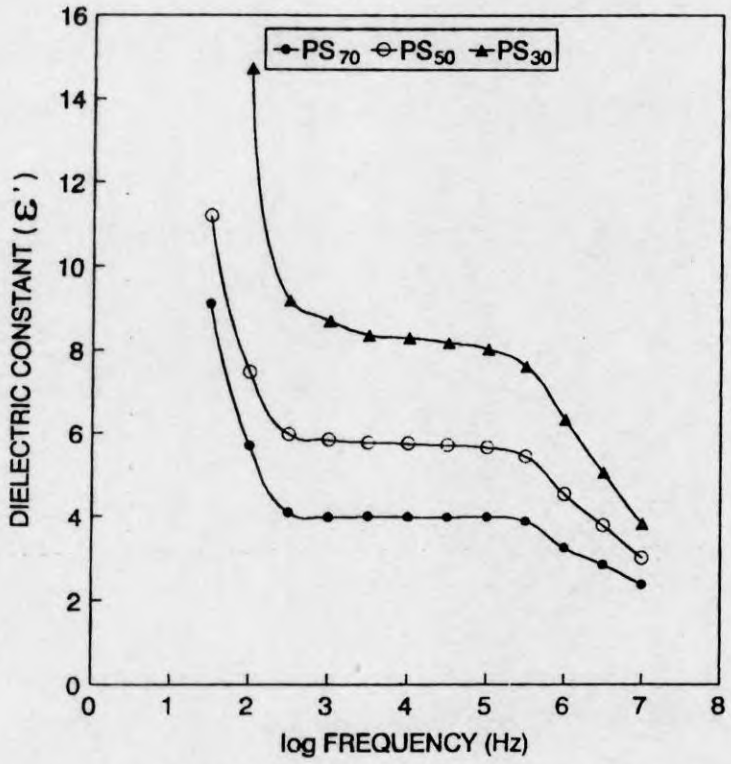

Figure 7.21. Variation of dielectric constant of dynamically vulcanised PP/NBR blends with frequency.

The relaxation spectra of 70/30 PP/NBR blends vulcanised with different vulcanising systems are shown in Figure 7.22. It is seen from the figure that the dissipation factor is not much affected by vulcanisation. But at high frequency region of 10^7 Hz the sulphur system shows the highest tan δ value and peroxide system showed the lowest. The mixed vulcanised system takes an intermediate

position. On dynamic vulcanisation, the magnitude of ε″ increases slightly. The blends vulcanised with peroxide and mixed systems have higher peak heights compared to unvulcanised and sulphur vulcanised systems. In the presence of DCP, the polypropylene phase is degraded and this may lead to the presence of some oxidised centres. The dielectric constant of the sample is also affected by the decrease in crystallinity. This will increase the dielectric relaxation and hence the peroxide and mixed vulcanised systems show higher values of ε″. It is seen from Figure 7.22 that the relaxation peak width increases upon dynamic vulcanisation. The variations of dissipation factor (tan δ) and loss factor with frequency for PP/NBR blends are shown in Figure 7.23. As the concentration of rubber increases to 50 and 70 wt % NBR, the relaxation peak frequency is shifted to lower value i.e., the relaxation time increases. The increase in relaxation time arises due to the increase in viscosity which creates more constraints to the relaxation of C≡N dipoles.

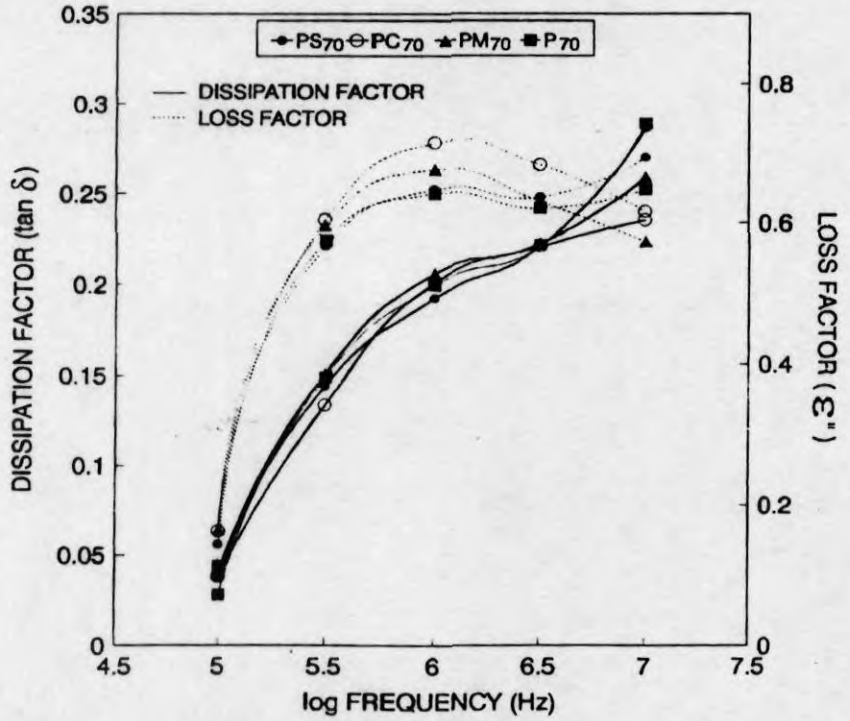

Figure 7.22. Variation of dissipation factor and loss factor of unvulcanised and dynamically vulcanised 70/30 PP/NBR blends with frequency.

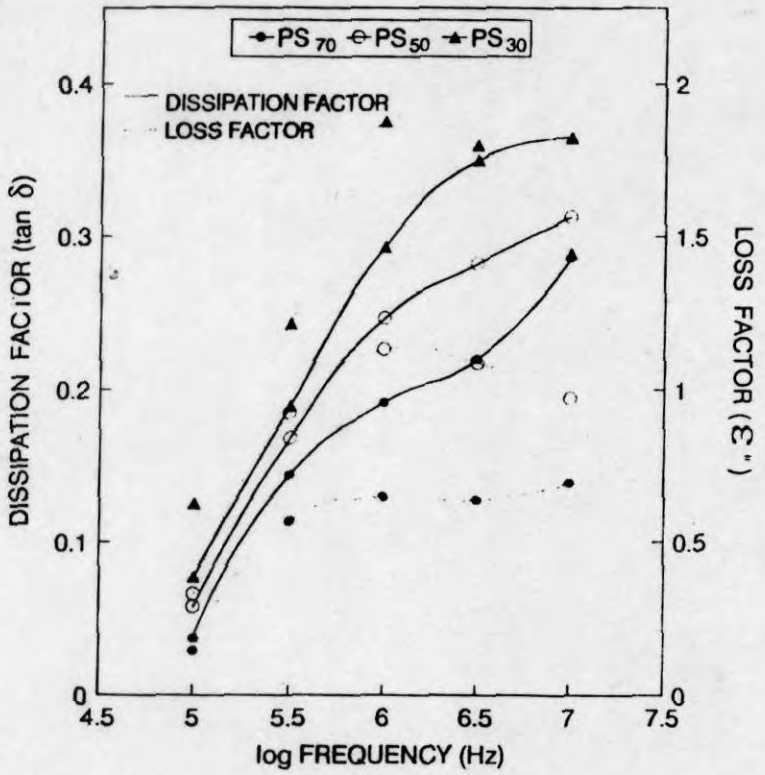

Figure 7.23. Variation of dissipation factor and loss factor of dynamically vulcanised PP/NBR blends with frequency.

7.3 References

1. B. M. Walker and C. P. Rader, (Eds.), *Handbook of Thermoplastic Elastomers,* Van Nostrand Reinhold, New York, 1979.
2. T. M. Malik and R. E. Prud'homme, *Polym. Eng. Sci.*, **24,** 2, 144 (1984).
3. K. Pathmanathan, J. Y. Cavaille and G. P. Johari, *Polymer,* **29,** 311 (1988).
4. G. M. Maistros, H. Block, C. B. Bucknall and I. K. Patridge, *Polymer*, **33**, 21, 4470 (1992).
5. P. K. C. Pillai, G. R. Narula and A. K. Tripathy, *Polym. J.*, **16**, 7, 575 (1984).
6. S. Radhakrishnan and D. R. Saini, J. Appl. *Polym. Sci.*, **52**, 1577 (1994).
7. A. Gustafsson, R. Salot and U. W. Gedde, *Polym. Comp.*, **14**, 5421 (1993).
8. A. A. Mansour, S. EL. Sabagh and A. A. Yehia, *J. Elastomers and Plastics*, **26**, 367 (1994).

9. R. Scarifani, G. Spadaro, F. Cassata and A. Valenza, *Eur. Polym. J.*, **31**, 9, 841 (1995).

10. B. G. Soares, F. Gubbels, R. Jerome, E. Vanlathem and R. Deltour, *Rubber Chem. Technol.*, **70**, 60 (1997).

11. M. Sumita, K. Sakata, S. Asai, K. Miyasaka and H. Nakagawa, *Polym. Bull.*, **25**, 265 (1991).

12. A. Abo-Hashem, H. M. Saad and A. H. Ashor, *Plast. Rubber Comp. Proc. Appl.*, **21**, 125 (1994).

13. A. K. Sircar, *Rubber Chem. Technol.*, **54**, 820 (1981).

14. F. Gubbels, R. Jerome, Ph. Teyssie, E. Vanlathem, R. Deltour, A. Calderone, V. Parente and J. L. Bredas, *Macromolecules*, **27**, 1972 (1994).

15. N. G. MacCrum, B. E. Read and G. Williams, *Anelastic and Dielectric effects in Polymeric solids*, John Wiley, New York, 1967.

16. J. A. Brydson, *Plastic Materials*, Butterworths, London, 1989, p. 105.

17. K. F. Mathes, in *Encyclopedia of Polymer Science and Engineering*, Vol 5 J. I. Kroschwitz, (Ed), John Wiley and Sons, New York, 1986, p. 507

18. C. C. Ku and R. Leiens, *Electrical properties of Polymers, Chemical Principles*, Hanser Publishers, Munich-Vienna, New York. 1987.

19. J. Bicerano, *Prediction of Polymer Properties*, Marcel Dekker Inc., Newyork, 1993 Chap. 9.

20. J. A. Reynolds and J, M. Hough, *Proc. Phys. Soc. London. Sect. B.*, **70**, 769 (1957).

21. S. Debnath, P. P. De and D. Khastgir, *Rubber Chem. Technol.*, **61**, 555 (1987)

Chapter 8

Molecular Transport of Aromatic Solvents

The results of this chapter have been submitted for publication in *Journal of Membrane Science*

8.1 Introduction

The transport behaviour of various organic solvents and gases through polymers is of great technological importance, since nowadays the polymer membranes are increasingly used in various barrier applications.[1] Nitrile rubber, which is an oil resistant elastomer is widely used in many applications like oil seals, gaskets, etc. For the last few decades, the performance of the nitrile rubber has been tried to improve by blending with various polymers.[2-4] Hence, it is necessary to analyse the transport behaviour and the mechanism of transport of various hydrocarbon solvents through PP/NBR blends in detail.

The transport of small molecules through polymers was widely studied by various research groups.[5-13] It was found that, the transport of the solvents through polymers is influenced by physical and chemical structure of polymers, the crosslink density, the shape and size of solvent molecules and temperature. The effect of various fillers on the transport behaviour of rubbery polymers was investigated[14-16] and it was observed that the presence of fillers makes a tortuous path to the transport of solvents through polymer samples and thereby reduces the solvent uptake. However, the transport behaviour is also affected by the interaction of filler between polymer and solvent.[16]

With the increasing importance of polymer blends, the research interest in the transport behaviour of organic solvents and gases have been directed to polymer blends as well.[17-20] In polymer blends, the transport behaviour depends on the

miscibility of the component polymers as well as the morphology of the system.[17] Hence the transport phenomena in polymer blends can be used as a characterisation technique, i e., in order to understand the miscibility as well as morphology of the system. In this chapter, the transport of a series of aromatic solvents through PP/NBR blends has investigated. The effects of blend ratio, nature of crosslinking and different fillers on the transport of aromatic solvents have been studied. The experimental results were compared with theoretical predictions.

8.2 Results and discussion

8.2.1 Effect of blend ratio

The transport behaviour of unvulcanised and dynamically vulcanised thermoplastic elastomers from PP and NBR were analysed. The results of the analysis of diffusion experiments of the unvulcanised and vulcanised blends in toluene are shown in Figures 8.1a and 8.1b, respectively as mol % uptake (Q_t) vs. square root of time.

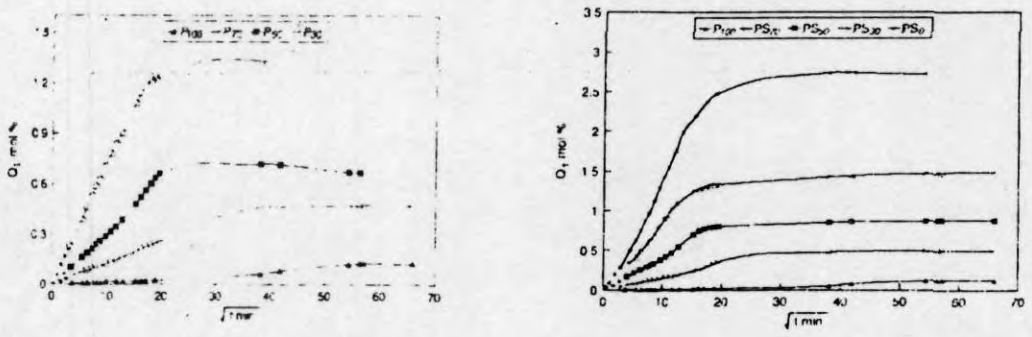

(a) (b)

Figure 8.1. Variation of mol % toluene uptake (Q_t) with square root of time of (a) unvulcanised and (b) vulcanised PP/NBR blends.

Polypropylene has the minimum uptake of toluene while NBR has the maximum level. The blends show an intermediate behaviour. The lowest value of mol % uptake for polypropylene in spite of the match in solubility parameter

between PP and toluene, is due to the crystallinity of PP (Table 8.1). In a semicrystalline polymer, some amorphous part is also present along with crystalline regions. Only this amorphous region will contribute to the uptake of solvent and hence PP has the lowest uptake value among all proportions of blend. In the case of blends, as the concentration of NBR increases in blends the crystalline content decreases. Hence, the hindrance for the transport of toluene decreases and uptake increases. In the blends the crystalline PP phase makes a tortuous path to the transport of solvent through the amorphous regions in blends. Figure 8.2 shows the variation of Q_∞ of PP/NBR blends with blend composition.

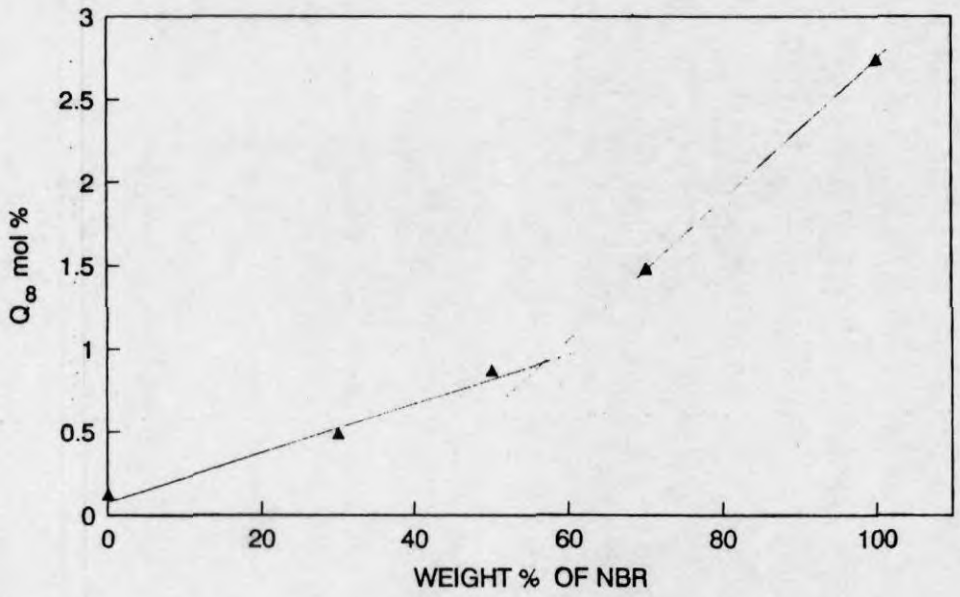

Figure 8.2. Variation of equilibrium uptake (Q_∞) of PP/NBR blends with weight percentage of NBR.

As the concentration of NBR increases, the Q_∞ value increases linearly up to 50 wt % NBR and after that a change in slope of the curve is observed. This difference in Q_∞ values with blend composition can be correlated with the morphology of the system. It was observed that in P_{70} and in P_{50}, the NBR is

dispersed as spheres in continuous PP matrix. In P_{30} blend, both NBR and PP form continuous phases leading to a co-continuous morphology (Figure 3.2). Because of the dispersed nature of NBR in P_{70}, the continuous PP phase act as a tortuous path for the diffusion process of solvent and hence the uptake is less. However, as the concentration of NBR increases from 30 to 50 wt%, the size of NBR domains increases which increases the contact between NBR particles and crystallinity of the blends decreases (Table 3.2). This leads to the high uptake in P_{50} compared to P_{70}. In P_{30}, where NBR forms the continuous phase the diffusion process is continuous through NBR phase and hence a sharp increase in uptake is observed

Table 8.1. Solubility parameter difference and crystallinity of PP/NBR blends.

Sample	Solubility parameter difference between polymer and toluene	% crystallinity (from DSC data)
P_{100}	0.2	55.3
P_{70}	0.124	33 9
P_{50}	0.34	20.9
P_{30}	0.556	13.7
P_0	0.88	-

The mechanism of transport of PP/NBR blends was analysed using the empirical relation.

$$\log Q_t/Q_\infty = \log k + n \log t \qquad (8.1)$$

where Q_t and Q_∞ are the mol % sorption at time t and at equilibrium respectively. k is a constant that depends on the structural characteristics of polymer gives information about the interaction between polymer and solvents The value of n=0.5, indicates a Fickian mode of transport, while n=1 indicates case II (relaxation

controlled) transport. The value of n between 0.5 and 1 indicates an anomalous transport behaviour. The values of n and k for PP/NBR blends are obtained by regression analysis of log Q_t/Q_∞ vs. log t plot. The results of the analysis are given in Table 8.2. Since the values range between 0.46 to 0.6, i.e., in PP/NBR blends, the mode of transport is close to Fickian. From the table it is seen that as the concentration of NBR increases the values of n slightly increase and approaches Fickian mode. For the Fickian mode of transport, the rate of diffusion of permeant molecules is much less than the relaxation rate of the polymer chains. Usually rubbers and semicrystalline polymers exhibit Fickian mode of diffusion.[17]

Table 8.2. n and k values for diffusion of toluene through PP/NBR blends

Sample	n	k (g/g min^n)
P_{100}	0.46	0.014
PS_{70}	0.47	0.036
PS_{50}	0.47	0.051
PS_{30}	0.51	0.05
PS_0	0.601	0.03

The transport of small molecules through polymers generally occurs through a solution diffusion mechanism, i.e., the penetrant molecules are first sorbed by the polymer followed by diffusion through the polymer. Thus the permeability (P) is the product of diffusivity (D) which is a kinetic parameter and sorptivity (S) which is a thermodynamic parameter.

Hence, the permeability, P is given by[5]

$$P = D \cdot S \qquad (8.2)$$

The thermodynamic factor, S is defined as grams of liquid sorbed per gram of rubber.

The kinetic parameter, D can be calculated using the equation,[5.12]

$$\frac{Q_t}{Q_\infty} = 1 - \sum_{n=0}^{\infty} \left[\frac{8}{(2n+1)^2 \pi^2} \right] e^{-(2n+1)^2 \pi^2 (Dt/h^2)} \tag{8.3}$$

where t is the time and h is the initial thickness of the polymer sheet. Although this equation can be solved readily, it is instructive to examine the short-time limiting expression as well.

$$\frac{Q_t}{Q_\infty} = \left[4/\pi^{1/2} \right] \left[Dt/h^2 \right]^{1/2} \tag{8.4}$$

From a plot of Q_t vs. $t^{1/2}$, a single master curve is obtained which is initially linear. Thus D can be calculated from a rearrangement of equation (8.4) as

$$D = \pi \left(\frac{h\theta}{4Q_\infty} \right)^2 \tag{8.5}$$

where h is the sample thickness, and θ is the slope of the initial linear portion of sorption curves, i.e., before the attainment of 50% of equilibrium uptake. The variation of diffusion and permeation coefficients with blend composition for PP/NBR blends is shown in Figure 8.3. It is seen from the figure that the polypropylene shows the lowest value for diffusion and permeation coefficient and NBR shows the highest. The blends take intermediate positions. As the concentration of NBR increases, the D and P increase. The increase in D and P values with increase in rubber content is due to the increase in concentration of NBR with a high diffusion coefficient and also due to the fact that the tortuousity exhibited by PP to the penetration of solvent molecules decreases with increase in NBR content. The change in P and D with rubber content is small up to 50 wt % NBR and after that a sharp increase is observed in these values. This sharp change in the values are due to the phase inversion of NBR from dispersed to continuous phase on passing from 50 to 70 wt % NBR which leads to an increased diffusion process.

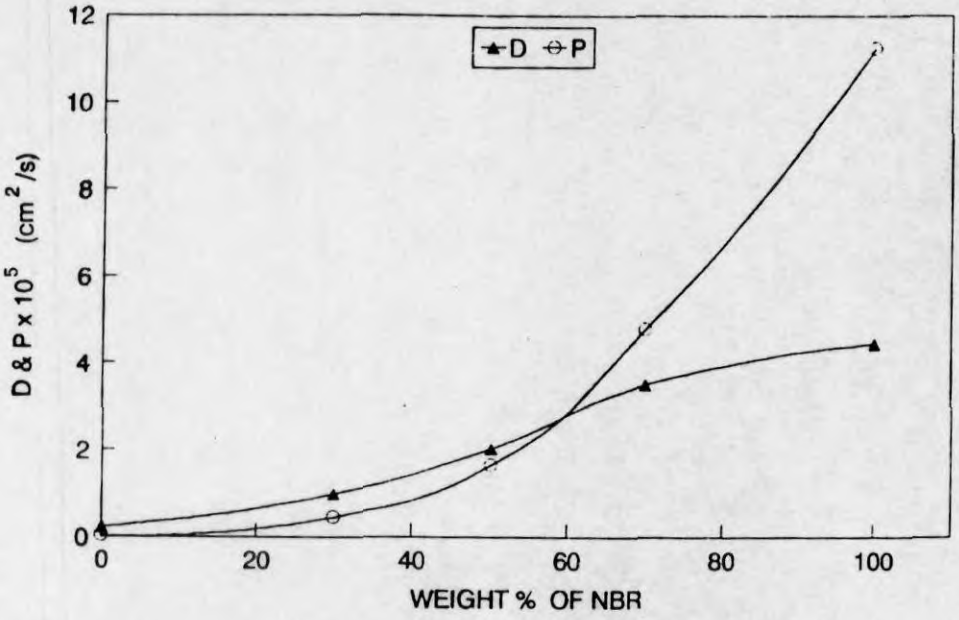

Figure 8.3. Variation of diffusion and permeation coefficient with weight percentage of NBR.

In the case of heterogeneous polymer blends, the permeability can be interpreted in terms of various theoretical models. Robeson's two limiting models, i.e., series and parallel models are generally used in the case of polymer blends.

According to parallel model

$$P_c = P_1\phi_1 + P_2\phi_2 \qquad (8.6)$$

and by series model

$$P_c = P_1P_2 / (\phi_1P_2 + \phi_2P_1) \qquad (8.7)$$

where P_c, P_1 and P_2 are the permeation coefficients of blend, component I and component II respectively and ϕ_1 and ϕ_2 are the volume fractions of components I and II, respectively.

Further for a conducting spherical filler, the overall composite permeation coefficient is given by Maxwell's equations as[19,21]

$$\bar{\rho}_c = P_m \frac{P_d + 2P_m - 2\phi_d(P_m - P_d)}{P_d + 2P_m + \phi_d(P_m - P_d)} \quad (8.8)$$

where the subscripts d and m correspond to dispersed phase and matrix respectively.

Robeson extended[21] Maxwell's analysis to include the continuous and discontinuous characteristic of both phases at intermediate compositions and expressed the equations as,

$$\bar{P}_c = X_a \bar{P}_1 \left[\frac{\bar{P}_2 + 2\bar{P}_1 - 2\phi_2(\bar{P}_1 - \bar{P}_2)}{\bar{P}_2 + 2\bar{P}_1 + \phi_2(\bar{P}_1 - \bar{P}_2)} \right] + X_b \bar{P}_2 \left[\frac{\bar{P}_1 + 2\bar{P}_2 - 2\phi_1(\bar{P}_2 - \bar{P}_1)}{\bar{P}_1 + 2\bar{P}_{21} + \phi_1(\bar{P}_2 - \bar{P}_1)} \right] \quad (8.9)$$

where X_a and X_b are fractional contributions to continuous phase so that $X_a + X_b = 1$.

Figure 8.4 shows the various theoretical and experimental curves showing the variation of P with NBR volume fraction. The P values of PP/NBR blends show an intermediate behaviour in between the two limiting models, parallel and series. The experimental data are close to Maxwell model with PP phase continuous at 70 wt % PP. At 30 wt % PP, the data is close to Maxwell model with NBR phase continuous. Again it is seen from the Figure 8.4 that the experimental curve coincides with Robeson's model for a co-continuous morphology at $X_a = 0.6$ and this suggest that a phase inversion occurs for NBR at this volume fraction. This result is consistent with our early observation from SEM micrographs that phase inversion occurs between 50 and 70 wt % of NBR in the blend.

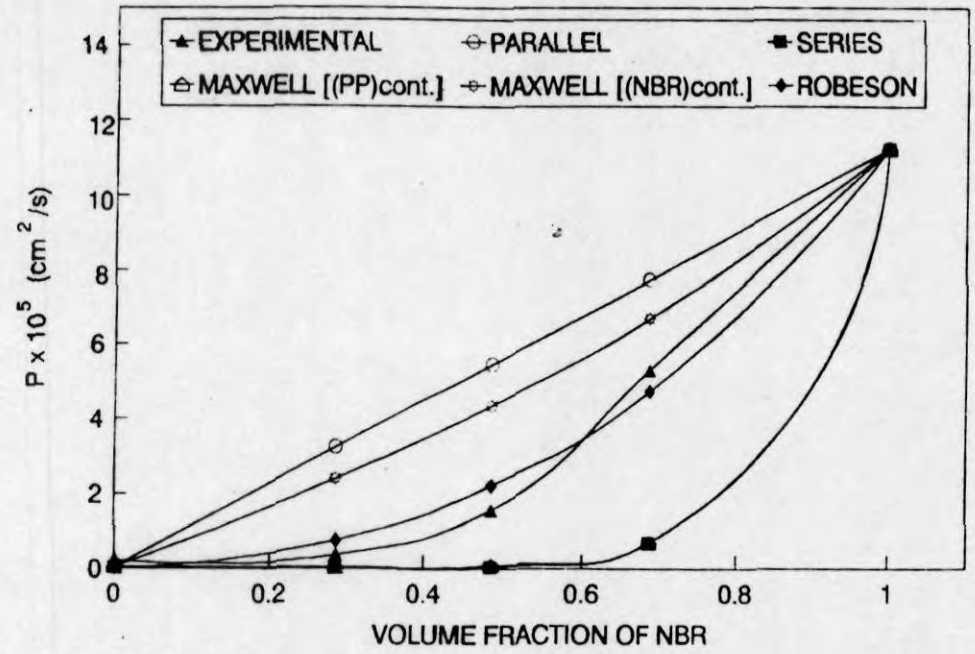

Figure 8.4. Experimental and theoretical variation of permeation coefficient with volume fraction of NBR is the blends.

8.2.2 Effect of type of crosslinking

The physical and mechanical properties of polymers are found to depend on the nature of crosslinking viz., sulphur or peroxide curing system. Figure 8.5 shows the Q_t vs. $\sqrt{t}$ curves of dynamically vulcanised P_{50} blends. Among the different vulcanising systems used, the DCP crosslinked system shows the lowest uptake. Sulphur cured system shows the highest solvent uptake and mixed system takes an intermediate position.

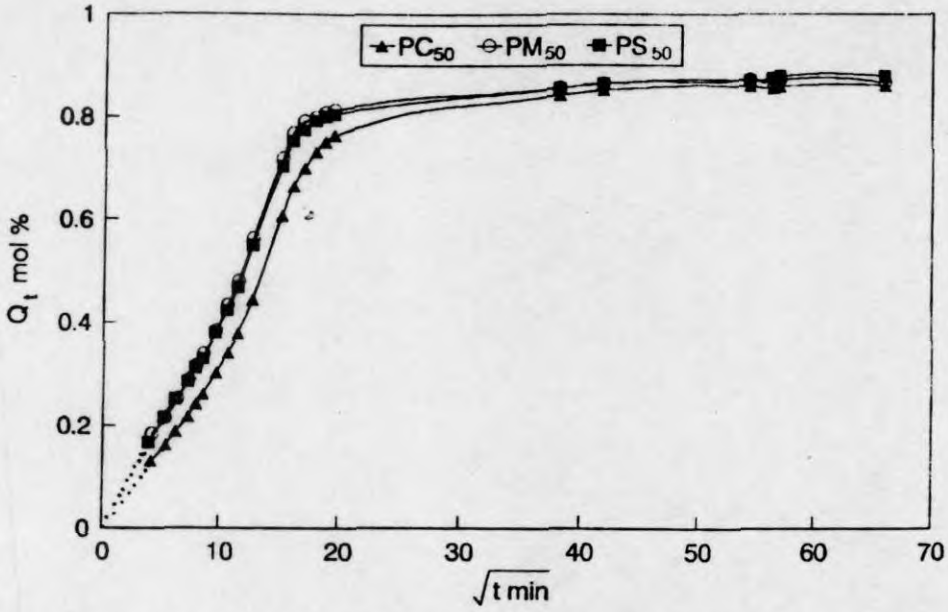

Figure 8.5. Variation of mol % uptake of toluene (Q_t) with square root of time for various dynamic crosslinked P_{50} blends.

The values of D, P, n and k for these samples are given in Table 8.3. It is seen from the table that the values of n vary from 0.46 to 0.52 for the three systems, i.e., sulphur system shows the lowest n value and DCP system shows the highest n value. All the three systems follow an almost Fickian mode of transport. When we examine the k values it is seen that the DCP crosslinked systems show the lowest k value and sulphur and mixed systems show almost similar values which is higher than that of DCP system. Hence the interaction between solvent and blend is low for DCP system compared to sulphur and mixed systems. The diffusion and permeation coefficients of toluene are low in the case of DCP compared to sulphur and mixed systems. The difference in the transport parameters of these three different vulcanising systems arises from the type of crosslinks formed and also due to the extent of crosslinking (i.e., crosslink density). Among the three vulcanising systems used, sulphur vulcanisation, leads to the formation of S-S linkages, while

DCP vulcanisation gives rise to rigid-C-C-linkages. In mixed system, both types of crosslinks are present i.e., -C-C- and -S-S- linkages (Figure 3.20). Since in DCP system the diffusion of solvents is more difficult due to the rigid nature of C-C linkages, it shows lowest uptake and low diffusion coefficient values. The presence of more flexible S-S linkages permits the solvents to permeate more easily through the sulphur vulcanised sample and hence show highest uptake. In mixed vulcanised system, an intermediate behaviour is expected, since it contains both C-C- and S-S-linkages. But the results indicate that the mixed system shows almost the same behaviour as that of sulphur system. This can be explained using crosslink density or molar mass between the crosslinks for the different vulcanising systems.

Table 8.3. Transport parameters for diffusion of toluene through dynamically vulcanised P_{50} blends.

Sample	n	k (g/g min^n)	D x 10^5 (cm^2/s)	P x 10^5 (cm^2/s)
PS_{50}	0.46	0.05	2.035	1.644
PC_{50}	0.52	0.032	1.807	1.432
PM_{50}	0.47	0.051	2.219	1.782

The values of M_c and crosslink density were calculated using equations (2.4 and 2.7) respectively and are given in Table 8.4. It is seen that the M_c values are in the order DCP < mixed ≅ sulphur system, i.e., the molar mass between the crosslinks is more in the case of mixed vulcanised system and lowest for DCP system. Since M_c is inversely proportional to crosslink density, the crosslink density follows the order DCP > mixed ≅ sulphur, i.e., the DCP vulcanised system with the highest crosslink density permeates less solvent molecules compared to sulphur and mixed vulcanised systems. Since blends vulcanised with sulphur and

mixed system have the same crosslink density, the uptake may be comparable. Hence the combined effect of the crosslink density and rigidity of bonds accounts for the transport behaviour in sulphur and mixed systems.

Table 8.4. M_c and crosslink density values of dynamically vulcanised P_{50} blends.

Sample	M_c	Crosslink density x 10^4 (gmol/cm^3)
PS_{50}	1673.02	5.97
PC_{50}	1252.08	7.99
PM_{50}	1671.78	5.98

8.2.3 Effect of penetrant size

The sorption behaviour of organic solvents through polymer samples is affected by the size, shape and polarity of penetrant molecules. Figure 8.6 shows the sorption curves of P_{50} blend crosslinked with sulphur for benzene, toluene and xylene. As expected as the size of penetrant molecules increases the solvent uptake decreases, i.e., the low molecular weight solvent benzene shows the highest uptake and xylene, the high molecular weight solvent shows the lowest uptake. The variation of Q_∞ with molar volume of solvent for different blend compositions are shown in Figure 8.7. It is seen from the figure that the Q_∞ values decrease linearly with the molar volume of penetrant for all the blend compositions. The rate of decrease in Q_∞ with molar volume increases with increase in concentration of NBR.

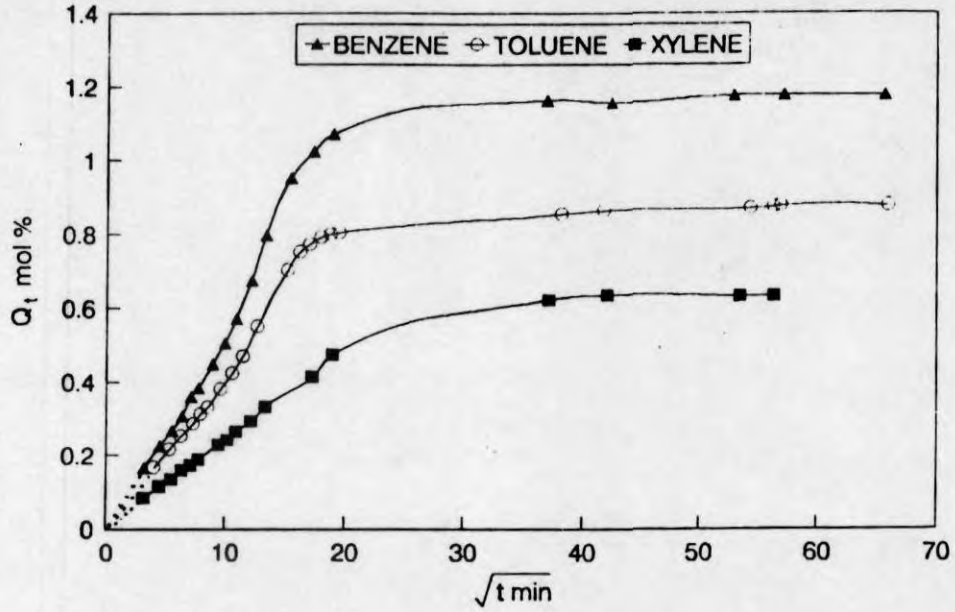

Figure 8.6. Variation of mol % uptake (Q_t) with square root of time for the diffusion of benzene, toluene and xylene through P_{50} blends.

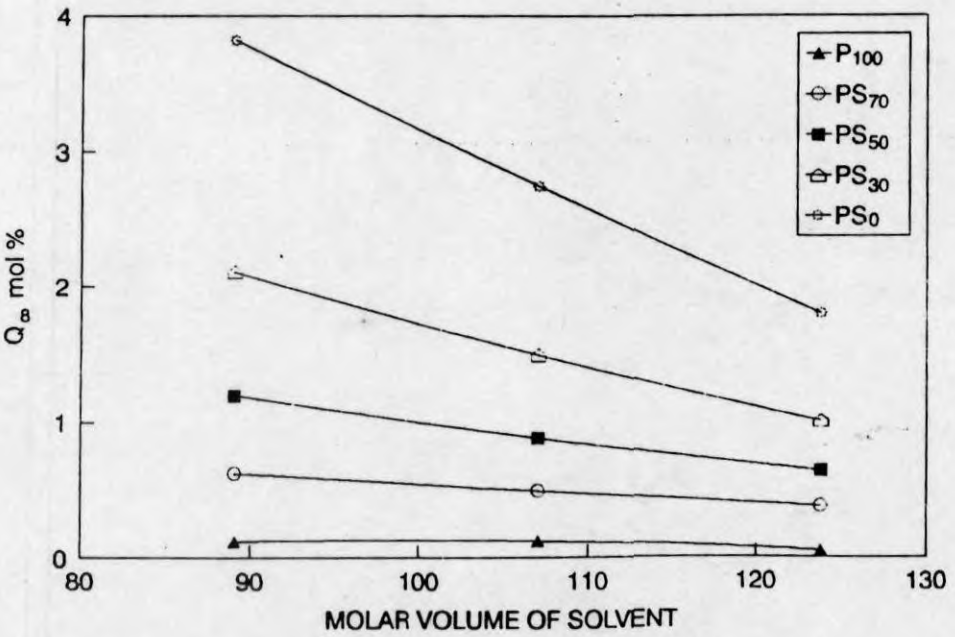

Figure 8.7. Variation of mol % uptake (Q_∞) of toluene in P_{50} blends with molar volume of solvents.

The influence of penetrant size on the mechanism of transport, diffusion and permeation coefficients of various polymer blends was analysed and the results are given in Table 8.5. It is seen from the table that the n values decrease with increase in molecular weight of penetrants. In the case of k values, there is no regular trend. However, in general the toluene shows highest k value and hence more interaction with the polymer. In the case of D and P values, both these parameters decrease with the penetrant size for pure NBR and blends.

Table 8.5. Transport parameters for diffusion of various solvents through PP/NBR blends.

		n	k (g/g min^n)	D x 10^5 (cm^2/s)	P x 10^5 (cm^2/s)
P_{100}	B	0.046	0.014	0.068	0.00088
	T	0.461	0.014	0.2191	0.025
	X	0.528	0.0095	0.763	0.0043
PS_{70}	B	0.466	0.039	0.0113	5.535×10^{-3}
	T	0.472	0.036	0.9885	4.488×10^{-1}
	X	0.426	0.041	0.584	0.232
PS_{50}	B	0.495	0.042	2.258	2.109
	T	0.468	0.051	2.035	1.649
	X	0.482	0.045	1.442	0.976
PS_{30}	B	0.511	0.051	3.544	5.53
	T	0.512	0.05	3.496	4.79
	X	0.482	0.051	2.504	2.664
PS_0	B	0.616	0.029	5.533	11.652
	T	0.601	0.03	4.447	11.28
	X	0.576	0.027	3.73	7.082

8.2.4 *Effect of fillers*

The incorporation of filler into polymer networks is found to decrease the sorption and diffusion of solvents. Figure 8.8 depicts the sorption curves of unfilled and 30 phr loaded silica, carbon black and cork filled P_{50} blends. It is seen from the figure that the initial uptake of toluene is not much affected by the presence of fillers. However, the equilibrium uptake values are lower for the filled blends compared to unfilled ones. Among the three fillers used, the C-black filled blends showed the lowest equilibrium uptake. The uptake behaviour of different blends follows the order $PS_{50} > P_{50}K_{30} > P_{50}Tsi_{30} > P_{50}C_{30}$.

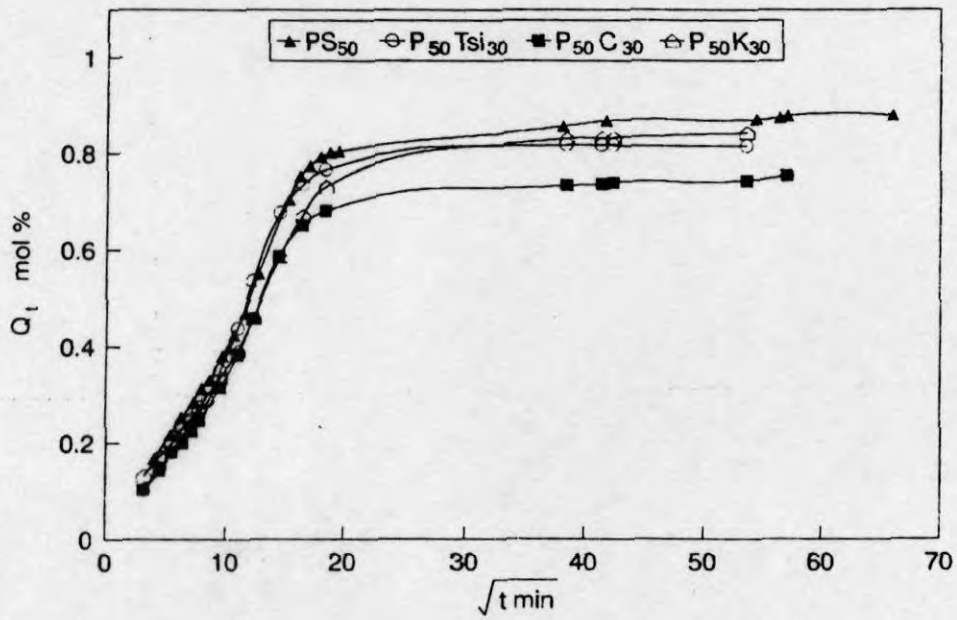

Figure 8.8. Variation of mol % uptake of toluene with square root of time for various filled P_{50} blends.

Table 8.6 shows the n, k, Q_∞, D and P values of these blends. Compared to the unfilled blend the n-values increase for silica and C-black loaded blend, while in cork filled sample n decreases. The k values increase upon the incorporation of cork while in the other two cases, the k value show a decrease. While considering

the diffusion and permeation coefficients, it is seen that the values are higher than the unfilled blend in the case of C-black and silica filled samples and lower for cork filled blend. The difference in the behaviour of the filled blends on the diffusivity and permeability and in the equilibrium values may be related to the interaction between the filler and polymer. It has been reported that in thermoplastic elastomers, the filler particles generally concentrate in the rubber phase. Since silica filler surface is polar, it shows better interaction with the polar NBR particles which may lead to more phase separation i.e., interaction between PP and NBR decreases, which leads to weak interphases. This weak interphase may enhance the diffusion and permeation of solvents through the membrane which increases the D and P values. However, the final equilibrium values depend mainly on the extent of crosslink density and reinforcement exerted by the filler.

The extent of reinforcement is assessed by using Kraus equation.[22] According to this equation,

$$V_{r0}/V_{rf} = 1\text{-}m[f/1\text{-}f] \qquad (8.10)$$

where V_{rf} is the volume fraction of swollen rubber in the fully swollen filled sample, f is the volume fraction of filler and m is a measure of the extent of reinforcement.

Table 8.6. Transport parameters for diffusion of toluene through filled PS_{50} blends.

	n	k ($g/g\ min^n$)	D x 10^5 (cm^2/s)	P x 10^5 (cm^2/s)
Silane treated silica	0.556	0.034	2.363	1.781
Carbon black	0.507	0.041	2.356	1.638
Cork	0.436	0.055	1.927	1.497

The crosslink density and extent of reinforcement (m) of different fillers obtained from Kraus equation for various filled and unfilled blends are shown in Table 8.7. It is seen that the crosslink density decreases in filled blends as compared to unfilled P_{50} blend. Hence, the reduction in equilibrium uptake in filled blends is due to the reinforcement exerted by the fillers Among the filled blends, the crosslink density varies in the order $P_{50}C_{30} > P_{50}Tsi_{30} > P_{50}K_{30}$ and the extent of reinforcement follows the order $P_{50}Tsi_{30} > P_{50}C_{30} > P_{50}K_{30}$. Hence cork filled P_{50} blend with lowest crosslink density and reinforcement shows the highest uptake among the filled samples. The carbon black filled sample with highest crosslink density and intermediate reinforcement shows the lowest uptake.

Table 8.7. Crosslink density and extent of reinforcement of filled PS_{50} blends

Sample	Crosslink density x 10^{-4}	m
Unfilled	2.276	
Silane treated silica	1.866	-1.7086
Carbon black	2.107	-0.53002
Cork	1.353	0.8197

8.2.5 Effect of temperature

The effect of temperature on mol % uptake of P_{50} blends is shown in Figure 8.9. As the temperature increases, the uptake of solvent increases as expected. The rates of diffusion and permeation also increase with increase in temperature. The temperature dependence of transport properties can be used to evaluate the activation energy for the diffusion and permeation process using the Arrhenius relation

$$X = X_0 \exp -(Ex/RT) \qquad (8.11)$$

where X is P or D; Ex, the activation energy; R, the universal gas constant; and T, the absolute temperature. The Arrhenius plots of log D and log P vs. 1/T for

different blend compositions are shown in Figures 8.10 and 8.11 respectively. From the Arrhenius plots, the values of activation energy for permeation and diffusion were calculated using regression analysis.

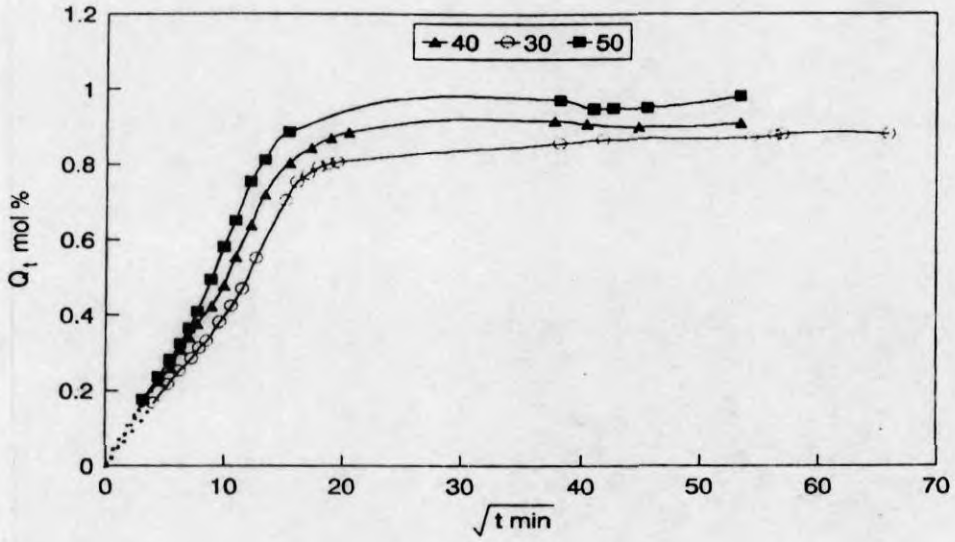

Figure 8.9. Variation of mol % uptake (Q_t) of toluene with square root of time a t various temperatures.

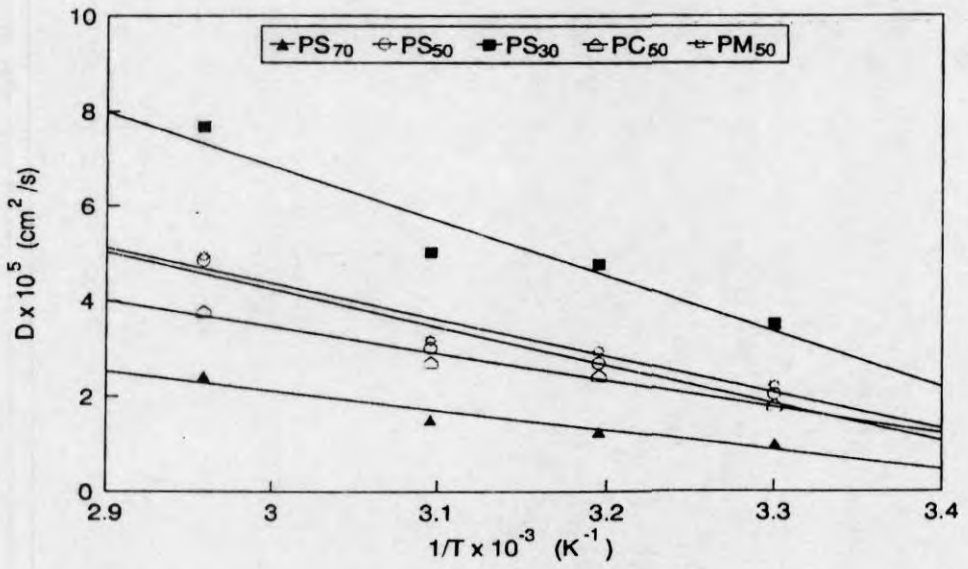

Figure 8.10. Arrhenius plots of log D vs. 1/T of dynamic vulcanised P_{50} blends.

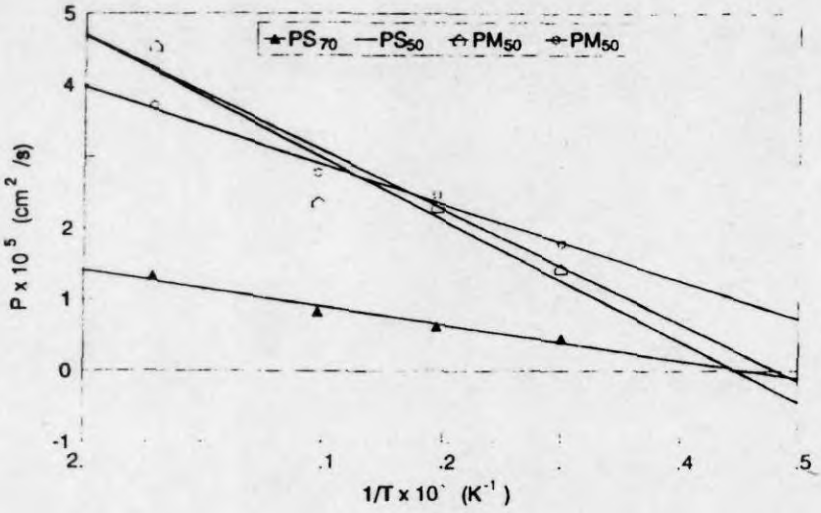

Figure 8.11. Arrhenius plots of log P vs. 1/T of dynamic vulcanised P_{50} blends.

The results are shown in Tables 8.8 and 8.9. In different blend compositions, the activation energy for diffusion decreases with increase in rubber concentration, while activation energy for permeation did not show a regular trend. Among the different vulcanising system used, the DCP vulcanised system shows the highest activation energy and mixed system shows the lowest. The highest activation energy observed in DCP crosslinked system may arise from the rigidity of C-C linkages compared to S-S linkages present in sulphur and mixed systems. It is also interesting to note that the activation energy decreases upon the incorporation of filler. The toluene shows the highest activation energy among the solvents used.

Table 8.8. Activation energy for diffusion and permeation of toluene in PP/NBR blends.

	E_P (kJ/mol)	E_D (kJ/mol)
PS_{70}	21.54	26.15
PS_{50}	20.31	23.66
PS_{30}	18.03	29.86
PC_{50}	23.48	26.31
PM_{50}	12.27	17.04
$P_{50}Tsi_{30}$	19.15	21.29

Table 8.9. Activation energy for diffusion and permeation of various solvents in PP/NBR blends.

		E_D (kJ/mol)	E_P (kJ/mol)
PS_{50}	B	17.95	21.48
	T	20.31	23.66
	X	18.40	21.36
$P_{50}Tsi_{5130}$	B	16.90	20.57
	T	19.15	21.29
	X	16.04	18.20

8.2.6 Thermodynamic parameters

The thermodynamic parameters for diffusion, ΔH and ΔS can be calculated using Van't Hoffs relation.

$$\log K_s = \frac{\Delta S}{2.303R} - \frac{\Delta H_s}{2.303RT} \qquad (8.12)$$

where K_s is equilibrium sorption constant which is given by

$$K_s = \frac{\text{No. of mols of solvent sorbed at equilibrium}}{\text{Mass of the polymer}} \qquad (8.13)$$

The values of ΔS and ΔH are obtained by regression analysis of the plots of log K_s vs. 1/T. The values of ΔH and ΔS are given in Table 8.10. It is seen from the table that the ΔH values are positive and vary from 2.2-4.6 kJ/mol. The positive values of ΔH indicate that the sorption is an endothermic process and is dominated by Henry's mode, i.e., the sorption proceeds through creation of new sites or pores in the polymer. In the case of blends with different NBR compositions, the ΔH value decreases with increase in NBR content.

Table 8.10. Thermodynamic parameters for diffusion of toluene through PP/NBR blends.

Sample	ΔH (kJ/mol)	ΔS (J/mol/deg)	-ΔG (kJ/mol)
PS_{70}	4.60	28.78	4.02
PS_{50}	3.16	28.86	5.49
PS_{30}	2.77	25.90	4.99
PM_{50}	4.70	24.00	2.49
PC_{50}	3.71	27.32	4.48
$P_{50}Tsi_{5130}$	2.13	32.94	4.48

8.2.7 Kinetics of diffusion

The first order kinetic model has been used to follow the kinetics of sorption and diffusion of solvents through PP/NBR blends. In order to apply this kinetic model it is assumed that during sorption of solvents, structural changes may occur in polymer chains which require a rearrangement of the polymer segments that can dominate the kinetic behaviour. According to first order kinetic equation,

$$dc/dt = k'(C_\infty - C_t) \qquad (8.14)$$

where k′ is the first order rate constant and C_t and C_∞ represent the concentrations at time t and at equilibrium respectively. Integration of the above equation gives

$$k't = 2.303 \log [C_\infty/(C_\infty - C_t)] \qquad (8.15)$$

Figures 8.12 and 8.13 show plots of log $(C_\infty - C_t)$ vs. t (time) for various blend compositions in toluene. From the plots of log $(C_\infty - C_t)$ vs. time, the first order rate constants were calculated by regression analysis and the results are given in Table 8.11. As expected, the rate constant values increase with increase in concentration of rubber in the blends. Among the vulcanised systems, DCP vulcanised system shows the lowest k′ value while mixed system shows the highest value. The sulphur vulcanised blend shows an intermediate behaviour. In filled systems, the rate constant values are higher as compared to unfilled system.

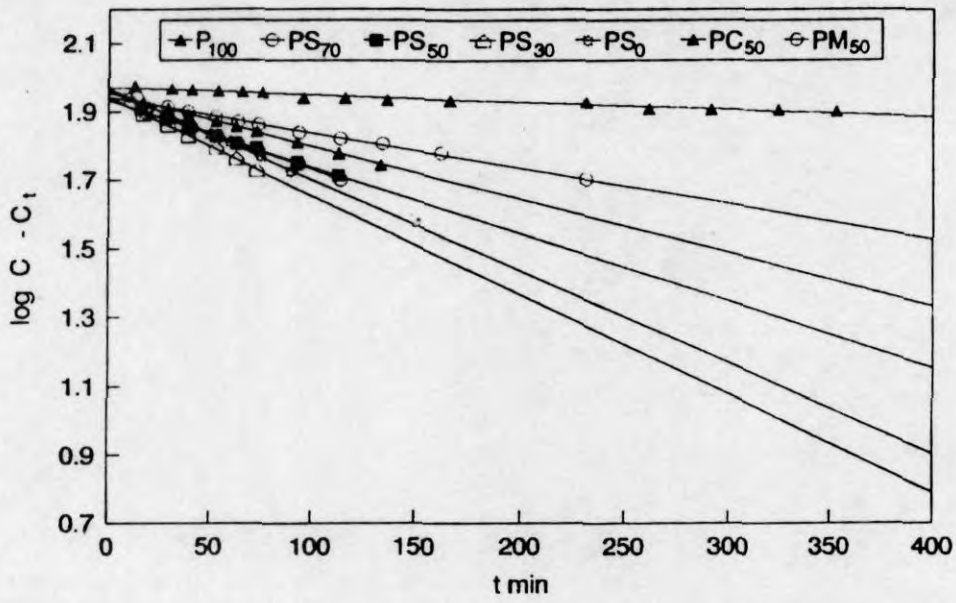

Figure 8.12. Variation of log $C_\infty - C_t$ vs. time of PP/NBR blends.

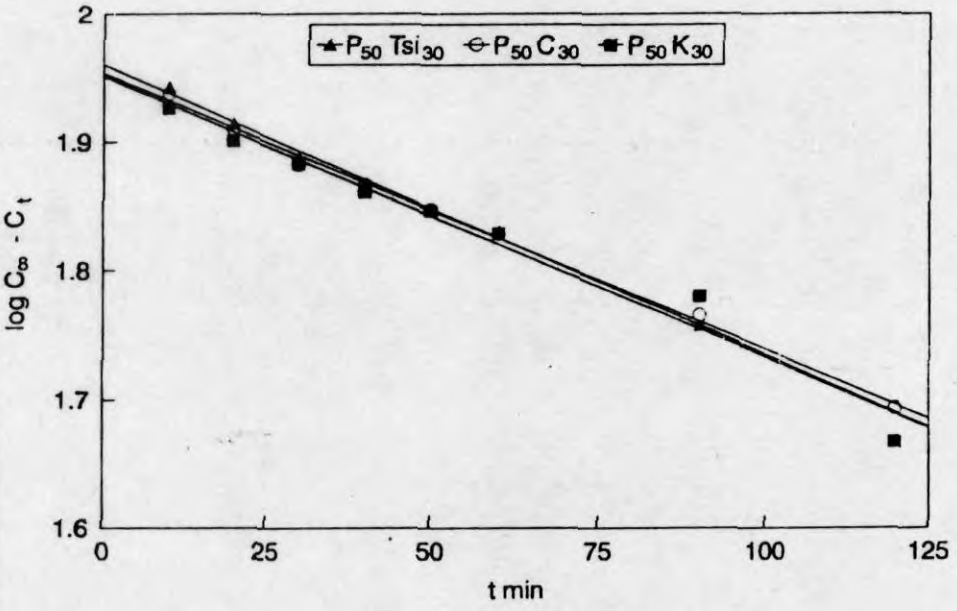

Figure 8.13. Variation of log $C_\infty - C_t$ vs. time of filled P_{50} blends.

Table 8.11. Rate constant values for the transport of toluene in PP/NBR blends.

Sample	Rate constant k x 10^3 (min^{-1})
P_{100}	0.22225
PS_{70}	1.041
PS_{50}	1.950
PS_{30}	2.80
PS_0	2.66
PC_{50}	1.55
PM_{50}	2.03
$P_{50}Tsi_{30}$	2.251
$P_{50}K_{30}$	2.186
$P_{50}C_{30}$	2.140

8.2.8 Comparison with theory

The chemical crosslink density calculated was correlated with those of affine and phantom network models.[7] In the affine network model, it is assumed that the junction points are embedded in the network without fluctuations, so that the components of each chain vector transform linearly with macroscopic deformation.

According to affine network model, the molecular weight between crosslinks is given by

$$M_c(aff) = \frac{\rho V_s \nu_{2c}^{2/3} \nu_{2m}^{1/3}\left(1 - \frac{\mu}{\nu}\nu_{2m}^{1/3}\right)}{-(\ln(1-\nu_{2m}) + \nu_{2m} + \chi\nu_{2m}^2} \qquad (8.16)$$

where V_s is the molar volume of solvent μ is the number of effective chains; ν, the number of junctions; ν_{2m}, the polymer volume fraction at equilibrium swelling; ν_{2c}, the polymer volume fraction during crosslinking; and ρ, the polymer density.

In the case of phantom network model, the chains can move freely through one another, i.e., the junction points fluctuate over time around their mean position without any hindrance from the neighbouring molecules. In phantom network model, M_c is calculated using the relation,

$$M_c(ph) = \frac{\left(1-\frac{2}{\phi}\right)\rho V_s \nu_{2c}^{2/3}\nu_{2m}^{1/3}}{-(\ln(1-\nu_{2m})+\nu_{2m}+\chi\nu_{2m}^2} \qquad (8.17)$$

where ϕ is the junction functionality.

The results obtained from these calculations are shown in Table 8.12. From the table it is seen that the experimental values are close to affine network model. Hence in PP/NBR blends, the crosslinked junctions are embedded in the network, so that they cannot fluctuate freely and the chain vector transforms linearly with macroscopic deformation.

Table 8.12. Theoretical and experimental M_c values for dynamic vulcanised PP/NBR blends.

	$M_{c\ chem}$	$M_{c\ affine}$	$M_{c\ phantom}$
PS_{70}	1196.32	520.401	173.46
PS_{50}	1673.02	1283.94	427.98
PC_{50}	1252.02	978.94	326.31
PM_{50}	1671.78	1282.99	427.66
PS_{30}	2992.19	2261.16	753.64

Attempts have been made to compare the experimental diffusion curves with the theoretical diffusion profile. The theoretical curves are constructed using the equation which describes the Fickian diffusion model.

$$\frac{Q_t}{Q_\infty} = 1 - \frac{8}{\pi^2} \sum_{n=0}^{\infty} 1/(2n+1)^2 \exp\left[-D(2n+1)^2 \pi^2 t / h^2\right] \qquad (8.18)$$

In order to generate the diffusion curves using the above equation, the experimentally determined D values are substituted in the above equation. Figure 8.14 shows the theoretical and experimental sorption curves of P_{70}, P_{50} and P_{30} blends in toluene. The overall agreement between the experimental and theoretical curves is fairly good. A similar behaviour was observed for other blend systems and solvents also.

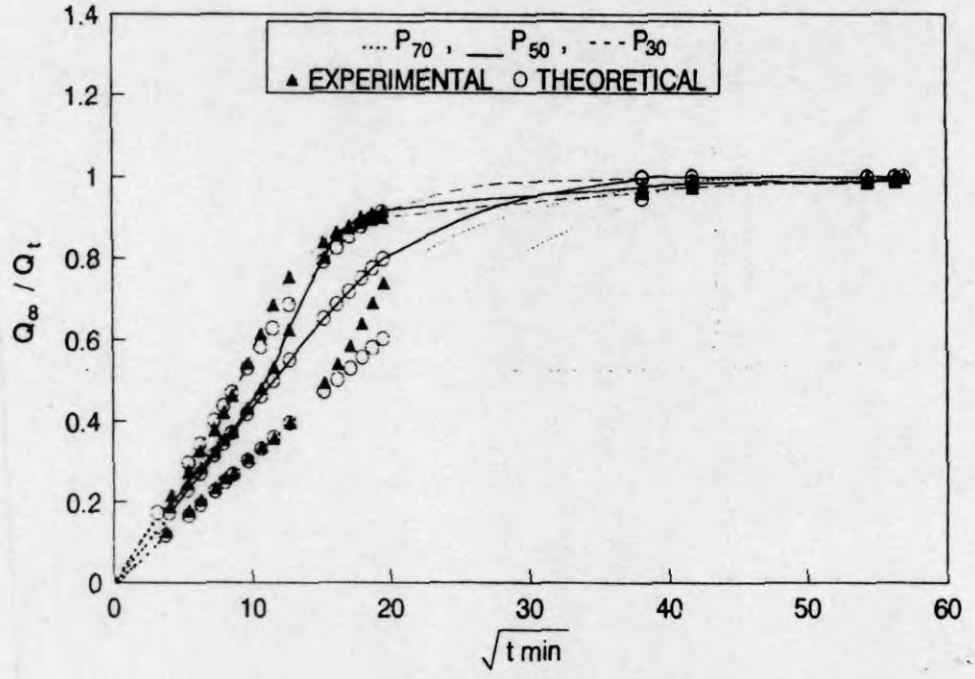

Figure 8.14. Experimental and theoretical diffusion curves of P_{70}, P_{50} and P_{30} blends.

8.3 References

1. K. T. Varughese, G. B. Nando, P. P. De and S. K. De, *J. Mater. Sci.*, **23,** 3894 (1988).
2. N. C. Liu, H. Q. Xie and W. E. Baker, *Polymer*, **34,** 4680 (1993).
3. J. George, R. Joseph, K. T. Varughese and S. Thomas, *J. Appl. Polym. Sci.*, **57,** 449 (1995).
4. A. Y. Coran and R. Patel, *Rubber Chem. Technol.*, **56**, 1045 (1983).
5. B. Shivaputrappa, Harogoppad and T. M. Aminabhavi, *Macromolecules*, **24,** 2598 (1991).
6. N. S. Schneider, J. L. Illinger and M. A. Cleaves, *Polym. Eng. Sci.*, **26**, 22, 1547 (1986).
7. D. C. Liao, Y. C. Chern, J. L. Han, K. H. Hseih, *J. Polym. Sci. B. Polym. Phys.*, **35,** 1747 (1997).
8. G. Unnikrishnan and S. Thomas, *J. Polym. Sci. Polym. Phys.*, **35**, 725 (1997).
9. A. P. Mathew, S. Pakirisamy, M.G. Kumaran and S. Thomas, *Polymer*, **36,** 26, 4935 (1995).
10. T. Johnson and S. Thomas, *J. Macromol. Sci. Phys.*, **B36(3)**, 401 (1997).
11. A. E. Mathai and S. Thomas, *J. Macromol. Sci. Phys.*, **B35(2),** 229 (1996).
12. S. C. George, S. Thomas and K. N. Ninan, *Polymer*, **37,** 26, 5839 (1996).
13. T. M. Aminabhavi, U. S. Aithal and S. S. Shukla, *JMS. Rev. Macromol. Chem. Phys.*, **C29(2&3)**, 319 (1989).
14. S. N. Lawandy and S. H. Botros, *J. Appl. Polym. Sci.*, **42,** 137 (1991).
15. F. Horkay, M. Zrinyi, E. Geissler, A. M. Hecht and P. Pruvost, *Polymer*, **32,** 835 (1991).
16. G. Unnikrishnan, S. Thomas and S. Varghese, *Polymer*, **37,** 13, 2687 (1996).
17. H. B. Hopfenberg and D. R. Paul, *In Polymer Blends*, Vol. I, (Ed., D. R. Paul), Academic Press, New York, 1976.
18. J. Kolarik and G. Gueskens, *Polym. Networks Blends*, **7(1),** 13 (1997).
19. T. M. Aminabhavi and H. T. S. Phayde, *J. Appl. Polym. Sci.*, **55,** 1335 (1995).
20. R. Asaletha, M. G. Kumaran and S. Thomas, *Polymer* (Communicated).
21. L. M. Robeson, A. Noshay, M. Matzner and C. N. Merriam, *Die. Angew. Makromol. Chem.*, **29/30,** 47 (1973).
22. G. Mathew, R. P. Singh, R. Lakshminarayan and S. Thomas, *J. Appl. Polym. Sci.*, **61,** 2035 (1996).

Chapter 9

Conclusion and Future Scope of the Work

9.1 Conclusion

Polymer blends have attracted much importance in the recent years since new materials of technological importance can be prepared by simple blending of two or more polymers. Among the different types of polymer blends, thermoplastic elastomers from rubber/plastic blends have gained lot of interest as they combine the excellent processing characteristics of plastic with the performance of rubbers. Thermoplastic elastomers based on blends of isotactic polypropylene (iPP)/acrylonitrile-co-butadiene rubber (NBR) blends combine the oil resistant properties of nitrile rubber and processability and mechanical properties of polypropylene. In this thesis we have made systematic investigations on the morphology and properties of PP/NBR blends. Since these blends are incompatible and immiscible, the effects of compatibilisation and dynamic vulcanisation on morphology and properties were also studied.

Since the morphology is a determining factor in the final properties of polymer blends, a systematic investigation of the morphology and its effect on mechanical properties of PP/NBR blends were conducted. The processability characteristics analysed from the Brabender plastographs show that the viscosity of NBR/PP blends increases with increase in NBR content. Morphology of the blends indicates a two phase structure in which rubber phase is dispersed as domains in the continuous PP matrix at lower proportions of NBR and the size of the domains increases with increase in rubber content. At 70 wt % of NBR, it also forms the continuous phase resulting in a co-continuous morphology. The

mechanical properties of the blends are found to be strongly influenced by the blend ratio. The Young's modulus, tensile strength and hardness of the blends were decreased with increase in NBR content. The tensile impact strength values decrease with NBR content up to 50 wt % and after that it shows an increase. In general, all the mechanical property-composition curves show a change in slope after 50 wt % NBR. This is associated with the change in morphology of the blends. A negative deviation from the additive line was observed for all the mechanical properties except hardness. Various composite models have been used to fit the experimental mechanical data. The tensile strength and Young's modulus of the blends could be predicted by the Coran's equation. The phenolic modified polypropylene and maleic modified polypropylene are found to act as compatibilisers in PP/NBR blend. With the increase in concentration of compatibilisers, the domain size of the dispersed NBR phase decreases, followed by a levelling off at higher concentrations which is an indication of interfacial saturation. The theories of Noolandi and Hong predict a linear decrease of interfacial tension with compatibiliser volume fraction for concentration less than CMC. Considering the fact that the interfacial tension is directly proportional to the domain size, it is demonstrated that the experimental data are in agreement with these theoretical predictions. The mechanical properties of the blend are also increased by the addition of compatibilisers followed by a levelling off at higher concentrations.

The dynamic vulcanisation of PP/NBR blends leads to fine and uniform distribution of rubber particles in the plastic matrix. The size of the dispersed rubber particles depend on the crosslinking systems used. Among the different vulcanising systems used, the sulphur system gives better properties for blends having high plastic content, while DCP system gives better properties for blends with high rubber content. The addition of fillers to PP/NBR blends has not much effect on the mechanical properties. It is observed that the addition of carbon black to PP/NBR blends adversely affects the properties.

The dynamic mechanical analysis of the blends is important as many of the polymeric materials usually undergo cyclic stresses during service. The analysis would also give an idea about the miscibility of the blend system. The effects of blend composition and compatibilisation on the dynamic mechanical properties were investigated in the temperature range -50 to +150°C. These investigations indicate that PP/NBR blends are incompatible as proved by the presence of two α-relaxation peaks corresponding to the Tgs of PP and NBR. As the concentration of rubber increases, the storage modulus of the system decreases, while the loss modulus and tan δ increase. The increase in loss modulus is more pronounced after 50 wt % of NBR in the blend. The change in viscoelastic properties with blend composition is correlated with the blend morphology. Various composite models have been used to fit the experimental viscoelastic data. Takayanagi's model is found to fit the experimental values for 20% parallel coupling. The addition of phenolic modified polypropylene and maleic anhydride modified polypropylene is found to increase the storage modulus at lower temperature which indicates an increase in interfacial adhesion upon the addition of these compatibilisers. At higher concentration of these compatibilisers the storage modulus decreases due to interfacial saturation. Among the vulcanised systems, the DCP system shows the highest modulus and sulphur system the lowest. The mixed system shows an intermediate behaviour.

The investigation of melt rheology of these blends would help to optimise the processing conditions required for the production of the material. Hence the melt rheological behaviour of PP/NBR blends has been investigated over a wide range of shear rates and temperatures. The blends show pseudoplastic behaviour which is indicated by a decrease in viscosity with shear rate. The viscosity of these blends increases with increase in NBR concentration and shows a sharp change after 50 wt % of NBR. The variation in viscosity is correlated with the phase change of NBR from dispersed to continuous phase. The blends show negative deviation which indicated lack of interaction between the polar nitrile rubber and non-polar polypropylene.

Various theoretical models have been used to predict the experimental viscosity values. The viscosity values fit well with the values calculated using altered free volume model. The compatibilisation of these blends using phenolic modified polypropylene is found to increase the viscosity of the system, indicating an increase in interfacial interaction. The variation of viscosity is correlated with the phase morphology. As the compatibiliser concentration increases the size of the domain decreases with a levelling off at high concentration. The dynamic vulcanisation of PP/NBR blends leads to fine and uniform distribution of NBR particles and the size of the dispersed NBR particles varies in the order DCP < mixed < sulphur cured system. Among the dynamic vulcanised blends the sulphur cured system has the highest viscosity and DCP cured system has the lowest. In peroxide and mixed cured systems PP is degraded in presence of DCP. The die swell values of the blends have decreased on dynamic vulcanisation. The temperature dependence of viscosity was studied using Arrhenius equation. The compatibilised system show higher values of activation energy compared to uncompatibilised one. A shear rate-temperature superposition master curve has also been developed for polypropylene and 70/30 PP/NBR blend. The melt flow index of PP/NBR blend decreases with increase in rubber concentration. The MFI data have been correlated with capillary rheometer data. The effect of annealing on the morphology of uncompatibilised and compatibilised blends has been investigated. The domain size of NBR particles increased in the uncompatibilised system upon annealing the samples for one hour. Interestingly, the morphology of the compatibilised system is really stable.

The analysis of thermal stability of polymeric materials is necessary for the development of durable products. The thermal degradation of polypropylene/nitrile rubber blends was investigated using thermogravimetric method. The incorporation of nitrile rubber into polypropylene improved the thermal properties of polypropylene. The initial degradation temperature of polypropylene is increased on blending. Among the different blends compositions

the P_{50} blend shows the lowest degradation temperature. The thermal behaviour of various blend compositions was correlated with blend morphology. The weight loss corresponding to different temperatures is also decreased upon blending. The effect of compatibilisation of PP/NBR blend using phenolic modified polypropylene and maleic anhydride modified polypropylene on thermal degradation was also investigated. The compatibilisation increased the degradation temperature. The dynamic vulcanisation of the blends using sulphur, peroxide and mixed system consisting of sulphur and peroxide, improved the thermal stability. Among the three vulcanised systems, the mixed vulcanised system has the highest degradation temperature and sulphur cured system the lowest. The thermal behaviour of the three types of dynamic vulcanised blends is correlated with the crosslink density and type of crosslinks formed. The melting behaviour of binary PP/NBR blends was also investigated using differential scanning calorimetry. The melting temperature and heat of fusion values decreased upon the addition of NBR. The crystallinity of PP/NBR blends also decreases with increase in nitrile rubber concentration. The crystalline structure of PP/NBR blends was also investigated. The pure polypropylene and the blends showed α-monoclinic structure as evident from the presence of four reflections corresponding to the four planes. The compatibilisation of the blends did not affect the α-monoclinic crystalline structure of PP. The incorporation of nitrile rubber in to polypropylene increased the inter planar distance, which indicates the presence of rubber phase in intra spherulitic regions

The dielectric properties of PP/NBR blends were also studied to explore the possibility of using these blends as insulating materials. The dielectric properties such as volume resistivity, dielectric constant and tan δ of PP/NBR blends were measured over a wide range of frequencies. The dielectric constant of the pure components and blends decrease with increase of frequency. The variation in dielectric constant is in three stages due to the relaxations in interfacial and orientation polarisation. With the increase of NBR content in the blend, the

dielectric constant increases and shows a sharp change after 50 wt % of loading. The sharp change above 50 wt % NBR is correlated with the morphology of the blend. The experimental dielectric constant values were compared with theoretical models. It is found that the experimental data fit well with the data obtained from Maxwell-Wagner-Sillers equation. The effects of various fillers such as HAF black, silane treated silica and cork on dielectric properties were also investigated. The incorporation of fillers into PP/NBR blends affected the dielectric properties. The dielectric constant increases upon the addition of carbon black and the increase is more pronounced in 30/70 PP/NBR blend. The change is correlated with the formation of network of carbon black particles in the continuous NBR phase at 70 wt % of NBR. In silane treated silica filled blends, the dielectric constant increases up to 20 wt % loading while at 30 wt % loading the ε' value decreases and in cork filled blends the ε' value increases by the addition of 10 wt % of cork, while further increase in loading decreases the ε' values. The increase in ε' value upon the addition of fillers was correlated with the presence of polar groups in the filler and to the interfacial polarisation. The loss factor increased upon the addition of carbon black and silica while the addition of cork decreased the ε'' values. The dynamic vulcanisation leads to an increase in ε' values. Among the different vulcanising systems used, the sulphur system shows the lowest value and DCP vulcanised system the highest. The mixed system shows an intermediate value. The dissipation factor and loss factor values also increased upon vulcanisation.

The investigation of the transport properties of these blends in various aromatic solvents was carried out to get an idea about the barrier properties of these materials. The mechanism of transport is close to Fickian in PP/NBR blends. As the concentration of NBR increases, in the blend, the equilibrium uptake values and diffusion and permeation coefficients increase. The variation in transport parameters was correlated with morphology of the system. The equilibrium uptake values show a sharp increase after 50 wt % of NBR which is due to the phase

inversion of NBR from dispersed to continuous phase. The experimental permeation coefficients were compared with various theoretical predictions. Maxwell and Robeson's models have been used to predict the experimental permeation coefficients. The effect of nature of crosslinking on transport behaviour was studied. Among the three vulcanising systems used [sulphur, DCP and mixed (S+DCP) systems], the sulphur system shows the highest uptake and DCP the lowest and mixed system shows intermediate behaviour. The difference in the behaviour is correlated with the type of crosslinks formed and crosslinking density. The diffusion and permeation coefficients and Q_∞ values decrease with increase in molar volume of solvents. The effect of different types of fillers on transport properties was also investigated. In the filled blends, the uptake values follow the order cork > silica > carbon black. The activation energy for diffusion and permeation was calculated and are found to decrease with increase in rubber content. Comparison of the crosslink density values with phantom and affine network models indicates that in PP/NBR blends, the network structure can be modelled by affine theory. The experimental and theoretical diffusion curves are in good agreement for the blend systems.

9.2 Future scope of the work

9.2.1 Crystallisation kinetics

The properties of rubber/plastic blends depend on the crystalline structure of plastic matrix. Hence a detailed investigation can be carried out on crystallisation kinetics and crystalline structure of PP/NBR blends. The spherulitic growth rate, spherulite structure and nucleation can be investigated using phase contrast optical microscopy and differential scanning calorimetry.

9.2.2 *Barrier property measurements*

The barrier properties of these blends can be studied to extend its application for the separation of various gases and liquids. The vapour permeation, pervaporation and gas separation studies can be carried out for this purpose.

9.2.3 *Interfacial characterisation*

In the present investigation we have seen that the compatibilisation of PP/NBR blends improved the properties. The investigation of interfacial tension and interfacial thickness in uncompatibilised and compatibilised blends can be studied using various modern techniques. The ellipsometry technique can be used to estimate the interfacial thickness in polymer blends. The small angle X-ray scattering (SAXS) and neutron scattering (SANS) can also be used to study the interfacial thickness. The interfacial tension can be measured using highly specialised pendant drop apparatus or breaking thread methods.

9.2.4 *Fabrication of useful products*

The application of PP/NBR blends for the fabrication of automobile parts such as dash boards, bumpers, etc. can be attempted.

Appendix

Curriculum Vitae

Name	*SNOOPPY GEORGE*
Age and Date of Birth	*29, 25.5.1969*
Permanent Address	*Chandrankunnel* *Pravithanam P. O., Pala* *Kerala - 686 651, INDIA* *Phone: 0482-246439*

Education *M.Sc. Chemistry (Distinction, First Rank)*

Research Interests

1. *Polymer blends: Characterisation and properties*
2. *Transport process through polymers, its kinetics and thermodynamics.*
3. *Polymer composites: Fabrication and properties*
4. *Interpenetrating networks: Latex IPNs and characterisation*

Work Experience

Five years research experience in Polymer Technology/Chemistry.

Skills

Instrumentation: Most of rubber/plastic processing and characterisation machineries.

Award

Senior Research Fellowship, CSIR, New Delhi.

Publications

Papers:	*9*
Papers presented in Conferences:	*4*

List of Publications

I. Papers published in International Journals

1. Blends of isotactic polypropylene and nitrile rubber: Morphology, mechanical properties and compatibilization.
S. George, R. Joseph, S. Thomas and K. T. Varughese, *Polymer*, 36, 23, 4405, 1995.

2. Tearing behaviour of incompatible and compatible blends of isotactic polypropylene and nitrile rubber.
S. George, L. Prasannakumari, Peter Koshy, S. Thomas and K. T. Varughese., *Material letters* 26, 51-58, 1996.

3. Thermoplastic elastomers from rubber-plastic blends morphology, mechanical properties and compatibilization.
J. George, S. George and S. Thomas, *International plastics engineering and technology*, 1, 35,1994.

4. Reactive compatibilization of immiscible polymer blends.
S. George, J. George and S. Thomas, *Handbook of Engineering Polymeric Materials*, Cheremisinoff (ed), Marcel Decker, Inc, New York, 1996.

5. Dynamic mechanical properties of Isotactic polypropylene/nitrile rubber blends: Effects of blend ratio, reactive compatibilisation and dynamic vulcanisation.
S. George, N. R. Neelakantan, K. T. Varughese and S. Thomas, *J. Polym. Sci. B. Polym. Phys.* 35, 2309, 1997.

6. Rheological behaviour of isotactic polypropylene/nitrile rubber blends: Effects of blend ratio, compatibilization and dynamic vulcanisation.
S. George, R. Ramamurthy, J. S. Anand, K. T. Varughese and S. Thomas., *Polymer* (In Press).

7. Dielectric behaviour of polypropylene/nitrile rubber blends: Effects of blend ratio and dynamic vulcanisation.
S. George, K. T. Varughese and S. Thomas, *J. Appl. Polym. Sci.* (communicated)

8. Molecular transport of aromatic solvents in isotactic polypropylene/ acrylonitrile-co-butadiene rubber blends.
S. George, K. T. Varughese and S. Thomas, *J. Membr. Sci.* (communicated)

9. Thermal and crystallisation behaviour of isotactic polypropylene/nitrile rubber blends.
S. George, K. T. Varughese and S. Thomas, *J. Therm. Analys.* (communicated)

II. Papers Presented in National/International Conferences

1. S. George, J. George, S. Thomas and K. T. Varughese
Morphology, properties and compatibilization of polyolefine/nitrile rubber blends, Macromolecules current trends, Vol. II., S. Venkatachalam. V. V. Joseph, R. Ramaswamy, V. N. Krishnamurthy (Eds), Allied Publishers, New Delhi, 789, 1995. Macro '95 held at VSSC, Thiruvananthapuram.

2. S. George, S. Thomas and K. T. Varughese.
Morphological and mechanical properties of thermoplastic elastomers from nitrile rubber and isotactic polypropylene, Proceedings of the 6th AGM Symposia of MRSI held in IIT, Kharagpur, February, 1995.

3. S. George, K. T. Varughese and S. Thomas.
Blends of isotactic polypropylene and nitrile rubber: Effect of blend ratio on morphology, dielectric and mechanical properties, Proceedings of the abstract of the national seminar of Rubber Blends held at RRII, Kottayam, India, Nov. 14, 1995.

4. S. George and S. Thomas
Tearing behaviour of isotactic polypropylene/nitrile rubber: Effect of blend ratio and compatibilization, Proceedings of the 8th Kerala Science Congress, held at Kochi, 1996.

ITTERWORTH
EINEMANN

Polymer Vol. 36 No. 23, pp. 4405–4416, 1995

0032-3861/95 $10.00+0.00

Blends of isotactic polypropylene and nitrile rubber: morphology, mechanical properties and compatibilization

Snooppy George, Reethamma Joseph* and Sabu Thomas†
School of Chemical Sciences, Mahatma Gandhi University, Priyadarshini Hills PO, Kottayam-686 560, Kerala, India

and K. T. Varughese
Central Power Research Institute of India, Bangalore-560 094, India
(Received 8 April 1994; revised 22 March 1995)

Morphology and mechanical properties of blends of isotactic polypropylene (PP) and nitrile rubber (NBR) have been investigated with special reference to the effects of blend ratio. Morphological observations of blends showed a two-phase system, in which the rubber phase was dispersed as domains in the continuous PP matrix at lower proportions of NBR (≤50%). The 30/70 PP/NBR blend was found to exist as a co-continuous system. Attempts have been made to correlate the changes in morphology with properties. The mechanical properties of blends were found to depend on the blend ratio. Various composite models, such as the series model, the parallel model, the Halpin–Tsai equation and Coran's model, have been used to fit the experimental mechanical properties. The effect of concentration of maleic-modified polypropylene (MA-PP) and phenolic-modified polypropylene (Ph-PP) as compatibilizers on the morphology and mechanical properties of the blend was also investigated. The compatibilizer concentrations used were 1, 5, 10 and 15 wt%. The domain size of the dispersed NBR particles decreased with the addition of a few per cent of the compatibilizer followed by a levelling off at higher concentrations. The levelling off was an indication of interfacial saturation. The mechanical properties of the blends were improved by the addition of the compatibilizer followed by a levelling off at higher concentrations. The levelling off was an indication of interfacial saturation. The mechanical properties of the blends were improved by the addition of the compatibilizers. The experimental results were compared with the current compatibilization theories of Noolandi and Hong.

(Keywords: blends; morphology; compatibilization)

NTRODUCTION

hermoplastic elastomers (TPEs) possess the excellent rocessing characteristics of thermoplastic materials at gher temperatures, and the wide range of physical roperties of elastomers at service temperature[1–5]. uring the last few years, a large number of studies on ermoplastic elastomeric blends have been reported[6–12]. thorough understanding of the blend morphology is portant, since the properties of polymer blends are rongly dependent on the blend morphology[13–17].

Most of the polymer blends are found to be compatible. These incompatible blends are characterized by a two-phase morphology, narrow interphase, poor physical and chemical interactions across the phase boundaries and poor mechanical properties. These problems can be alleviated by the addition or *in situ* rmation of compatibilizers or interfacial agents[18,19]. ccording to Paul and Barlow[20], the addition of a itably selected compatibilizer to binary immiscible lends should (1) reduce the interfacial energy between the phases, (2) permit a finer dispersion during mixing, (3) provide a measure of stability against gross segregation, and (4) result in improved interfacial adhesion. The effect of addition of block and graft copolymers as compatibilizers in binary polymer blends has been studied in detail[21–27]. Recently, the reactive compatibilization technique has been used for compatibilizing polyethylene (PE)/polystyrene (PS), polypropylene (PP)/nylon-6, PS/nylon-6, PP/PE, PS/EPDM and NR/PP systems[28–35].

Finally, thermodynamic theories concerning the emulsifying effect of block copolymers in polymer blends have been developed by Leibler[36,37], and Noolandi and Hong[38–40]. The theory of Noolandi and Hong[38–40] states that localization of some of the block copolymer at the interface results in a lowering of the interaction energy between two immiscible homopolymers, broadening of the interphase between homopolymers, and a decrease in free energy, and ultimately limits the amount of copolymer present at the interphase.

Blends of nitrile rubber (NBR) and PP combine the oil-resistant properties of nitrile rubber and the excellent mechanical and processing characteristics of PP. They can be successfully used for high-temperature, oil-

Present address: Rubber Research Institute of India, Kottayam-686009, India
To whom correspondence should be addressed

resistant applications. However, these blends are found to be immiscible and incompatible. They are characterized by a sharp interface, coarse morphology and poor physical and chemical interactions across the phase boundaries. Although some studies have been reported[41,42] on the thermodynamics, structural properties and compatibilization of NBR/PP blends, detailed investigations relating morphology to the properties and compatibilizing efficiency to the nature and concentration of the copolymer are lacking. The purpose of the present study is to investigate systematically the influence of blend ratio on the morphology and mechanical properties of NBR/PP blends. The effects of concentration of two compatibilizers, maleic-modified PP and phenolic-modified PP, on the morphology and mechanical properties of the blend were investigated quantitatively. The experimental results were applied to test the current compatibilization theories of Noolandi and Hong.

EXPERIMENTAL

Materials

Isotactic PP (Koylene M3060) with a melt flow index of 3 g/10 min was supplied by IPCL, Vadodara, India. NBR, with 32% acrylonitrile content, was supplied by Synthetics and Chemicals, Bareli, U.P., India.

Maleic-modified PP (MA-PP) was prepared by melt mixing PP with maleic anhydride (5 parts), benzoquinone (0.75 parts) and dicumyl peroxide (3 parts) in a Brabender Plasticorder at 180°C (ref. 11). Phenolic-modified PP (Ph-PP) was prepared by melt-mixing PP with dimethylol phenolic resin (Sp-1045; 4 parts) and stannous chloride (0.8 parts) at 180°C (ref. 11).

Blend preparation

The blends are referred to as P_0, P_{30}, P_{50}, P_{70} and P_{100}, where the subscripts denote the weight percentage of PP in the blend. These blends were prepared in a Brabender Plasticorder (model PLE-330) at a temperature of 180°C. The rotor speed was 60 rev min^{-1} and the blending was carried out for 6 min. The compatibilizer concentrations used were 1, 5, 10 and 15 wt%.

Physical testing of the samples

The samples for physical property measurements were prepared by compression-moulding the mixes at 180°C in a hydraulic press into sheets with dimensions 15 cm × 15 cm × 0.15 cm. The tensile property measurements were done on a Zwick Universal Testing machine (model 1474) using dumb-bell shaped specimens at a crosshead speed of 500 mm min^{-1}, in accordance with ASTM D412-81. The tensile impact strength of the samples was measured on a Ceast Impact Tester (model 6545/000) using dumb-bell shaped specimens. The hardness of the samples was measured using shore A and shore D Hardness Durometer. The crystallinity of the samples was measured using a Perkin–Elmer DSC differential scanning calorimeter. The weight percentage crystallinity of PP was determined from the ratio of the heat of fusion of the blend to that of the 100% crystalline PP ($\Delta H_{pp} = 138\ J\ g^{-1}$ (ref. 43).

Morphology studies

The samples for morphology studies were prepared by cryogenically fracturing the samples in liquid nitrogen. The fractured end of the sample was kept immersed in chloroform for two weeks. The samples were then dried in an oven. For morphology studies, samples (the NBR phase was preferentially extracted) were sputter-coated with gold and photographs were taken in a JEOL scanning electron microscope. The domain size was measured from the scanning electron photomicrographs. Several micrographs were taken for each blend and about 100 domains were taken for number-average domain diameter measurements. The apparent domain diameter was obtained from the measurement of hole diameter obtained as a result of the extraction of the rubber phase.

RESULTS AND DISCUSSION

Processing characteristics

The processing characteristics of the blends have been studied from the Brabender Plastographs. The torque–time and torque–temperature relationships obtained from Brabender plastographs are shown in *Figure 1*. In all cases, the mixing torque falls rapidly up to 3 min of mixing time and then levels off to give uniform values at the end of the mixing cycle, indicating a good level of mixing. Favis[17] has reported that the final morphology of the blend is strongly influenced by the time of mixing. All the blends show a higher mixing torque than PP, and the torque is found to increase with increase in NBR content. This is due to the higher melt viscosity of NBR as compared to PP. This result clearly indicates that all the blends have higher melt viscosity than PP. It is also seen from *Figure 1* that the mixing temperature of the blends increases with increase in NBR content. This is due to the fact that high shear forces are involved as the NBR content increases owing to its higher viscosity as compared to PP.

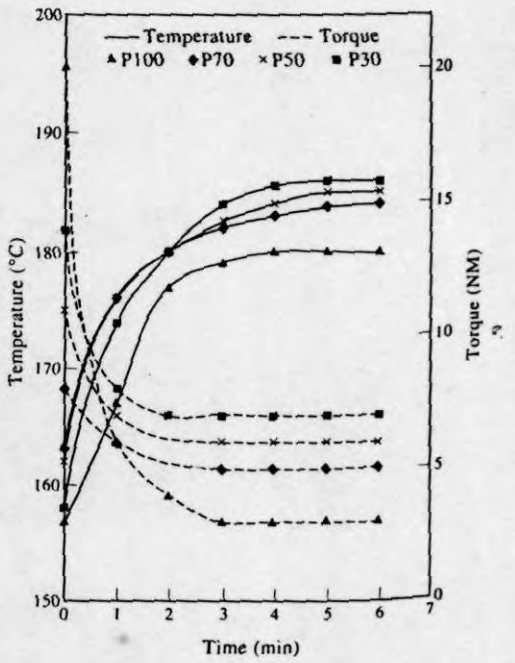

Figure 1 Brabender plastograph showing the variation of mixing torque and temperature with time of mixing

orphology of the binary blends

The morphology of heterogeneous polymer blends epends on blend composition, viscosity of individual omponents and processing history. Danesi and Porter[14] ave shown that for blends with the same processing istory, the morphology is determined by the melt iscosity ratio and composition. Generally, the least iscous component was observed to form the continuous hase over a larger composition range[44].

The scanning electron micrographs of blends P_{70}, P_{50} nd P_{30}, from which the NBR phase has been extracted, re shown in *Figures 2a* to *c*. In the P_{70} blend, NBR is und to be dispersed as domains in the continuous PP atrix. This is due to the higher melt viscosity and lower ntent of NBR compared to PP in the blend. As the ubber content in the blend increases from 30 to 50 wt% BR. the average size of the dispersed NBR phase creases from 5.87 to 17.90 μm. The bigger particle size f the rubber phase with increase in rubber content is tributed to the reagglomeration or coalescence of the spersed rubber particles. The occurrence of coalescence higher concentrations of one of the components has en reported by many authors[45–47]. In the P_{30} blend, oth NBR and PP phases exist as co-continuous phases. his is associated with the higher proportions of NBR nd low viscosity of the PP phase.

Mechanical properties

The properties of rubber–plastic blends are determined by (1) material properties of rubber and plastic phases, (2) rubber/plastic proportions, (3) the phase morphology, and (4) the interaction at the interface[48]. The stress–strain curves of the P_{100}, P_{70}, P_{50}, P_{30} and P_0 blends are shown in *Figure 3*. From the stress–strain curves it is possible to determine the differences in the deformation characteristics of the blends under an applied load. The stress–strain curve of PP is similar to that of a brittle material. It shows very high initial modulus with a definite yield point. The addition of NBR changes the nature of stress–strain curves considerably. The stress–strain curves of PP and blends containing a higher proportion of PP have distinct elastic and inelastic regions. In the inelastic region they undergo yielding. The elastic moduli of the blends are found to be considerably reduced with the increase in rubber concentration. The improved rubbery behaviour of P_{30} blend compared to P_{70} and P_{50} can be explained in terms of the phase inversion of NBR from dispersed to continuous phase on passing from P_{50} to P_{30}. The stress–strain behaviour of NBR is typical of uncross-linked soft elastomer.

Table 1 and *Figure 4* show the variation of mechanical properties as a function of weight percentage of NBR.

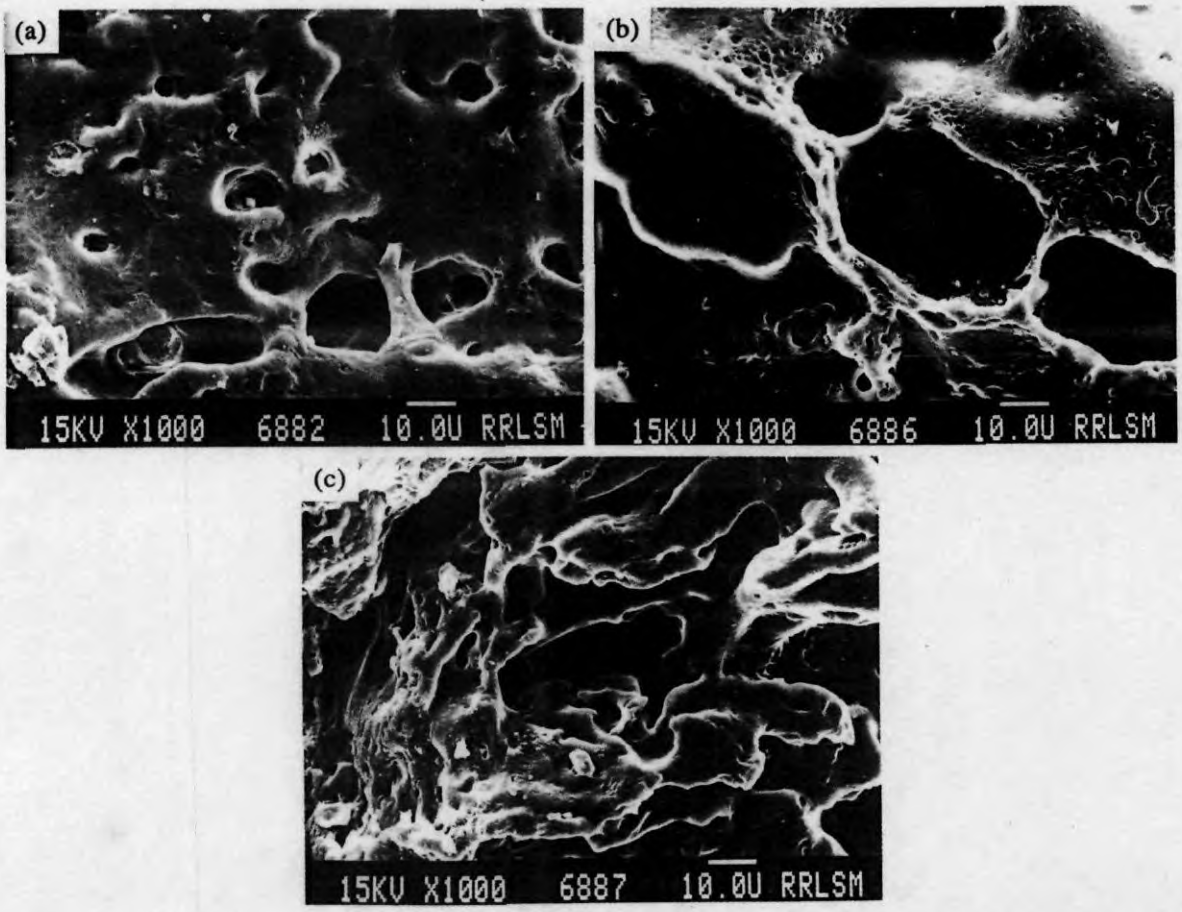

ure 2 Scanning electron photomicrographs of NBR/PP blends from which NBR was extracted with chloroform. (a) 30/70 NBR/PP blend: NBR is spersed as domains in the continuous PP matrix. (b) 50/50 NBR/PP blend: NBR is dispersed as domains in the continuous PP matrix. (c) 70/30 NBR/ blend with co-continuous morphology

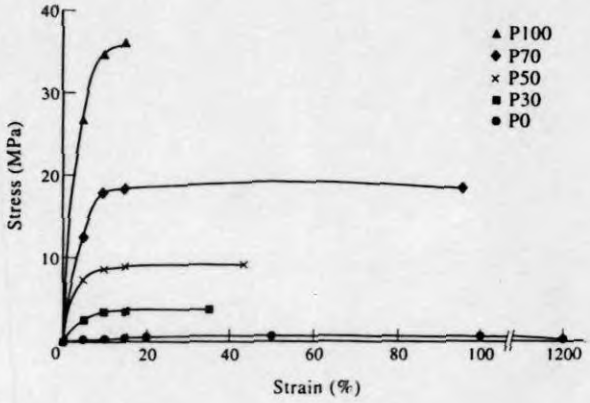

Figure 3 Stress–strain curves of the samples

Pure isotactic PP has the highest tensile strength and Young's modulus. From the table it is seen that with increase in NBR content, the tensile strength and Young's modulus decrease. The strength of NBR/PP blends depends on the strength of the PP phase, which in turn depends on the extent of crystallinity. It has been observed that the crystallinity of the blend was decreased by the incorporation of NBR (*Table 2*). Martuscelli *et al.*[49] have shown that the spherulite growth of isotactic PP in blends with rubber is hindered by the presence of the rubber phase. Hence the observed decrease in tensile strength and Young's modulus with increase in NBR content is due to the presence of the soft rubber phase and fall in crystallinity of the PP phase. It can be noticed from *Figure 4* that the tensile strength–composition curve shows a negative deviation, i.e. blend properties lie below the additivity line. The observed negative deviation is due to the poor interfacial adhesion between the non-polar PP and polar NBR phases, which causes poor stress transfer between the matrix and the dispersed phase. A clear change in the slope of this tensile strength–composition curve is seen between the composition range 50/50 PP/NBR to 30/70 PP/NBR. The observed change in slope is attributed to phase inversion of NBR from dispersed phase to continuous phase. This type of slope change in a mechanical property–composition curve has been reported by Danesi and Porter for the PP/EPDM system[14].

The elongation at break of the PP/NBR blend is found to increase with the addition of 30 wt% NBR and after that it decreases with increase in rubber content (*Table 1*). The elongation at break also shows negative deviation. This decrease in elongation at break at higher rubber content is due to the poor interfacial adhesion between the homopolymers.

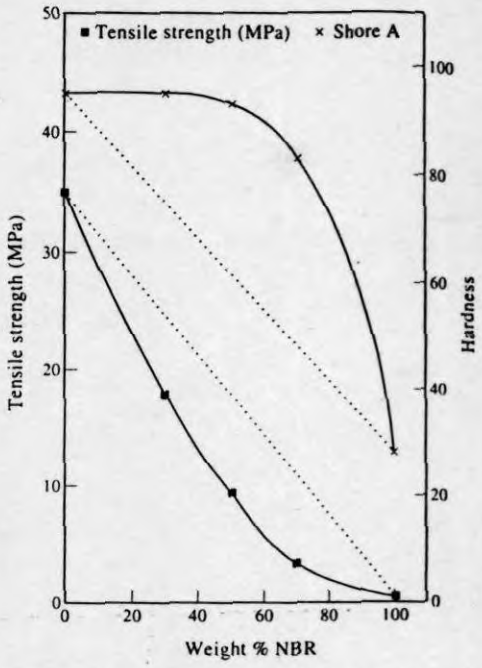

Figure 4 Effect of weight percentage of NBR on tensile strength and shore A hardness of NBR/PP blends

Table 2 Crystallinity of PP/NBR blends

Composition	Crystallinity (%)
P_{100}	55.3
P_{70}	33.9
P_{50}	20.9
P_{30}	13.7

From *Table 1* it is also seen that the tensile impact strength decreases with the addition of NBR up to 50 wt%. In immiscible blends, the tensile impact strength usually depends on the particle size of the dispersed phase. Smaller and uniformly distributed particles are more effective at initiating crazes and terminating them before they develop into catastrophic sizes. The decrease in tensile impact strength in PP/NBR blends up to 50 wt% NBR content is due to the poor interfacial adhesion and bigger particle size of the dispersed NBR phase, as seen in the scanning electron photographs of P_{70} and P_{50} blends. The poor interfacial adhesion causes

Table 1 Variation of mechanical properties with blend composition

Property	Composition				
	P_{100}	P_{70}	P_{50}	P_{30}	P_0
Tensile strength (MPa)	35	18.30	9.20	3.50	0.475
Young's modulus (MPa)	500	250	135	47	1.5
Elongation at break (%)	15.6	95.58	43.45	38.64	1267
Tensile impact strength ($J\,m^{-1}$)	1110	1008	920	1448	–
Hardness shore A	95	95	93	83	28
Hardness shore D	55	55	45	18	–

premature failure as a result of the usual crack-opening mechanism. Karger-Kocsis *et al.*[50] have shown that with increase in particle size of the dispersed rubber phase, the tensile impact strength of the PP/EPDM blend decreases. Above 50 wt% NBR content, the tensile impact strength is found to increase sharply. This sharp increase in impact strength may be due to the continuous nature of the NBR phase, which forms a co-continuous structure with the plastic phase (*Figure 2*). Similar results were reported in the case of the PP/EVA system[51].

From *Table 1* it is seen that the addition of 30 wt% NBR does not change the hardness. However, further addition of NBR decreases the hardness. The hardness–composition curve shows a slope change beyond 50 wt% NBR (*Figure 4*). The reduction in hardness and the slope change in the curve at higher proportions of NBR (>50%) can be explained by the phase inversion of NBR from dispersed to the continuous phase on passing from the 50/50 PP/NBR to the 30/70 PP/NBR blend. It is interesting to see that the hardness values show a positive deviation.

Various composite models, such as the parallel model, the series model, the Halpin–Tsai equation and Coran's equation, have been used to predict the mechanical properties of these blends. The highest-upper-bound

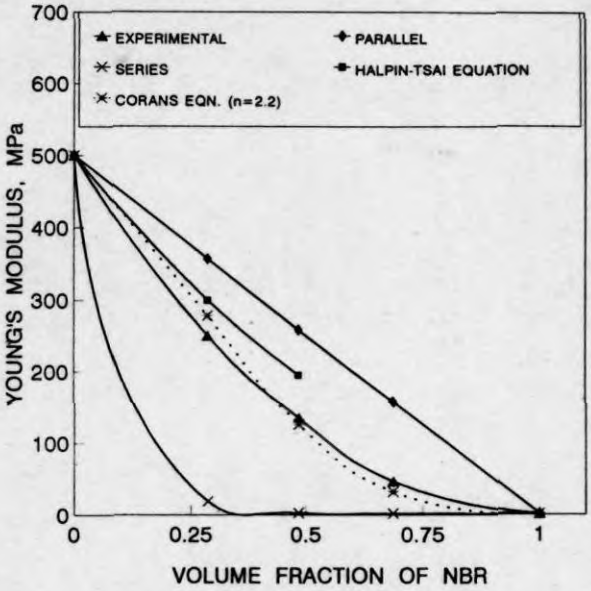

Figure 5 Experimental and theoretical values of Young's modulus as a function of volume fraction of NBR phase

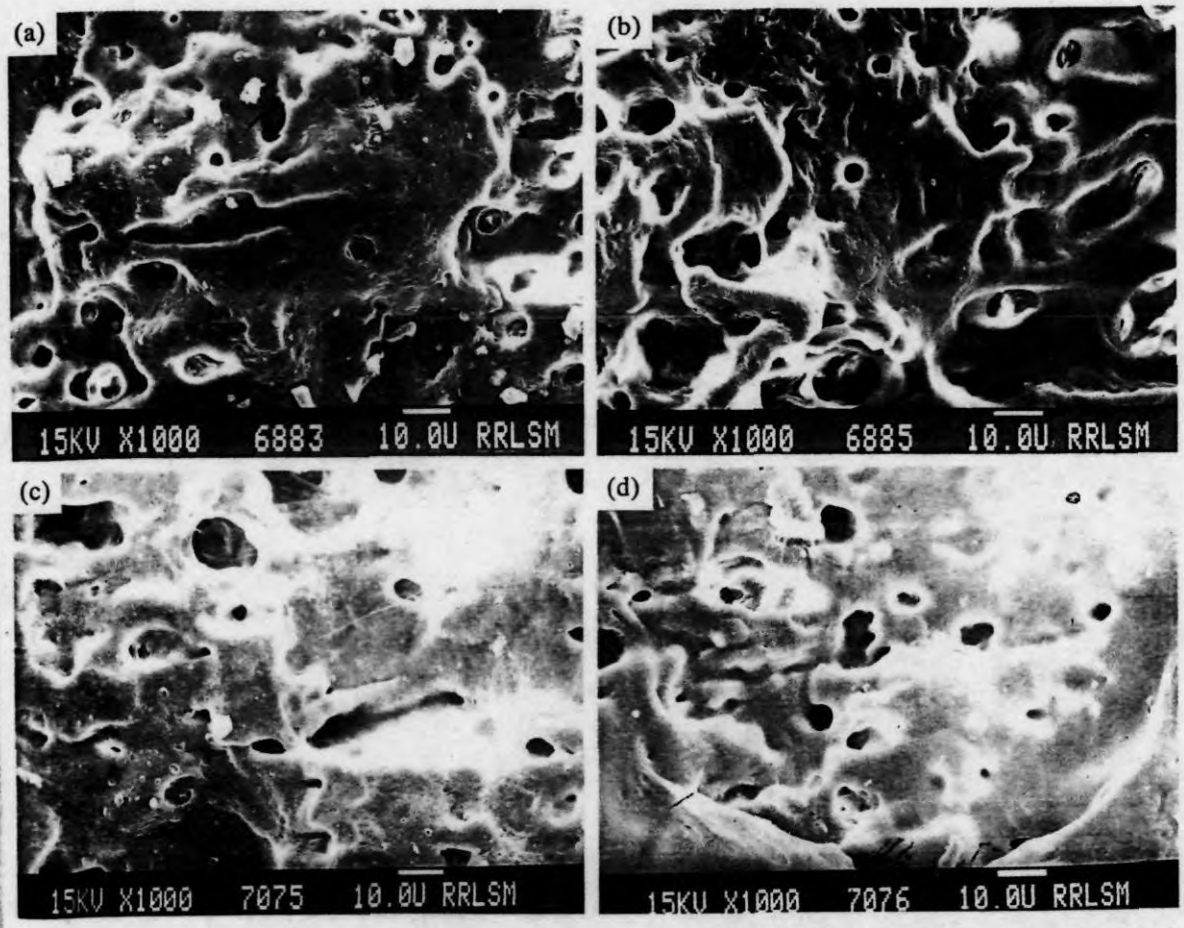

Figure 6 Scanning electron micrographs of 30/70 NBR/PP blend compatibilized with MA-PP: (a) 1% MA-PP; (b) 5% MA-PP; (c) 10% MA-PP; (d) 15% MA-PP

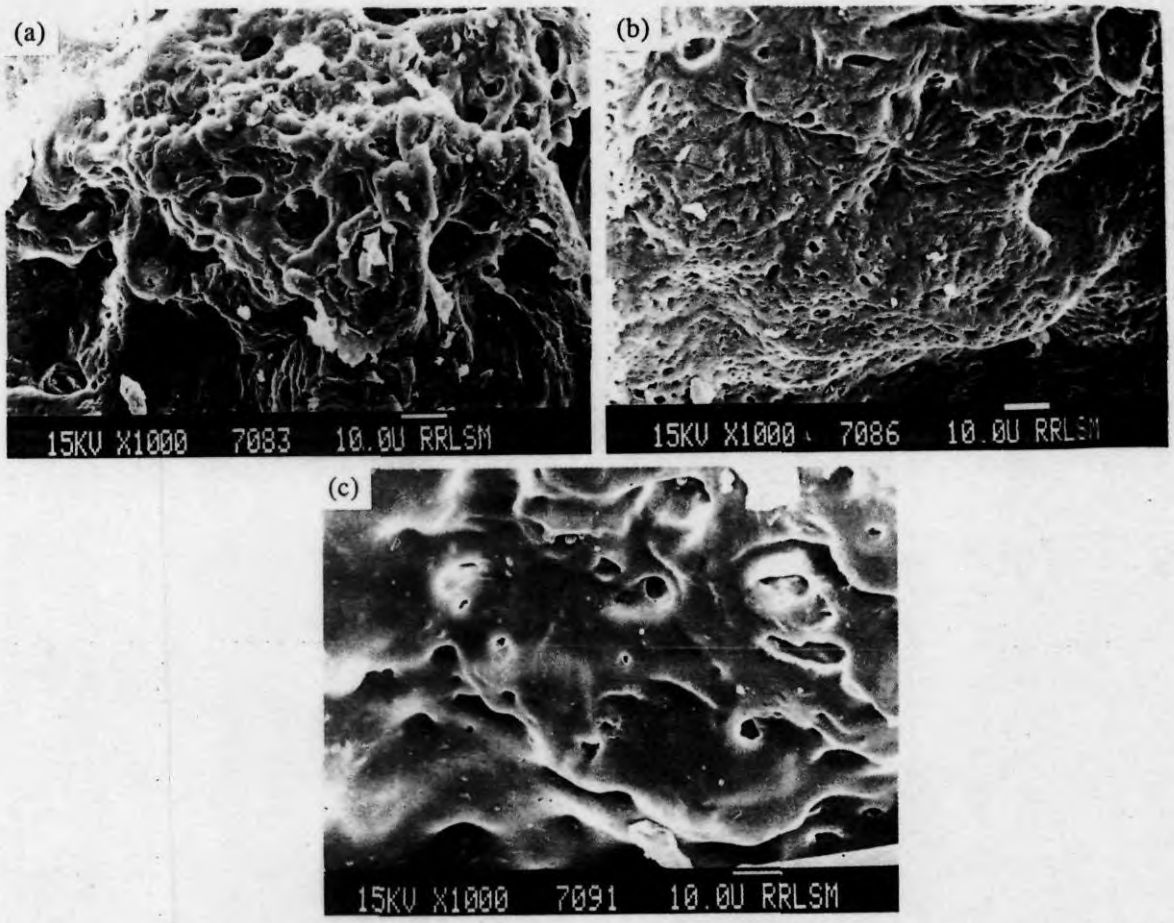

Figure 7 Scanning electron micrographs of 30/70 NBR/PP blend compatibilized with Ph-PP: (a) 1% Ph-PP; (b) 10% Ph-PP; (c) 15% Ph-PP

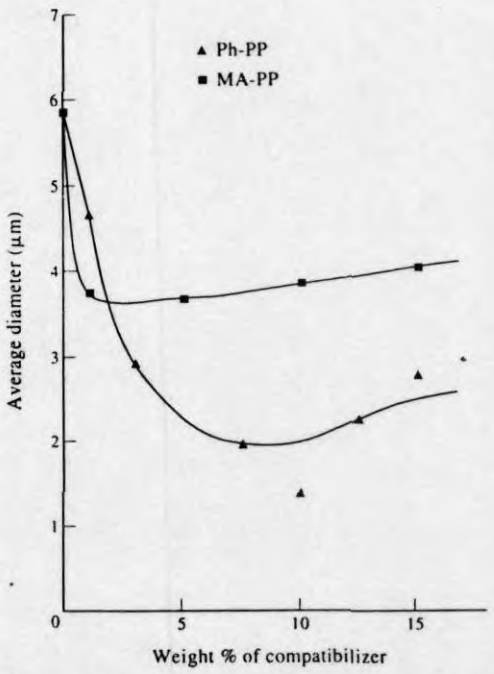

Figure 8 Effect of compatibilizer concentration on the domain size of the dispersed phase of 30 70 NBR PP blend

parallel model is given by the rule of mixtures:

$$M = M_1\phi_1 + M_2\phi_2 \quad (1)$$

where M is any mechanical property of the composite, M_1 and M_2 are the mechanical properties of components 1 and 2, respectively, and ϕ_1 and ϕ_2 are the volume fractions of components 1 and 2, respectively. This equation holds for models in which the components are arranged parallel to one another so that an applied stress elongates each component by the same amount. The lowest-lower-bound series model is found in models in which the components are arranged in series with the applied stress. The equation for this case is:

$$1/M = \phi_1/M_1 + \phi_2/M_2 \quad (2)$$

According to the Halpin–Tsai equation[52,53]:

$$M_1/M = (1 + AiBi\phi_2)/(1 - Bi\phi_2) \quad (3)$$

$$Bi = (M_1/M_2 - 1)/(M_1/M_2 + Ai) \quad (4)$$

In the Halpin–Tasai equation, subscripts 1 and 2 refe to the continuous phase and dispersed phase respec tively. The constant Ai is defined by the morphology o the system. For elastomer domains dispersed in continuous hard matrix, $Ai = 0.66$.

For an incompatible blend, mechanical properties ar generally between the parallel model upper bound (M_U and the series model lower bound (M_L). According t

an's equation[45]:

$$M = f(M_U - M_L) + M_L \quad (5)$$

ere f can vary between zero and unity. The value of f function of phase morphology. The value of f is en by:

$$f = V_H{}^n(nV_S + 1) \quad (6)$$

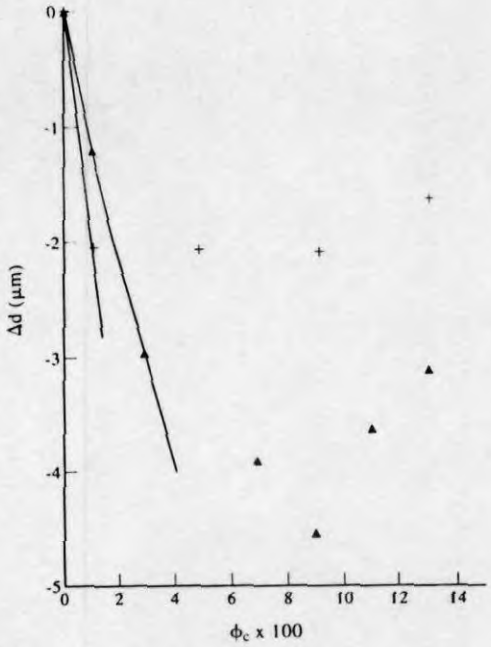

e 9 Effect of volume fraction of compatibilizer on the particle eduction of 30/70 NBR PP blend

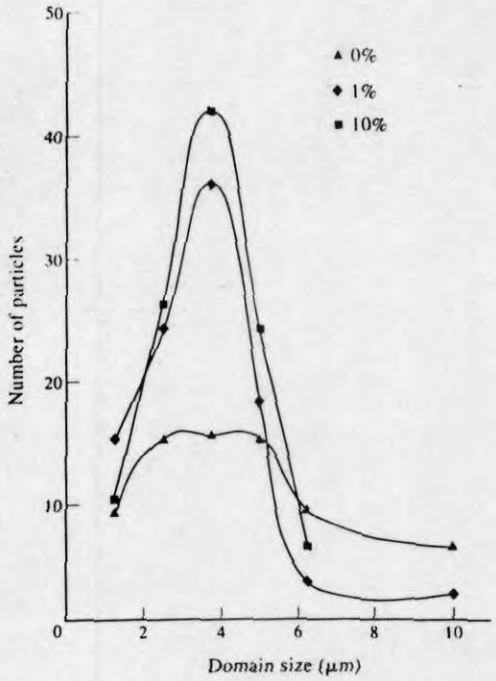

e 10 Effect of MA-PP concentration on domain size distribution 70 NBR/PP blend

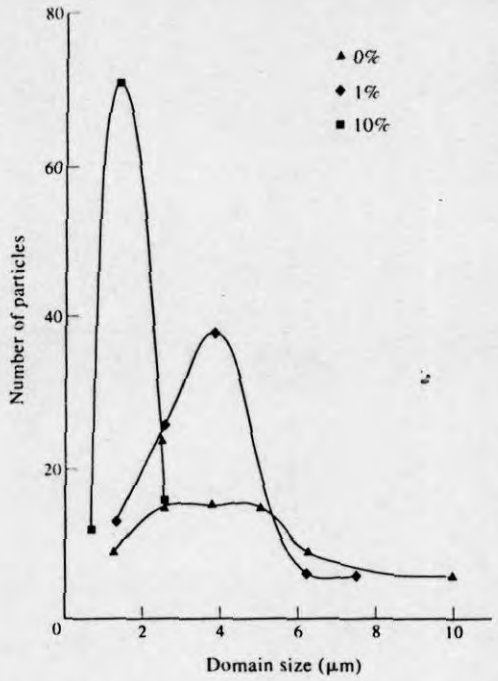

Figure 11 Effect of Ph-PP concentration on domain size distribution of 30/70 NBR/PP blend

where n contains the aspects of phase morphology, and V_H and V_S are the volume fractions of the hard-phase and soft phase, respectively. The change in f with respect to V_H is greatest when $V_H = (n-1)/n$, thus the value of $(n-1)/n$ could be considered as the volume fraction of hard-phase material that corresponds to a phase inversion.

Figure 5 shows the experimental and theoretical curves of Young's modulus as a function of soft-phase volume fraction. It can be seen that experimental data are very close to Coran's model, in which $n = 2.2$. The value of $n = 2.2$ corresponds to $V_H = 0.545$, as the hard-phase volume fraction that corresponds to a phase inversion of NBR from dispersed phase to continuous phase. This result is consistent with our experimental results from morphology and mechanical property studies.

COMPATIBILIZATION

Morphology of compatibilized blends

The effect of MA-PP and Ph-PP as compatibilizers on the morphology of the 70/30 PP/NBR blend is shown by the scanning electron micrographs of *Figures 6* and *7*, respectively. *Figures 6a–d* show blends containing 1%, 5%, 10% and 15% MA-PP compatibilizer, respectively, and *Figures 7a–c* show blends containing 1%, 10% and 15% Ph-PP compatibilizer, respectively. The morphology of an uncompatibilized blend has been given in *Figure 2a*. From the scanning electron micrographs it is seen that the size of the dispersed NBR phase decreases with the addition of modified polymers. This reduction in particle size with the addition of modified polymers is due to the reduction in interfacial tension between the dispersed NBR phase and PP matrix.

The average domain sizes of the compatibilized blends were analysed as a function of compatibilizer concentration (*Figure 8*). The average domain size of the

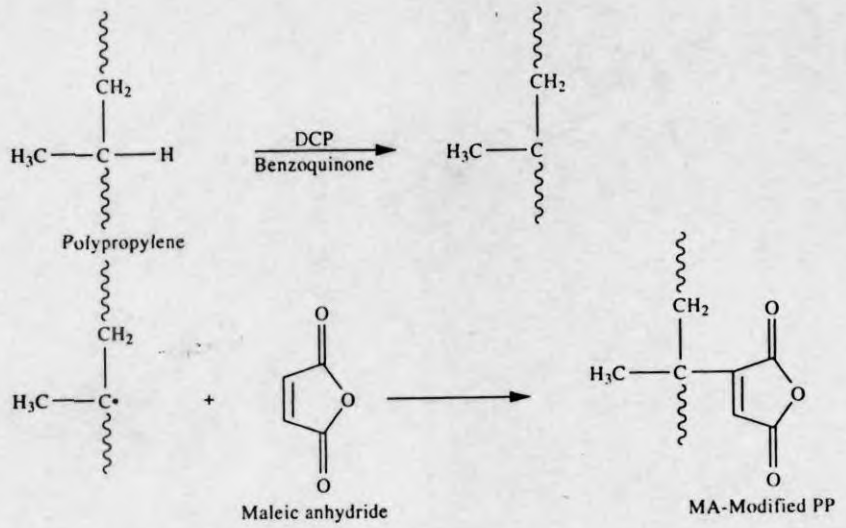

Figure 12 Reaction scheme for the maleic anhydride modification of polypropylene

unmodified blend is 5.87 μm. From *Figure 8*, it is seen that in the case of MA-PP compatibilized blends, addition of 1% MA-PP causes a reduction in domain size of 35%. Further addition of MA-PP does not change the domain size considerably, but a levelling off is observed. In the case of Ph-PP compatibilized blends, the average diameter of the dispersed NBR phase decreases up to the addition of 10 wt% Ph-PP. With 10 wt% Ph-PP, the domain size is reduced by 77% of the domain size of the unmodified blend. However, further addition of compatibilizer increases the domain size. The equilibrium concentration at which the domain size levelled off can be considered as the critical micelle concentration (*CMC*), i.e. the concentration at which micelles are formed. Generally, *CMC* is estimated from the plot of interfacial tension *versus* copolymer concentration. Since the interfacial tension is directly proportional to the domain size, the estimation of *CMC* from the plot of domain size *versus* concentration is warranted[54]. The *CMC* indicates the critical amount of compatibilizer required to saturate unit volume of interface. The increase in domain size above *CMC* may be due to the formation of micelles of compatibilizer at the continuous PP phase. Several authors have reported on the interfacial saturation of binary polymer blends by the addition of compatibilizers[27,35,55,56]. Thomas and Prud'homme[27] reported that in PS/poly(methyl methacrylate) blends at lower concentrations of copolymer, the dispersed phase size decreased linearly with increasing copolymer concentration, whereas at higher concentration, it levelled off. Noolandi and Hong also suggested that there is a critical concentration of block copolymer at which micelles are formed in the homopolymer phases. All the above experimental observations, including the present study and theoretical predictions of Noolandi and Hong, suggest that a critical concentration of compatibilizer is required to saturate the interface of a binary blend. Above this critical concentration the compatibilizer may not modify the interface any more, but forms compatibilizer micelles in the bulk phase.

The interfacial saturation point can be further explained by Taylor's theory. In Taylor's theory[57] c particle deformation, the critical Weber number, We, given by the equation:

$$We = \frac{\eta_m d n \dot{\gamma}}{2\tau_{12}} \quad (7$$

where η_m is the viscosity of the matrix, dn is the numbe average diameter of the dispersed phase, $\dot{\gamma}$ is the shea rate and τ_{12} is the interfacial tension. From the equatio it is clear that there is a critical value of We below whic there is no particle deformation and, as a result, a critic particle size. At this point the compatibilizer attains th maximum possible interfacial area and therefore the must be a maximum quantity of compatibilizer require to saturate the interface.

The theories of Noolandi and Hong can be applied t these highly incompatible PP/NBR blends for concer trations less than *CMC*. According to them the inte facial tension is expected to decrease linearly with th addition of compatibilizer below *CMC*, and above th *CMC* a levelling off is expected. The expression fc interfacial tension reduction (Δr) in a binary blend A/ upon the addition of divalent copolymer A–b–B is give by[40]:

$$\Delta r = d\phi_c[(1/2\chi + 1/Z_c) - 1/Z_c \exp(Z_c\chi/2)] \quad (8$$

where d is the width at half-height of the copolyme profile given by the Kuhn statistical segment length, ϕ_c i the bulk volume fraction of the copolymer in the syste χ is the Flory–Huggins interaction parameter between A and B segments of the copolymer, and Z_c is the degree c polymerization of the copolymer. According to thi equation, the plot of interfacial tension reduction *versu* ϕ_c should yield a straight line. Although this theory wa developed for the action of symmetrical diblock copc lymer A–b–B in incompatible binary systems (A/B), thi theory can be successfully applied to other systems i which the compatibilizing action is not strictly by th addition of symmetrical block copolymers[58]. Sinc interfacial tension reduction is directly proportional t the particle size reduction, as suggested by Wu[54], we ca replace the interfacial tension reduction term by th

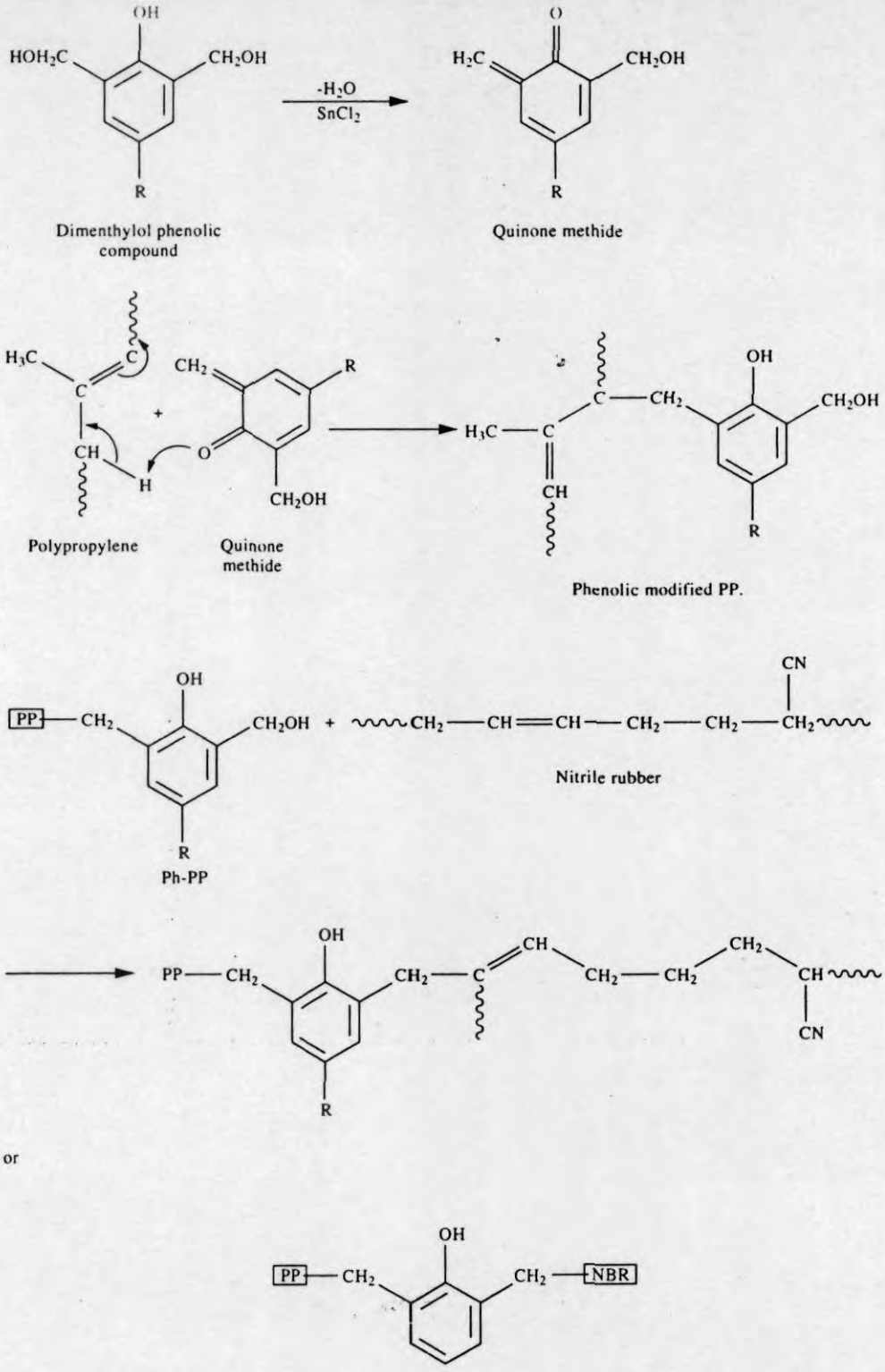

Figure 13 Reaction scheme for the dimethylol phenolic resin modification of polypropylene

Particle size reduction (Δd) term in Noolandi and Hong's equation. Therefore:

$$\Delta d = Kd\phi_c[(1/2\chi + 1/Z_c) - 1/Z_c \exp(Z_c\chi/2)] \quad (9)$$

where K is a proportionality constant.

The plot of particle size reduction as a function of the volume percentage of compatibilizer is shown in *Figure 9*. It can be seen that at low copolymer concentrations (below the *CMC*), d decreases linearly with increasing copolymer volume fraction, whereas at higher concentrations (above the *CMC*) it levels off, in agreement with the theories of Noolandi and Hong.

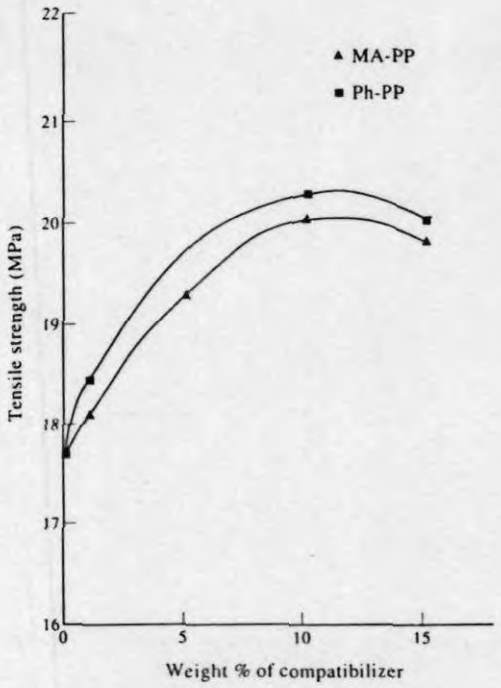

Figure 14 Effect of compatibilizer concentration on the tensile strength of 30/70 NBR/PP blend

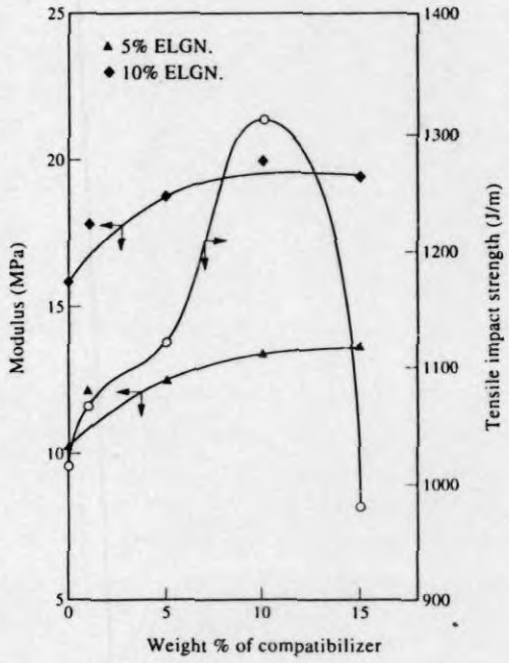

Figure 15 Effect of Ph-PP concentration on the modulus at 5% and 10% elongation and tensile impact strength of 30/70 NBR/PP blend

The domain size distribution curves for the MA-PP and Ph-PP compatibilized blends are shown in *Figures 10* and *11*, respectively. In the case of the unmodified blend, a high degree of polydispersity is evident by the large width of the distribution curve. With increasing concentration of compatibilizer (Ph-PP and MA-PP), the polydispersity decreases, as evident by the decrease in the width of the distribution curve. In the case of the Ph-PP compatibilized blend, a very narrow distribution is obtained with the addition of 10% Ph-PP. Willis and Favis[35] have also shown that the addition of compatibilizer to polyolefin/polyamide system not only reduces the dimensions of the minor phase, but also results in uniform distribution of the minor phase.

The mechanism of compatibilization and the difference in the behaviour of MA-PP and Ph-PP as compatibilizers in NBR/PP blends can be explained as follows. In the MA-PP, maleic anhydride groups are grafted onto the PP chain backbone[11] as shown in *Figure 12*. The compatibilizing action of MA-PP is due to the dipolar interaction between the maleic anhydride groups of MA-PP and NBR. This causes a reduction in interfacial tension, which reduces the domain size of the dispersed phase. In Ph-PP, dimethylol groups are grafted onto the PP chain, as shown in *Figure 13*. At low concentration of Ph-PP (≤5%), the compatibilizing action is only due to the dipolar interaction between the dimethylol phenolic groups and NBR. But on reaching 10% Ph-PP concentration, there is a possibility of the formation of graft copolymer between Ph-PP and NBR[11], as shown in *Figure 13*. This graft copolymer acts as an emulsifier at the interface and thus reduces the interfacial tension, leading to small and uniform distribution of the NBR phase as seen in the scanning electron micrograph of the 10% Ph-PP compatibilized blend.

Mechanical properties of compatibilized blends

The mechanical properties of immiscible polymer blends are affected by the addition of compatibilizers. *Figure 14* shows the variation of tensile strength of the 70/30 PP/NBR blend with weight percentage of two compatibilizers, Ph-PP and MA-PP. With increase in compatibilizer concentration the tensile strength is found to increase up to 10 wt% of compatibilizer and then levels off for both compatibilizers. This increase in tensile strength is due to the increase in interfacial adhesion between PP and NBR phases which is evident from the scanning electron micrographs. The highest tensile strength of the 10 wt% Ph-PP compatibilized blend is due to the lowest particle size of NBR domains in this system. In the case of MA-PP compatibilized blends, the increase in tensile strength is due to the increased dipolar interaction between the MA-PP and NBR phase, which causes an increase in interfacial adhesion between PP and NBR phases, although there is no reduction in particle size with the increase in MA-PP concentration beyond 1%. Similar results have been reported for the Nylon/PP system[29].

The variation of tensile modulus at 5% and 10% elongation and tensile impact strength with the Ph-PP concentration is shown in *Figure 15*. The tensile modulus is found to increase with increase in concentration of Ph-PP up to 10%, and after that it levels off.

From *Figure 15* it is seen that the tensile impact strength of the blend increases significantly with the addition of up to 10% Ph-PP, and after that it decreases drastically. This result is consistent with the literature reports on the increase of tensile impact strength with reduction in particle size of the dispersed phase. The reduction in tensile impact strength for the blend containing 15 wt% Ph-PP is due to the formation of

compatibilizer micelles in the homopolymer phases. Similar results have been reported for the low-density polyethylene/polydimethylsiloxane system[59].

CONCLUSION

The morphology and properties of thermoplastic elastomers from nitrile rubber (NBR) and polypropylene (PP) have been studied, with special reference to the effects of blend ratio and compatibilizing agents. The processability characteristics analysed from the Brabender plastographs show that the viscosity of NBR/PP blends increases with increase in NBR content. The morphology of the blends indicates a two-phase structure in which the rubber phase is dispersed as domains in the continuous PP matrix at lower proportions of NBR, and the size of the domains increases with increase in rubber content. At 70 wt% of NBR, it also forms the continuous phase, resulting in a co-continuous morphology. The mechanical properties of the blends are found to be strongly influenced by the blend ratio. The Young's modulus, tensile strength and hardness of the blends were decreased with increase in NBR content. The tensile impact strength decreases with up to 50 wt% NBR content and after that it shows an increase. In general, all the mechanical property–composition curves show a change in slope after 50 wt% NBR. This is associated with the change in morphology of the blends. A negative deviation from the additive line was observed for all mechanical properties except hardness. Various composite models have been used to fit the experimental mechanical data. The tensile strength and Young's modulus of the blends could be predicted by Coran's equation. The phenolic-modified PP and maleic-modified PP are found to act as compatibilizers in PP/NBR blends. With increase in concentration of compatibilizers, the domain size of the dispersed NBR phase decreases, followed by a levelling off at higher concentrations, which is an indication of interfacial saturation. The theories of Noolandi and Hong predict a linear decrease of interfacial tension with compatibilizer volume fraction for concentrations less than the *CMC*. Considering the fact that the interfacial tension is directly proportional to the domain size, it is demonstrated that the experimental data are in agreement with these theories. The mechanical properties of the blend are found to increase with the addition of compatibilizers, followed by a levelling off at higher concentration.

ACKNOWLEDGEMENT

The authors are grateful to the University Grants Commission, New Delhi, for financial assistance, and to the authorities of the Central Power Research Institute for providing mixing facilities.

REFERENCES

1 Walker, B. M. (Ed.) 'Handbook of Thermoplastic Elastomers', Van Nonstrand Reinhold, New York, 1979
2 Legge, N. R., Holden, G. and Schoeder, H. E. (Eds) 'Thermoplastic Elastomers – A Comprehensive Review', Hanser Publishers, Munich, 1987
3 Bhowmick, A. K. and Stephens, H. L. (Eds) 'Handbook of Elastomers – New Developments and Technology', Marcel Dekker, New York, 1988
4 De, S. K. and Bhowmick, A. K. (Eds) 'Thermoplastic Elastomers from Rubber – Plastic Blends', Ellis Horwood, New York, 1990
5 Wheelan, A. and Lee, K. S. (Eds) 'Thermoplastic Rubbers in Developments in Rubber Technology', Applied Science Publishers, New York, 1988
6 Kresge, E. N. *J. Appl. Polym. Sci. Appl. Polym. Symp.* 1984, **39**, 37
7 Campbell, D. S., Elliot, D. J. and Wheelans, M. A. *NR Technol.* 1978, **9**, 21
8 Kuriakose, B. and De, S. K. *Polym. Eng. Sci.* 1985, **25**, 630
9 Akhtar, S., De, P. P. and De, S. K. *Mater. Chem. Phys.* 1985, **12**, 235
10 Coran, A. Y., Patel, R. and Williams, D. *Rubber Chem. Technol.* 1982, **55**, 116
11 Coran, A. Y. and Patel, R. *Rubber Chem. Technol.* 1983, **56**, 1045
12 Coran, A. Y., Patel, R. and Williams, D. *Rubber Chem. Technol.* 1985, **58**, 1014
13 Thomas, S., De, S. K. and Gupta, B. R. *Kautschuk + Gummi Kunststoffe* 1987, **40**(7), 665
14 Danesi, S. and Porter, R. S. *Polymer* 1978, **19**, 448
15 Stehling, F. C., Huff, T., Speed, C. S. and Wissler, G. *J. Appl. Polym. Sci.* 1981, **26**, 2693
16 Jancar, J., Di Anselmo, A., Di Benedetto, A. T. and Kucera, J. *Polymer* 1993, **34**, 1684
17 Favis, B. D. *J. Appl. Polym. Sci.* 1990, **39**, 285
18 Paul, D. R. and Newman, S. (Eds) 'Polymer Blends', Academic Press, New York, 1978
19 Olabisi, O., Robeson, L. M. and Shaw, M. T. 'Polymer–Polymer Miscibility', Academic Press, New York, 1978
20 Paul, D. R. and Barlow, G. W. *ACS, Adv. Chem. Ser.* 1979, **176**, 315
21 Molau, G. E. *J. Polym. Sci.* 1965, **A3**, 4235
22 Molau, G. E. and Wittbrodt, W. M. *Macromolecules* 1968, **1**, 260
23 Riess, G., Kohler, J., Tournut, C. and Banderet, A. *Makromol. Chem.* 1967, **101**, 58
24 Riess, G., Kohler, J., Tournut, C. and Banderet, A. *Eur. Polym. J.* 1968, **4**, 187
25 Fayt, R., Jerome, R. and Teyssie, Ph. *J. Polym. Sci., Polym. Phys. Edn* 1982, **20**, 2209
26 Fayt, R., Jerome, R. and Teyssie, Ph. *Polym. Eng. Sci.* 1987, **27**, 328
27 Thomas, S. and Prud'homme, R. E. *Polymer* 1992, **33**, 4260
28 Baker, W. E. and Saleem, M. *Polymer* 1987, **28**, 2057
29 Ide, F. and Hasegawa, A. *J. Appl. Polym. Sci.* 1974, **18**, 963
30 Choudhury, N. R. and Bhowmick, A. K. *J. Appl. Polym. Sci.* 1989, **38**, 1091
31 Cheung, P., Suwanda, D. and Balke, S. T. *Polym. Eng. Sci.* 1990, **30**, 1063
32 Mori, E., Pukanszky, B., Kelen, T. and Tudos, F. *Polym. Bull.* 1984, **12**, 157
33 Ballegooie, Van P. and Rudin, A. *Polym. Eng. Sci.* 1988, **28**, 21
34 Ballegooie, Van P. and Rudin A. *Macromol. Chem.* 1989, **190**, 3153
35 Willis, J. M. and Favis, B. D. *Polym. Eng. Sci.* 1990, **30**, 1073
36 Leibler, L. *Makromol. Chem. Macromol. Symp.* 1985, **16**, 17
37 Leibler, L. *Macromolecules* 1982, **15**, 1283
38 Noolandi, J. *Polym. Eng. Sci.* 1984, **24**, 70
39 Noolandi, J. and Hong, K. M. *Macromolecules* 1982, **15**, 482
40 Noolandi, J. and Hong, K. M. *Macromolecules* 1984, **17**, 1531
41 Liu, N. C., Xie, H. Q. and Baker, W. E. *Polymer* 1993, **34**, 4680
42 Frenkel, R., Duchacek, V., Kirillove, T. and Kuzmin, E. *J. Appl. Polym. Sci.* 1987, **34**, 1301
43 Boder, G. 'Structural Investigations of Polymers', Ellis Horwood, New York, 1991
44 White, J. L. *Polym. Eng. Sci.* 1973, **13**, 46
45 Dao, K. C. *Polymer* 1984, **25**, 1527
46 Heikens, D. and Barentsen, W. M. *Polymer* 1977, **18**, 69
47 Walczak, Z. K. *J. Appl. Polym. Sci.* 1973, **17**, 169
48 Coran, A. Y. 'Handbook of Elastomers – New Development and Technology' (Eds A. K. Bhowmick and H. L. Stephens), Marcel Dekker, New York, 1988, p. 249
49 Martuscelli, E., Silvestre, C. and Abate, G. *Polymer* 1982, **23**, 229
50 Karger-Kocsis, J., Kiss, L. and Kuleznev, V. N. *Int. Polym. Sci. Technol.* 1981, **8**, T/21
51 Thomas, S. *Mater. Lett.* 1987, **5**, 360
52 Nielsen, N. E. *Rheol. Acta* 1974, **13**, 86
53 Halpin, J. C. *J. Compos. Mater.* 1970, **3**, 732
54 Wu, S. *Polym. Eng. Sci.* 1987, **27**, 335
55 Spiros, H. A., Gancarz, I. and Koberstein, J. T. *Macromolecules* 1989, **22**, 1449

56 Fayt, R., Jerome, R. and Teyssie, Ph. *Makromol. Chem.* 1986, **187,** 837
57 Willis, J. M. and Favis, B. D. *Polym. Eng. Sci.* 1988. **28,** 1416
58 Oommen, Z., Thomas, S. and Gopinathan Nair, M. R. *Polym. Eng. Sci.* (in press)
59 Santra, R. N., Samantaray, B. K., Bhowmick, A. K. and Nando, G. B. *J. Appl. Polym. Sci.* 1993, **49,** 1145

Reprinted from

MATERIALS LETTERS

AN INTERDISCIPLINARY JOURNAL AFFILIATED WITH THE **MATERIALS RESEARCH SOCIETY** AND THE **MATERIALS RESEARCH SOCIETY-JAPAN** DEVOTED TO THE RAPID PUBLICATION OF SHORT COMMUNICATIONS ON THE SCIENCE, APPLICATIONS AND PROCESSING OF MATERIALS

Materials Letters 26 (1996) 51–58

Tearing behavior of blends of isotactic polypropylene and nitrile rubber: influence of blend ratio, morphology and compatibilizer loading

Snooppy George [a], L. Prasannakumari [b], Peter Koshy [b], K.T. Varughese [c], Sabu Thomas [a,*]

[a] *School of Chemical Sciences, Mahatma Gandhi University, Priyadarshini Hills P.O., Kottayam 686 560, Kerala, India*
[b] *Regional Research Laboratory, Thiruvananthapuram, India*
[c] *Materials Technology Division, Central Power Research Institute, Bangalore 560 094, India*

Received 11 August 1995; accepted 26 August 1995

N·H
ELSEVIER

MATERIALS LETTERS

An interdisciplinary journal affiliated with the Materials Research Society and the Materials Research Society-Japan devoted to the rapid publication of short communications on the science, applications and processing of materials.
Founding Editor: F.F.Y. Wang

Aims and Scope

Materials Letters is a fast publication journal on the science and technology of materials. The journal provides a rapid communication forum for scientists and engineers engaged in the field of ceramics, metals and alloys, composites and novel materials. The rapid publication of advances in these fields contributes to their further development and stimulates cross-fertilization and interdisciplinary studies. Contributions include, but are not restricted to, a variety of topics such as:

Materials:	Crystalline and amorphous, synthetic superlattices and composites.
Novel materials:	Microstructures, nanostructures, thin films and fullerenes.
Characterization:	Analytical, microscopic, acoustic, optical, spectroscopic and diffractive.
Properties:	Mechanical, magnetic, optical, electrical, interfacial, phase transformational and transport.
Applications:	Structural, opto-electronic, magnetic, smart materials, ferroelectrics, novel semiconductors, environmental materials.
Processing:	Crystal growth, beam processing, sol–gel processing and deformation processing.
Synthesis:	High pressure, powder preparation, explosive forming, rapid quenching, extrusion and milling.

Abstracted/indexed in:
Ceramic Abstracts; Chemical Abstracts; Current Contents; Engineering, Technology & Applied Sciences; EI Compendex Plus; Engineering Index; INSPEC; Metals Abstracts; Physics Briefs.

Subscription Information 1996
Materials Letters is published twelve times per year. For 1996 three volumes (volumes 26–28) have been announced. The subscription price for these volumes is available upon request from the Publisher. Subscriptions are accepted on a prepaid basis only and are entered on a calendar year basis. Issues are sent by SAL (Surface Air Lifted) mail wherever this service is available.

Airmail rates are available upon request. Please address all enquiries regarding orders and subscriptions to:

Elsevier Science B.V.
Order Fullfilment Department
P.O. Box 211, 1000 AE Amsterdam
The Netherlands
Tel. +31 20 4853642, Fax: +31 20 4852598

Claims for issues not received should be made within six months of our publication (mailing) date.

US mailing notice – *Materials Letters* (ISSN 0167-577x) is published monthly by Elsevier Science B.V., P.O. Box 211, 1000 AE Amsterdam, The Netherlands. Annual subscription price in the USA is US$ 863.00 (valid in North, Central and South America only), including air speed delivery. Second class postage paid at Jamaica, NY 11431.
USA POSTMASTERS: Send address changes to Materials Letters, Publications Expediting, Inc., 200 Meacham Avenue, Elmont, NY 11003.
AIRFREIGHT AND MAILING in the USA by Publications Expediting, Inc., 200 Meacham Avenue, Elmont, NY 11003.

⊖ The paper used in this publication meets the requirements of ANSI/NISO 239.48-1992 (Permanence of Paper).

Printed in the Netherlands

ELSEVIER

North-Holland, an imprint of Elsevier Science

MATERIALS LETTERS

An interdisciplinary journal affiliated with the Materials Research Society and the Materials Research Society-Japan devoted to the rapid publication of short communications on the science, applications and processing of materials.
Founding Editor: F.F.Y. Wang

Aims and Scope

Materials Letters is a fast publication journal on the science and technology of materials. The journal provides a rapid communication forum for scientists and engineers engaged in the field of ceramics, metals and alloys, composites and novel materials. The rapid publication of advances in these fields contributes to their further development and stimulates cross-fertilization and interdisciplinary studies. Contributions include, but are not restricted to, a variety of topics such as:

Materials:	Crystalline and amorphous, synthetic superlattices and composites.
Novel materials:	*Microstructures, nanostructures, thin films and fullerenes.*
Characterization:	Analytical, microscopic, acoustic, optical, spectroscopic and diffractive.
Properties:	Mechanical, magnetic, optical, electrical, interfacial, phase transformational and transport.
Applications:	Structural, opto-electronic, magnetic, smart materials, ferroelectrics, novel semiconductors, environmental materials.
Processing:	Crystal growth, beam processing, sol–gel processing and deformation processing.
Synthesis:	High pressure, powder preparation, explosive forming, rapid quenching, extrusion and milling.

Abstracted/indexed in:
Ceramic Abstracts; Chemical Abstracts; Current Contents; Engineering, Technology & Applied Sciences; EI Compendex Plus; Engineering Index; INSPEC; Metals Abstracts; Physics Briefs.

Subscription Information 1996
Materials Letters is published twelve times per year. For 1996 three volumes (volumes 26–28) have been announced. The subscription price for these volumes is available upon request from the Publisher. Subscriptions are accepted on a prepaid basis only and are entered on a calendar year basis. Issues are sent by SAL (Surface Air Lifted) mail wherever this service is available.

Airmail rates are available upon request. Please address all enquiries regarding orders and subscriptions to:

Elsevier Science B.V.
Order Fullfilment Department
P.O. Box 211, 1000 AE Amsterdam
The Netherlands
Tel. +31 20 4853642, Fax: +31 20 4852598

Claims for issues not received should be made within six months of our publication (mailing) date.

US mailing notice – *Materials Letters* (ISSN 0167-577x) is published monthly by Elsevier Science B.V., P.O. Box 211, 1000 AE Amsterdam, The Netherlands. Annual subscription price in the USA is US$ 863.00 (valid in North, Central and South America only), including air speed delivery. Second class postage paid at Jamaica, NY 11431.
USA POSTMASTERS: Send address changes to Materials Letters, Publications Expediting, Inc., 200 Meacham Avenue, Elmont, NY 11003.
AIRFREIGHT AND MAILING in the USA by Publications Expediting, Inc., 200 Meacham Avenue, Elmont, NY 11003.

♾ The paper used in this publication meets the requirements of ANSI/NISO 239.48-1992 (Permanence of Paper).

Printed in the Netherlands

North-Holland, an imprint of Elsevier Science

ELSEVIER

ELSEVIER

January 1996

Materials Letters 26 (1996) 51–58

MATERIALS LETTERS

Tearing behavior of blends of isotactic polypropylene and nitrile rubber: influence of blend ratio, morphology and compatibilizer loading

Snooppy George [a], L. Prasannakumari [b], Peter Koshy [b], K.T. Varughese [c], Sabu Thomas [a,*]

[a] *School of Chemical Sciences, Mahatma Gandhi University, Priyadarshini Hills P.O., Kottayam 686 560, Kerala, India*

[b] *Regional Research Laboratory, Thiruvananthapuram, India*

[c] *Materials Technology Division, Central Power Research Institute, Bangalore 560 094, India*

Received 11 August 1995; accepted 26 August 1995

Abstract

Tearing behavior of blends of isotactic polypropylene (PP) and nitrile rubber (NBR) has been investigated with special reference to the effect of blend ratio and addition of compatibilizing agents. It has been observed that the tear strength of blends depends on the rubber concentration. Attempts have been made to correlate the tear strength with the morphology of the blends. Various composite models such as parallel model, series model, Halpin–Tsai equation and Coran's model have been used to fit the experimental values. The effect of addition of phenolic modified polypropylene (Ph-PP) as a compatibilizer on the tear strength of PP/NBR blend was investigated. The observed increase in tear strength with increase of Ph-PP concentration has been explained in terms of the reduction in particle size of dispersed NBR domains.

Keywords: Polymer blends; Polypropylene; Nitrile rubber; Tearing behavior

1. Introduction

Thermoplastic elastomers (TPEs) prepared by simple blending of a crystalline plastic and an elastomer have gained considerable interest as a class of rapidly growing materials due to their easy preparation and combined properties of thermoplastic and elastomer. Usually, thermoplastic elastomers possess the excellent processing characteristics of thermoplastic materials at higher temperatures and a wide range of physical properties of elastomers at service temperatures [1–5]. However, most of the thermoplastic elastomer blends are found to be incompatible due to the poor interfacial interaction between the homopolymers. These incompatible blends exhibit poor mechanical properties. In such cases it is necessary to compatibilize these blends in order to control the morphology and mechanical properties. Usually, the incompatible blends are compatibilized by the addition of block or graft copolymers or by the in situ formation of copolymers [6]. These block and graft copolymers are found to reduce the surface tension between the homopolymers and thereby improve the interfacial adhesion and mechanical properties [7].

Thermoplastic elastomers from blends of polypropylene (PP) and nitrile rubber (NBR) have gained

* Corresponding author.

SSDI 0167-577x(95)00212-X

much attention due to their easy processability, low density, excellent oil resistance and good mechanical properties. However, these blends are found to be immiscible and incompatible. They are characterized by a coarse morphology, narrow interphase and poor physical and chemical interactions across the phase boundaries. These materials find applications in cables, oil seals, hoses and other molded articles. Recently, the morphology and mechanical properties of these blends have been studied in our laboratory [8]. However, the tearing behavior of these blends has not yet been reported.

Several studies have been reported on the rubber modification of polypropylene. The morphology and mechanical properties of PP/EVA blends have been studied by Thomas and co-workers [9,10]. Kuriakose et al. reported on the NR modification of PP [11]. Blends of polypropylene with ethylene propylene rubbers have been studied by different research groups [12,13]. The mechanical and thermal properties of PP/polybutadiene blends have been reported by Gupta and Ratnam [14]. Coran and Patel [15] reported the technological compatibilization of PP/NBR and PE/NBR blends. They studied the effect of graft copolymer and dynamic vulcanization on the mechanical properties of these blends. Recently, Baker and co-workers [16] studied the effectiveness of various basic functional groups in polypropylene as compatibilizers in a PP/NBR system using morphological and impact property measurements. The thermodynamic and structural aspects of PE/NBR blends have been reported by Frenkel et al. [17].

The major applications of NBR/PP blends are in oil seals, hoses, gaskets, etc. These materials usually undergo tearing action during the course of their application. Therefore, it is important to study the tear resistance of these materials in order to understand the final properties of the material. The role of rubber particles in the mechanism of tear propagation in rubber modified thermoplastics and thermosets has been reported [18–21]. Thomas et al. [10] studied the tear resistance of PP/EVA blends and attempted to correlate the change in tear resistance with the morphology. They also studied the mechanism of tear failure. The tear resistance of the silica filled thermoplastic polypropylene–natural rubber blend was studied by Kuriakose et al. [11].

In this paper we have studied the effect of blend ratio on the tear resistance of PP/NBR blends. The influence of phenolic modified polypropylene as a compatibilizer on the tearing behavior was also investigated. Various composite models have been used to fit the experimental tear resistance values.

2. Experimental

2.1. Materials

Isotactic polypropylene (PP) Koylene M3060 having MFI of 3 g/10 min was supplied by IPCL, Baroda. Nitrile rubber (NBR) having 32% acrylonitrile content was supplied by Synthetics and Chemicals, Bareli, U.P.

Phenolic modified polypropylene (Ph-PP) was prepared by melt mixing polypropylene with dimethylol phenolic resin sp-1045 (4 parts) and stannous chloride (0.8 parts) at 180°C.

2.2. Blend preparation

The blends are denoted by P_0, P_{30}, P_{50}, P_{70} and P_{100}, where the subscripts denote the weight percent of polypropylene in the blend. The blends were prepared in a Brabender plasticorder (Model PLE-330) at a temperature of 180°C. The rotor speed was 60 rpm and the blending was carried out for 6 min. PP was first melted for 2 min in the chamber and then NBR was added and mixing continued for another 6 min. In the case of compatibilized blends the compatibilizers were added to molten PP followed by NBR. The compatibilizer concentrations were varied from 1 to 15 wt%.

2.3. Physical testing of the samples

The samples for tear resistance measurements were prepared by compression molding the samples at 180°C in a hydraulic press into 15 cm × 15 cm × 0.15 cm size sheets. The tear strength of the samples was determined using unnicked 90° angle test pieces at a cross head speed of 500 mm/min in a Zwick Universal Testing machine in accordance with ASTM D624-81.

2.4. Morphology studies

Samples for SEM studies were prepared by cryogenically fracturing the samples in liquid nitrogen. From

: cryogenically fractured samples, the NBR phase .s preferentially extracted with chloroform. The frac-ed end of the sample was kept immersed in chloro-m for two weeks to remove the NBR phase. The ed samples were sputter coated with gold and the otographs were taken in a JEOL scanning electron croscope.

Results and discussion

The physical properties of immiscible polymer nds depend on (1) material properties of rubber and stic phases, (2) rubber–plastic proportions, (3) ase morphology and (4) the interaction at the inter-ase. Fig. 1 shows the tear load–displacement curves PP/NBR blends. Polypropylene tears at a high load d at the smallest displacement. NBR undergoes the gest displacement with the minimum tearing force. e tearing behavior of NBR/PP blends is intermediate tween PP and NBR. As the NBR content in the blend reases the load required to tear the samples decreases d the displacement increases. This increase in dis-acement with rubber content may be due to the reased stretching of rubber particles which bridge matrix crack. From Fig. 1 it is also seen that the odulus of the blends decreases with increase in rubber ntent and this reduction is more pronounced in the se of the P_{30} blend. In PP/EVA blends similar behav-

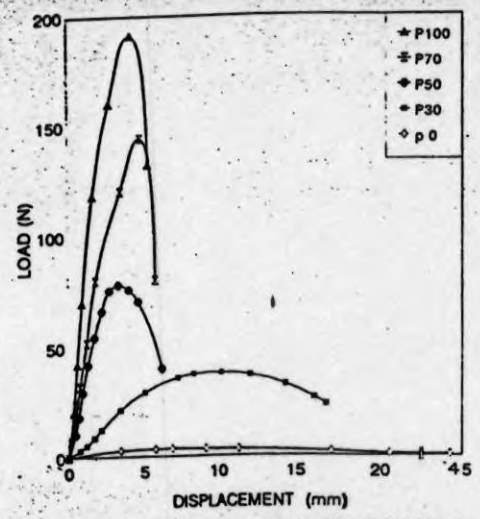

Fig. 1. Tear load–displacement curves of NBR/PP blends.

ior has been reported by Thomas et al. [10]. They correlated this behavior with the morphology of the blends.

The scanning electron micrographs of the PP/NBR blends shown in Fig. 2 indicate the morphology of the blends. With the increasing proportion of NBR, from 30 to 50 wt%, the size of the dispersed NBR phase increased from 5.37 to 17.90 μm. At 70 wt% NBR, NBR also forms a continuous phase resulting in a co-continuous morphology. In our previous publication, we have correlated the mechanical properties such as tensile strength, modulus, elongation at break and impact strength with the morphology of the system [8].

The tear strength values of the blends as a function of weight per cent of NBR are given in Fig. 3. From the figure it is seen that the tear strength of the samples decreases with increase in NBR content. The strength of NBR/PP blends depends on the strength of PP which in turn depends on the extent of crystallinity. Martuscelli and co-workers [22,23] have shown that the spherulitic growth rate of PP is hindered by the presence of rubber particles in blends of PP with rubbers. The decrease in crystallinity of PP/NBR blends with the addition of NBR was reported in our previous paper [8]. Hence the observed drop in tear strength with the addition of NBR is due to the drop in crystallinity of the PP phase and the increase in particle size of the dispersed NBR phase (Fig. 2) with the increase in NBR proportion. The bigger particles of the dispersed phase are unable to bridge the growing crack during tearing. It is also observed that the tear strength composition curve shows a negative deviation after 30 wt% NBR, i.e. the tear strength values lie below the additivity line. This negative deviation is due to the poor interfacial adhesion between the nonpolar PP phase and the polar NBR phase. The tear strength–composition curve shows a change in slope after 50 wt% NBR. This change in slope can be explained in terms of the change in morphology of the blend. In P_{70} and P_{50} blends, NBR is dispersed as domains in the continuous PP matrix, while in P_{30} NBR also forms a continuous phase resulting in a co-continuous morphology. Thus the change in slope of the tear strength–composition curve is due to the phase inversion of NBR from dispersed to continuous.

Composite models such as parallel model, series model, Halpin–Tsai equation and Coran's model have been applied to the PP/NBR system to predict the tear

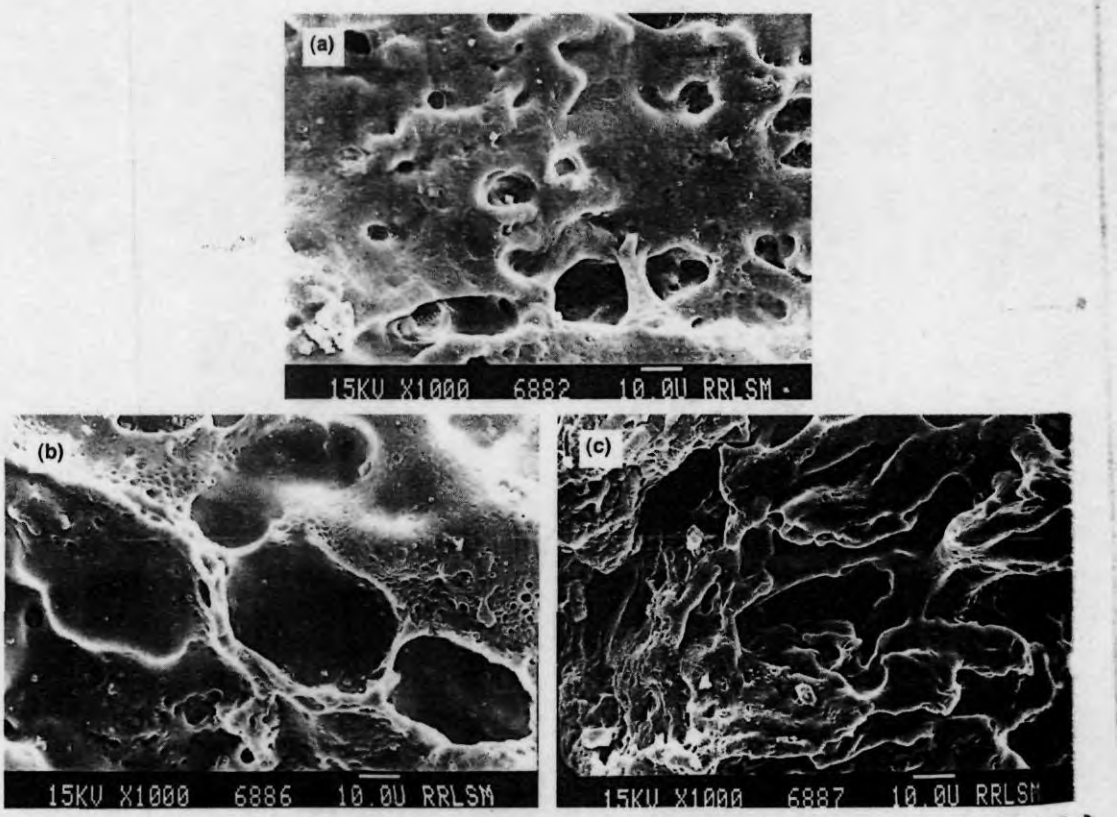

Fig. 2. Scanning electron photomicrograph of NBR/PP blends from which NBR was extracted with chloroform. (a) 30/70 NBR/PP blend: NBR is dispersed as domains in the continuous PP matrix. (b) 50/50 NBR/PP blend: NBR is dispersed as domains in the continuous PP matrix. (c) 70/30 NBR/PP blend with co-continuous morphology.

properties of these blends. In the parallel model, the highest bound tear strength is given by the equation

$$M = M_1\phi_1 + M_2\phi_2, \tag{1}$$

where M is the tear strength of the blend, M_1 and M_2 are the tear strengths of components 1 and 2, respectively, and ϕ_1 and ϕ_2 are the volume fractions of components 1 and 2, respectively. The parallel model is applicable to the systems in which the components are arranged parallel to one another so that an applied stress elongates each component by the same amount. The lowest lower bound series model is found in models in which the components are arranged in series with the applied stress. The equation for this case is

$$1/M = \phi_1/M_1 + \phi_2/M_2. \tag{2}$$

According to the Halpin–Tsai equation [24,25]

$$M_1/M = (1 + A_iB_i\phi_2)/(1 - B_i\phi_2), \tag{3}$$

$$B_i = (M_1/M_2 - 1)/(M_1/M_2 + A_i). \tag{4}$$

The subscripts 1 and 2 refer to the continuous phase and dispersed phase, respectively. The constant A_i is defined by the morphology of the system. For elastomer domains dispersed in a continuous hard matrix $A_i = 0.66$.

The mechanical properties of an incompatible blend are generally in between upper bound parallel model (M_u) and lower bound series model (M_L).

According to Coran's equation

$$M = f(M_u - M_L) + M_L, \tag{5}$$

where f can vary between zero and unity. The value of f is a function of phase morphology. When the soft phase is continuous, f would be low and if the hard phase only is continuous f would be closer to 1.0. In

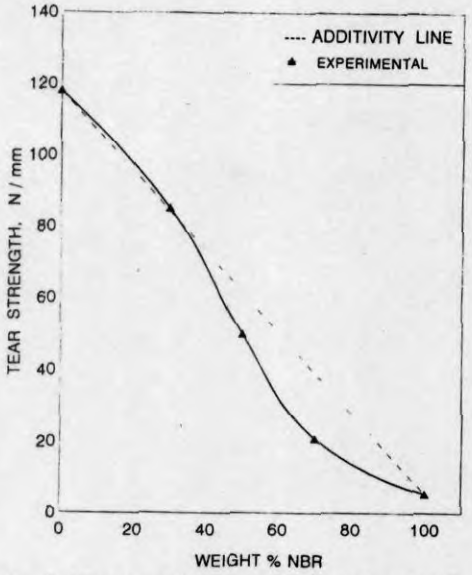

Fig. 3. Effect of weight per cent of NBR on tear strength.

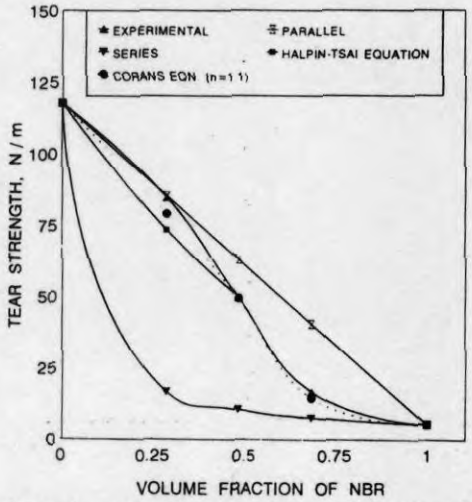

Fig. 4. Experimental and theoretical values of the tear strength as a function of volume fraction of the NBR phase.

the case of interpenetrating phases, f has an intermediate value. The value of f is given by

$$f = V_H^n(nV_S + 1), \quad (6)$$

where n contains the aspects of phase morphology, V_H and V_S are the volume fractions of the hard phase and soft phase, respectively.

Fig. 4 shows the experimental and theoretical curves of tear strength as a function of soft phase volume fraction. It can be seen from Fig. 4 that the experimental data are close to the parallel model and it can be well explained using Coran's model in which the value of $n = 1.1$.

The effect of phenolic modified polypropylene on the tear strength of the 70/30 PP/NBR blend is shown in Fig. 5. It is observed that the tear strength of the blend increases with increase in Ph-PP concentration up to 10 wt% and after that it levels off. It can be noticed that the tear strength of the blend is increased by 50% upon the addition of 10% compatibilizer. The increase in tear strength with Ph-PP concentration is due to the increased interfacial adhesion between the PP and NBR phase and also due to the reduction in particle size of the dispersed NBR phase. The change in tear strength of the blend with Ph-PP concentration can be explained in terms of the morphology of the system. The scanning electron micrographs of 1, 7.5, 10 and 15 wt% Ph-PP compatibilized blends are shown in Figs. 6a, 6b, 6c and 6d, respectively. The SEM photograph of the unmodified blend was already given in Fig. 2a. From the SEM photographs it is observed that the size of the NBR domains decreases with the addition of Ph-PP. The distribution of the particles also became more uniform with the addition of compatibilizers.

Fig. 7 depicts the domain size of NBR particles versus compatibilizer concentration of the 70/30 PP/NBR blend. The average domain size of the unmodified blend is 5.87 μm. The addition of 1 wt% Ph-PP causes a reduction in domain size of 30%. By the addition of

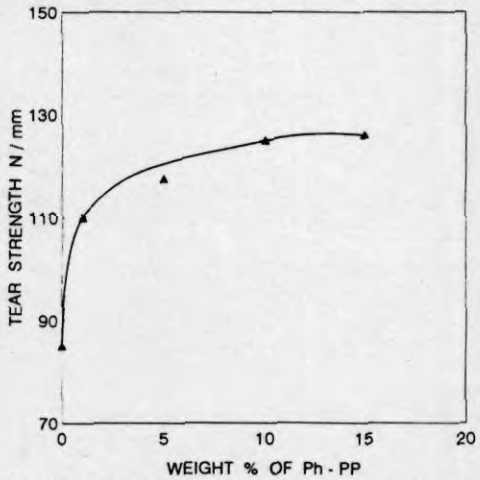

Fig. 5. Effect of Ph-PP concentration on the tear strength of the 30/70 NBR/PP blend.

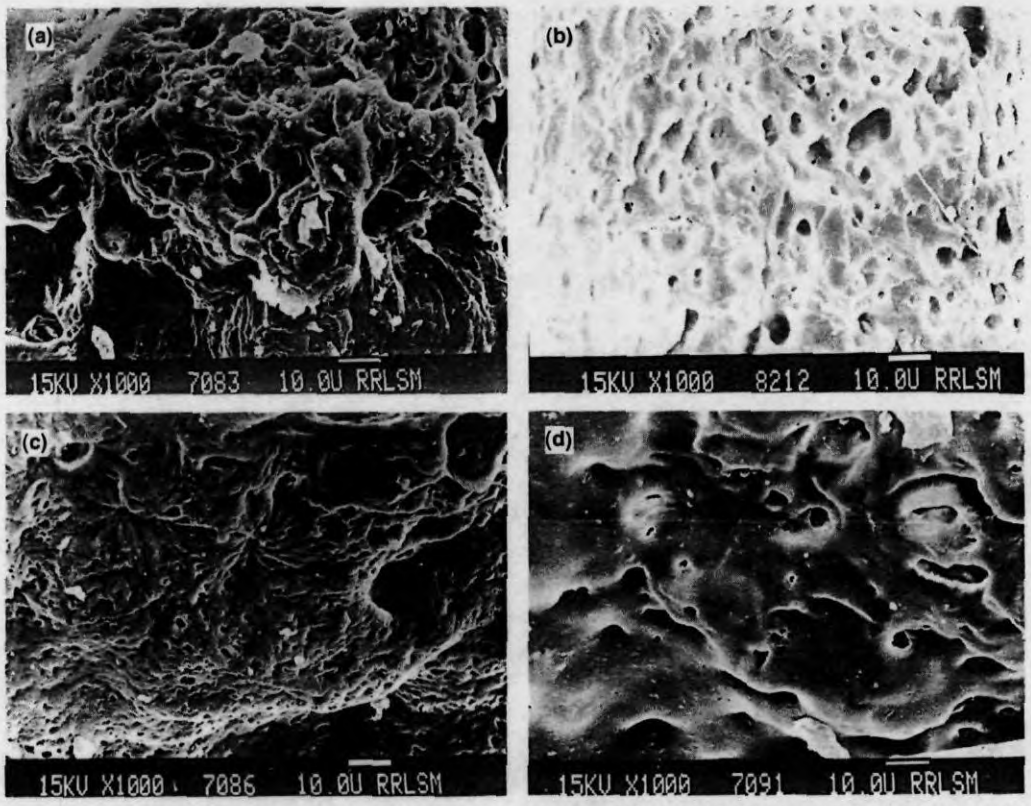

Fig. 6. Scanning electron micrographs of the 30/70 NBR/PP blend compatibilized with Ph-PP. (a) 1% Ph-PP, (b) 7.5% Ph-PP, (c) 10% Ph-PP, (d) 15% Ph-PP.

10 wt% Ph-PP, the domain size is further reduced to 77% of the domain size of the unmodified blend. However, further addition of compatibilizer increases the domain size. This reduction in particle size with the addition of Ph-PP is due to the reduction in interfacial tension between PP and NBR phases and also due to the increased interfacial adhesion. During tearing usually, the rubber particles which bridge the growing crack stretch to large extent before failing [18–21]. The tearing strain of the rubber particles increases with the reduction in particle size. It has been reported that the stretched rubber particles span the crack during crack propagation by acting like little springs between its faces [21]. As the crack is wedged further open, first the larger and then only the smaller particles fail. Thus in the PP/NBR blend, the addition of Ph-PP decreases the domain size of the NBR phase which bridges the growing crack and this reduction in domain size leads to increased stretching of NBR particles during tearing.

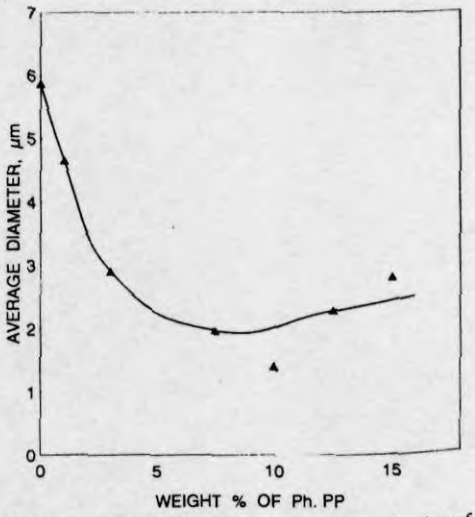

Fig. 7. Effect of Ph-PP concentration on the domain size of the dispersed phase of the 30/70 NBR/PP blend.

Table 1
Mechanical properties of 70/30 PP/NBR blends containing Ph-PP

wt% Ph-PP	Properties	
	tensile strength MPa)	tensile impact strength (J/m)
0	17.7	1013.5
1	18.45	1065
5	18.4	1120
10	20.3	1310
15	20.05	980

Again the increased interfacial adhesion between PP and NBR phases helps to inhibit the propagation of growing crack during tearing. This will obviously increase the tear strength of PP/NBR blends with the addition of Ph-PP. The levelling off observed in the tear strength after 10 wt% of Ph-PP is due to the interfacial saturation. Other mechanical properties like tensile strength and tensile impact strength are also found to increase with increase in Ph-PP content followed by a levelling off at high concentrations of the compatibilizer (Table 1).

The mechanism of compatibilizing action of Ph-PP in PP/NBR blends can be explained as follows. When PP is melt mixed with dimethylol phenolic resin and $SnCl_2$, dimethylol groups are grafted on the PP backbone chain as shown in Fig. 8. When Ph-PP is added to PP/NBR blend, there is a possibility of formation of a graft copolymer between PP and NBR as shown in Fig. 8. This graft copolymer acts as an emulsifier at the interface and thus reduces interfacial tension leading to

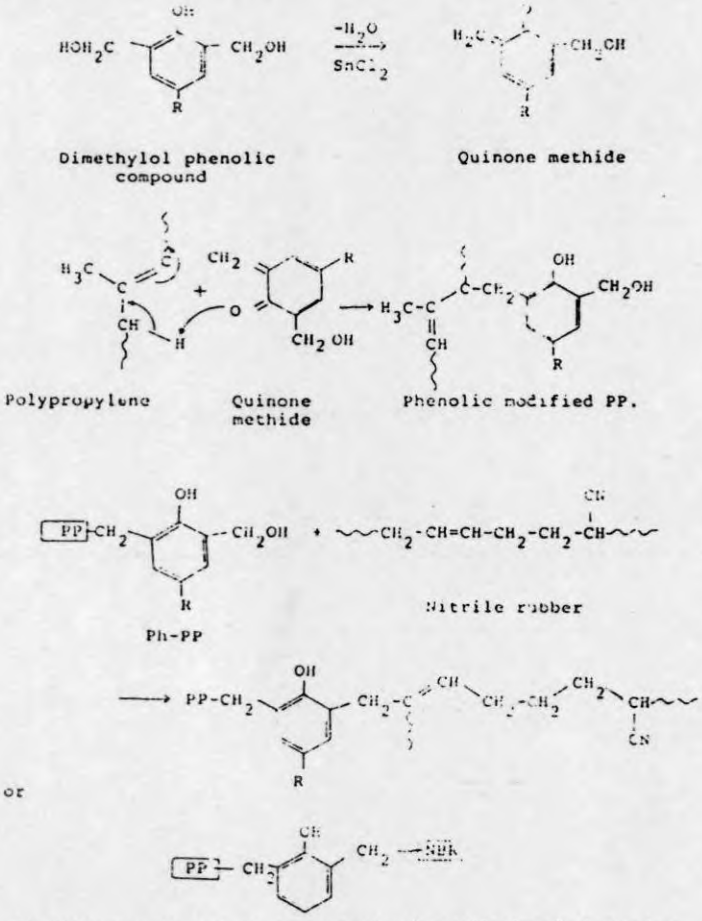

Fig. 8. Reaction scheme for the dimethylolphenolic modification of polypropylene.

small and uniform distribution of the NBR phase as seen in the SEM micrographs. It is also important to mention that Ph-PP can also act as compatibilizer by the dipolar interaction between the dimethylol groups of Ph-PP and polar NBR.

4. Conclusion

The present study indicates that the tear strength of the PP/NBR blends decreases with increase in NBR concentration. The tear strength of the blends depends on the morphology of the blends. The tear strength–composition curve shows a negative deviation from the additivity line. Various composite models have been used to fit the experimental tear strength data. The tear strength of blends could be predicted by Coran's equation. The phenolic modified polypropylene (Ph-PP) is found to act as a compatibilizer in PP/NBR blends. With the increase in Ph-PP concentration, the tear strength increases up to 10 wt% Ph-PP and after that it levels off. The increase in tear strength with Ph-PP concentration is associated with the decrease in the domain size of the NBR phase and the increase in interfacial adhesion.

Acknowledgements

Thanks are due to the University Grants Commission for the financial support of the work.

References

[1] J.C. West and S.L. Cooper, Science and technology of rubber, ed. F.R. Eirich (Academic Press, New York, 1978) ch. 13.
[2] N.R. Legge, G. Holden and H.E. Schoeder, eds., Thermoplastic elastomers – a comprehensive review (Hanser Publishers, Munich, 1987).
[3] A. Wheelan and K.S. Lee, eds., Thermoplastic rubbers in developments in rubber technology (Applied Science Publishers, New York, 1988).
[4] A.K. Bhowmick and H.L. Stephens, eds., Handbook of elastomers – new developments and technology (Dekker, New York, 1988).
[5] S.K. De and A.K. Bhowmick, eds., Thermoplastic elastomers from rubber – plastic blends (Horwood, New York, 1990).
[6] D.R. Paul and S. Newman, eds., Polymer blends (Academic Press, New York, 1978).
[7] D.R. Paul and G.W. Barlow, ACS, Adv. Chem. Ser. 176 (1979), 315.
[8] S. Goerge, R. Joseph, S. Thomas and K.T. Varughese, Polymer, in press.
[9] S. Thomas, S.K. De and B.R. Gupta, Kautschuk + Gummi Kunststoffe 40 (1987) 665.
[10] S. Thomas, B.R. Gupta and S.K. De, J. Mater. Sci. 22 (1987), 3209.
[11] B. Kuriakose and S.K. De, Intern. J. Polym. Mater. 11 (1986) 101.
[12] E.N. Kresge, J. Appl. Polym. Sci. Polym. Symp. 39 (1984) 37.
[13] R. Greco, C. Mancarella, E. Martuscelli, G. Ragosta and J. Jinghua, Polymer 28 (1987) 1929.
[14] A.K. Gupta and B.K. Ratnam, J. Appl. Polym. Sci. 42 (1991) 297.
[15] A.Y. Coran and R. Patel, Rubb. Chem. Technol. 56 (1983) 1045.
[16] N.C. Liu, H.Q. Xie and W.E. Baker, Polymer 34 (1993) 4680.
[17] R. Frenkel, V. Duchacek, T. Kirrillove and E. Kuzmin, J. Appl. Polym. Sci. 34 (1987) 1301.
[18] G.B. Bucknall and R.R. Smith, Polymer 6 (1965) 437.
[19] J.A. Schmitt and H. Keskkula, J. Appl. Polym. Sci. 3 (1960) 132.
[20] W.D. Bascom, R.E. Cottingham, R.L. Jones and P. Peyser, J. Appl. Polym. Sci. 19 (1975) 2545.
[21] S. Kunz Douglass, P.W.R. Beaumont and M.F. Ashby, J. Mater. Sci. 15 (1980) 1109.
[22] E. Martuscelli, C. Silvestre and G. Abate, Polymer 23 (1982) 229.
[23] Z. Bartczak, Z.A. Galeski and E. Martuscelli, Polym. Eng. Sci. 24 (1984) 1155.
[24] N.E. Nielson, Rheol. Acta. 13 (1974) 86.
[25] J.C. Halpin, J. Compos. Mater. 3 (1970) 732.

MATERIALS LETTERS

Instructions to Authors (short version)

(A more detailed version of these instructions is published in the preliminary pages to each volume.)

Submission of papers

Manuscripts (one original + two copies), accompanied by a covering letter, should be sent to one of the Principal Editors, or to a Corresponding Editor (German, Japanese and Russian authors only) indicated on page 2 of the cover. Manuscripts may also be submitted to an Associate Editor whose area of interest covers the contents of the manuscript. For addresses and areas of interest see the List of Associate Editors in the preliminary pages to each volume.

Original material. By submitting a paper for publication in Materials Letters the authors imply that the material has not been published previously nor has been submitted for publication elsewhere and that the authors have obtained the necessary authority for publication.

Refereeing. Submitted papers will be refereed and, if necessary, authors may be invited to revise their manuscript. If a submitted paper relies heavily on unpublished material, it would be helpful to have a copy of that material for the use of the referee.

Types of contributions

Letters are intended as brief reports of significant, original and timely research results on the science, applications and processing of materials which warrant rapid publication. In considering a manuscript for publication, particular attention will be given to theoriginality of the research, the desirability of speedy publication, the clarity of the presentation and the validity of the conclusions. There is no strict page limit, however, the length should be suitable for consideration in the letter format, viz. manuscripts should, in general, not exceed 2000 words (8 typewritten pages of text, including the list of authors, abstract, references and figure captions). As proofs will *not* be sent, authors should check their papers carefully before submission.

Manuscript preparation

All manuscripts should be written in good English. The paper copies of the text should be prepared with double line spacing and wide margins, on numbered sheets. See notes opposite on electronic version of manuscripts.

Structure. Please adhere to the following order of presentation: Article title, Author(s), Affiliation(s), Abstract, PACS codes and keywords, Main text, Acknowledgements, Appendices, References, Figure captions, Tables.

Corresponding author. The name, complete postal address, telephone and fax numbers and the e-mail address of the corresponding author should be given on the first page of the manuscript.

Keywords. Please supply up to six keywords of your own choice that describe the content of your article in more details.

References. References to other work should be consecutively numbered in the text using square brackets and listed by number in the Reference list. Please refer to the more detailed instructions for examples.

Illustrations

Illustrations should also be submitted in triplicate: one master set and two sets of copies. The *line drawings* in the master set should be original laser printer or plotter output or drawn in black india ink, with careful lettering, large enough (3–5 mm) to remain legible after reduction for printing. The *photographs* should be originals, with somewhat more contrast than is required in the printed version. They should be unmounted unless part of a composite figure. Any scale markers should be inserted on the photograph, not drawn below it.

Colour plates. Figures may be published in colour, if this is judged essential by the Editor. The Publisher and the author will each bear part of the extra costs involved. Further information is available from the Publisher.

After acceptance

Notification. You will be notified by the Editor of the journal of the acceptance of your article and invited to supply an electronic version of the accepted text, if this is not already available.

Copyright transfer. You will be asked to transfer the copyright of the article to the Publisher. This transfer will ensure the widest possible dissemination of information.

No proofs. In order to speed up publication, all proofreading will be done by the Publisher and proofs are *not* sent to the author(s).

Electronic manuscripts

The Publisher welcomes the receipt of an electronic version of your accepted manuscript. If you have not already supplied the final, revised version of your article (on diskette) to the journal Editor, you are requested herewith to send a file with the text of the accepted manuscript directly to the Publisher by e-mail or on diskette (allowed formats 3.5″ or 5.25″ MS-DOS, or 3.5″ Macintosh) to the address given below. Please note that no deviations from the version accepted by the Editor of the journal are permissible without the prior and explicit approval by the Editor. Such changes should be clearly indicated on an accompanying printout of the file.

Author benefits

No page charges. Publishing in Materials Letters is free.

Free offprints. The corresponding author will receive 50 offprints free of charge. An offprint order form will be supplied by the publisher for ordering any additional paid offprints.

Discount. Contributors to Elsevier Science journals are entitled to a 30% discount on all Elsevier Science books.

Contents Alert. Materials Letters is included in Elsevier's prepublication service CoDAS.

Further information (after acceptance)

Elsevier Science B.V., Materials Letters
Desk Editorial Department
P.O. Box 103, 1000 AC Amsterdam,
The Netherlands
Tel.: +31 20 4852651
Fax: +31 20 4852319
E-mail: NHPDESKED@ELSEVIER.NL

ELSEVIER

North-Holland, an imprint of Elsevier Science

1994 PHYSICS and MATERIALS SCIENCE JOURNALS

Applied Surface Science
Volumes 72-81 in 40 issues. Price: US $ 2114.00 / Dfl. 3910.00

Astroparticle Physics
Volume 2 in 4 issues. Price: US $ 182.00 / Dfl. 336.00

Computational Materials Science
Volume 2 in 4 issues. Price: US $ 211.00 / Dfl. 391.00

Computer Physics Communications
Volumes 79-85 in 21 issues. Price: US $ 2236.00 / Dfl. 4137.00

International Journal of Applied Electromagnetics in Materials
Volume 5 in 4 issues. Price: US $ 203.00 / Dfl. 376.00

Journal of Crystal Growth
Volumes 135-145 in 44 issues. Price: US $ 4822.00 / Dfl. 8921.00

Journal of Geometry and Physics
Volumes 13 and 14 in 8 issues. Price: US $ 358.00 / Dfl. 662.00

Journal of Luminescence
Volumes 59-62 in 24 issues. Price: US $ 1083.00 / Dfl. 2004.00

Journal of Magnetism and Magnetic Materials
Volumes 126-137 in 36 issues. Price: US $ 3347.00 / Dfl. 6192.00

Journal of Non-Crystalline Solids
Volumes 162-176 in 45 issues. Price: US $ 3535.00 / Dfl. 6540.00

Journal of Nuclear Materials
Volumes 206-216 in 33 issues. Price: US $ 3098.00 / Dfl. 5731.00

Materials Letters
Volumes 19-22 in 24 issues. Price: US $ 899.00 / Dfl. 1664.00

Nuclear Instruments and Methods in Physics Research - Section A
Accelerators, Spectrometers, Detectors & Associated Equipment
Volumes 337-351 in 45 issues. Price: US $ 5441.00 / Dfl. 10,065.00

Nuclear Instruments and Methods in Physics Research - Section B
Beam Interactions with Materials and Atoms
Volumes 83-94 in 48 issues. Price: US $ 4352.00 / Dfl. 8052.00
Reduced combined 1994 subscription price to Nuclear Instruments and Methods - A and B: US $ 9063.00 / Dfl. 16,767.00

Nuclear Physics A
Volumes 566-580 in 60 issues. Price: US $ 4792.00 / Dfl. 8865.00

Nuclear Physics B
Volumes 409-432 in 72 issues. Price: US $ 7537.00 / Dfl. 13,944.00

Nuclear Physics B - Proceedings Supplements
Volumes 34-38 in 15 issues. Price: US $ 881.00 / Dfl. 1630.00
Reduced combined 1994 subscription price to
Nuclear Physics A + Nuclear Physics B + NPB-Proceedings Supplements: US $ 11,202.00 / Dfl. 20,724.00

Optical Materials
Volume 3 in 4 issues. Price: US $ 206.00 / Dfl. 381.00

Optics Communications
Volumes 103-111 in 54 issues. Price: US $ 2121.00 / Dfl. 3924.00

Physica A - Statistical and Theoretical Physics
Volumes 201-211 in 44 issues. Price: US $ 2503.00 / Dfl. 4631.00*

Physica B - Condensed Matter Physics
Volumes 192-202 in 44 issues. Price: US $ 2503.00 / Dfl. 4631.00*

Physica C - Superconductivity
*Volumes 219-236 in 72 issues. Price: US $ 4096.00 / Dfl. 7578.00**

Physica D - Nonlinear Phenomena
Volumes 70-78 in 36 issues. Price: US $ 2048.00 / Dfl. 3789.00*

**Reduced rates are available for combined subscriptions to Physica: please contact the publisher for details.*

Physics Letters A
Volumes 185-197 in 78 issues. Price: US $ 2537.00 / Dfl. 4693.00

Physics Letters B
Volumes 317-340 in 96 issues. Price: US $ 4683.00 / Dfl. 8664.00

Physics Reports
Volumes 240-251 in 72 issues. Price: US $ 2342.00 / Dfl. 4332.00
Reduced combined 1994 subscription price to Physics Letters A, *Physics Letters B + Physics Reports*: US $ 8502.00 / Dfl. 15,729.00

Solid State Ionics
Volumes 68-76 in 36 issues. Price: US $ 1805.00 / Dfl. 3339.00

Surface Science
(including Surface Science Letters)
Volumes 296-318 in 69 issues. Price: US $ 6104.00 / Dfl. 11,293.00

Surface Science Reports
Volume 18-20 in 24 issues. Price: US $ 618.00 / Dfl. 1143.00
Reduced combined 1994 subscription price to Surface Science (including Surface Science Letters), Applied Surface Science and Surface Science Reports: US $ 8192.00 / Dfl. 15,156.00

Ultramicroscopy
Volumes 52-56 in 20 issues. Price: US $ 1151.00 / Dfl. 2130.00

Dutch Guilder price(s) quoted applies worldwide, except in the Americas (North, Central and South America). US Dollar price(s) quoted applies in the Americas only. Journals are sent by Surface Mail to all countries except to the following where Air Delivery via SAL mail is ensured at no extra cost to the subscriber: Argentina, Australia/New Zealand, Brazil, Hong Kong, India, Israel, Japan, Malaysia, Mexico, Pakistan, P.R. China, Singapore, S. Africa, S. Korea, Taiwan, Thailand, USA & Canada. Customers in the European Community should add the appropriate VAT rate applicable in their country to the price(s).

ELSEVIER SCIENCE

ELSEVIER SCIENCE B.V.

P.O. Box 103, 1000 AC Amsterdam, The Netherlands

Elsevier Science Inc., Journal Information Center, PO Box 882, Madison Square Station, New York, NY 10159, U.S.A.

415/j/jnls.chp

Dynamic Mechanical Properties of Isotactic Polypropylene/ Nitrile Rubber Blends: Effects of Blend Ratio, Reactive Compatibilization, and Dynamic Vulcanization

SNOOPPY GEORGE, N. R. NEELAKANTAN,* K. T. VARUGHESE,† SABU THOMAS

School of Chemical Sciences, Mahatma Gandhi University, Priyadarshini Hills, P.O., Kottayam-686 560, Kerala, India

Received 11 December 1996; revised 7 April 1997; accepted 25 April 1997

ABSTRACT: The effect of blend ratio and compatibilization on dynamic mechanical properties of PP/NBR blends was investigated at different temperatures. The storage modulus of the blend decreased with increase in rubber content and shows two T_g's indicating the incompatibility of the system. Various composite models have been used to predict the experimental viscoelastic data. The Takayanagi model fit well with the experimental values. The addition of phenolic modified polypropylene (Ph–PP) and maleic modified polypropylene (MA–PP) improved the storage modulus of the blend at lower temperatures. The enhancement in storage modulus was correlated with the change in domain size of dispersed NBR particles. The effect of dynamic vulcanization using sulfur, peroxide, and mixed system on viscoelastic behavior was also studied. Among these peroxide system shows the highest modulus. © 1997 John Wiley & Sons, Inc. J Polym Sci B: Polym Phys **35:** 2309–2327, 1997

Keywords: polypropylene; nitrile rubber; compatibilization; dynamic vulcanization; dynamic mechanical properties

INTRODUCTION

Polypropylene is a versatile polymer widely used in many consumer and engineering applications. Its area of application has been extended by blending with other polymers. By the blending of two polymers it is possible to tailor their individual properties in a single material. Several studies have been reported on the modification of polypropylene using different rubbers and plastics.[1–5] Blends of polypropylene with rubbers have gained serious attention because they possess the processing characteristics and mechanical properties of polypropylene and the flexibility of rubbers.[6] The polypropylene/ethylene–propylene–diene terpolymer (EPDM)[7,8] system is one of the systems widely studied. The other systems investigated are polypropylene/ethylene-*co*-vinyl acetate (PP/EVA),[9] polypropylene/butyl rubber (PP/BR),[10] polypropylene/natural rubber (PP/NR),[11] etc.

Although it is possible to combine the properties of two or more polymers in a single material by blending, many of the polymer pairs are immiscible and incompatible. This leads to poor mechanical properties. However, the properties of these polymer blends can be improved by the addition of compatibilizers or emulsifying agents.[12] A suitably chosen compatibilizer will locate at the interface between the two components and thereby reduce the interfacial tension and improve the interfacial adhesion and mechanical properties. The effects of compatibilization on the properties of binary blends have been widely investigated. Recently, Thomas and co-workers[13–16] investigated the effect of compatibilization using copolymers and modified polymers in different

* *Present address:* Indian Institute of Technology, Chennai-36

† *Present address:* Materials Technology Division, Central Power Research Institute, Bangalore-560 094, India

Correspondence to: S. Thomas

Journal of Polymer Science: Part B: Polymer Physics, Vol. 35, 2309–2327 (1997)

CCC 0887-6266/97/142309-19

polymer blends. For example, they found that the addition of natural rubber-graft-polymethyl methacrylate (NR-*g*-PMMA) and natural rubber-graft-polystyrene (NR-*g*-PS) as compatibilizers in PMMA/NR and PS/NR blends, respectively, leads to fine and uniform distribution of the minor phase in the major matrix polymer. They have also reported on the influence of molecular weight of homo- and copolymers and mode of addition on the properties of the blends.

Miscibility between two polymers is usually characterized by dynamic mechanical analysis or viscoelastic data. The viscoelastic properties like storage modulus, loss modulus, and loss tangent of polymer depend on structure, crystallinity, extent of crosslinking, etc.[17] Karger–Kocsis and Kiss[18] have investigated the effect of morphology on the dynamic mechanical properties of PP/EPDM blends. They have found that the storage modulus (E') of blends decreases with increasing concentration of EPDM. But these blends are incompatible and have a two-phase morphology because of the presence of two separate damping peaks of blend components remaining at their original positions in the dynamic mechanical spectrum. Influence of microstructure on the viscoelastic behavior of polycarbonate/styrene acrylonitrile copolymer (PC/SAN) blend has been studied by McLaughlin[19] and Guest and Daly.[20] The compatibility of polycarbonate with polystyrene and polyester was investigated by Li et al.[21] using dynamic mechanical and DSC measurements. Their investigations indicated that the polystyrene/PC system is partially miscible because the T_g values corresponding to PC and PS are composition dependent. Wippler[22] reported on the dynamic mechanical properties of PC/PE blends. They have used the Takayanagi model to predict the behavior of experimental storage modulus.

The effect of polychloroprene (CR) content on the storage moduli of ABS was reported by Kang et al.[23] They found that the storage moduli of the blends increase with increase in the CR content. Recently, in this laboratory the influence of blend composition on the viscoelastic properties of NR–EVA and NBR–EVA blends has been investigated.[24,25] The damping factors of these blends are found to increase with increase in rubber content, and correlated with the phase morphology of the system.

The miscibility of poly(vinyl chloride) (PVC) with 50% epoxidized natural rubber (ENR) was investigated by Varughese et al.[26] using dynamic mechanical and DSC measurements. These blends showed a single T_g lying between the T_gs of pure components, which indicated the miscibility of the system. They also found that a moderate level of broadening of the glass transition temperature region occurs with increasing PVC concentration.

The effect of compatibilization on the dynamic mechanical properties of various polymer blends have been reported. The effect of diblock copolymers on the dynamic mechanical properties of polyethylene/polystyrene (PE/PS) blend has been reported by Brahimi et al.[27] Their investigations indicated that the addition of pure and tapered diblock copolymers enhances the phase dispersion and interphase interactions of the blends and that the addition of excess copolymers create micelles. Ramesh and De[28] investigated the effect of carboxylated nitrile rubber as a reactive compatibilizer in PVC/ENR blends in terms of dynamic mechanical data. The DMA results indicated that an immiscible composition of PVC/ENR blends becomes progressively miscible by the addition of XNBR. The effect of addition of ethylene–methyl acrylate copolymer as a compatibilizer in LDPE/PDMS blends was investigated by Santra et al.[29] The T_g values corresponding to the homopolymers shifted by the addition of a compatibilizer. Holsti–Miettinen and co-workers[30] investigated the dynamic mechanical properties of PA6/PP/SEBS-*g*-MA ternary blends. Cohen and Ramos[31] have used the mechanical model of Takayanagi to describe the viscoelastic behavior of binary and ternary blends of *cis*-1,4-polyisoprene, 1,4-polybutadiene, and the polyisoprene–polybutadiene block copolymer.

The effect of dynamic vulcanization on the dynamic mechanical properties of polymer blends has been reported. Kuriakose et al.[32] investigated the effect of dynamic vulcanization of PP/NR blends on the viscoelastic properties. They found that the increase in storage modulus and decrease in loss modulus becomes more remarkable as the extent of crosslinking increases. Thomas et al.[24] investigated the effect of dynamic vulcanization on the dynamic mechanical properties of NR/EVA blends. The damping behavior of dynamically cured butyl rubber/polypropylene blends was investigated by Liao et al.[33] They found that the damping characteristics of the dynamically cured BR/PP blend depend on the blend composition and the curative level. The dynamic mechanical properties of dynamically vulcanized PVC/ENR blends were investigated by Varughese et al.[34]

These blends upon dimaleimide vulcanization showed a lowering in storage and loss moduli in the glassy zone. The damping peak became narrow upon dynamic vulcanization.

Blends of polypropylene (PP) and nitrile rubber (NBR) possess the hot oil-resistant properties of NBR and the excellent processability and mechanical properties of polypropylene. However, these blends are incompatible with poor physical and chemical interactions across the phase boundaries. Hence, this system requires compatibilization to improve the properties. The effect of phenolic-modified polypropylene and maleic anhydride-modified polypropylene as compatibilizers on the properties of PP/NBR blends was investigated.[16,35] However, no systematic study has been reported on the viscoelastic properties of the PP/NBR blends. In many practical applications, because these materials usually undergo cyclic stressing, the study of viscoelastic properties are very important.

In this article we have investigated the effect of blend composition and morphology on the dynamic mechanical properties of the PP/NBR blends. The effect of compatibilizer concentration and dynamic vulcanization was also investigated. The dynamic mechanical properties have been correlated with the morphology of the blend. Attempts have also been made to predict the experimental dynamic mechanical properties using existing theoretical models.

EXPERIMENTAL

Materials

Isotactic polypropylene (PP) Koylene M 3060 having MFI of 3 g/10 min was supplied by IPCL, Baroda. Nitrile rubber (NBR) having 32% acrylonitrile content was supplied by Synthetic and Chemicals, Bareli, UP.

Maleic anhydride-modified polypropylene was prepared by melt mixing PP with maleic anhydride (5 parts), dicumyl peroxide (DiCUP) (3 parts), and benzoquinone (0.75 parts) at 180°C. Phenolic-modified polypropylene was prepared by melt mixing PP with dimethylol phenolic resin SP-1045 (4 parts) and stannous chloride (0.8 parts) at 180°C.[16]

Blend Preparation

The blends were prepared in a Brabender plasticorder (PLE-330) at a temperature of 180°C.

Table I.

Ingredients	Sulfur System	DiCUP System	Mixed System
PP	70	70	70
NBR	30	30	30
ZnO	5	—	5
Stearic acid	2	—	2
CBS*	2	—	2
TMTD†	2.5	—	2.5
S	0.2	—	0.1
DiCUP‡	—	2	1.0

* *N*-cyclohexyl benzothiazyl sulfenamide.
† Tetramethyl thiuram disulfide.
‡ Dicumyl peroxide.

The rotor speed was 60 rpm and the blending was carried out for 6 min. PP was first melted for 2 min in the chamber and then NBR was added and mixing continued for another 6 min. In the case of compatibilized blends, the compatibilizers were added prior to the addition of NBR. The binary blends are designated as P_0, P_{30}, P_{50}, P_{70}, and P_{100}, where the subscripts denote the weight percentage of polypropylene in the blend. Dynamic vulcanization of P_{70} blend was done by using three crosslinking systems, sulfur, peroxide, and a mixed system consisting of sulfur and peroxide. The recipe used for dynamic vulcanization is given in Table I.

Morphology Studies

Samples for SEM studies were prepared by cryogenically fracturing the samples in liquid nitrogen. From the cryogenically fractured samples, the NBR phase was preferentially extracted with chloroform. The dried samples were sputter coated with gold and the photographs were taken on a JEOL scanning electron microscope.

Dynamic Mechanical Testing

The dynamic mechanical properties of the blends were measured using a Rheovibron DDV at a frequency of 35 Hz. Compression molded samples of dimensions $5 \times 0.5 \times 0.05$ cm^3 were used for testing. The temperature range used was from -50 to $+150$°C.

RESULTS AND DISCUSSION

Binary Blends

The dynamic mechanical properties such as storage modulus (E'), loss modulus (E''), and damp-

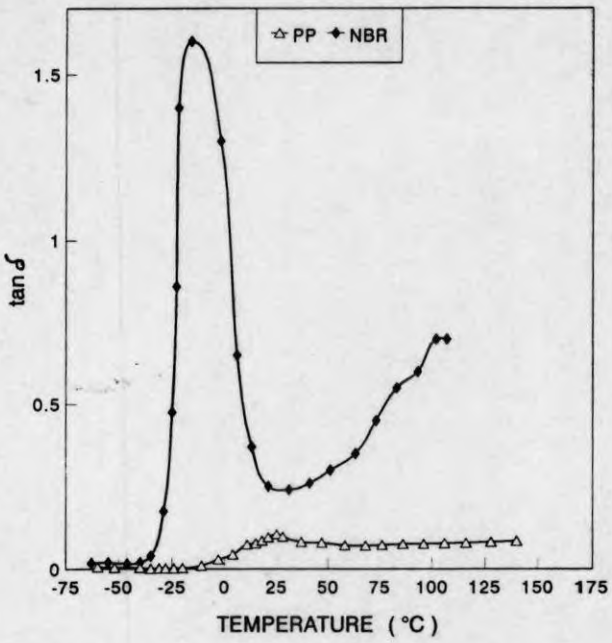

Figure 1. Variation of tan δ of PP and NBR with temperature.

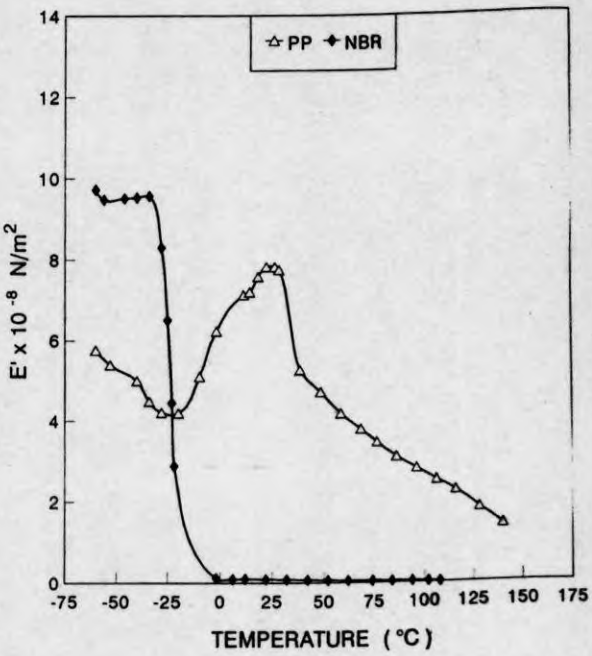

Figure 3. Variation of storage modulus (E') of PP and NBR with temperature.

ing (tan δ) of the pure components and the blends were evaluated from −50 to 150°C. Figures 1–3 show the variation of tan δ, E'', and E' Vs temperature for the homopolymers. The tan δ curve of nitrile rubber shows a peak at −16°C due to the α-transition arising from the segmental motion. This corresponds to the glass transition temperature (T_g) of nitrile rubber. Polypropylene shows the glass transition temperature at 25°C, as shown by a tan δ peak at 25°C in the tan δ Vs temperature curve. Nitrile rubber has higher damping than polypropylene because of its rubbery nature. The loss modulus (E'') curve also shows the presence of loss maximum for NBR and PP at −20 and 25°C, respectively (Fig. 2). Nitrile rubber has higher storage modulus than polypropylene below the T_g region, and the trend is reversed beyond the relaxation stage. In the case of nitrile rubber, the storage modulus shows a drastic fall around T_g, while for polypropylene, because of its crystalline nature, the modulus drop is at a slower rate. The higher modulus of NBR compared to PP below the transition region is due to the fact that at this stage the entire molecular chains of amorphous NBR is frozen to form a fully glassy state. As NBR undergoes transition from the fully formed glassy to the rubbery state, the storage modulus decreases considerably. In crystalline materials, during transition, only the amorphous part undergoes segmental motion, while the crystalline region remains as solid until its temperature of melting (T_m). Hence, in the case of polypropylene, which is a crystalline material, the storage modulus drops only in a lesser

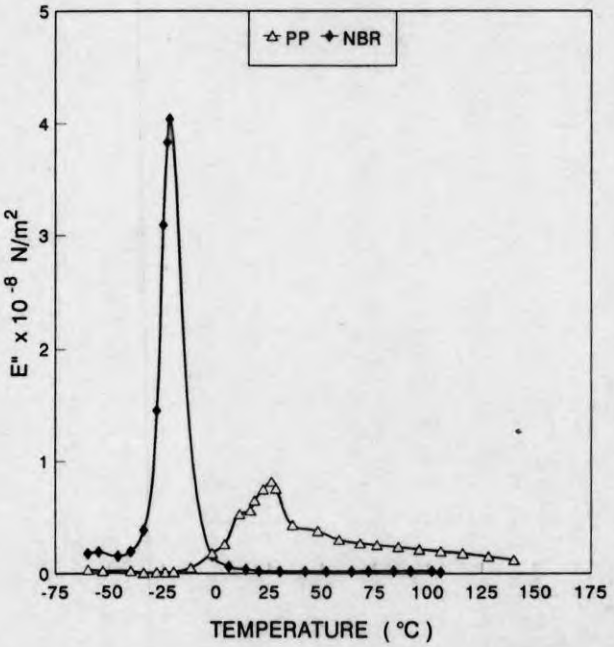

Figure 2. Variation of loss modulus (E'') of PP and NBR with temperature.

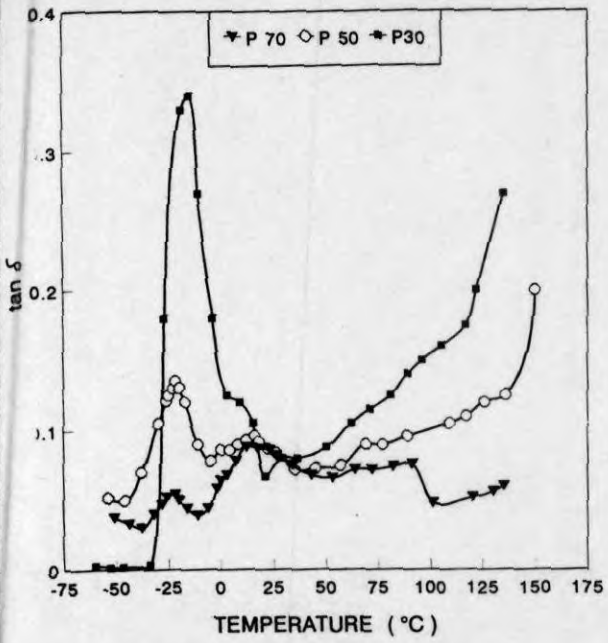

Figure 4. Variation of tan δ of PP/NBR binary blends with temperature.

extent than that in NBR as a result of the relaxation process.

Dynamic mechanical investigation was used to predict the miscibility of the system by various researchers.[26,36–38] Generally, for an incompatible blend, the tan δ Vs temperature curve shows the presence of two tan δ or damping peaks corresponding to the glass transition temperatures of individual polymers.[36] For a highly compatible blend the curve shows only a single peak[26] in between the transition temperatures of the component polymers, whereas broadening of transition occurs in the case of partially compatible system.[38] In the case of compatible and partially compatible blends the T_gs are shifted to higher or lower temperatures as a function of composition. The variation of tan δ with temperature of the PP/NBR blends is shown in Figure 4. The blends show two tan δ peaks around −20 and +20°C, which correspond to the T_gs of nitrile rubber and polypropylene, respectively. Two separate peaks corresponding to the T_gs of PP and NBR indicate that the blends are not compatible. The T_g corresponding to PP component is shifted to a lower temperature upon the addition of NBR. This may be due to the plasticizing effect of NBR, by which the chain mobility of PP is increased. The damping of the blends increases with an increase in the concentration of nitrile rubber. The variation of tan δ_{max} of the blends as a function of NBR content is shown in Figure 5. The increase in the damping and tan δ_{max} with increase in NBR content is due to the reduction in the crystalline volume of the system on increasing the concentration of NBR whose damping is always higher than PP. The variation of tan δ_{max} is more pronounced above 50 wt % NBR. This behavior can be explained in terms of the morphology of the blends. The scanning electron micrographs of the blends P70, P50, and P30 are shown in Figure 6(a), (b), and (c). In P_{70} and P_{50} the NBR phase is dispersed as domains in the continuous PP matrix. As the concentration of NBR increases, the size of the dispersed NBR domains increases. The average domain size of the dispersed NBR domains in P_{70} and P_{50} are 5.87 and 17.90 μm, respectively. In P_{30}, the NBR phase also forms a continuous phase, resulting in a cocontinuous morphology. Because above 50 wt % NBR, the NBR forms a continuous phase, the tan δ_{max} shows a pronounced variation due to the higher contribution of tan δ_{max} from the NBR phase.

The variation of storage modulus E' of various blends as a function of temperature is shown in Figure 7. As in the case of blend components, the modulus of the blends decrease with increase in temperature. It is seen from this figure that the modulus of the blends decreased with increase in the NBR content. At the glassy region E' becomes

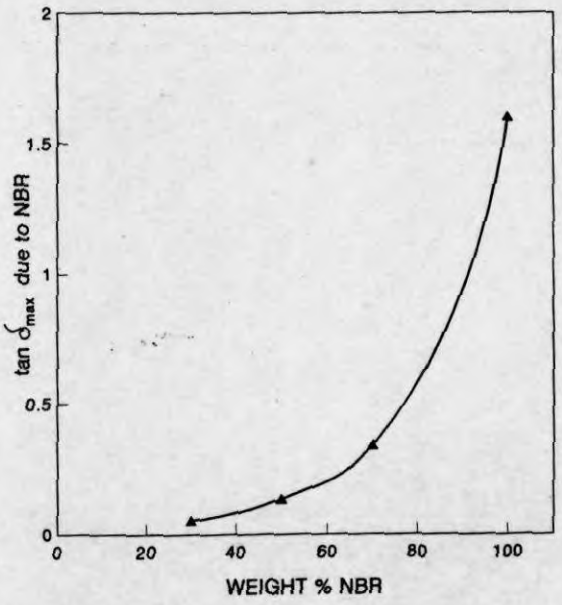

Figure 5. Variation of tan δ_{max} due to NBR of PP/NBR binary blends with wt % of NBR.

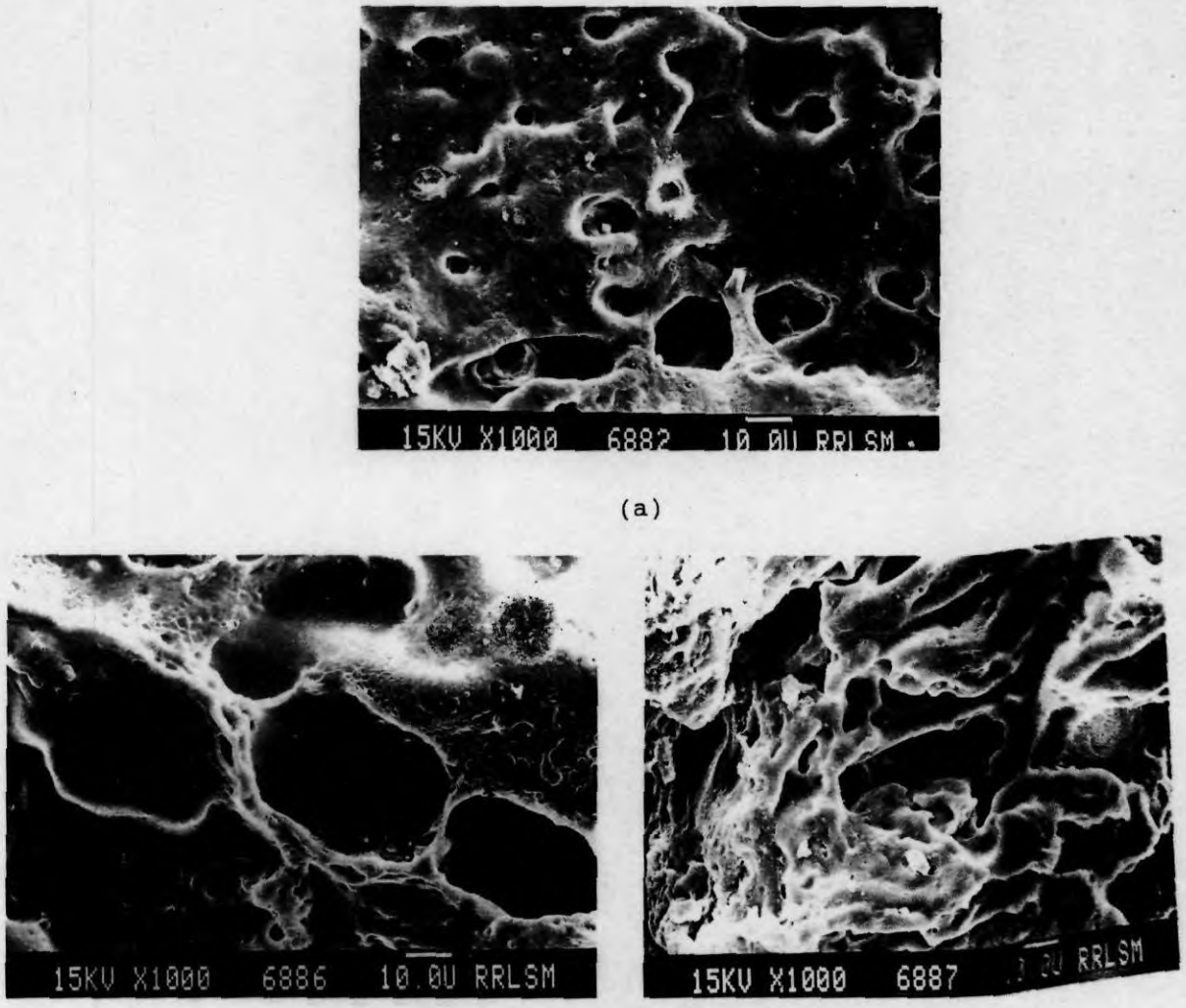

Figure 6. Scanning electron micrographs of the morphology of PP/NBR binary blends (a) 70/30, (b) 50/50, and (c) 30/70 PP/NBR.

higher for the high NBR blends and its value drops down several decades faster above T_g. This behavior can be attributed to the better glass-forming characteristics of NBR with a higher degree of modulus value. Thus, P_{30}, in which NBR is also distributed as a continuous phase, has the higher storage modulus below the transition than the remaining P_{70} and P_{50} blends in which NBR is in the form of a dispersed phase only. Beyond the transition region, E' is higher for low NBR content blends due to the influence of crystalline polymer, PP.

Figure 8 shows the variation of storage modulus at 30°C as a function of NBR content. As we have already discussed, the modulus decrease with the increase in rubber concentration. The curve shows a negative deviation from the additivity line. This negative deviation is due to the lack of interfacial interaction and adhesion between the nonpolar crystalline PP and polar nitrile rubber phases. The curve shows a slope change from P_{50} to P_{30} due to the phase inversion of NBR from the dispersed to continuous phase.

The variation of loss modulus with temperature (Fig. 9) also shows the same trend as that of tan δ, i.e., the curves show two maxima corresponding to the glass transition temperatures of polypropylene and nitrile rubber. The loss modu-

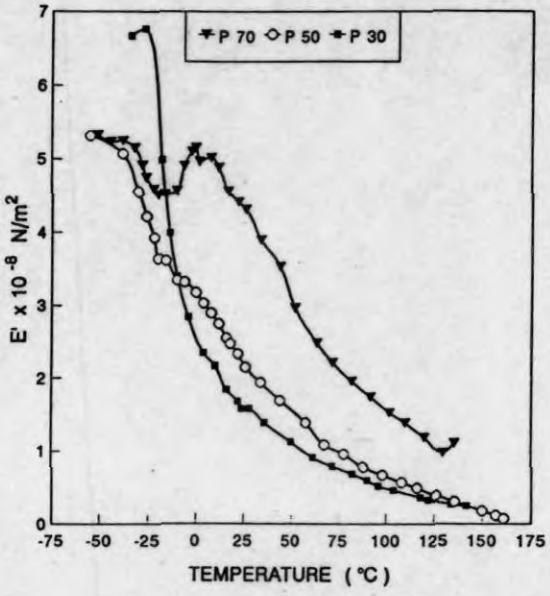

Figure 7. Variation of storage modulus (E') of binary PP/NBR blends with temperature.

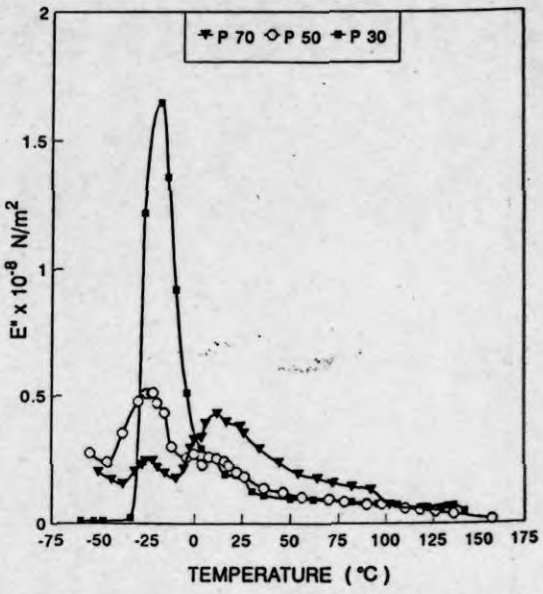

Figure 9. Variation of loss modulus (E'') of binary PP/NBR blends with temperature.

lus also increases with an increase in the NBR content.

Modeling of Viscoelastic Properties

Various composite models such as the parallel model, the series model, the Halpin–Tsai equation, Coran's equation, and Takayanagi's model have been applied to predict the viscoelastic behavior of the binary blends. The upper bound parallel model is given by

$$M = M_1\phi_1 + M_2\phi_2 \qquad (1)$$

where M is property of the composite, M_1 and M_2 are the corresponding properties of component 1 and 2, respectively and ϕ_1 and ϕ_2 are the volume fractions of components 1 and 2, respectively. In a parallel model the components are arranged parallel to one another so that an applied stress elongates each component by the same amount. In the case of the lower bound series model, where the components are arranged in series with the applied stress, the equation is

$$1/M = \phi_1/M_1 + \phi_2/M_2 \qquad (2)$$

According to the Halpin–Tsai[39,40] model, the equation that relates the morphology of the polymer to the properties is,

$$M_1/M = (1 + A_i B_i \phi_2)/(1 - B_i \phi_2) \qquad (3)$$

where

$$B_i = (M_1/M_2 - 1)/(M_1/M_2 + A_i) \qquad (4)$$

In this equation, the subscripts 1 and 2 refer to the continuous phase and dispersed phase, respectively. The constant A_i is determined by the

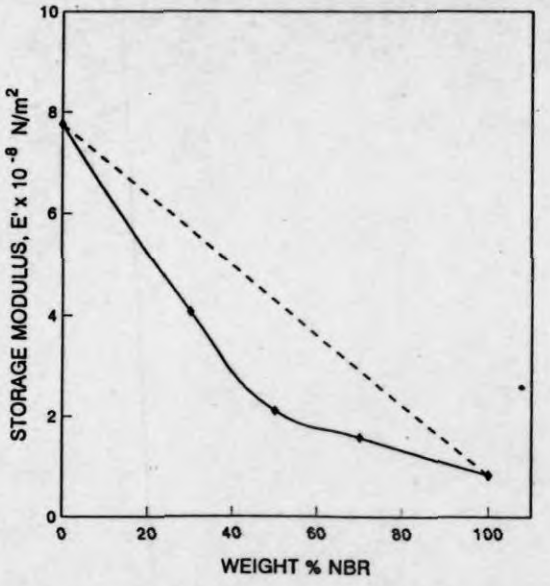

Figure 8. Variation of storage modulus (E') of binary PP/NBR blends with wt % of NBR at 30°C.

morphology of the system. For elastomer domains dispersed in a continuous hard matrix, $A_i = 0.66$.

The properties of an incompatible blend usually are in between upper bound parallel model (M_U) and lower bound series model. According to Coran's equation[41]

$$M = f(M_U - M_L) + M_L \quad (5)$$

where f can vary between zero and unity. The value of f is given by

$$f = V_H^n(nV_S + 1) \quad (6)$$

where n contains the aspects of phase morphology. V_H and V_S are the volume fractions of the hard phase and soft phase, respectively.

The viscoelastic behavior of heterogeneous polymer blends can be predicted using Takayanagi's model. The Takayanagi model is given by[30]

$$E^* = (1 - \lambda)E_M^* + [[(1 - \phi)/E_M^*] + (\phi/E_N^*)]^{-1} \quad (7)$$

where

E_M^* = complex modulus of matrix phase.
E_N^* = complex modulus of the dispersed phase.
$\lambda\phi$ = volume fraction of the dispersed phase and the values of λ and ϕ related to the degree of series-parallel coupling.

As suggested by Cohen and Ramos, the degree of parallel coupling of the model can be expressed by

$$\% \text{ parallel} = [\phi(1 - \lambda)/(1 - \phi\lambda)] \times 100 \quad (8)$$

Figure 10 shows the experimental and theoretical curves of the storage modulus of the PP/NBR blends as a function of NBR volume fraction. As expected, the storage modulus values of these blends lie in between those of the parallel and series models. The experimental values are close to the Halpin–Tsai and Coran models ($n = 2.2$) up to 50 wt % NBR. In the case of the Takayanagi model, which is widely used for the prediction of viscoelastic data, the experimental values can be described with 20% parallel coupling. However, for the P_{30} blend, the experimental values are higher than those obtained from any other theoretical models. This may be due to the fact that

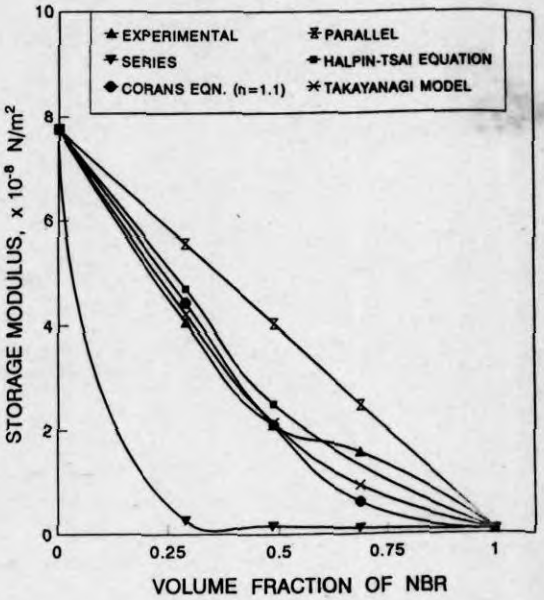

Figure 10. Experimental and theoretical curves o storage modulus of binary PP/NBR blends as a functio of wt % of NBR at 30°C.

all theoretical values are calculated, base on th assumption that NBR phase is dispersed in th continuous PP matrix. But in the case of P_{30}, th NBR also forms a continuous phase leading to cocontinuous morphology of the blend [Fig. 6(c)]

Effect of Compatibilization

The addition of suitably selected compatibilizer to immiscible blends should (1) reduce the in terfacial energy of the phases, (2) permit a fine dispersion while mixing, (3) provide a measure stability against gross phase segregation, and (4 result in improved interfacial adhesion.[42] In poly mer blends the physical properties are always a fected by the resulting morphology of the compat bilized blends.[13,14,27] In this article, we have mad a correlation between phase morphology d namic mechanical properties.

The effect of maleic anhydride-modified poly propylene and phenolic-modified polypropylene compatibilizers on the morphology of the 70/3 PP/NBR blend is shown by the SEM micrograph of Figures 11 and 12, respectively. From the SE micrographs, it is seen that the size of the di persed NBR phase decreases with the additio of compatibilizers. This reduction in part si with the addition of modified polymers is due the reduction in interfacial tension between t

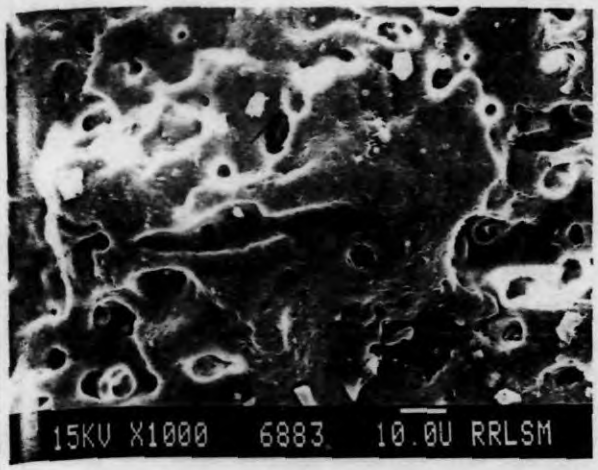

(a)

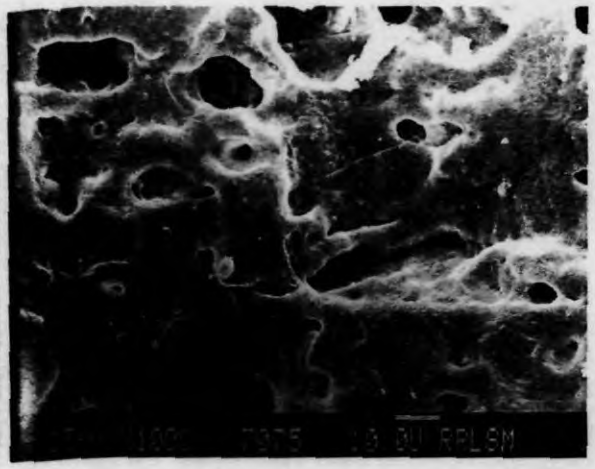

(b)

Figure 11. Scanning electron micrographs of the morphology of MA–PP compatibilized PP/NBR blends with (a) 1 and (b) 10 wt % MA–PP.

dispersed NBR phase and the polypropylene matrix.

The average domain size of the compatibilized blends as a function of the compatibilizer concentration is shown in Figure 13. The average domain size of the unmodified blend is 5.87 μm. In the case of MA–PP compatibilized blends, addition of 1% MA–PP causes a reduction in domain size of 55%. Further addition of MA–PP does not change the domain size considerably, but a leveling off is observed. In Ph–PP compatibilized blends, the average diameter of the dispersed NBR phase decreases up to the addition of 10 wt % Ph–PP. By the addition of 10 wt % Ph–PP, the domain size is reduced by 77% of the domain size of the unmodified blend. However, further addition of a compatibilizer increases the domain size. The equilibrium concentration at which the domain size leveled off can be considered as the so-called critical micelle concentration (CMC), i.e., the concentration at which micelles are formed. The CMC has been estimated by the intersection of the straight lines at the low and high concentration regions.[13,14] The CMC values for MAPP and Ph–PP are 1.5 and 4.5%, respectively. The CMC value indicates the critical amount of compatibilizer required to saturate the unit volume of the interface. The increase in domain size above CMC may be due to the formation of micelles of the compatibilizer at the continuous polypropylene phase. This is schematically shown in Figure 14. As the micelle formation starts, some of the compatibilizer already at the interface leaves the interface. This leads to an increase in domain size. Several authors have reported on the interfacial saturation of binary polymer blends by the addition of compatibilizers.[43–45] Thomas and Prud'homme[45] reported that in PS/PMMA blends at lower concentrations of the copolymer, the dispersed phase size decreases linearly with increasing copolymer concentration, whereas at a higher concentration it leveled off. Noolandi and Hong[46,47] theoretically predicted that there is a critical concentration of block copolymer at which micelles are formed in the homopolymer phases. All the above experimental observations including the present study and theoretical predictions of Noolandi and Hong suggest that there is a critical concentration of compatibilizer required to saturate the interface of a binary blend. The compatibilizer concentration above this critical concentration may not modify the interface any more, but forms compatibilizer micelles at the bulk phase.

The theories of Noolandi and Hong can be applied to these highly incompatible PP/NBR blends for concentrations less than CMC. According to them, the interfacial tension is expected to decrease linearly with the addition of the compatibilizer below CMC, and above the CMC a leveling off is expected. The expression for interfacial tension reduction ($\Delta\nu$) in a binary blend A/B upon the addition of the divalent copolymer A-b-B is given by[47]

$$\Delta\nu = d\phi_c[(1/2\chi + 1/Z_c) - 1/Z_c\exp(Z_c\chi/2)] \quad (9)$$

where d is the width at half height of the copoly-

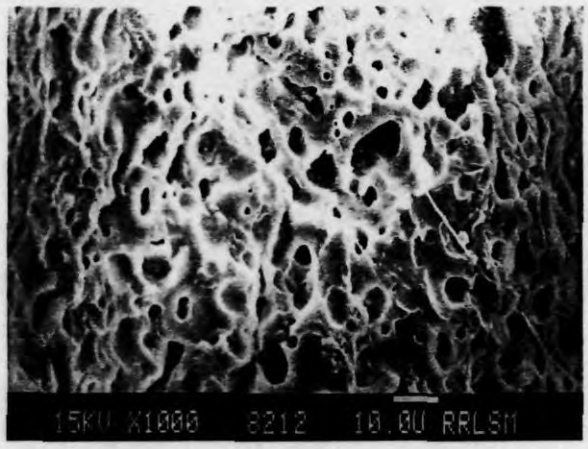

(a)

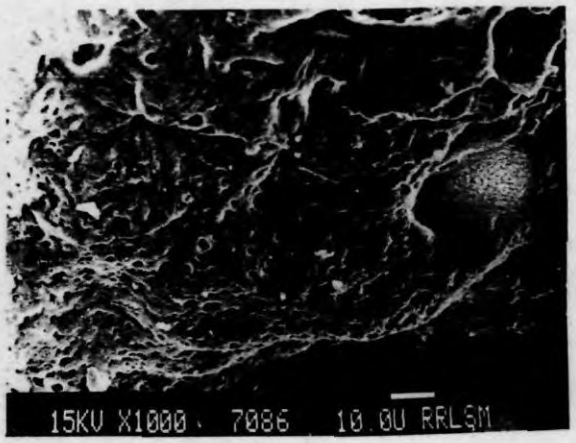

(b) (c)

Figure 12. Scanning electron micrographs of the morphology of Ph–PP compatibilized PP/NBR blends with (a) 3, (b) 7.5, and (c) 10 wt % Ph–PP.

mer profile by the Kuhn statistical segment length, ϕ_c is the bulk volume fraction of the copolymer in the system. χ is the Flory–Huggins interaction parameter between the A and B segments of the copolymer, and Z_c is the degree of polymerization of the copolymer. According to this equation, the plot of interfacial tension reduction vs. ϕ_c should yield a straight line. Although this theory was developed for the action of symmetrical diblock copolymer A-b-B in incompatible binary systems (A/B), this theory can be successfully applied to other systems, in which the compatibilizing action is not strictly by the addition of symmetrical block copolymers.[14] Because interfacial tension reduction is directly proportional to the particle size reduction as suggested by Wu,[48] we can replace the interfacial tension reduction term by the particle size reduction (Δd) term in Noolandi and Hong's equation.

Therefore,

$$\Delta d = Kd\phi_c[(1/2\chi + 1/Z_c) - 1/Z_c\exp(Z_c\chi/2)] \quad (10)$$

where K is a proportionality constant.

The plot of the particle size reduction as a function of the volume percent of the compatibilizer is shown in Figure 15. It can be seen that at low copolymer concentrations (below the CMC) Δd

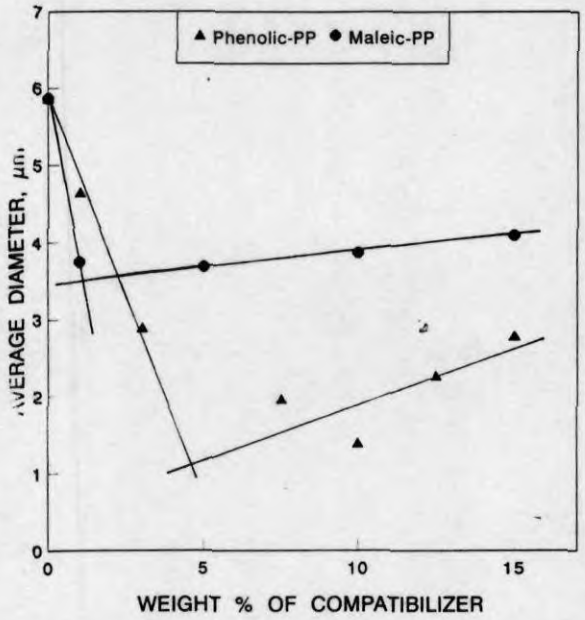

Figure 13. Variation of the average size of dispersed NBR domains as a function of compatibilizer concentration.

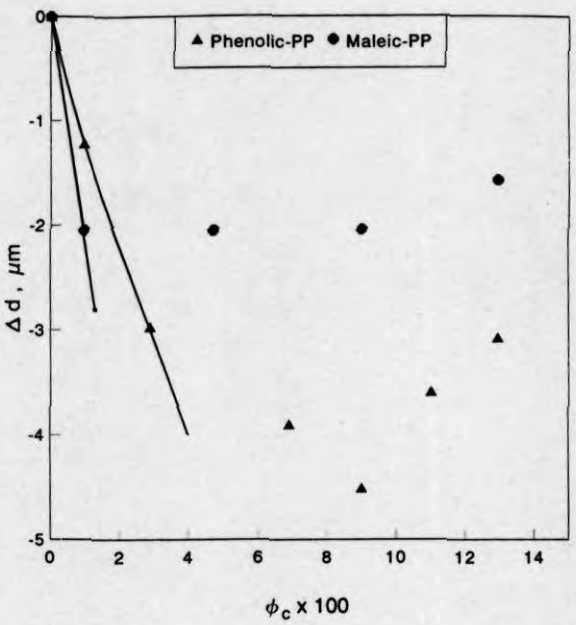

Figure 15. Variation of particle size reduction as a function of compatibilizer volume fraction.

decreases linearly with increasing the copolymer volume fraction, whereas at higher concentrations (above the CMC), it levels off, in agreement with the theories of Noolandi and Hong.

The domain size distribution curves for the MA–PP and Ph–PP compatibilized blends are shown in Figures 16 and 17, respectively. In the case of an unmodified blend, a high degree of polydispersity is evident by the large width of the distribution curve. With the increasing concentration of the compatibilizer (Ph–PP and MA–PP) the polydispersity decreases, as evident by the decrease in the width of the distribution curve. In the case of the Ph–PP compatibilized blend, a very narrow distribution is obtained with the addition of 10% Ph–PP. Willis and Favis[49] have also shown that the addition of a compatibilizer to the polyolefin/polyamide system not only reduces the dimensions of the minor phase, but also results in uniform distribution of minor phase.

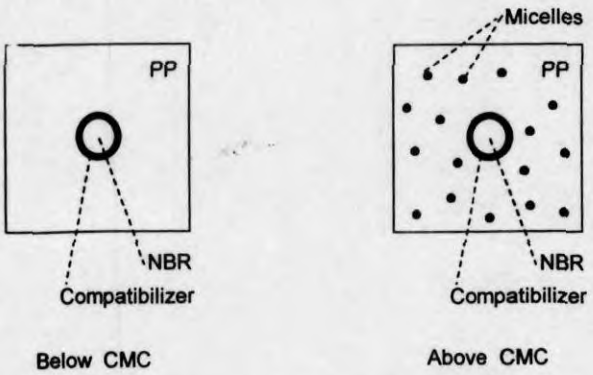

Figure 14. Schematic representation of the formation of micelles above critical micelle concentration.

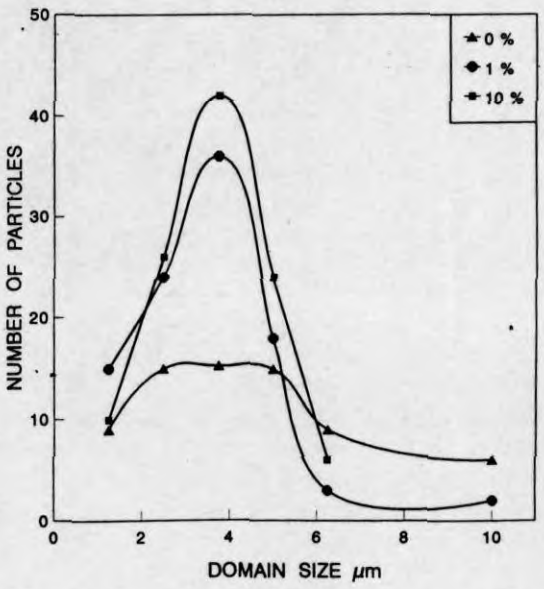

Figure 16. Domain size distribution curves of MA–PP compatibilized PP/NBR blends.

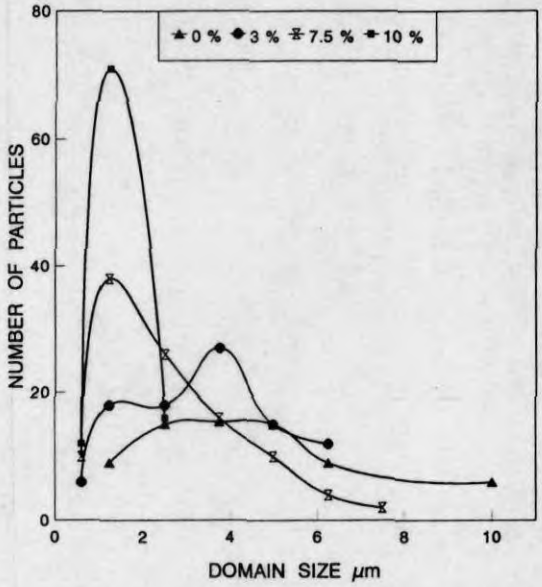

Figure 17. Domain size distribution curves of Ph–PP compatibilized PP/NBR blends.

The mechanism of the compatibilizing action and the difference in the behavior of MA–PP and Ph–PP as compatibilizers in NBR/PP can be explained as follows. In the maleic anhydride-modified polypropylene, maleic anhydride groups are grafted on PP chain back bone,[35] as shown in Figure 18. The compatibilizing action of this MA–PP is due to the dipolar interaction between the maleic anhydride groups of MA–PP and NBR. This causes a reduction in interfacial tension, which reduces the domain size of the dispersed phase. In phenolic-modified polypropylene dimethylol groups are grafted on polypropylene chain, as shown in Figure 19.[35] Here the compatibilizing action is due to the dipolar interaction between the dimethylol phenolic groups and NBR and also due to the emulsifying action of the graft copolymer formed between PP and NBR. The compatibilizing action of the copolymer at the interface is schematically shown in Figure 20.

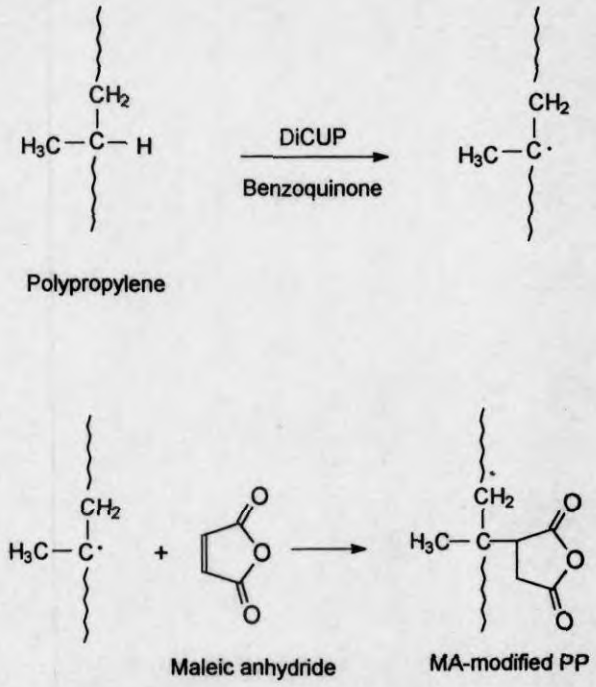

Figure 18. Schematic representation of the maleic anhydride modification of polypropylene.

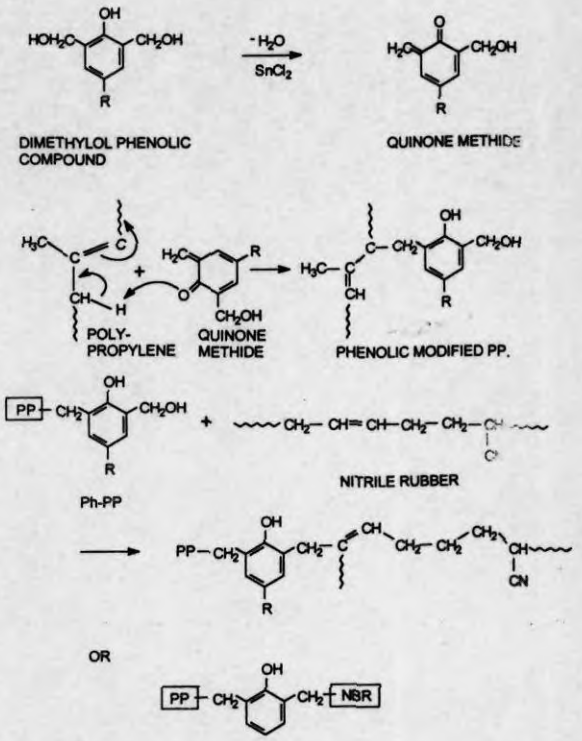

Figure 19. Schematic representation of the dimethylol phenolic modification of polypropylene and the formation of copolymer.

The variation of the storage modulus as a function of the temperature of the 70/30 PP/NBR blends compatibilized with different concentrations of phenolic-modified polypropylene is shown in Figure 21. With the addition of 3% Ph–PP the modulus of the unmodified blend is increased at lower temperatures, i.e., below glass transition temperatures. However, with further addition of the compatibilizer (7.5 and 10 wt % Ph–PP) the storage modulus is decreased from the levels of P_{70} containing the 3% Ph–PP. The increase in the

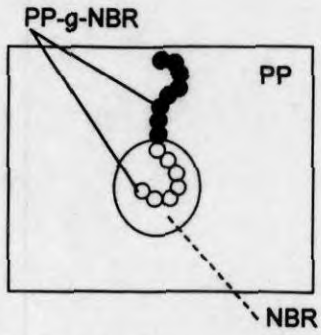

Figure 20. Schematic illustration of the conformation of the block copolymer at the interface.

modulus upon the addition of 3% Ph–PP is due to the increase in the interfacial adhesion caused by the emulsifying effect of the block copolymer formed by the interaction between the phenolic-modified polypropylene and nitrile rubber. The better interaction between PP and NBR in the presence of Ph–PP is evident from the morphology observed in SEM micrographs. At a lower concentration of the compatibilizer the average domain size of NBR particles decreased due to interfacial tension reduction and high interfacial interaction. The decrease in modulus at a higher concentration of the copolymer is due to the formation of micelles of the compatibilizer in the polypropylene matrix. As the micelle formation starts, some of the copolymer already at the interface leaves the interface, as explained earlier. This increases the domain size. Similar behavior has been reported in the compatibilization of PS/PE blends by HPB-*b*-PS copolymers.[27] Brahimi et al.[27] reported that the modulus of the PE/PS blend increased by compatibilization using PS–PE block copolymers up to interface saturation concentration, and after that the modulus decreased. At higher temperatures all the blends of PP/NBR showed approximately the same modulus.

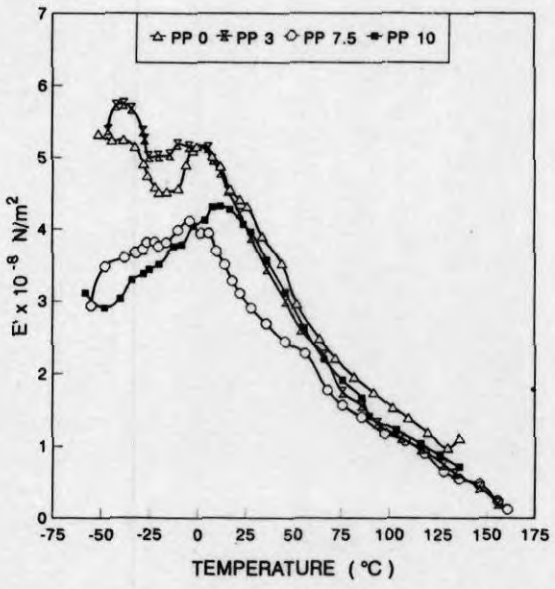

Figure 21. Variation of storage modulus (E') of Ph–PP compatibilized PP/NBR blends with temperature.

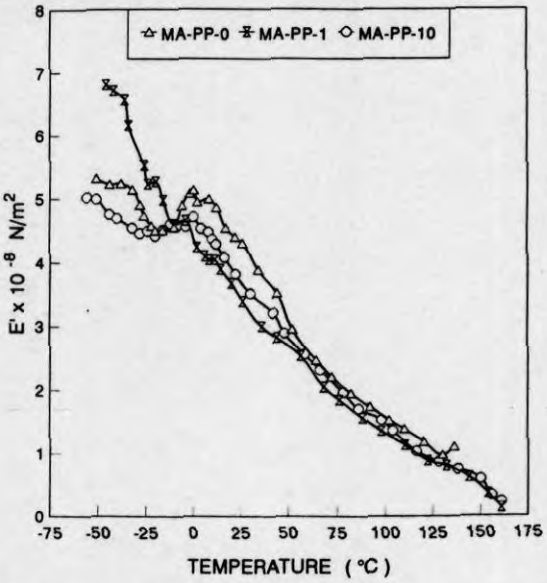

Figure 22. Variation of modulus (E') of MA–PP compatibilized PP/NBR blends.

Figure 22 depicts the variation of storage modulus E' of the 70/30 PP/NBR blend compatibilized with maleic anhydride-modified polypropylene. In this case, the addition of 1% maleic anhydride-modified polypropylene also increases the modulus of the blend compared to the unmodified one at lower temperatures, i.e., below the grass transition temperature of PP. At high temperatures the values are lower than the P_{70} blend. When the concentration of MA–PP is increased to 10% the modulus shows lower values than that of P_{70}. At higher temperatures it shows values higher than that of the blend modified with 1% MA–PP. At a temperature above 50°C all the blends show nearly the same values of E'. In the modification of PP/NBR with maleic anhydride-modified polypropylene (MA–PP), the MA–PP increases the interfacial interaction between PP and NBR by the dipolar interaction between polar maleic anhydride groups of MA–PP and polar

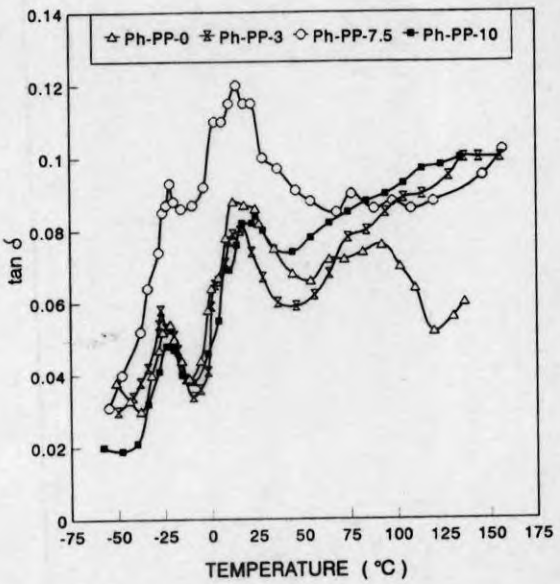

Figure 23. Variation of tan δ of Ph–PP compatibilized PP/NBR blends as a function of temperature.

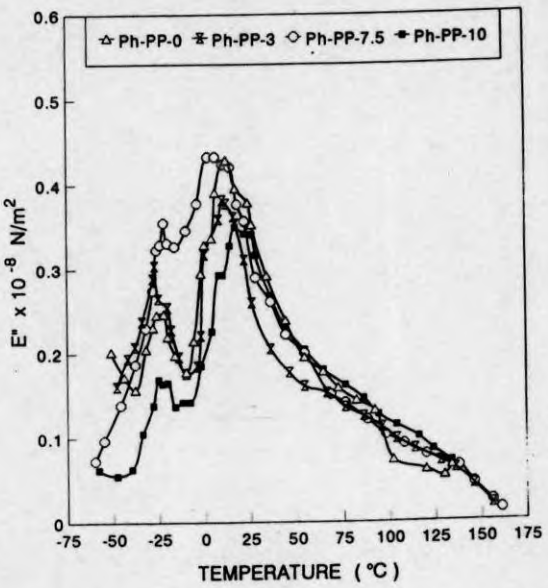

Figure 25. Variation of loss modulus (E'') of Ph–PP compatibilized PP/NBR blends as a function of temperature.

NBR. The increased interaction at the interface may be the reason for the increase in the modulus upon the addition of 1% MA–PP. The further decrease in E' by the addition of 10 wt % MA–PP indicates the formation of micelles in the PP matrix. Here, also, the increased interfacial interaction is evident from the small and uniform dispersion of NBR particles upon the addition of MA–PP. Above 1 wt % MA–PP the domain size leveled off due to interfacial saturation (Fig. 13).

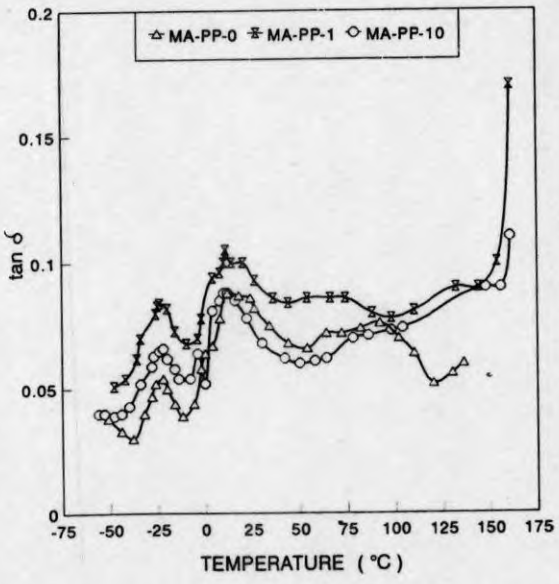

Figure 24. Variation of tan δ of MA–PP compatibilized PP/NBR blends as a function of temperature.

The variation of tan δ as a function of temperature of Ph–PP compatibilized blends is shown in Figure 23. The compatibilized blends also show the same behavior for the tan δ curve as that of unmodified blend, i.e., the compatibilized blends show the presence of two maximas corresponding to the glass transition temperature of polypropylene and nitrile rubber. This indicates that the compatibilization does not alter the level of miscibility. In other words, the presence of a compatibilizer does not promote molecular level miscibility. This is in agreement with the conclusions made by Paul,[12] who suggested that if two polymers are far from being miscible, then no copolymer is likely to make a one-phase system. In a completely immiscible system, the main role of the compatibilizer is to act as an interfacial a[illegible]. At lower temperatures the tan δ values show an increase for 3 and 7.5 wt % of Ph–PP. However, at intermediate temperatures the tan δ values of these blends are lower than that of the unmodified blend. When the concentration of Ph–PP is increased to 10 wt % the tan δ values decrease and the values are lower than those of P_{70}. All the compatibilized systems show higher values of tan δ than an unmodified blend at higher temp[illegible]tures. This increase in tan δ indicates that the interfacial interaction caused by the presence of

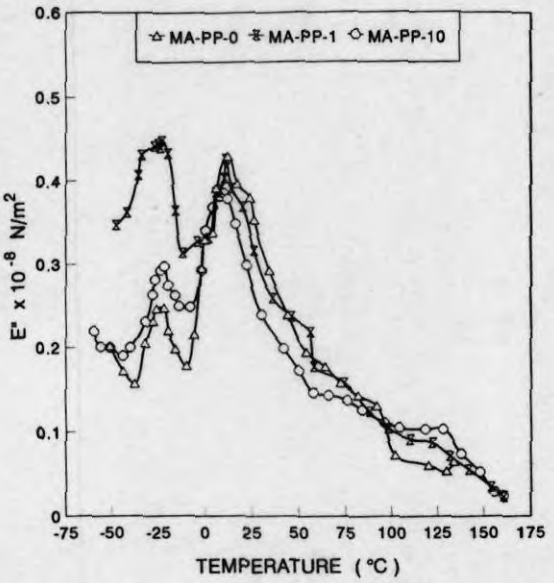

Figure 26. Variation of loss modulus (E'') of MA–PP compatibilized blends as a function of temperature.

the Ph–PP in PP/NBR blend may be weakened at higher temperatures. The decrease in the interfacial interaction at a higher temperature will decrease the interfacial adhesion and, hence, leads to increased segmental motion. The glass transition temperatures corresponding to NBR remains unaltered by the incorporation of Ph–PP. However, T_g values corresponding to PP changes slightly with the incorporation of Ph–PP. Upon the addition of 3% Ph–PP the T_g value remains the same as that of P_{70}. However, in the case of 7.5 and 10 wt % Ph–PP incorporation, the T_g values shift to slightly higher temperatures.

The variation of tan δ of MA–PP-compatibilized PP/NBR blends is shown in Figure 24. By the incorporation of 1% MA–PP, the tan δ values increase at the whole temperature range. When the concentration of MA–PP is increased to 10 wt

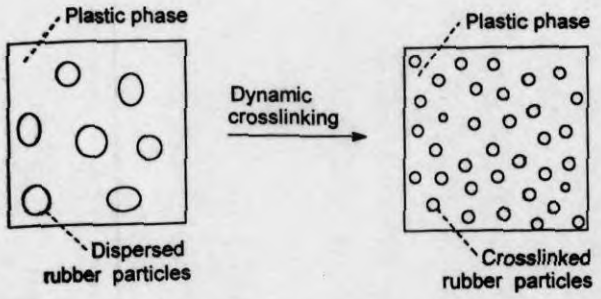

Figure 27. Schematic representation of the morphology of dynamic vulcanized thermoplastic elastomer.

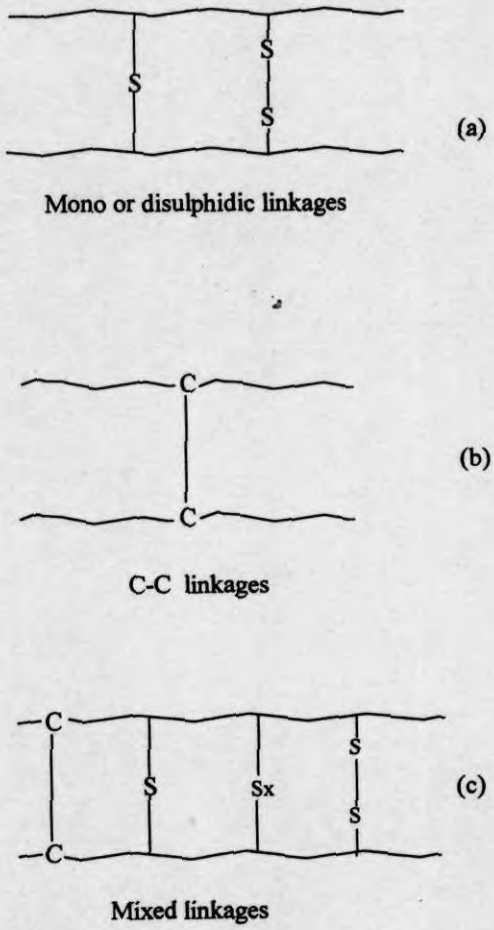

Figure 28. Schematic representation of the network structure in (a) sulfur, (b) DiCUP, and (c) mixed (DiCUP + sulfur) vulcanized systems.

% the tan δ shows an increase at a lower temperature, and at an intermediate temperature it decreases. In this case, also, the decrease in tan δ is due to the increase in interfacial interaction caused by the presence of MA–PP. The compatibilized blends indicate higher tanδ values than the uncompatibilized system at higher temperatures.

Figure 25 depicts the variation of loss modulus (E'') as a function of temperature of Ph–PP-compatibilized blends. The loss modulus shows a similar trend as that of tan δ curves. The E'' curves show the presence of two peaks corresponding to the glass transition temperature of PP and NBR. Similar to tan δ curves here, the addition of 3 and 7.5 wt % Ph–PP also increases the E''. The values are lower than those of the P_{70} at lower temperatures. At intermediate temperatures all the compatibilized blends show slightly lower E'' values than P_{70}.

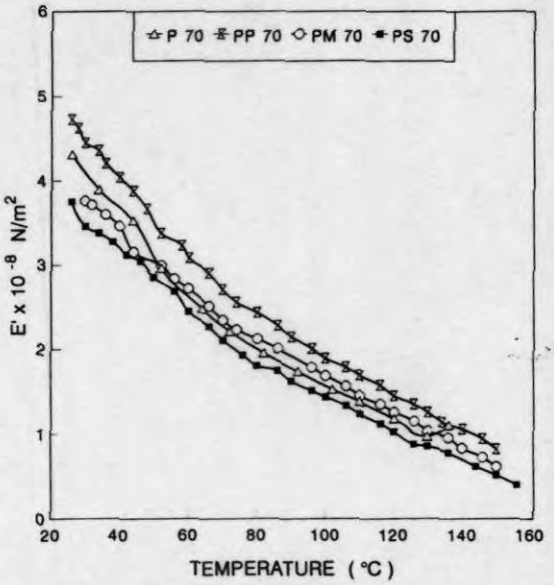

Figure 29. Variation of storage modulus (E') of sulfur, DiCUP, and mixed (DiCUP + sulfur) vulcanized 70/30 PP/NBR blends with temperature.

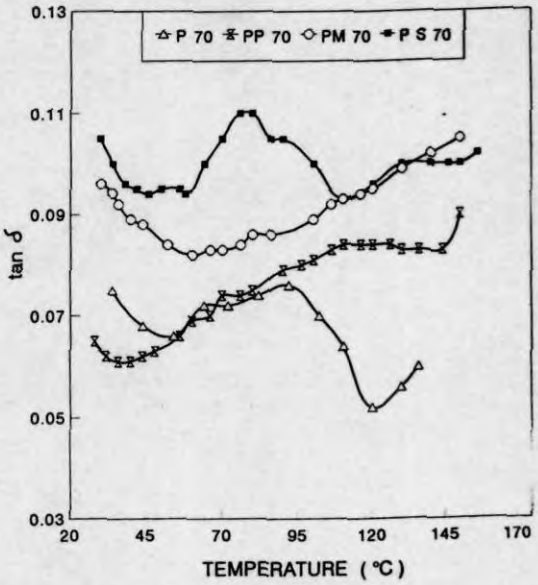

Figure 31. Variation of tan δ of sulfur, DiCUP, and mixed (DiCUP + sulfur) vulcanized PP/NBR blends with temperature.

In MA–PP compatibilized blends, the variation of loss modulus is shown in Figure 26. The behavior is similar to tan δ curves. It shows the presence of two peaks corresponding to NBR and PP. At lower temperatures, 1 and 10% MA–PP-modified blends show higher values of E'' than those of the unmodified blend. At intermediate temperatures the values of E'' lie below that of the unmodified blend. Here, also, at higher temperatures the compatibilized blends show higher values of E''.

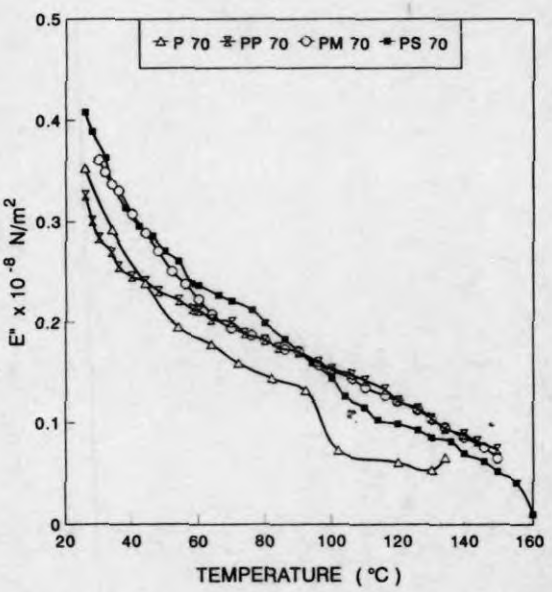

Figure 30. Variation of loss modulus (E'') of sulfur, DiCUP, and mixed (DiCUP + sulfur) vulcanized PP/NBR blends with temperature.

Effect of Dynamic Vulcanization

The vulcanization of the rubber phase during mixing has been investigated as a way to improve the physical properties of several thermoplastic elastomers based on rubber/plastic blends.[28,30] During dynamic vulcanization the crosslinked rubber phase becomes finely and uniformly distributed in the plastic matrix and attains a stable morphology, as shown schematically in Figure 27. Dynamic vulcanization has been applied to several rubber/plastic blends.[6] In the present study, three types of crosslinking systems have been used. These include accelerated sulfur vulcanization, which produces predominantly polysulfidic linkages, a peroxide system, which gives rise to C—C linkages, and a mixed system, which produces both polysulfide linkages and C—C linkages. The schematic representation of the network structure in the three cases are shown in Figure 28.

The variation of E', E'', and tan δ of the P_{70} blend crosslinked with sulfur, dicumyl peroxide, and mixed systems are shown in Figures 29–31. The modulus of the blends vulcanized with the DiCUP and mixed systems shows higher values

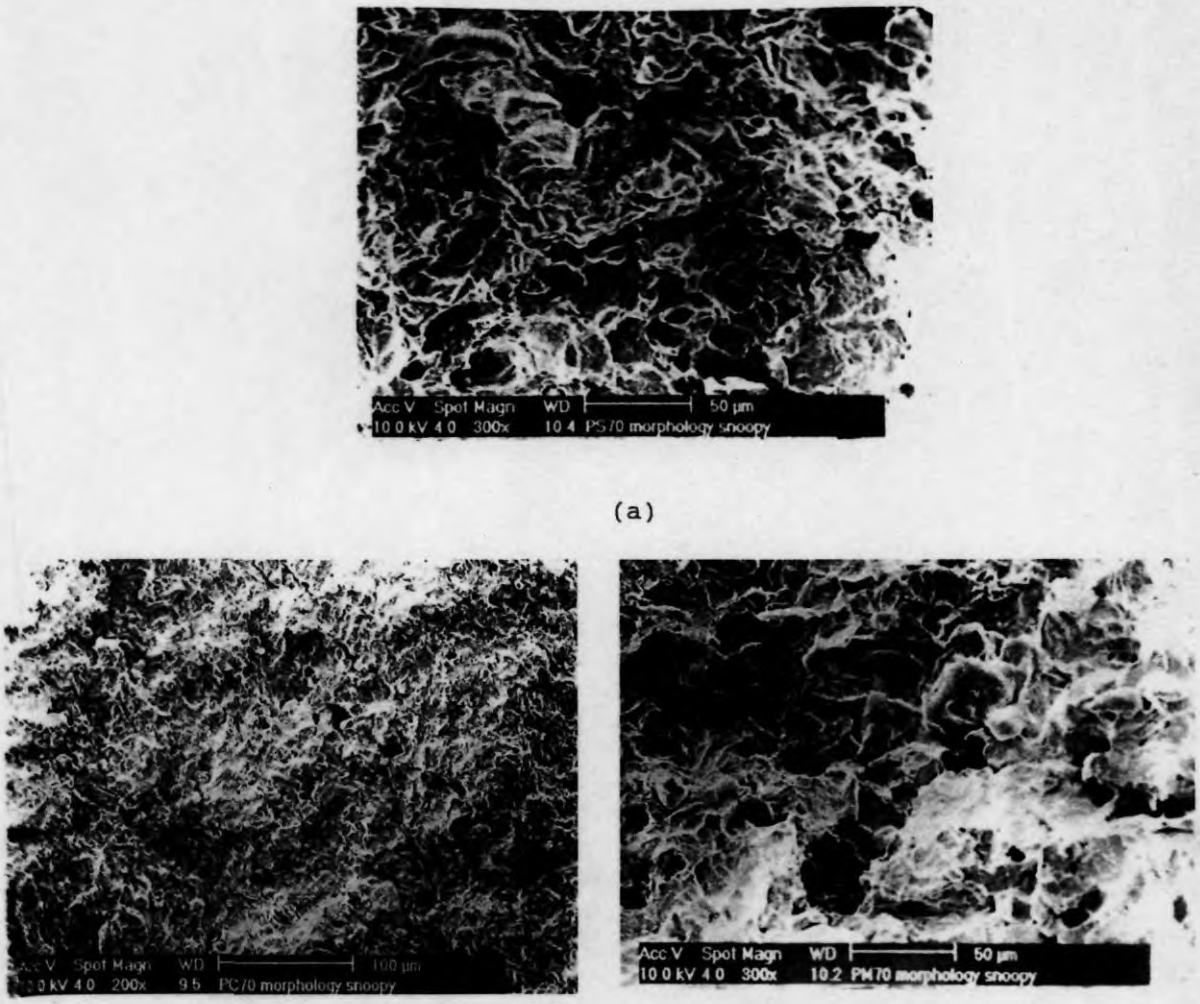

Figure 32. Scanning electron micrographs of the morphology of dynamically vulcanized PP/NBR blends (a) sulfur, (b) DiCUP, and (c) mixed (sulfur + DiCUP) cured samples.

than the uncrosslinked system, while the sulfur crosslinked system shows the lowest value. In the PP/NBR blends on peroxide vulcanization there is a possibility of degradation of the PP phase in the presence of DiCUP. However, the results from the figure indicates that the crosslinking reaction predominates over degradation reactions in the case for DiCUP vulcanization. The increase in modulus for the DiCUP system is also due to the crosslinking of the NBR phase. In the case of the sulfur system, sulfur crosslinks only the NBR phase and shows the lowest modulus value. The mixed system, as expected, shows intermediate behavior.

The loss modulus of the vulcanized systems shown in Figure 30 indicates that the loss modulus increases upon vulcanization. Here, also, the DiCUP system shows the lowest E'' and sulfur system shows the highest E'' values. The mixed system shows intermediate behavior.

The variation of tan δ with temperature (Fig. 31) also shows the same trend as that of the loss modulus, i.e., the DiCUP crosslinked system shows the lowest tan δ values and the sulfur system the highest value. The mixed system shows intermediate values. In all cases the introduction of crosslinks increases the tan δ values.

The morphology of the PP/NBR blends vulcan-

ized with sulfur, DiCUP, and the mixed system is shown in Figure 32. From the figures it is seen that in the sulfur cured system, the size of the dispersed NBR domains is larger than those of the peroxide and mixed-cured systems. In the peroxide-cured system, the distribution is fine and uniform and, hence, the crosslinking is more effective in the DiCUP system. However, this effect of crosslinking is not so predominant on the properties of the peroxide-vulcanized system due to the degradation of the PP phase in the presence of DiCUP.

CONCLUSION

The effect of the blend composition and compatibilization on the dynamic mechanical properties was investigated in the temperature range −50 to +150°C. These investigations indicate that the PP/NBR blends are incompatible, as shown by the presence of two relaxation peaks corresponding to the T_g's of PP and NBR. As the concentration of rubber increases, the storage modulus of the system decreases, while the loss modulus and tan δ increase. The increase in loss modulus is more pronounced after the 50 wt % NBR phase. The change in viscoelastic properties with blend composition can be correlated with the blend morphology. Various composite models have been used to fit the experimental viscoelastic data. The Takayanagi model was found to fit the experimental values for a 20% parallel coupling. The addition of phenolic-modified polypropylene and maleic anhydride-modified polypropylene are found to increase the storage modulus at a lower temperature, which indicate an increase in interfacial adhesion on the addition of these compatibilizers. At a higher concentration of these compatibilizers the storage modulus decreases due to interfacial saturation. As the concentration of the compatibilizers increased, the domain size of the dispersed NBR particles decreased initially, followed by a leveling off or increase at a higher concentration, indicating the presence of interfacial saturation concentration. Among the vulcanized systems, the DiCUP system shows the highest modulus, and sulfur system the lowest. The mixed system showed an intermediate behavior.

One of the authors (S.G.) is grateful to Council for Scientific and Industrial Research (CSIR), New Delhi, for Senior Research Fellowship and Mr. Vijayan of IIT, Chennai, for his help in doing this work.

REFERENCES AND NOTES

1. P. Cheung, D. Suwanda, and S. T. Balke, *Polym. Eng. Sci.*, **30,** 17, 1063 (1990).
2. R. M. Holsti-Miettinen, M. T. Heino, and J. V. Seppala, *J. Appl. Polym. Sci.*, **57,** 573 (1995).
3. F. C. Stehling, T. Huff, C. S. Speed, and G. Wissler, *J. Appl. Polym. Sci.*, **26,** 2693 (1981).
4. M. S. Lee and S. A. Chen, *Polym. Eng. Sci.*, **33,** 11, 686 (1993).
5. C. Els and W. J. McGill, *Plast. Rubber Comp. Process. Appl.*, **21,** 115 (1994).
6. S. K. De and A. K. Bhowmick, Eds., *Thermoplastic Elastomers from Rubber-Plastic Blends*, Ellis Horwood, New York, 1990.
7. C. S. Ha, D. J. Ihm, and S. C. Kim, *J. Appl. Polym. Sci.*, **32,** 6281 (1986).
8. A. Coppola, R. Greco, and G. Ragosta, *J. Mater. Sci.*, **21,** 1775 (1986).
9. S. Thomas, S. K. De, and B. R. Gupta, *Kaust. Gumm. Kunst.*, **40,** 7, 665 (1987).
10. D. Havata, J. Plastil, D. Zuchowska, and R. Steiler, *Polymer*, **32,** 18, 3313 (1991).
11. B. Kuriakose and S. K. De, *Polym. Eng. Sci.*, **25,** 630 (1985).
12. D. R. Paul and S. Newman, Eds., *Polymer Blends*, Academic Press, New York, 1978.
13. R. Asaletha, M. G. Kumaran, and S. Thomas, *Rubber Chem. Technol.*, **68,** 671 (1995).
14. Z. Oommen, M. R. Gopinathan Nair, and S. Thomas, *Polym. Eng. Sci.*, **36,** 1 (1996).
15. J. George, R. Joseph, K. T. Varughese, and S. Thomas, *J. Appl. Polym. Sci.*, **57,** 449 (1995).
16. S. George, R. Joseph, K. T. Varughese, and S. Thomas, *Polymer*, **36,** 23, 4405 (1995).
17. T. M. Murayama, Ed., *Dynamic Mechanical Analysis of Polymeric Materials*, Elsevier, New York, 1978.
18. J. Karger-Kocsis and L. Kiss, *Polym. Eng. Sci.*, **27,** 4, 254 (1987).
19. K. W. McLaughlin, *Polym. Eng. Sci.*, **29,** 22, 1560 (1989).
20. M. J. Guest and J. H. Daly, *Eur. Polym. J.*, **26,** 6, 603 (1990).
21. Y. Li and H. L. Williams, *J. Appl. Polym. Sci.*, **40,** 1891 (1990).
22. C. Wippler, *Polym. Eng. Sci.*, **30,** 17 (1990).
23. D. IL. Kang, C. S. Ha, and W. J. Cho, *Eur. Polym. J.*, **28,** 6, 565 (1992).
24. A. T. Koshy, B. Kuriakose, S. Varghese, and S. Thomas, *Polymer*, **34,** 3428 (1993).
25. H. Varghese, S. S. Bhagawan, and S. Thomas, *Eur. Polym. J.*, **31,** 957 (1995).
26. K. T. Varughese, G. B. Nando, P. P. De, and S. K. De, *J. Mater. Sci.*, **23,** 3894 (1988).
27. B. Brahimi, A. Ait-Kadi, A. Ajji, and R. Fayt, *J. Polym. Sci., Part B: Polym. Phys.*, **29,** 946 (1991).
28. P. Ramesh and S. K. De, *J. Appl. Polym. Sci.*, **50,** 1369 (1993).

29. R. N. Santra, B. K. Samantaray, A. K. Bhowmick, and G. B. Nando, *J. Appl. Polym. Sci.*, **49,** 1145 (1993).
30. R. M. Holsti–Miettinen, J. V. Seppala, O. T. Ikkala, and I. T. Reima, *Polym. Eng. Sci.*, **34,** 5, 395 (1994).
31. R. E. Cohen and A. R. Ramos, *J. Macromol. Sci. Phys.*, **B17,** 625 (1980).
32. B. Kuriakose, S. K. De, S. S. Bhagawan, R. Sivaramakrishnan, and S. K. Athithan, *J. Appl. Polym. Sci.*, **32,** 5509 (1986).
33. F. S. Liao, A. C. Su, and Tzu–Chien J. Hsu, *Polymer*, **35,** 2579 (1994).
34. K. T. Varughese, P. P. De, and S. K. Sanyal, *Angew. Makromol. Chem.*, **182,** 73 (1990).
35. A. Y. Coran and R. Patel, *Rubber Chem. Technol.*, **56,** 1045 (1983b).
36. S. Thomas and A. George, *Eur. Polym. J.*, **28,** 145 (1992).
37. D. J. Walsh and J. S. Higgins, *Polymer*, **23,** 336 (1982).
38. S. Thomas, B. R. Gupta, and S. K. De, *J. Vinyl Technol.*, **9,** 71 (1987).
39. N. E. Nielson, *Rheol. Acta*, **13,** 86 (1974).
40. J. C. Halpin, *J. Compos. Mater.*, **3,** 732 (1970).
41. A. Y. Coran, *Hand Book of Elastomers: New Development and Technology*, A. K. Bhowmick and H. L. Stephens, Eds., Marcel Dekker, New York, 1988, p. 249.
42. D. R. Paul and G. W. Barlow, *ACS, Adv. Chem. Ser.*, **176,** 315 (1979).
43. H. A. Spiros, G. Irena, and J. T. Koberstein, *Macromolecules*, **22,** 1449 (1989).
44. R. Fayt, R. Jerome, and Teyssie Ph., *Makromol. Chem.*, **187,** 837 (1986).
45. S. Thomas and R. E. Prud'homme, *Polymer*, **33,** 4260 (1992).
46. J. Noolandi and K. M. Hong, *Macromolecules*, **15,** 482 (1982).
47. J. Noolandi and K. M. Hong, *Macromolecules*, **17,** 1531 (1984).
48. S. Wu, *Polym. Eng. Sci.*, **27,** 335 (1987).
49. J. M. Willis and B. D. Favis, *Polym. Eng. Sci.*, **30,** 1073 (1990).
50. C. S. Ha, *J. Appl. Polym. Sci.*, **35,** 2211 (1988).